THE DESIGN OF ACYL MODIFIED CO-ENZYME-A ESTER ANALOGUES AS ENZYME INHIBITORS

Maria Grazia Rubanu

A Thesis Submitted for the Degree of PhD
at the
University of St Andrews

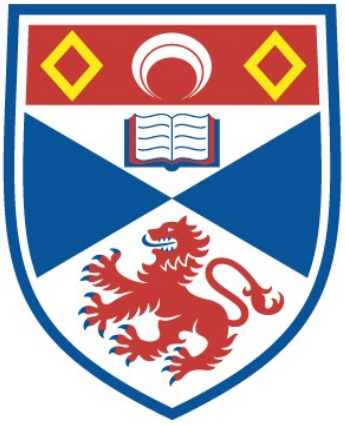

2019

The design of acyl modified co-enzyme-A ester analogues as enzyme inhibitors

University of
St Andrews

Maria Grazia Rubanu

This thesis is submitted in partial fulfilment for the degree of

Doctor of Philosophy (PhD) at the University of St Andrews

May 2019

Declarations

Candidate's declarations

I, Maria Grazia Rubanu, do hereby certify that this thesis, submitted for the degree of PhD, which is approximately 40,000 words in length, has been written by me, and that it is the record of work carried out by me, or principally by myself in collaboration with others as acknowledged, and that it has not been submitted in any previous application for any degree.

I was admitted as a research student at the University of St Andrews in September 2015.

I received funding from an organisation or institution and have acknowledged the funder(s) in the full text of my thesis.

Date Signature of candidate

Supervisor's declaration

I hereby certify that the candidate has fulfilled the conditions of the Resolution and Regulations appropriate for the degree of PhD in the University of St Andrews and that the candidate is qualified to submit this thesis in application for that degree.

Date Signature of supervisor

Permission for publication

In submitting this thesis to the University of St Andrews we understand that we are giving permission for it to be made available for use in accordance with the regulations of the University Library for the time being in force, subject to any copyright vested in the work not being affected thereby. We also understand, unless exempt by an award of an

embargo as requested below, that the title and the abstract will be published, and that a copy of the work may be made and supplied to any bona fide library or research worker, that this thesis will be electronically accessible for personal or research use and that the library has the right to migrate this thesis into new electronic forms as required to ensure continued access to the thesis.

I, Maria Grazia Rubanu, confirm that my thesis does not contain any third-party material that requires copyright clearance.

The following is an agreed request by candidate and supervisor regarding the publication of this thesis:

Printed copy

No embargo on print copy.

Electronic copy

No embargo on electronic copy.

Date Signature of candidate

Date Signature of supervisor

Underpinning Research Data or Digital Outputs

Candidate's declaration

I, Maria Grazia Rubanu, hereby certify that no requirements to deposit original research data or digital outputs apply to this thesis and that, where appropriate, secondary data used have been referenced in the full text of my thesis.

Date Signature of candidate

Abstract:

This thesis is focused on the design and synthesis of analogues of thioesters of Co-enzyme A which are involved in many important biosynthetic pathways.

Acetyl-CoA is converted into citrate by citrate synthase in the first step of the Krebs cycle that is central for the cellular respiration.

Chapter 2 is focused on the successful synthesis of five analogues of acetyl-CoA and their investigation as inhibitors of citrate synthase. This project is based on the finding that Fluorovinyl thioether-CoA (FV-CoA) is a micromolar inhibitor of citrate synthase (K_i^{app} = 4.4 µM).[1] Sulfoxide-CoA, with a sulfonyl and a methylene group replacing the carbonyl group and the sulfur atom of acetyl-CoA, was found to be a modest micromolar inhibitor of citrate synthase (11.1 µM), indicating its potential as hydrogen bonding acceptor. The remaining compounds showed poor or too low binding affinity for the enzyme. Although these compounds showed poor inhibitory capacity towards citrate synthase, they could be potential inhibitors of other acetyl-CoA utilizing enzymes, such as malate synthase that catalyzes the conversion of acetyl-CoA into malate. Its activity is correlated to different pathogens pathway (*Mycobacterium tubercolosis*) and its regulation could potentially prevent the bacterial growth.

Chapter 3 describes the attempted synthesis of a fluorovinyl thioacrylate derivative as malonyl-CoA analogue and potential covalent inhibitor of acetyl-CoA carboxylase (ACC). ACC catalyzes the irreversible conversion of acetyl-CoA into malonyl-CoA in the first step of fatty acid synthesis. The regulation of ACC is associated to many cardiovascular diseases such as diabetes, obesity and its inhibition can lead to the development of novel antibiotics for their treatment. Due to the challenging synthesis of the precursor thioester, this malonyl-CoA analogue could not be prepared.

Chapter 4 reports the synthesis of α,α,β-trifluoro cyclopropane-CoA and was found to be a poor inhibitor of citrate synthase (K_i = 65.2 µM). However, this compound has potential to be a covalent inhibitor of citrate synthase and other enzymes such as malate synthase, thus future investigations will be carried out to this purpose.

Furthermore, chapter 4 reports the attempted synthesis of an α,α-difluoroethyl thioether-CoA as an acetyl-CoA analogue. This compound bears two electronegative fluorine atoms, thus it could interact electrostatically with the active site residues of citrate synthase through hydrogen bonds, leading to its inhibition. Unfortunately, due to the instability of the difluoro moiety under the enzymatic reaction conditions, this was not converted to the corresponding acetyl-CoA analogue.

Acknowledgements:

First of all, I would like to thank my supervisor Professor David O'Hagan for giving me the opportunity of doing my PhD in his multidisciplinary research group, for all his support and guidance during these years. I feel privileged and honoured to have worked in one of the most prestigious universities of UK which allowed me to do research at high levels. A special thank goes to the amazing NMR and Mass Spectrometry team that has always provided us excellent services.

I would compare my PhD experience to a roller coaster, feeling a constant excitement, panic and fear at the same time for almost four years. Likely, I am a masochist and stubborn person so despite the ups and downs I am really proud of my hard work and what I have learned all these years.

To all the members of my group, I am very grateful for all the help and support you gave me. You have been a great supporting system so I thank you all for making me feel welcome from day one.

A special thanks goes to Davide which has been there for me since I walked in those laboratories for the first time, for his guidance and his PDs. I have learned so much from you and I own you sardinian food forever. Also, thanks for introducing me to your family, your wonderful kids and wife.

To Nouchali and Tanya, the DOH girl team, thanks for all the laughs, the talks, the girl nights and all the beautiful moments we have spent together. To all the people from the 4th floor of the BMS building (Marta, Ed, Guillame, Virginie, David, Maria) it has been a pleasure to get to know all of you, I could not think to a better and chilled environment to work in. To Cristina and Nicolas, thank you so much for all the support and the good moments we have shared during these years.

To Giulia, my wonderful flatmate, thanks for your friendship and for being always there not matter what.

To my family, word can not express my gratitude. Dad and Mom, I will never be able to repay you for all the sacrifices you have made to get us the best education we could get. I am deeply thankful and I hope you are proud of me.

To all my friends from my hometown and my former university, I am lucky to always have you in my life. Thanks for all the support despite the distance.

To my guardian angels, these last words are for you. I wish you were here to celebrate with me, I love you and I miss you.

Abbreviations:

AANAT	N-acetylserotonin O-methyltransferase
AcCo-A	acetyl-CoA
ACP	acyl carrier protein
ACC	acetyl-CoA carboxylase
ADP	adenosine Diphosphate
AgF	silver Fluoride
Ala	alanine
ALS	acetolactate synthase
Arg	arginine
Asn-	asparagine
Asp-	aspartic acid
ATCase	aspartate transcarbamoyltransferase
ATP	adenosine triphosphate
Au-1	gold pre-catalyst
BC	biotin Carboxylase
BCCP	biotin carboxyl carrier protein
$B(OH)_3$	boric acid
br	broad
cAMP	cyclic adenosine monophosphate
cal	calories
CAII	carbonic anhydrase
CatK	cathepsin K
CCD	charge Coupled Device
$CDCl_3$	deuterated chloroform
$(CD_3)_2SO$	deuterated dimethyl sulfoxide
CD_3OD	deuterated methanol
CHP	cumene hydroperoxide
CoA-SH	co-enzyme A
CO_2	carbon dioxide
CO	carbon monoxide
COSY	correlated spectroscopy
CPT	carnitine palmitoyltransferase
CS	citrate synthase
CT	carboxyl transferase
CTP	cytidine triphosphate

CuI	coper iodide
$CuCl_2$	coper chloride
D_2O	deuterated oxide
D_2	dopamine receptor
d	doublet
Da	dalton
Ds	double-standed
DAST	diethylaminosulfur trifluoride
DBU	1,8-Diazabicyclo[5.4.0]undec-7-ene
DCM	dichloromethane
DCE	dichloroethane
DET	diethyl tartrate
DMF	dimethylformamide
DNA	deoxyribonucleic acid
DMPU	N,N′-Dimethylpropyleneurea
DPCK	dephosphocoenzyme A kinase
DQF	double quantum filter
dTMP	deoxythymidine monophosphate
DTNB	(5,5'-dithiobis-(2-nitrobenzoic acid)
dUMP	deoxyuridine monophosphate
EBX	ethynylBenziodoXolone
EC_{50}	effective concentration
EDCI	1-ethyl-3-(3-dimethylaminopropyl)carbodiimide
Et_3N	triethyl amine
EtOH	ethanol
EI	electron ionization
Et_2O	diethyl ether
EtONa	sodium ethoxide
ES	enzyme-substrate complex
ESI	electron spray ionization
EtSH	ethanthiol
FAD	flavin adenine dinucleotide
FAS	fatty acids synthase
FDA	food and drug administration
FdUMP	fluorine deoxyuridine monophosphate
5-FHPA	5-Fluoro-2,3,4-trihydroxypentanoic acid

FV-CoA	fluorovinyl thioether co-enzyme A
g	grams
GCT	gas chromatographer
Gly-	glycine
h	hour
HAT	histone acetyltransferase
HCl	hydrochloric acid
HCV	hepatitis C virus
HDAC	histone deacetylase
HEPES	(4-(2-hydroxyethyl)-1-piperazineethanesulfonic acid
HF	hydrogen fluoride
His-	histidine
HIV	human immunodeficiency virus
HMG-CoA	β-Hydroxy β-methylglutaryl-CoA)
HOBt	hydroxybenzotriazole
HPLC	high pressure liquid chromatography
HR	high resolution
5-HT	5-hydroxytryptamine
Hz	hertz
IBX	2-iodo peroxybenzoic acid
IC_{50}	inhibition constant
Ile-	isoleucine
Imm-H	immucillin-H
J	coupling costant
John-Phos	(2-Biphenyl)di-*tert*-butylphosphine
K_{cat}	turnover enzyme
K_i	inhibition constant
K_m	michaelis-menten constant
LB	luria broth
LCD	liquid crystal display
LCT	liquid chromatography time of flight
LiOH	lithium hydroxide
n	nano
NMR	nuclear magnetic resonance
mCPBA	meta-Chloroperoxybenzoic acid
M	molar
MCD	malonyl decarboxylase

MCPA	methylene cyclopropyl acetic acid
MCPG	methylenecyclopropylglycine
MCPF	methylenecyclopropyl formyl
MeCN	acetonitrile
MeCOCl	methyl chloroformate
MeOH	methanol
MeONa	sodium methoxide
MES	2-(*N*-morpholino)ethanesulfonic acid
$MgCl_2$	magnesium chloride
mGluR4	glutamate metabotropic receptor 4.
MS	mass spectrometry
m/z	mass/charge
NADH	nicotinamide adenine dinucleotide
NaH	sodium hydride
NaOAc	sodium acetate
NAT	N-acetyl transferase
n-BuLi	normal-butyl lithium
NBS	N-bromo succinimide
NFSI	N-Fluorodibenzenesulfonimide
NFOBS	N-fluoro-o-benzenedisulfonimide
NMR	nuclear magnetic resonance
NS5B	non-structural protein 5B
NSI	nanospray ionization
OD	optical density
ODC	ornithine decarboxylase
p	pico
p	pentet
PABA	para-aminobenzoic acid
PAGE	polyacrylamide gel electrophoresis
PanK	pantothenate kinase
Pd	palladium
PDH	pyruvate dehydrogenase
PEG	polyethylene glycol
PEP	phosphoenolpyruvic acid
PGs	prostaglandins
PI	protease inhibitor
PMR	modified retro peptides

Phe-	phenylalanine
PKS	polyketide synthesis
PNP	purine nucleoside phosphorylase
PP	pyrophosphate
PPAT	phosphopantetheine adenylyltransferase
PPHF	poly (pyridine fluoride)
ppm	part per milion
PPVE	perfluoro(propyl vinyl ether)
Pro-	proline
PTFE	polytetrafluoroethylene
pTsOH	p-toluenesulfonic acid
QM/MM	quantum mechanics/molecular mechanics
q	quartet
R	relaxed
RNA	ribonucleic acid
s	singlet
SBB	N-(4-sulfamylbenzoyl)benzylamine
SDS	sodium dodecyl sulphate
Ser-	serine
SFM	super fluorinated materials
SM	starting material
Ss	single stranded
t	triplet
T	transition
T-cells	tumoral cells
TBAF	tetra-n-butylammonium fluoride
TBD	1,5,7-triazabicyclo[4.4.0]dec-5-ene
TBHP	tert-Butyl hydroperoxide
TCA	the citric acid cycle
TEA	triethyl amine
TF/VIIa	tissue factor VIIa
THF	tetrahydrofuran
Ti $(OiPr)_4$	titanium isopropoxide
TLC	thin layer chromatography
TMS	trimethyl silane
TNB^-	2-nitro-5-thiobenzoate
TPP	thiamine pyrophosphate

t_r	retention time
TS	transition state
TS	thymidylate synthase
Ts	tosyl
Tyr-	tyrosine
V-CoA	vinyl-CoA
V_{max}	maximum velocity rate
w/v	weight/volume
δ	chemical shift

Contents

1. INTRODUCTION

Coenzyme A and its thioesters derivatives are resourceful molecules involved in many biosynthetic pathways such as glycolysis, fatty acid metabolism and cell respiration. It has been estimated that 4% of key enzymes require Co-A or Co-A thioesters as substrates. Analogues of Co-A thioesters have been useful tools for the study of the activity and mechanism of enzymes, generally mimicking their intermediate states. This thesis will focus mainly on the design and synthesis of fluorinated and non-fluorinated acetyl-CoA analogues targeting citrate synthase.

1.1. Co-enzyme A discovery and its key role in cell metabolism

Co-enzyme A (Co-A) is a co-factor which was identified by Fritz Lipmann in 1946 and its structure was reported in 1953. The structure, which is highlighted in Figure 1.1, includes a pantetheine domain derived from pantothenic acid which is part of the Vitamin B family and an adenosine diphosphate moiety.[2] Co-A promotes the activation and transfer of acyl groups in many enzymatic reactions through its thiol group (-SH), it acts as an acyl group carrier transferring the moiety from one enzyme catalyzed reaction to an other.[3]

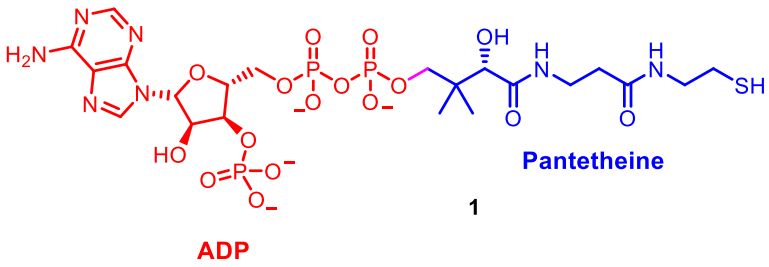

Fritz Lipmann

Figure 1.1. Co-enzyme A structure.[2]

1.2. Acetyl-CoA as a central metabolite: biosynthesis pathways

Acetyl-CoA **2** is the coenzyme-A thioester of acetate. The thioester facilitates the transfer of the acetyl moiety to a variety of acceptor molecules. Thioesters are less conjugated than amides or oxygen esters, and sulfur is an excellent nucleophile and leaving group more so than nitrogen or oxygen.

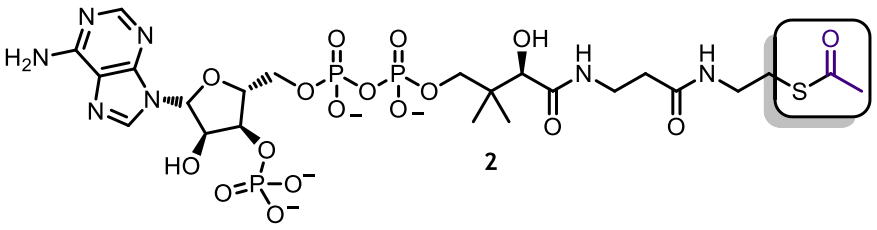

Figure 1.2. Acetyl-CoA structure.[2]

Acetyl-CoA **2** is synthesised in mitochondria by oxidative decarboxylation of pyruvate, itself originated from glycolysis and β-oxidation of fatty acids. The degradation of pyruvate **3** described in Scheme 1, is catalysed by an enzyme complex called pyruvate dehydrogenase (PDH). The reaction involves a sequence of group transfers and redox steps carried out by three different catalytic subunits: pyruvate dehydrogenase (E_1), dihydrolipoyl transacetylase (E_2) and dihydrolipoyl dehydrogenase (E_3).

Pyruvate interacts with thiamine pyrophosphate (TPP), prosthetic group of E_1 via decarboxylation to generate hydroxyethyl-TPP **4**. This is then simultaneously oxidised to acetyl and transferred to lipoamide, prostethic group of E_2, to give acetyllipoamide **6**. Transfer of the acetyl group to CoA-SH generates acetyl-CoA **2** and dihydrolipoamide which is re-oxidised to lipoamine by FAD prostethic group of E_3. The overall reaction converts pyruvate **3** (three carbons) to acetyl-CoA **2** (two carbons) releasing carbon dioxide (CO_2) and producing NADH in the process.[4]

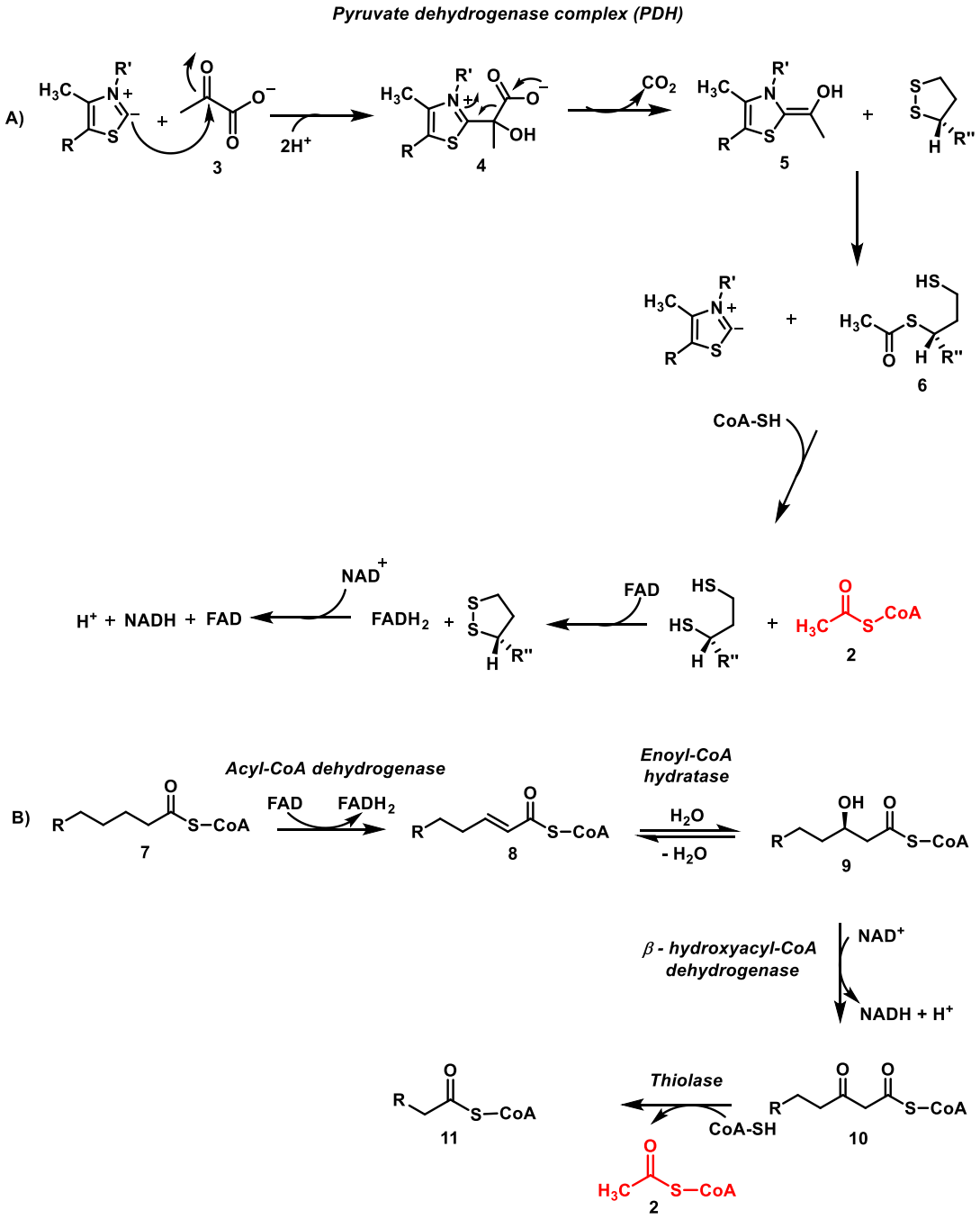

Scheme 1.1. Two biosynthetic pathways to acetyl-CoA: A) Oxidation of pyruvate and B*)* *β*-oxidation of fatty acids.[4]

Acetyl-CoA is also obtained by *β*-oxidation, degradation of fatty acids. The catabolic process involves four steps. Fatty acyl-CoA **7** undergoes a dehydrogenation forming an *α,β*-unsaturated bond to form *trans*- Δ^2- enoyl-CoA **8** catalysed by acyl-CoA dehydrogenase. The second step mediated by enoyl-CoA hydratase, involves the hydration of the double bond to form *β*-hydroxyacyl-CoA **9** that undergoes oxidation to generate *β*-ketoacyl-CoA **10**, catalysed by *β*-hydroxyacyl-CoA dehydrogenase. The forth

step involves a thiolysis mediated by thiolase where *β*-ketoacyl-CoA **10** is broken down into acetyl-CoA **2**.[4]

Acetyl-CoA is central in cholesterol synthesis and ketogenesis. Ketone bodies (acetoacetate **14**, β-hydroxybutyrate **16**, acetone **15**) are produced in the mitochondria during fasting or triggered by low blood sugar. Both metabolic pathways have the first two steps in common. The first is mediated by thiolase and involves the conversion of two molecules of acetyl-CoA to generate acetoacetyl-CoA **12**. This is then converted to β-hydroxy-β-methylglutaryl-CoA (HMG-CoA) **13** by condensation with an other acetyl-CoA, in a reaction mediated by HMG-CoA synthase.

Ketone bodies are synthesised by HMG-CoA lyase conversion of HMG-CoA **13** to form acetoacetate **14**, the first ketone body generated. This can undergo a decarboxylation to generate acetone **15** or a reduction to yield β-hydroxybutyrate **16**. β-Hydroxybutyrate **16** and acetoacetate **14** are released into circulation, the ratio depends on the amount of NADH accumulated in the liver mitochondria whereas acetone **15** is excreted *via* lungs as a volatile waste (Scheme 1.2).[6]

Cholesterol **24** is a steroid that modulates the fluidity of animal cell membranes and is the precursor of many steroid hormones such as progesterone, testosterone, estradiol, cortisol and bile acids production. Its synthesis takes place in the cytosol.

The key step for the synthesis of cholesterol **24** is the irreversible conversion of HMG-CoA **13** to mevalonate **18** mediated by HMG-CoA reductase. Mevalonate **18** is progressed to two isoprene units: isopentenyl-pyrophosphate (PP) **20** and dimethylallyl-pyrophosphate (PP) **21**. These engage in head to tail condensation reactions to give farnesyl-PP **22**. Condensation of two farnesyl-PP **22** gives squalene **23** which undergoes a series of reactions to form cholesterol **24**. [5]

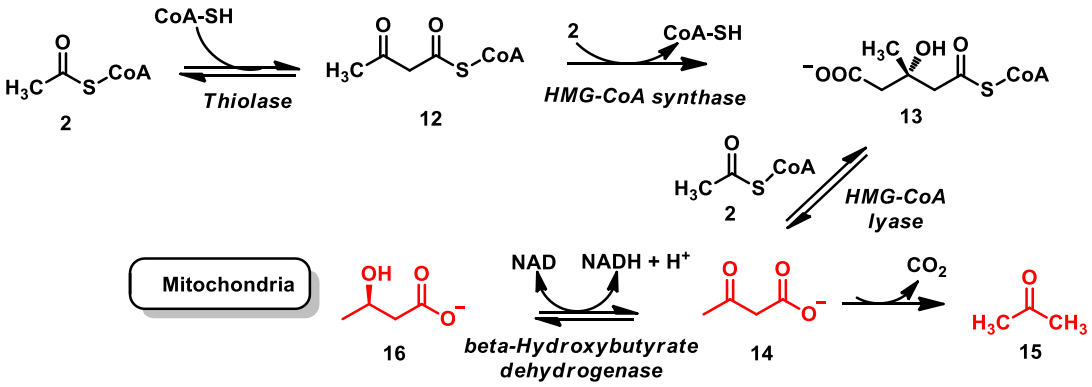

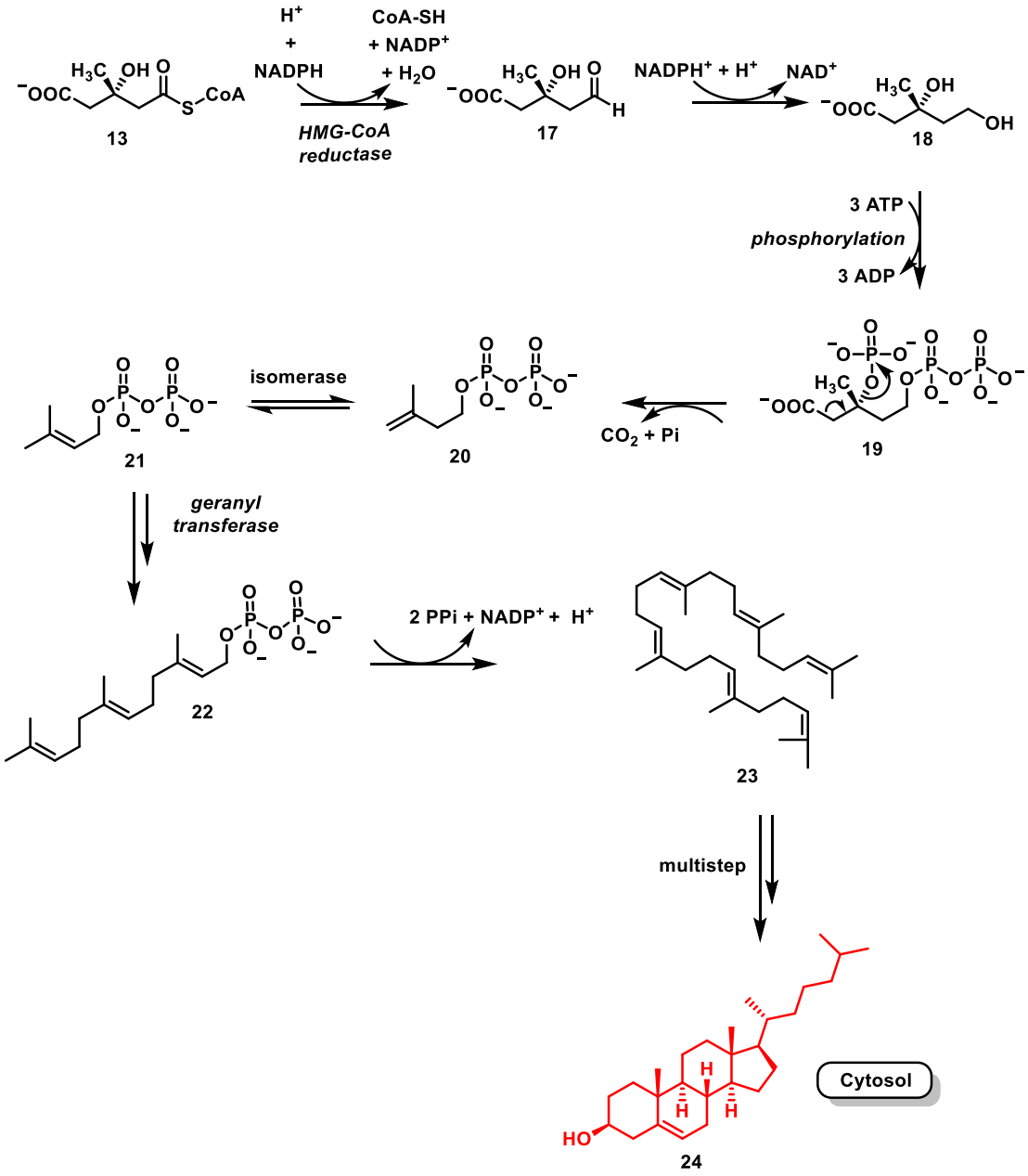

Scheme 1.2. The metabolic pathways to ketone bodies and cholesterol.[4–6]

Acetyl-CoA **2** is also a key metabolite that links metabolism with cell signaling, chromatin structure, and transcription. It can be transferred by N-acetyltransferases (NATs) to arylamines, such as the aromatic amines serotonin **26** which is a neurotransmitter. Serotonin **25** is intermediate in the biosynthesis of melatonin **27** mediated by N-acetylserotonin O-methyltransferase (AANAT), thus it is involved in the regulation of the body circadian's rhythm.

Histone acetyltransferases (HATs) affects N-terminal acetylation of some human proteins, influencing their stability, localization and function. HATs are enzymes that

mediate the acetylation reaction of lysines on histone proteins, key components of chromosomes. Acetylation of the lysine residue **28** decreases the affinity of the entire histone complex for DNA, exposing other areas of DNA to the transcription machinery. Deacetylation processes catalyzed by histone deacetylase enzymes (HDAC), play a key role in the repression of the transcription. Balancing the acetylation and deacetylation of histones is central for the control of gene transcription. Such imbalances seem to be associated with Huntington diseases (HD). The mutation of the Huntington protein has been observed to interact with HATs and HDAC enzymes deactivating them and consequently disrupting DNA transcription (Scheme 1.3).[7]

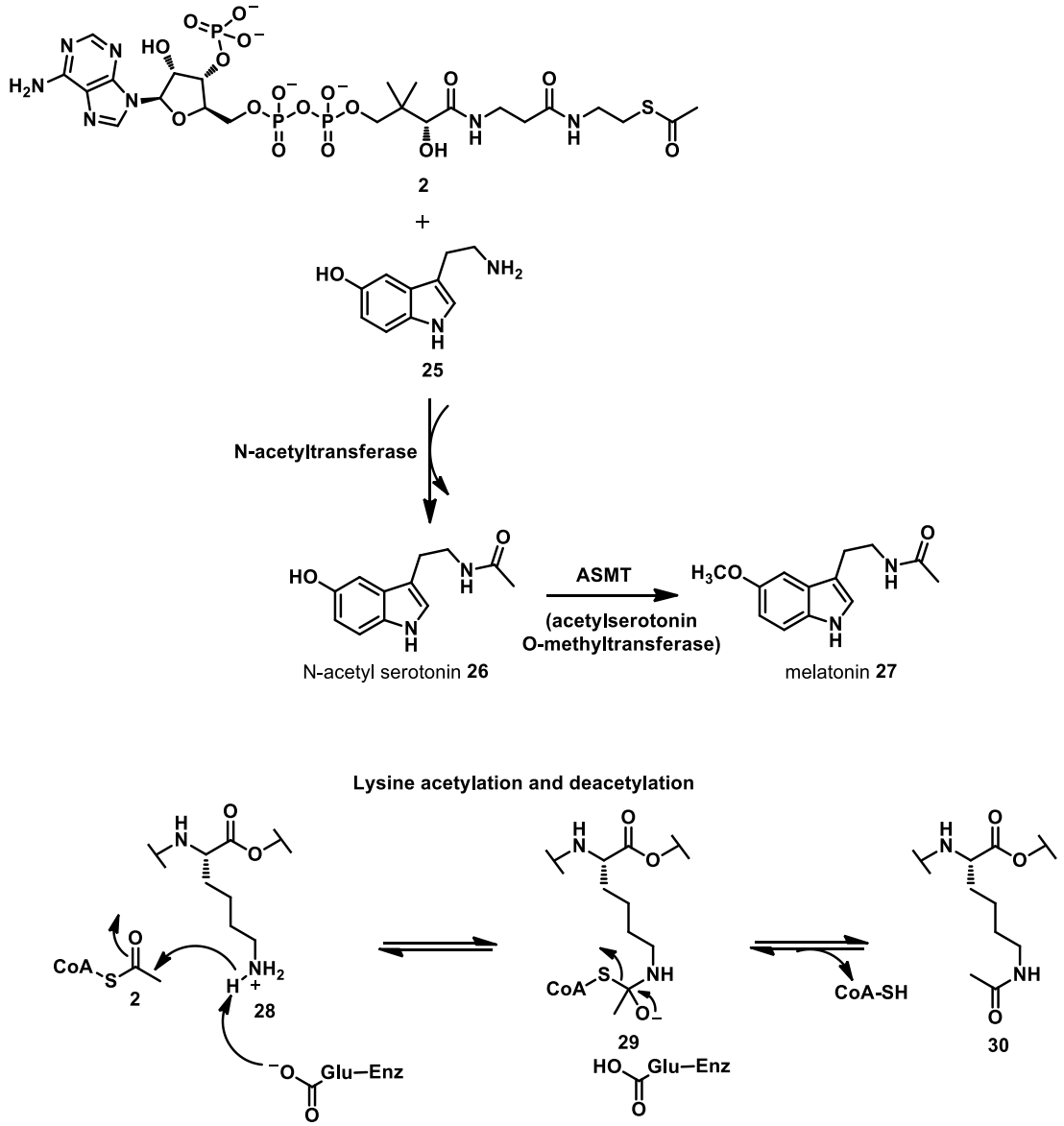

Scheme 1.3. N-Acetyl transferase mediated acetyl group transfer reaction.[7]

1.3. Fatty acid synthesis

Acetyl-CoA **2** is a starter unit in the chain elongation process of fatty acid biosynthesis. The first step in fatty acid assembly involves an irreversible carboxylation of acetyl-CoA **2**, through its enolate form **31**, to malonyl-CoA **33** with biotin that acts as CO_2 carrier in **32**. Malonyl-CoA is then transferred onto the fatty acid synthase (FAS) by acyl carrier protein (ACP), which effects a first transacylation from malonyl-CoA **33** to malonyl-ACP **34**. In turn, the malonyl unit is loaded onto the FAS complex for a series of decarboxylative condensations, reductions, dehydrations and reductions, extending the C-C backbone for the production of long-chain fatty acids.[8,9] The mechanism is described in detail in Chapter 3.

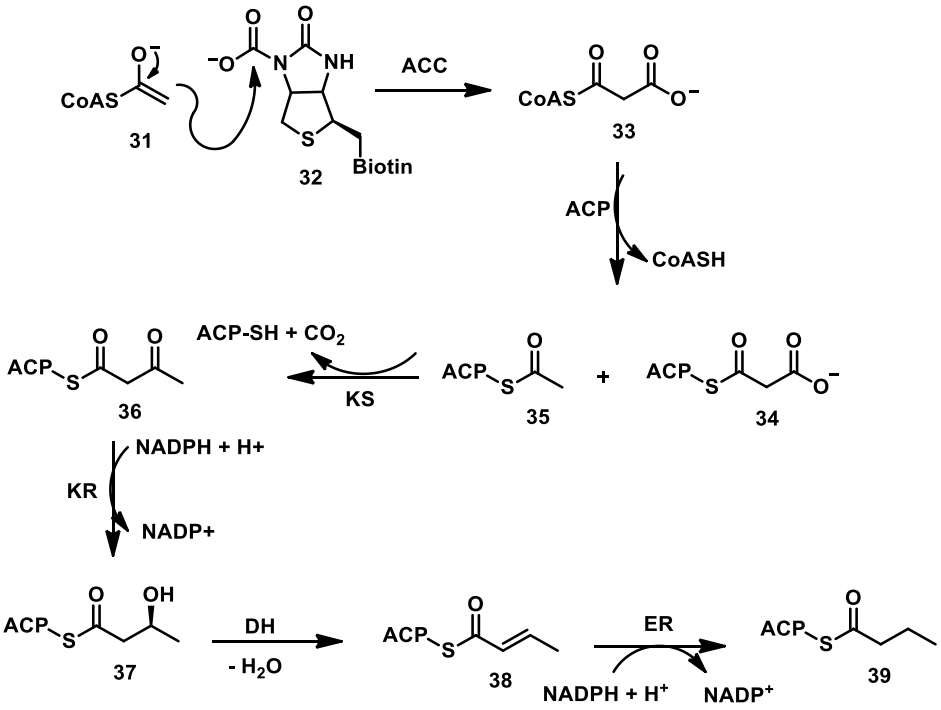

Scheme 1.4. Summary of fatty acid biosynthesis.[8,9]

1.4. Polyketide Biosynthesis

Polyketide synthases (PKS) are a family of multi-domain enzyme complexes present in bacteria, fungi, plants and a few animal families.

PKS exhibit Type-I, Type-II organizations as well as Type III which lacks the ACP domain. Similar to the FAS enzymes, the introduction of acetyl-CoA **2** (starter unit) or its analogues into the polyketide chain proceeds *via* malonyl-CoA and then a decarboxylative Claisen with the ACP thioester of the developing fatty acid chain, adding a two carbon unit with each cycle. PKS are an important source of common antibiotics such as tetracyclines **44**, a family of antibiotics that exert antibacterial activity. They inhibit the synthesis of proteins by binding to the ribosome of bacteria, thus disabling the binding of aminoacyl-tRNA to the mRNA ribosome complex. An other useful antibiotic is Lovastatin **45**, a fungal metabolite shown to target HMG-CoA reductase and therefore used to reduce cholesterol **24** levels and generally the risks associated in acquiring cardiovascular diseases (Scheme 1.5).[10,11]

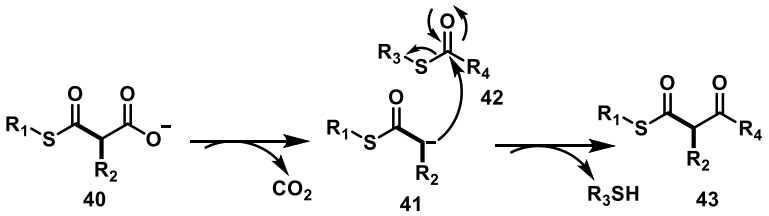

Type I PKSs:

R_1= ACP
R_2= H, CH_3, CH_3CH_2, CH_2CH_2Cl OH, OCH_3, NH_2
R_3= KS
R_4= CH_2R

Type II PKSs:

R_1= ACP
R_2= H
R_3= KS
R_4= CH_2R

Type III PKSs:

R_1= CoA
R_2= H, CH_3, CH_3CH_2
R_3= PKS
R_4= CH_2R

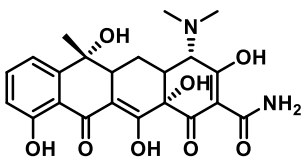

Tetracycline **44**

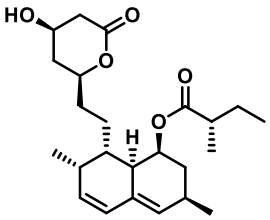

lovastatin **45**

Scheme 1.5. Polyketides synthesis.[10,11]

1.5. The role and impact of fluorine substitution in bio-organic chemistry

Given that fluorinated compounds are rare in nature, it is interesting that 20-25% of marketed pharmaceuticals have at least one fluorine atom. Fluorine displays some advantageous properties, it has the highest electronegativity (3.98) and electron affinity (3.448 eV) of all the elements as it is the first element with *p* orbitals to achieve a noble gas configuration with the uptake of one electron. Its atomic radius is the smallest along the Period 2 elements; this contraction is due to its high nuclear charge and consequently fluorine is not polarisable as the 2p electrons are held closely to the nucleus. Due to fluorine high electronegativity, the C-F bond is highly polarised and its strength can be associated with an ionic more than a covalent nature of the bond with the electronic density significantly located on fluorine. This makes it highly polarisable, short and one of the strongest bond in organic chemistry compared to other common bonds (Table 1.1).[12]

Bond	**Bond dissociation energy (Kcal/mol)**
C-F	105.4
C-H	98.8
C-C	84.0
C-O	83.1
C-Cl	78.5
C-N	69.7

Table 1.1. The bond dissociation energy of the most common C-X bonds in organic chemistry.[12]

The incorporation of a small and highly electronegative atom such as fluorine into a therapeutic or diagnostic molecule can enhance pharmacokinetic and pharmacodynamic properties such as metabolic stability, membrane permeability as well as increasing the binding affinity towards specific macromolecular target proteins.[13,14]

1.6. pKa modulation by introduction of fluorine

Fluorine substitution can affect the basicity or acidity of nearby functional groups. Van Niel *et al.*[15] investigated how the incorporation of fluorine into basic molecules decreases their pKa. They prepared a series of 4-fluoropiperidines and 3-fluoro-4-aminopiperidines as analogues of propyl piperidine derivatives as a class of $5HT_{1D}$ receptor ligands such as Sumatriptan **46**. Propyl-piperazine **49** is rapidly absorbed and orally bioavailable compared to compound **47** which lacks these properties. Molecular modelling showed that piperazine **49** could be replaced by a 4-fluoropiperidine as in **48** having a similar electron density distribution. The introduction of fluorine lowers the pKa of the amine affecting oral absorption, whereas, the effect on oral bioavailability cannot always be accurately anticipated.[15,16]

Methotrexate **50** is a potent antifolate widely used for the treatment of diverse forms of cancer, and for rheumatoid arthritis. Methotrexate **50** inhibits dihydrofolate reductase, an enzyme that reduces di-hydrofolic acid to tetra-hydrofolic acid and it is activated intracellularly to generate polyglutamate derivatives by addition of glutamic acid residues mediated by polyglutamate synthase.

The polyglutamation of methotrexate **50** increases its retention intracellularly, thus enhancing its inhibitory effect as an antifolate. One of the major side effects of an excessive dosage of this potent antimetabolite is an elevated cytotoxicity. Fluoro methotrexane **51** was found to be less toxic than methotrexane **50**. The lower toxicity of **51** may be correlated to an increased acidity of the *γ*-carboxyl group, blocking the poly-glutamination process (Figure 1.3).[15,17]

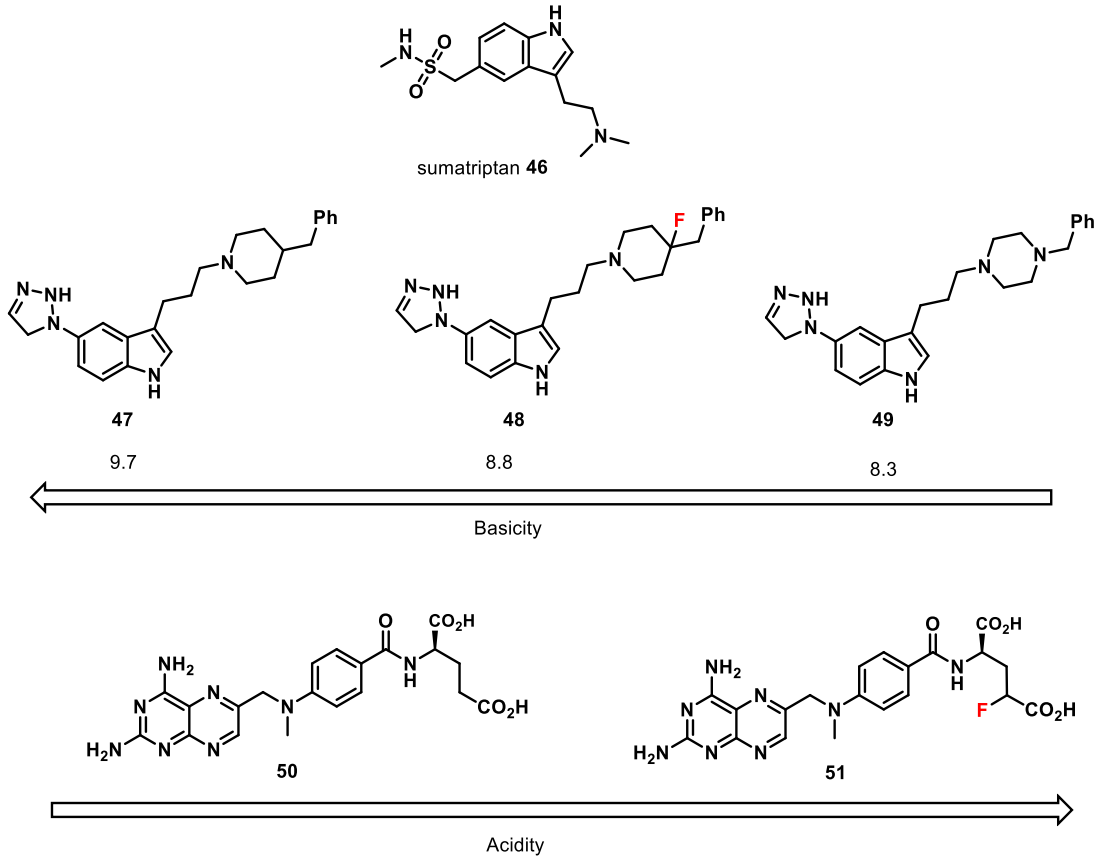

Figure 1.3. Fluorine substitution to tune the pKa.[15–17]

1.7. *Change of the lipophilicity profile with fluorine incorporation in drug design.*

Generally, incorporation of fluorine modulates lipophilicity, a parameter in medicinal chemistry that influences the absorption and distribution of a drug. The lipophilicity is measured as the octanol/water partition coefficient P (logP), quantifying the ability of a molecule to pass through a lipidic membrane. High logP values are representative of strong lipophilicity and high hydrophobicity. It is frequently stated that in the case of aromatic substituents, the replacement of ring hydrogen atoms by fluorine or fluoroalkyl groups such as CF_3, CF_3O and CF_3S enhances lipophilicity. Böhm *et al.*[18] investigated the effect of replacing hydrogen with fluorine for 293 compounds selected from the Roche database and reported the results on a Gaussian distribution curve. They concluded that fluorine introduction on aromatics led to an increase of lipophilicity by 0.25 logP units. Conversely, mono-, di-, and tri- fluorination of saturated alkyl substituents usually decreases lipophilicity due to the relative polarity of the corresponding fluoroalkanes and their associated dipoles (Figure 1.4A). For fluorinated compounds containing heteroatoms, the modulation of the lipophilicity is related to the distance between fluorine and the heteroatom, and a decrease in logP (not shown) is recorded when fluorine is at least three C-C bonds away from the heteroatom (Figure 1.4B).[18]

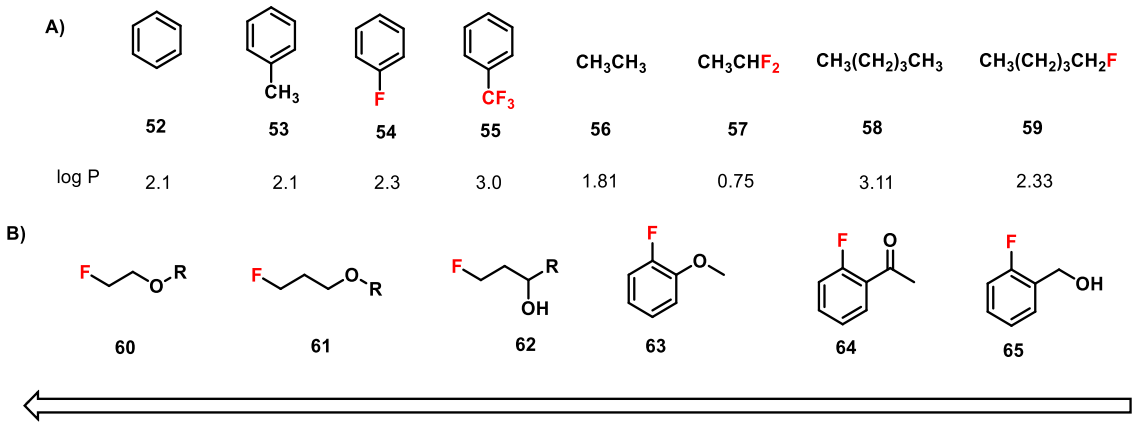

Figure 1.4. Lipophilicity modulation with the incorporation of fluorine into chemical compounds.[18,19]

1.8. Fluorine influences conformation

The high polarisation of the C-F bond indicates that it reacts preferentially through electrostatic interactions (dipole-dipole, charge-dipole) and its incorporation into molecules can impact their conformation. It has been observed that 1,2-difluoroethane **66** possesses a more stable *gauche* relative to *anti* conformation by 2.4 to 3.4 Kj/mol. This preference is related to the hyper-conjugative effect. This suggests that the donation of electron density from the σ-bonding orbital of a vicinal C-H bond to the parallel σ^*-anti-bonding orbital of the C-F bond, is regarded as the source of stabilisation. For the *gauche* isomer **66**, the C-F bond (σ*-acceptor) is anti-periplanar to the C-H bond (σ-donor), offering maximum overlap.[19,20]

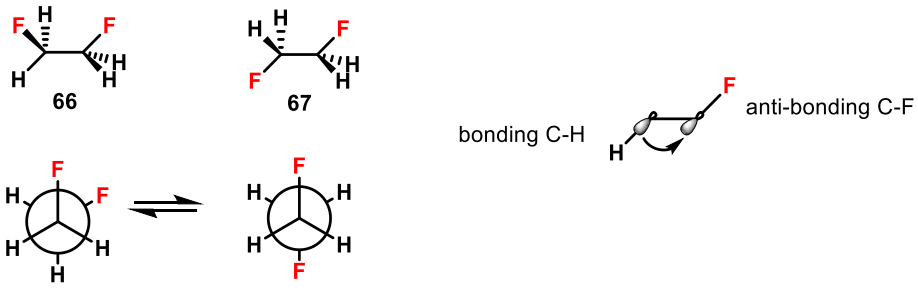

Figure 1.5. *Gauche* effect and hyperconjugation.[19,20]

The conformational effects of the C-F bond are highlighted in compound **68** and **69**. They are inhibitors of the cholesteryl ester transfer protein and thus are good candidates for the treatment of coronary heart disease. Compound **69** binds more efficiently to the target protein, due to sp^3 hybridisation of the ether oxygen allowing electron density donation from its two lone pairs to the two σ* CF antibonding orbitals. Thus, the fluorinated side chain CF_2CF_2H in **69** adopts an orthogonal rather than a planar conformation which is related to the fluorine-oxygen interaction being more predominant than that between the ether oxygen and the aromatic ring (Figure 1.6).[21]

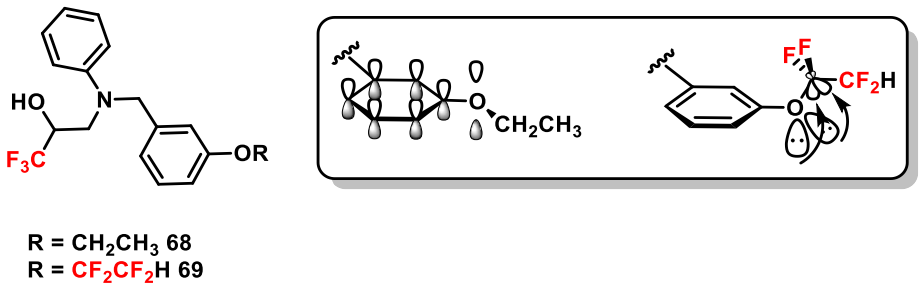

R = CH_2CH_3 68
R = CF_2CF_2H 69

Figure 1.6. Cholesteryl ester transfer protein inhibitors **68** and **69**.[21]

Diastereoisomers **71** and **72** are analogues of HIV protease Indinavir **70**, developed by Merck. Compound **71** shows a comparable affinity to Indinavir for the protein, whereas **72** has a much lower inhibitory potency than **71**. This is related to the F-C-C-OH *gauche* effect which in the case of **72**, destabilises the bioactive chain conformation decreasing its affinity to the enzyme (Figure 1.7).[21]

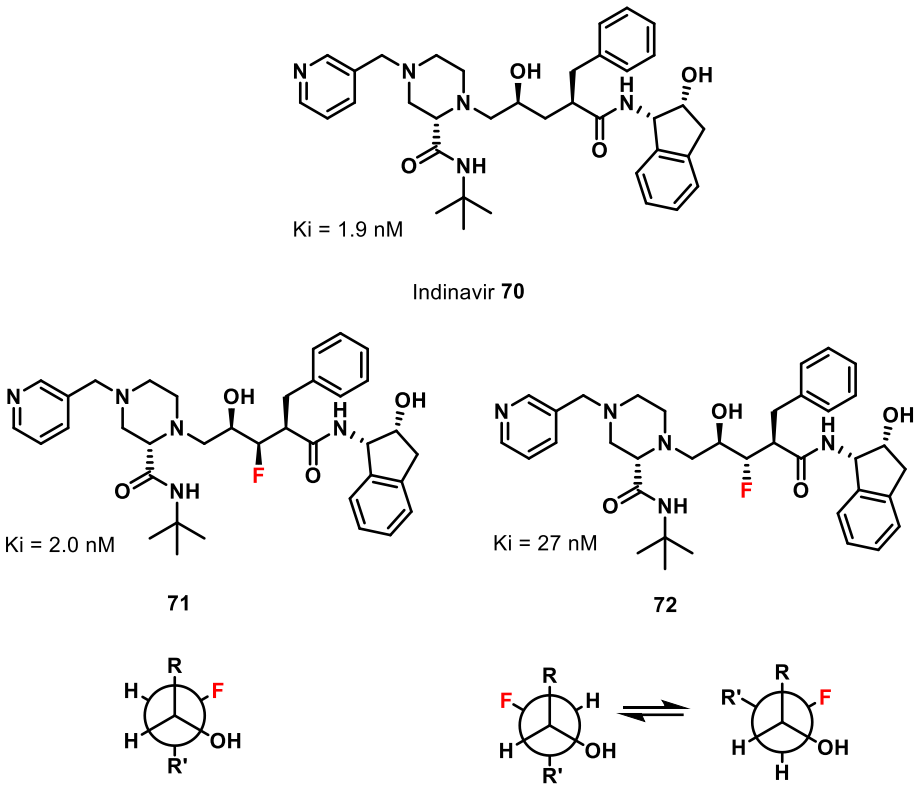

Figure 1.7. The *Gauche* effect on the conformation of HIV protease inhibitors **71** and **72**.[21]

1.9. The fluorine metabolism block effects

The bioavailability of pharmaceuticals can be improved by introducing fluorine into their metabolically labile sites. The C-F bond is less susceptible to metabolic attack than other bonds, thus its incorporation in the metabolic site or at an adjacent one can prevent undesired metabolic transformations from happening. This is the case of Ezitimibe **73** which was developed as analogue of SCH 48461 **74**, a potent cholesterol adsorption ihibitor. In **73**, fluorine is introduced as a replacement for hydrogen and methoxide that are subject to metabolic hydroxylation and demethylation respectively (**74**). Compound **73** was found to be more metabolically stable and a more potent inhibitor than **74**.[22]

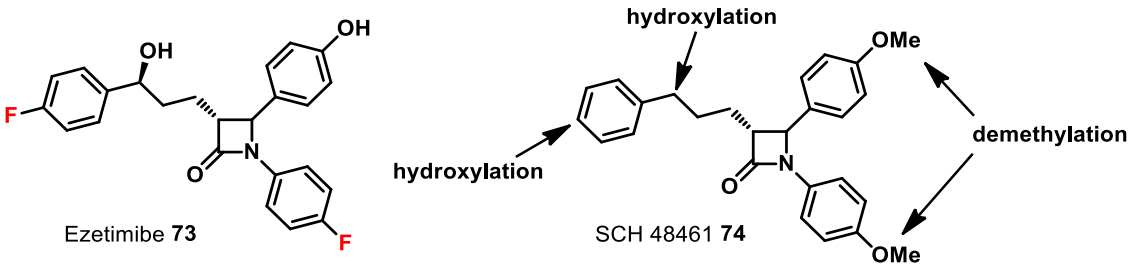

Figure 1.8. Introducing fluorine as metabolic blocker in drug candidates

1.10. Fluorine in natural organic compounds

Although fluorine is the 13th most abundant element in the Earth crust, fluorine containing natural products are extremely rare.

The most widely distributed is sodium fluoroacetate **78**, produced by a large number of Australian, Brazilian and African plants. Fluoroacetate **78** is responsible for their toxic properties. It was identified in 1943 by Marais in South Africa from the shrub *Cymosum*. In 1986, the soil bacterium *Streptomyces cattleya* was shown to be able to produce fluoroacetate **78** and the antibiotic 4-fluorothreonine **75** when grown in the presence of fluoride ion. The enzyme which catalyses the enzymatic C-F bond formation, was isolated in 2002 and was informally named "fluorinase".[13,23]Fluorinase has subsequently had applications as a catalyst for PET radiosynthesis forming the C -^{18}F bond from aqueous [^{18}F] fluoride probe.[24]

Fluoroacetate **78**, as analogue of acetyl-CoA **2**, exerts its toxicity upon conversion to fluoroacetyl-CoA **76** and then conversion to F-citrate by citrate synthase. F-citrate binds strongly to the enzyme aconitase interrupting the citric acid cycle.

Nucleocidin **81** is a fluorine containing antibiotic which was isolated in 1957 from the bacterium *Streptomyces calvus*. It possesses a fairly broad antibiotic spectrum, but it was never approved for clinical use due to its high toxicity in mammals. The presence of fluorine in the molecule was established 12 years after its discovery by Morton *et al.*[25] in 1969 and was regarded as very surprising since no apparent fluoride source was added to the culture medium. Unfortunately attempts to re-isolate the antibiotic from *S. calvus* were unsuccessful for many years until recently.[26]

Fluoroacetone **80** which is highly toxic, has been suggested to be the metabolite of *Acacia georginae* but the metabolite was never properly identified and characterised.

ω-Fluorooelic acid and ω-fluoropalmitic acid **77** were isolated and identified by Peters and coworkers in 1959 from the seed of *West African shrub D. toxicarium*. For the synthesis of *ω*-fluoro fatty acids, fluoroacetyl-CoA replaces acetyl-CoA in the fatty acid biosynthesis.[20] The toxicity of *ω*-fluoro fatty acids are related to their conversion to fluoro acetate. An other fluorometabolite, named (2R3S4S)-5-fluoro-2,3,4-trihydroxypentanoic acid (5-FHPA) **79**, was discovered and identified from soil bacterium *Streptomyces sp.MA37* at the University of Saint Andrews (Figure 1.9).[27] Genomic analysis led to the identification of a gene cluster, enconding a biosynthetic pathway for 5-FHPA.

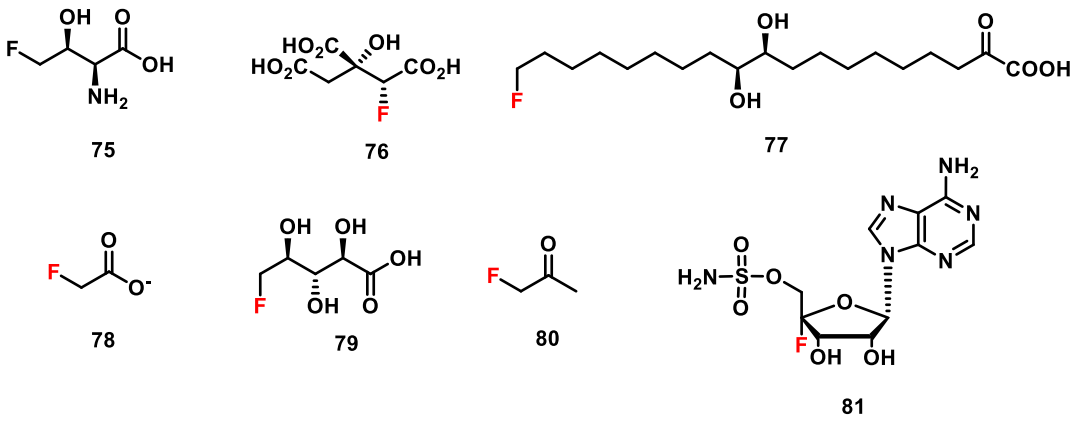

Figure 1.9. Fluorinated natural compounds.[13,23–27]

1.11. General applications of organofluorine compounds

Fluorinated organic compounds find application in different fields ranging from pharmaceutical, polymers to electronic devices manufacturing. Polytretrafluoroethylene (PTFE) **82** was discovered by Plunkett in 1936. It is one of the most common fluoropolymers, chemically and thermally stable. It has been used in the fabrication of anti-stick frying pans and Goretex garments (low molecular weight PTFE). A second generation of fluoropolymers were synthetised from PTFE copolymerisation with trifluoro vinyl ether such as heptafluoropropyl trifluorovinyl ether PPVE **83**. These polymers combine the unique PTFE properties (chemical, thermal stability, elasticity) and are more chemically accessible than PTFE.

Fluorinated compounds have been successfully used in the design of liquid crystals due to the small size and high polarity of fluorine. The C-F incorporation enhances the liquid crystal stability without altering its characteristic ordered structure and improving important phisycal properties such as optical, dielectric and viscoelastic properties. The number and the position of fluorinated groups can affect the liquid crystal phase sequence and can impact its transition temperatures. Figure 1.10 shows the most common “super-fluorinated” materials (SFM) used for the design of LCD technology. They contain fluorinated aliphatic bridges as link of their mesogenic structures, enhancing some of the material properties such as the temperature and nematic phase range and reducing the rotational viscosity. Fluorine containing compounds find also application in the agrochemical industry as herbicides, fungicides and inceticides. Norflurazon **86** is a carotenoid inhibitor whose function is to block the photosynthesis process of plants. Primsulfuron **87** belongs to the class of herbicides and contain sulfonylureas wich are inihbitors of acetolactate synthase (ALS). It is commonly used in the planting of maize. Flutolanil **88** is a trifluoro methyl benzamide derivative and is used as fungicide on rice, cereal and vegetables. Fluorinated benzoylureas such as diflubenzuron **89** and teflubenzuron **90** are known inseticides and inhibit chitin biosynthesis, interfering in the moulting process (Figure 1.10).[21]

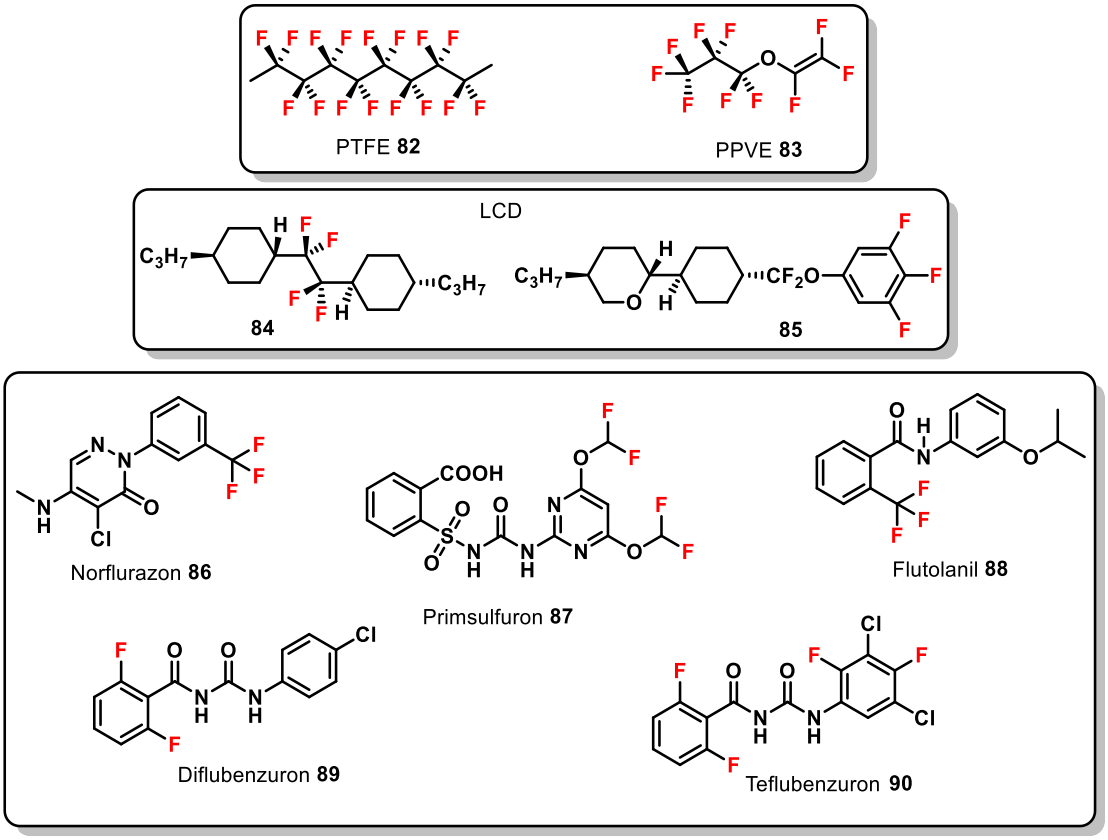

Figure 1.10. The versatility of organofluorine compounds.[21]

1.12. Fluorine in the design and application of bioisosteres: drug design and enzymatic inhibition

The concept of an isostere was introduced by Irving Langmuir in 1919 and defines atoms or group of atoms having similar physical and chemical properties. The bioisostere concept fits the broadest definition for isosteres but the mimetic also exhibits a similar biological activity. They find application in medicinal chemistry for the design of new drugs as the bio-isosteric replacement can modulate the pharmacokinetic properties of a certain molecular target.

The electronic properties and small size of fluorine make it a versatile bioisostere of different functional groups or atoms. It has been found to be a good substitute for the hydrogen atom and the methyl group in certain circumstances, also a suitable functional mimetic of the carbonyl group, hydroxyl and amide moiety, when appropriately incorporated. As previously discussed, fluorine incorporation into drugs can influence many properties such as the potency, conformation, metabolism and membrane permeability (Table 1.2).[15,18,28]

Element	Electronegativity	Bond lenght	Van der Waals Radius (Å)	Bond energy (Kcal/mol)
H	2.1	1.09	1.20	99
F	4.0	1.39	1.35	116
O (OH)	3.5	1.43	1.40	85

Table 1.2. Physical properties of fluorine.[15,18,28]

1.13. Fluorine as hydrogen bioisostere

The replacement of hydrogen with fluorine has been extensively explored in drug design, usually replacing hydrogen atoms bound to aromatic rings or those on alkyl chains. This substitution can lead to minor steric perturbations of the molecular functionality but has consequences on the physical-chemical and biological properties of a compound.
5-Fluorouracil **92**, as a mimic of uracil **91**, was one of the first fluorinated antitumor drugs when it was reported in 1957.

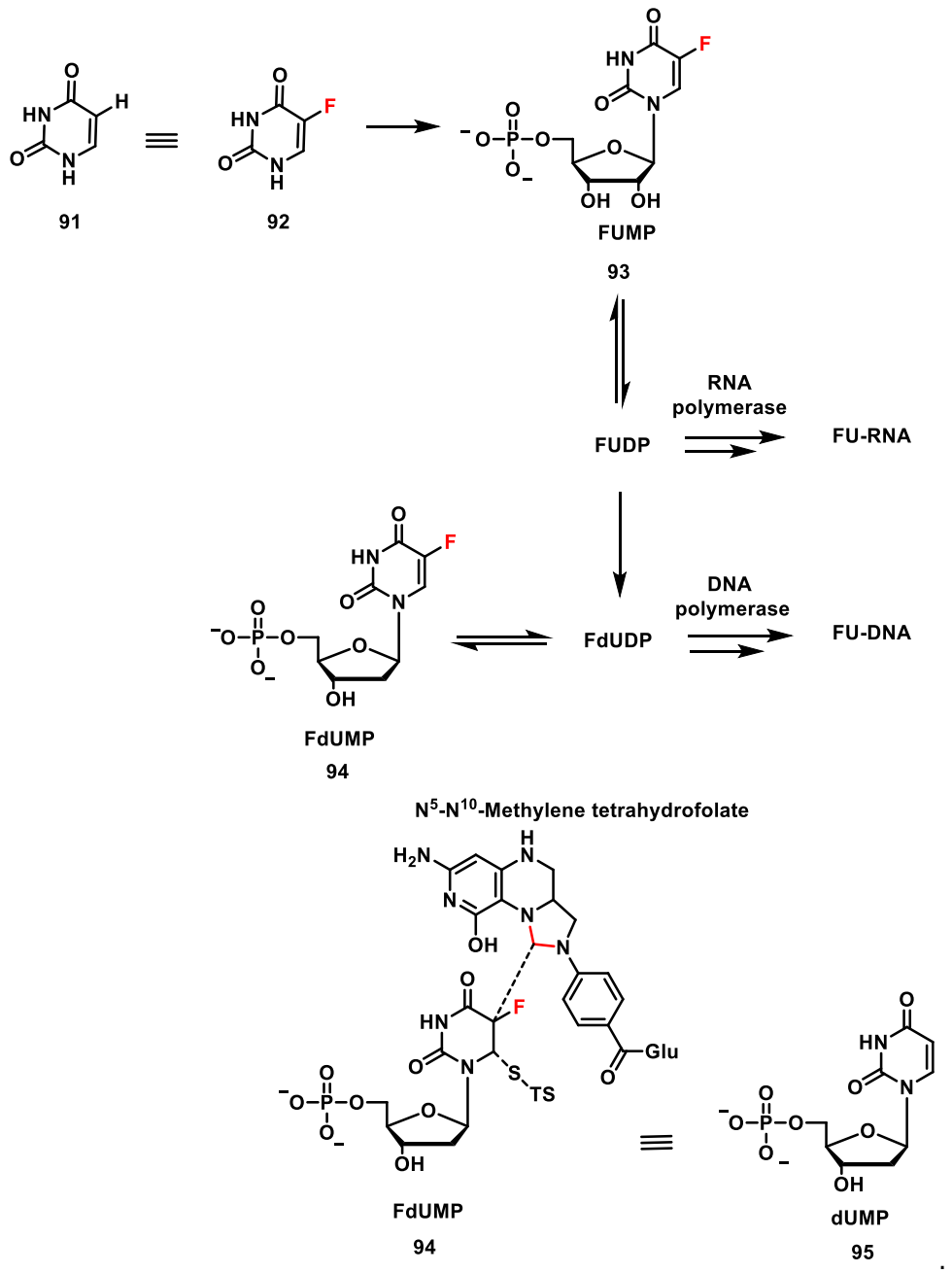

Scheme 1.6. 5-fluorouracil **92** as inhibitor of TS (thymidylate synthase).[29,30]

Nucleotide **94** was found to be a potent inhibitor of thymidylate synthase (TS), the enzyme that mediates the conversion of 2-deoxyuridine-5-monophosphate (dUMP) into 2-deoxythimidine-5-monophosphate (dTMP), a nucleoside required for DNA replication. Upon accessing the cell, the fluorinated compound is converted to a variety of active metabolites, one of which is FdUMP (fluoro-deoxyuridine monophosphate) **94** that inhibits thymidylate synthase with a *K*i 1000-fold lower than the Michaelis-Menten constant (Km) for dUMP (2 μM). Thus, the replacement of the hydrogen *α* C-5 with fluorine inhibits TS by a mechanism based inhibition process (Scheme 1.6). [29,30]

One of the first synthetic pathways to 5-fluorouracil **91** reported involved the use of fluoroacetic acid **78** in a reaction with propanoic acid **96** via addition-elimination to generate fluoroacrylate **97**. A Diels-Alder [4+2] cycloaddition generated **99** that under acidic conditions leads to **91**. Uracil **91** reacts with fluoroxy-trifluoro methane or fluoride (F_2) to give 5-fluorouracil **92** (Scheme1.7A). For industrial scale production of fluorouracil, the synthetic procedure involves the direct fluorination of uracil **91** with nitrogen diluted fluorine gas (N_2/F_2 mixture) in water, followed by dehydration of the intermediate fluorohydrin **100** (Scheme 1.7B).[31]

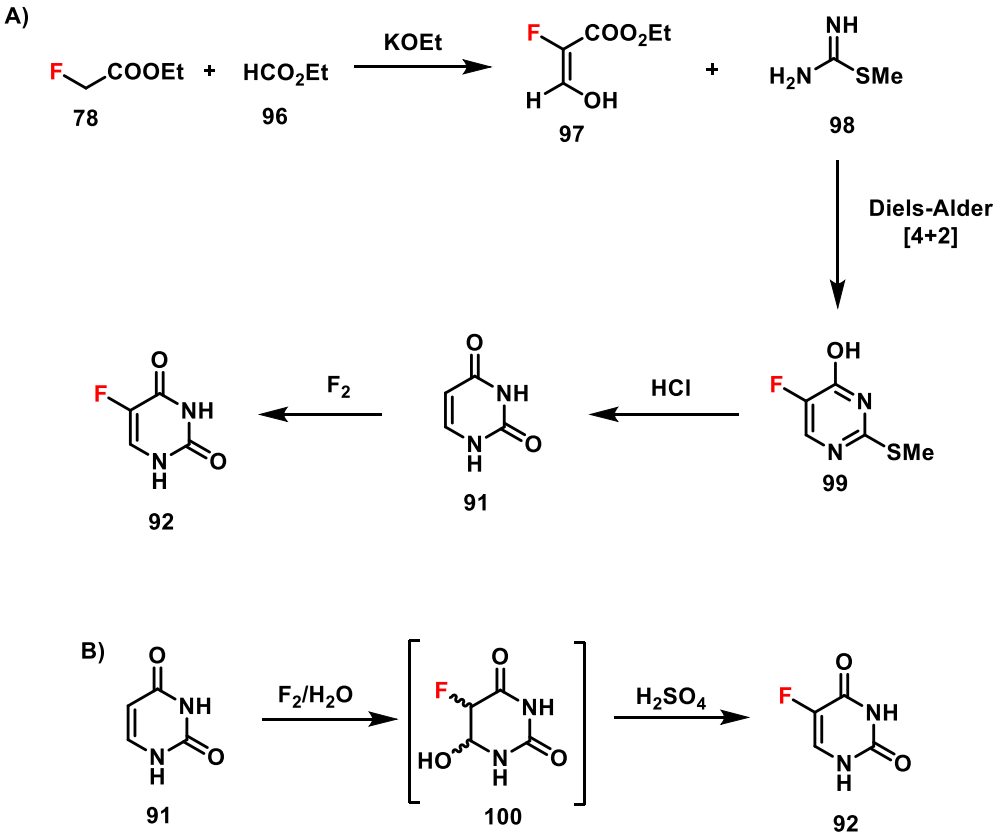

Scheme 1.7. Synthetic routes to 5-fluoro uracil.[31]

Carbonic anhydrase (CAII) is a zinc metalloenzyme that catalyses the converting carbon dioxide to bicarbonate. CAII inhibitors have had a significative impact in ophthalmology, since inhibition lowers the intraocular pressure, which is found elevated in patients suffering with glaucoma. One of the most potent inhibitor of CAII is 4-(aminosulfonyl)-*N*-phenylmethylbenzamide (SBB) **101** with a *K*i of 2.1 nM (Figure 1.11). Kim *et al.*[32] demonstrated that the introduction of fluorine into an aromatic ring of SBB **102** and **103**, improved the enzyme-inhibitor binding affinity, enhancing polar interactions with Pro-202 and Phe-131. The X-ray crystal structures of carbonic anhydrase (CAII) with inhibitors **102** and **103** reveals a significant contribution from the fluoroaromatic ring of each inhibitor that moves closer to the Phe-131 residue with increasing fluorination, and enhancing binding affinity.[32,33]

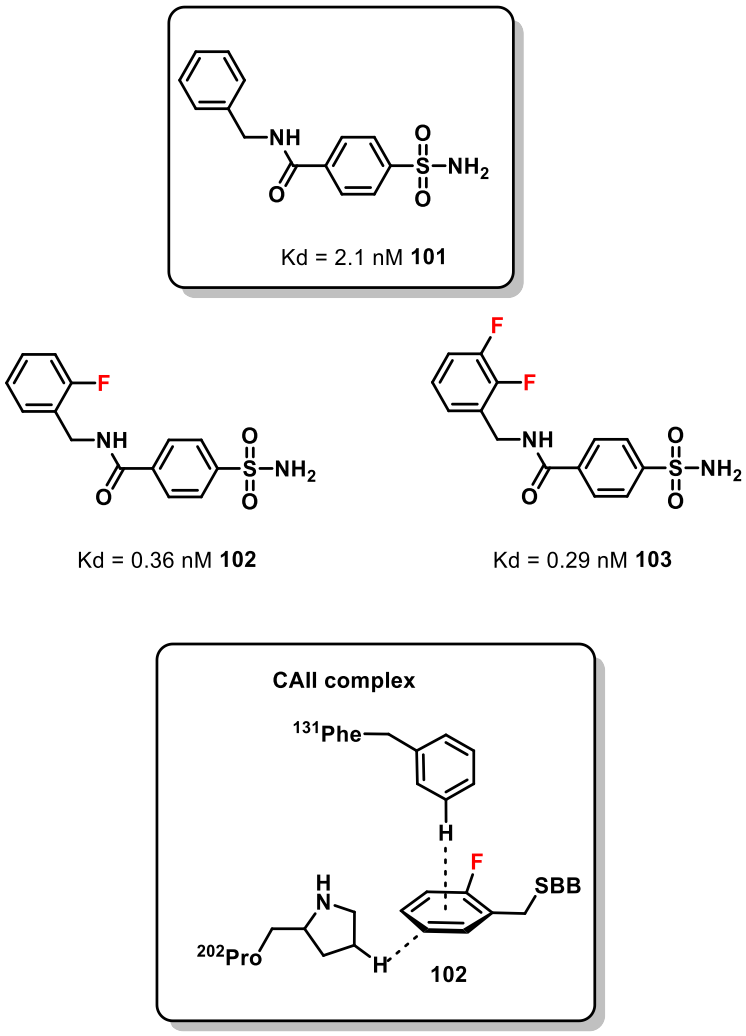

Figure 1.11. Modulation of the binding affinity of the enzyme-inhibitor complex by fluorination of SBB inhibitor of carbonic anhydrase.[32,33]

Fluoroquinolone derivates were found to be specific inhibitors of DNA gyrase which is a bacterial type of topoisomerase II. Topoisomerase II unwinds DNA supercoiling during cell replication and transcription. The inhibition of DNA gyrase leads to the death of the bacterial cell making it an attractive target for antibacterial agents. Nalidixic acid **110** is a quinolone derivative and a potent inhibitor of DNA replication. It was discovered as a by-product in the synthesis of chloroquinone, used for malaria treatment.

Norfloxacin **109** inhibits DNA gyrase with a Ki 60-fold greater than nalidixic acid **110**. Hence, the introduction of fluorine at the 6-position of the aromatic ring in **109** improves both binding affinity and the ability of these drugs to penetrate the bacterial cell. Norfloxacin **109** bears a piperazine substituent at C7 which also contributes to the overall improvement of the pharmacokinetic profile of the drug (Scheme 1.8).[33]

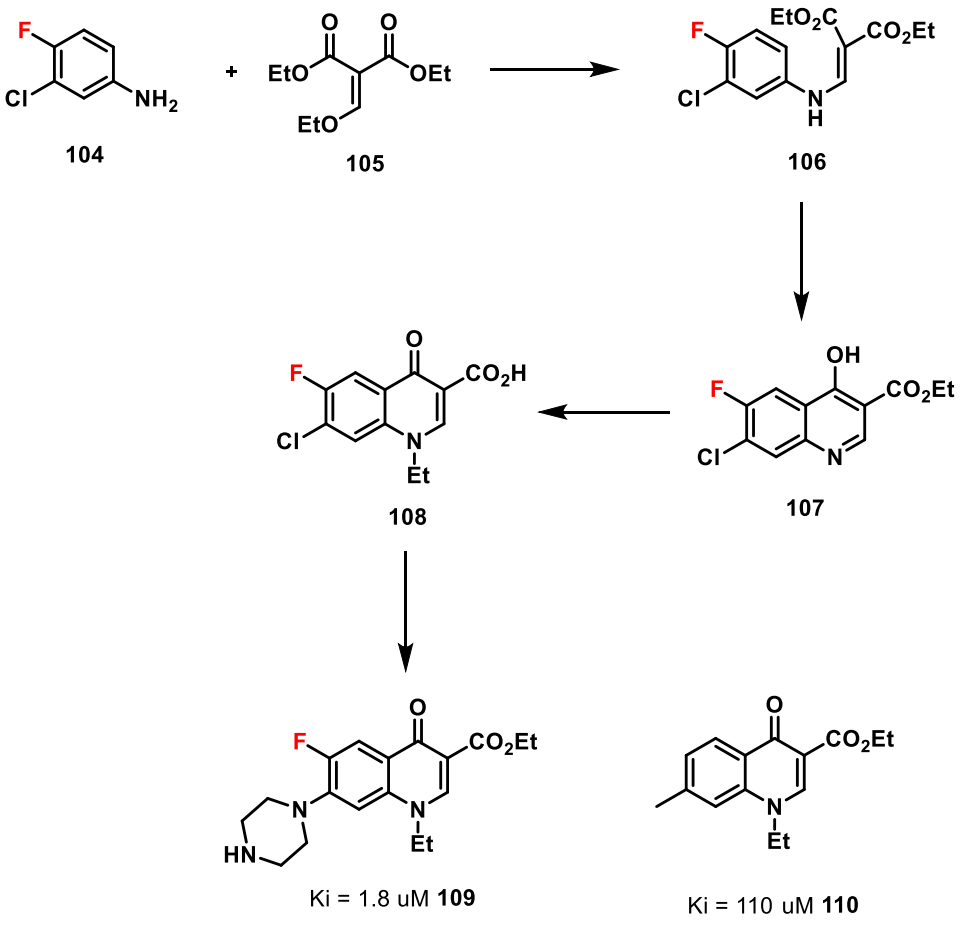

Scheme 1.8. DNA gyrase inhibitor binding affinity enhanced by fluorine incorporation.[33,34]

Examples of methyl group-fluorine replacement providing positive effects on metabolism, are represented by taxoids derivatives **111** and **112**. These compounds were designed to overcome susceptibility to multidrug resistance and the lack of tumor specificity that characterises the common chemotherapeutic agents such as paclitaxel **113**. The iso-butenyl groups in **112** are subject to P450 oxidation affecting their metabolic stability. The replacement of the two allylic methyl substituents in **112** with fluorine (**111**) improved the metabolic stability suppressing oxidation. A series of difluorovinyl taxoids were synthesised by Ojima-Houlton coupling of the enantiopure lactam and various baccatins bearing different substituents at C10 and/or C2.[33]

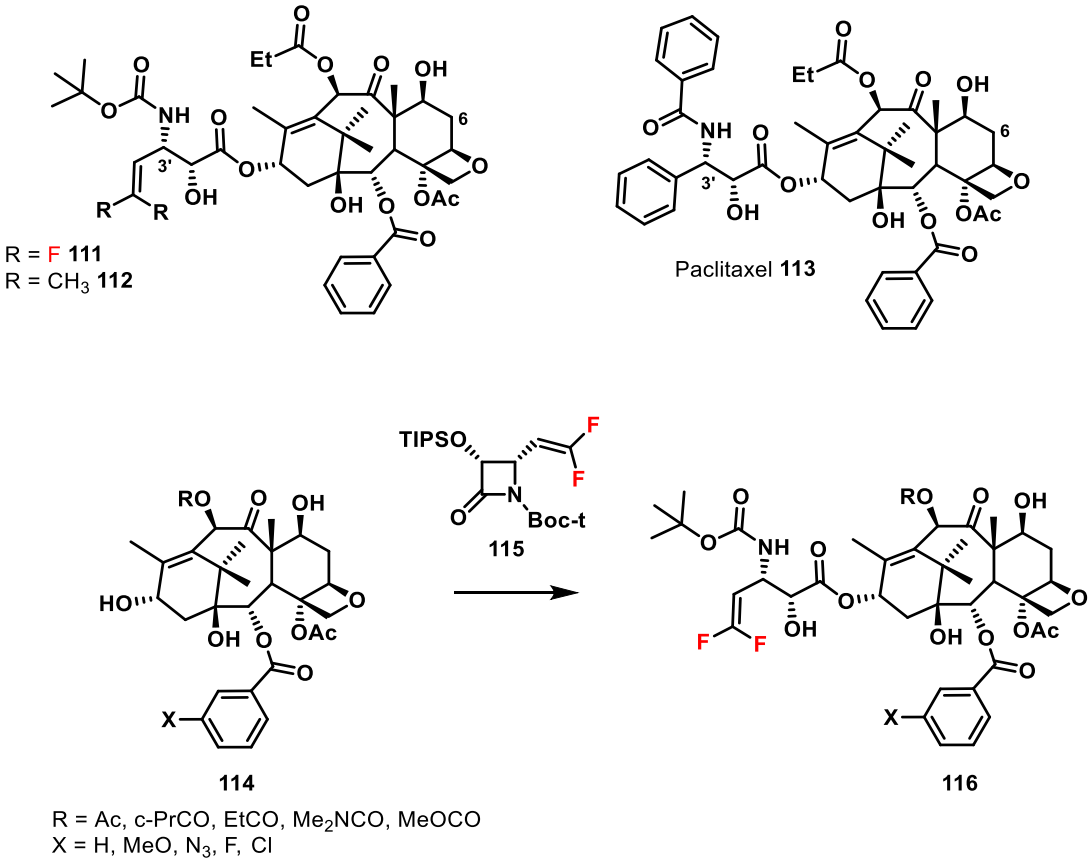

Scheme 1.9. Synthesis of difluorovinyl taxoids.[33]

1.14. Fluorine and carbonyl bioisosterism

The C-F bond has been explored as a C=O replacement due to the similarity in bond lengths, dipole moments and Van der Waals radii of the two functionalities, as well the close electronegativity of fluorine and oxygen. An example of C-F to C=O bioisosterism has been observed in the case of campothecin **117**, a potent alkaloid inhibitor (Ki = 0.45 μM) of topoisomerase I that catalyses the relaxation of the left handed double helical form of DNA, preventing the proliferation of tumoral cells. However, campothecin **117** was found to be metabolic unstable due to rapid hydrolysis of the lactone ring to the inactive carboxylic acid. To overcome this liability to hydrolysis, the C=O group was replaced by a C-F moiety to generate isomers **118** and **119** which were more stable at pH 7.4 than campothecin **117**, but less potent as inhibitors of topoisomerase. The inhibitory potency of **119** was enhanced by introducing a cyclohexyl substituent at C7 position of the quinolone ring to give **120** whose binding affinity was closer to **117** (Figure 1.12).[33]

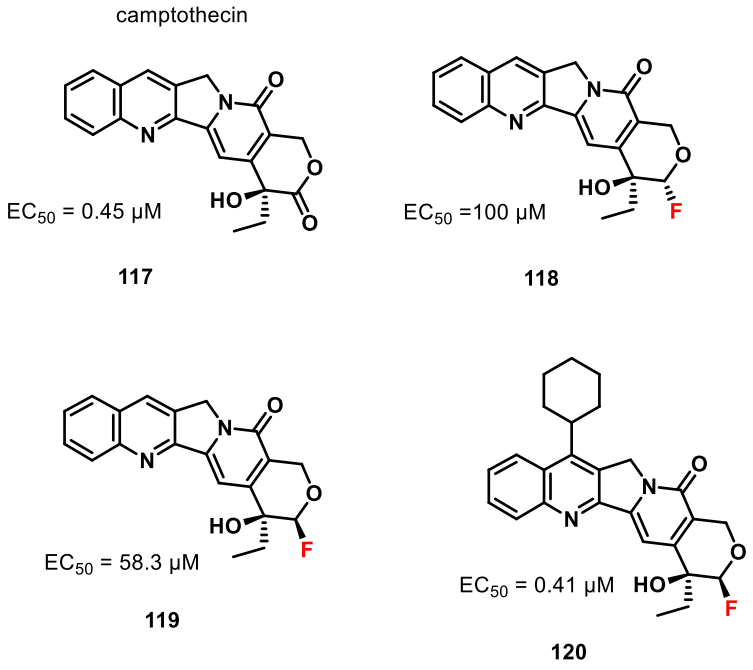

Figure 1.12. Topoisomerase inhibitors.[33]

The aryl fluoride **122** was also found to be a good mimic of quinone **121**. Compound **121** acts as an inhibitor of the tissue factor VIIa enzyme complex (TF/VIIa), a protein that causes blood to clot in the coagulation process. Compound **122** exhibited a greater inhibitory potency than **123**, with the fluorine acting as hydrogen bond acceptor engaging with the amide nitrogen of Gly-216, as observed from crystal structures of **121** and **122** bound to TF/VIIa complexes (Figure 1.13).[35]

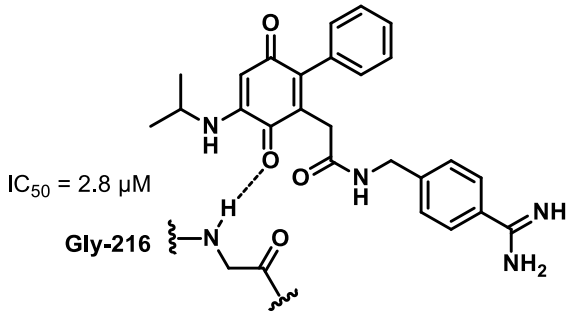

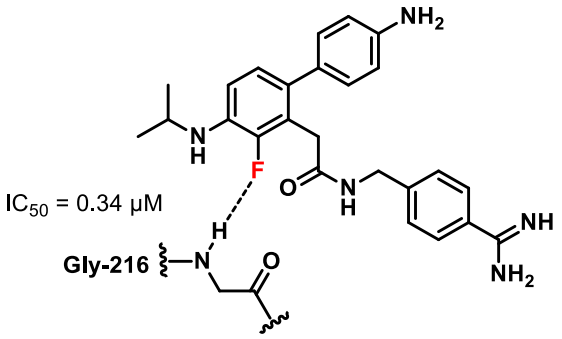

Figure 1.13. Fluorine alkenyl moiety as quinone mimic in the inhibition of TF/VIIa.[35]

1.15. Fluorinated motifs as amide mimetics

The replacement of an amide group with an appropriate isostere is a common strategy in medicinal chemistry. An ideal amide mimic has to retain both the geometry and the hydrogen bonding capabilities of the functional group.

Zanda *et al.*[33] reported the synthesis of partially modified retro peptides **124** (PMR) where the [NHCH(CF_3)] moiety replaces the -NHC(O)- unit. The presence of the CF_3 group was found to constrain the molecule, leading to peptidomimetics with defined conformations. The new mimetics **124** adopt a turn-like conformation similar to the non-fluorinated peptides **123** with comparable torsion angles, suggesting that the CF_3 motif is important in stabilising the turn. Furthermore, since the C-F bond is similarly polarised with respect to the C=O bond, the low basicity of the NH is maintained, fundamental for peptide stability (Figure 1.14).[33]

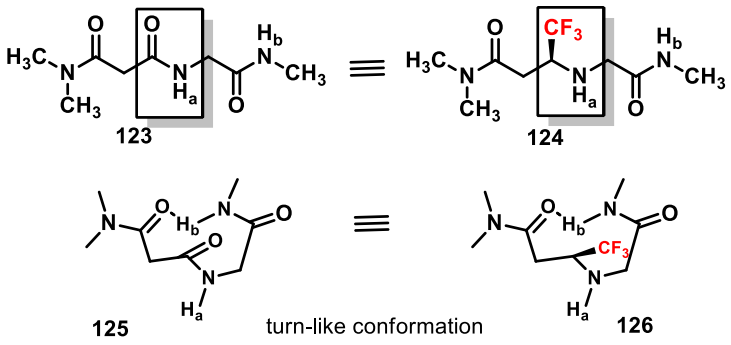

Figure 1.14. Synthesis of a retropeptide motif reported by Zanda *et al*.[33]

The NHCH(CF_3) moiety has also found application in the design and synthesis of potent inhibitors of cathepsin K, the key enzyme responsible for the degradation of Type I collagen in osteoporosis.[33] Cathepsin K is involved in the degradation of triple helical collagen but its mechanism of action is still under investigation. It was demonstrated that Cat K interacts with glycosaminoglycan derivatives to generate high molecules weight oligomeric complexes that are believed to be involved in the unwinding process of triple helical collagens. The trifluoro-ethyl amino group was an excellent amide isostere generating the most potent dipeptide inhibitor of Cat K (K_i = 5 pM) **129**, highly selective and stable to amide bond cleavage. Its compatibility as an amide bond mimetic was confirmed by X-ray studies showing the trifluoroethylamine N-H interacting with the carbonyl oxygen of Gly-66 residue of the enzyme while the trifluoromethyl moiety was oriented towards the bulk solvent.[35]

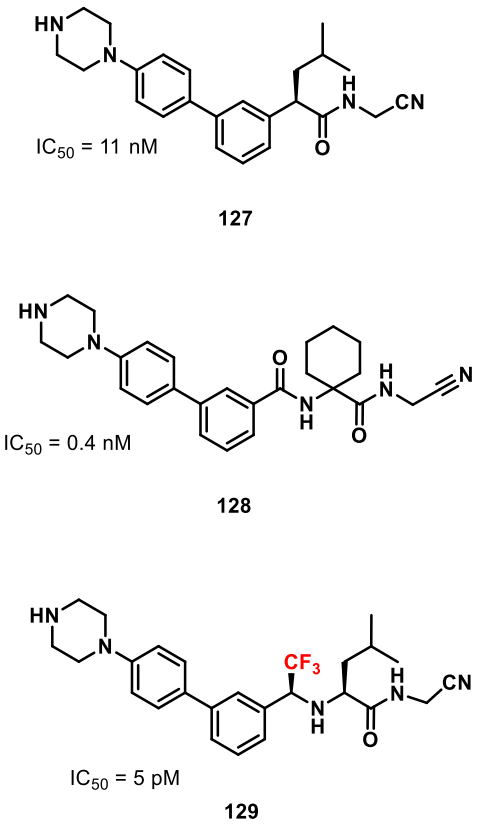

Figure 1.15. The CF_3 group as an analogue of amide units in peptides.[33,35]

Difluorotoluene **132** has been shown to be a mimetic of thymine **130**, and the corresponding deoxynucleoside **134** has been explored as a substrate for the DNA polymerase enzyme. DNA polymerase catalyses the formation of DNA from the appropriate nucleotides. These enzymes operate coding a complementary DNA from a DNA template. Specifically, DNA polymerase inserts deoxyadenosine opposite to thymidine, and thus it will not incorporate thymidine, deoxyguanosine or deoxycitidine. When assaying difluorotoluene **132**, as a template surrogate in place of thymine **130**, deoxynucleoside **134** was efficiently inserted as a replacement of thymine **130**. Difluorotoluene **134** retains the shape and the conformation of the natural nucleoside **133**. Furthermore, the enzyme actively recognises difluorotoluene **134** despite its non-polar nature and the perceived wisdom that Watson-Crick-type hydrogen bonding is regarded as the primary source of the specificity in DNA replication (Scheme 1.10).[36]

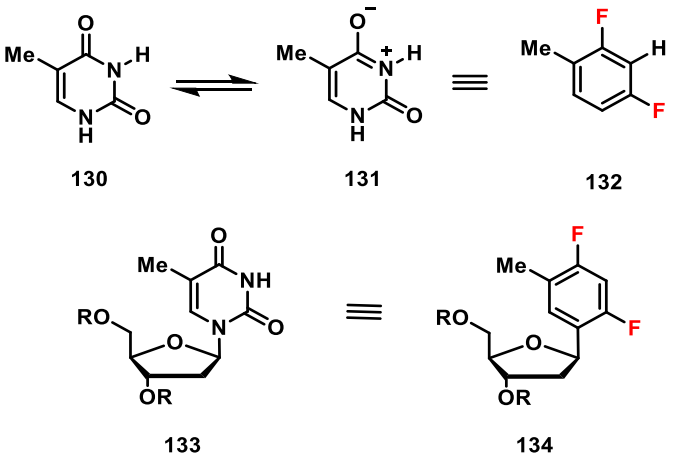

Scheme 1.10. Difluorotoulene as a mimetic of thymine.[36]

1.16. Fluorine as a hydroxyl mimetic (C-OH)

The replacement of a hydroxyl group with fluorine has been extensively investigated, especially due to their similar bond lengths with carbon (C-F = 1.35 Å; C-O = 1.43 Å) and the potential for fluorine to be a hydrogen bond acceptor.

This replacement led to the discovery of exciting therapeutic agents. Nucleosides are fundamental for all living organism as building blocks of DNA and RNA. The introduction of fluorine atoms into the ribose ring influences the structure of the nucleoside analogue. The C-F bond interacts with the environment through electrostatic interactions; in a fluorine containing drug target, the C-F bond can be oriented towards a partial positive charge, engaging in intermolecular electrostatic interactions. The C-F bond dipole can also adopt an antiparallel arrangement when interacting with other polarised bonds such as a carbonyl (dipole-dipole interactions). These dipole-dipole interactions stabilise or destabilise a conformation. Thus, antiperiplanar effects, dipole-dipole and *gauche* interactions all influence the preferential conformation adopted by a nucleoside.

Sofosbuvir **138** was designed as an analogue of nucleoside **139**. It is a potent inhibitor of Hepatitis C virus (HCV) whose replication is catalysed by NS5B polymerase. NS5B polymerase is an RNA dependent RNA polymerase involved in the viral life cycle. It creates double stranded RNA (ds RNA) from single stranded RNA (ssRNA). The binding affinity for the enzyme is correlated to the conformation adopted by the nucleoside. Sofosbuvir **138** bears a fluorine in 2'-β position adopting a South conformation. Whereas its 2'-α-fluoro isomer prefers a North conformation. The 2'-β-fluoro conformer **138** binds HCV NS5B while the 2'-α-fluoro analogue **136** does not. Sofosbuvir **138** (South conformation) interacts with the NH side chain of amino acid Asn-291 through a hydrogen bond and is a good analogue of nucleoside **139** in terms of the geometry and its interactions with the enzyme (Figure 1.16). [33]

Sofosbuvir is the largest selling small molecule in medicinal chemistry at present.

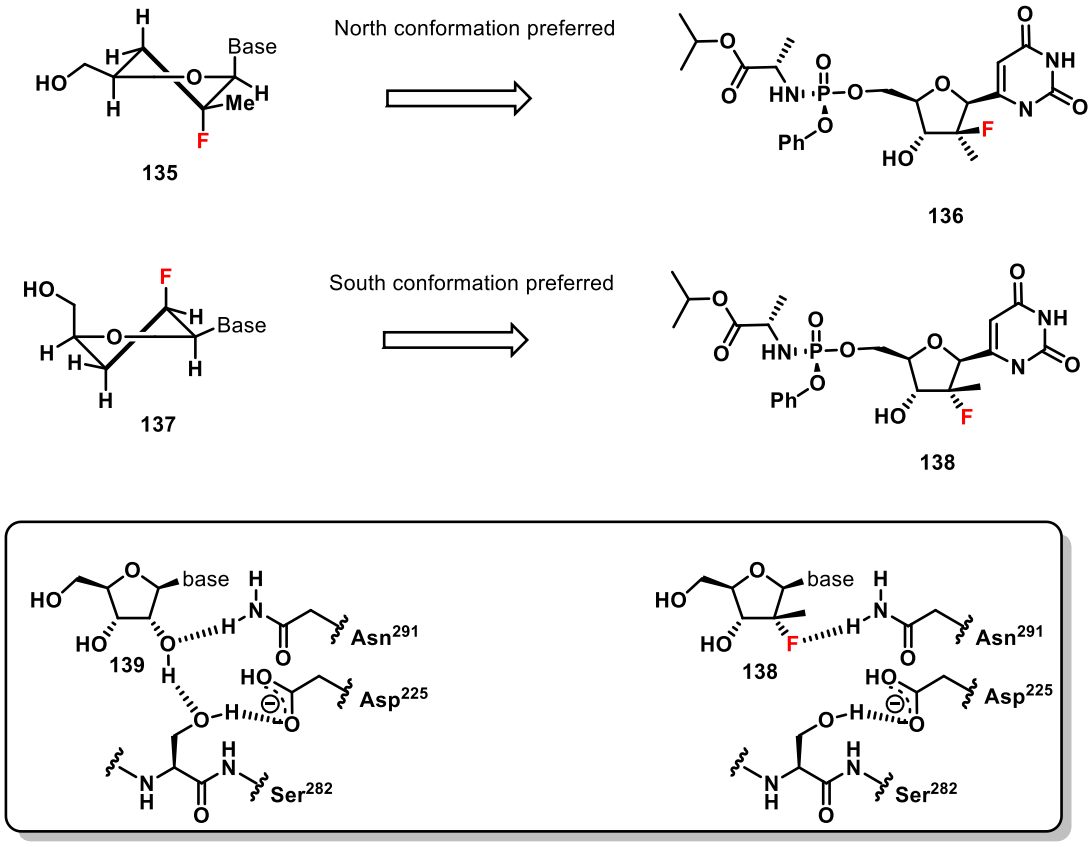

Figure 1.16. Fluorine as an isopolar and isoelectronic mimic of the hydroxyl group.[33]

1.17. Alkenyl fluoride as enol mimetic

In developing the analogy between oxygen and fluorine, vinyl fluorides have been explored as isoelectronic and isosteric replacements for an enol/ate. For example, fluorovinyl steroids **147** and **148** were investigated as mimetics of pregnenolone **140**, a metabolic intermediate in the biosynthesis of estrogens and androgens. They are processed by cytochrome P450 17A1, a hydroxylase. Inhibitors of this family of enzymes block the synthesis of androgens whose high levels are associated with prostate cancer, thus cytochrome P450 17A1 inhibitors have potential as therapeutics. Pregnenolone **140** is converted to dehydroepiandrosterone **146** as illustrated in Scheme 1.11. Pregnenolone **140** is believed to be an intermediate in the $C_{17\alpha}$ hydroxylation step followed by subsequent cleavage of the $C_{17(20)}$ bond to generate the C17 keto androgens. Steroids **147** and **148** mimic the enol tautomers of pregnenolone **141** and were found to be potent inhibitors of P450 17A1 enzyme (Scheme 1.11).[37]

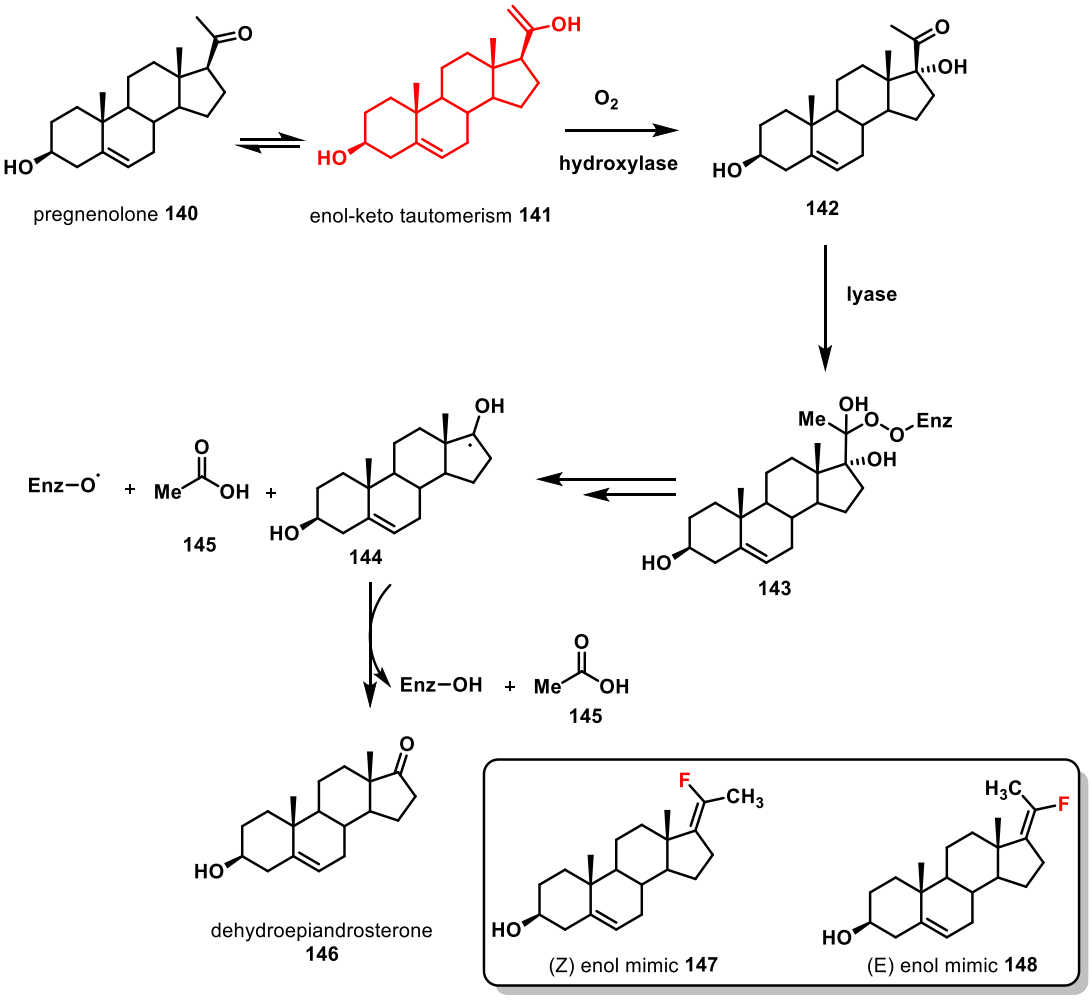

Scheme 1.11. Novel steroidal fluoroalkene derivatives as enol intermediate mimetics for C17α hydroxylase/C17(20) lyase inhibition.[37]

3-Dehydroquinate **150** is a common intermediate in the shikimate and quinate pathways, in bacteria, fungi and higher plants. The pathway generates essential aromatic compounds from acyclic carbohydrates.

3-Dehydroquinate **150** is irreversibly converted to dehydroshikimate **151** by the enzyme dehydroquinase, which occurs in two different forms: Type-I enzymes are dimers that mediate a *syn*- elimination of water from an intermediate Schiff's base, whereas Type-II enzymes (found in *Mycobacterium Tuberculosis)* are thermally stable dodecameric complexes able to dehydrate a stabilised enolate **150** in an *anti*- manner (Scheme 1.12). A vinylfluoride **152** was designed as a mimic of enolate **150** and found to be a highly selective (1000 fold) competitive inhibitor of the Type II dehydroquinase enzyme. This vinylfluoride appears to be a good enolate mimetic.[38]

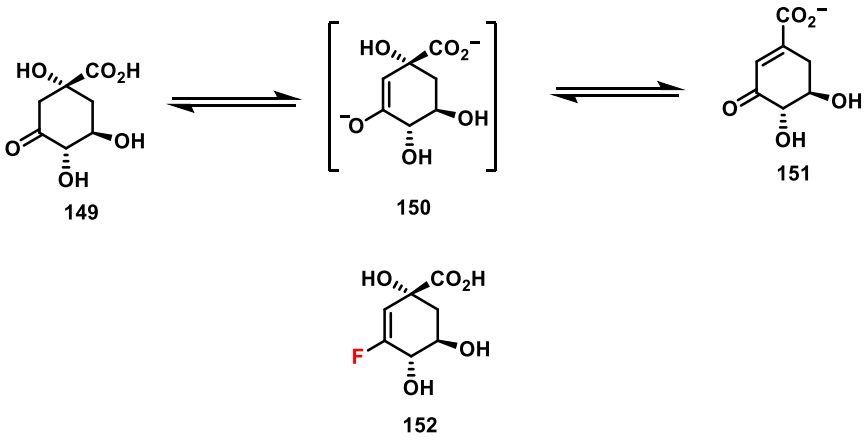

Scheme 1.12. Inhibition of Type II dehydroquinase enzyme.[38]

1.18. Enzymes: basic concepts on enzyme catalysed reactions

Enzymes are macromolecular catalysts required for the processes required for sustaining life; they accelerate biochemical reactions by reducing the activation energy and thus effectively allowing these transformations to occur. A basic enzymatic reaction can be represented by the equation described in Figure 1.17. They are generally first order with respect to the substrate:

Figure 1.17. The enzyme mediated reaction.[5]

The most general evidence for the enzyme-substrate formation is the so called "saturation effect". At constant concentration of enzyme, the reaction shows a maximal velocity (V_{max}) where all the catalytic sites are occupied with substrate, thus the reaction rate cannot increase shifting from first order to zero order. This saturation effect is typical of an enzyme catalysed reaction. The first kinetic model introduced for an enzymatic reaction was proposed by Michaelis-Menten. They suggested that an enzyme interacts with a substrate with a rate costant k_1 to generate the enzyme-substrate complex ES, necessary for enzymatic catalysis. The ES complex can dissociate to E and S with a rate constant k_{-1} or it can generate the product P with a k_2 rate constant (Figure 1.18).[5]

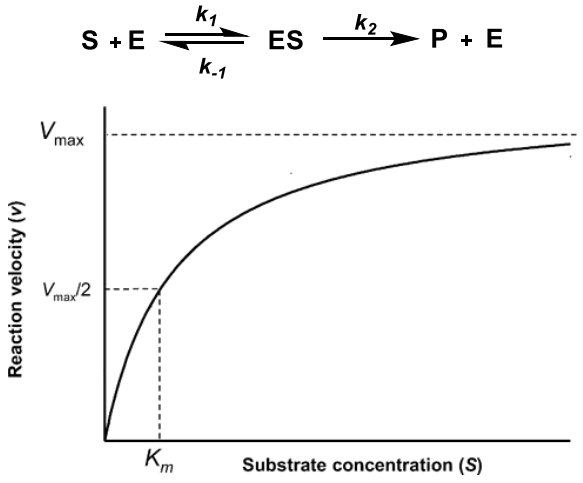

$$v = \frac{Vmax[S]}{Km + [S]}$$

Figure 1.18. The Michaelis-Menten equation: reaction velocity (v) vs substrate concentration(S).[5]

The Michaelis-Menten equation correlates the reaction rate (v) to the substrate concentration for a system where the substrate (S) binds reversibly to the enzyme (E) to form an ES complex that reacts irreversibly to form the product P releasing the enzyme E. V_{max} is the maximum velocity reached by the system at maximum substrate concentration (saturation effect). The Michaelis-Menten equation K_M is equal to the substrate concentration at which the reaction velocity is one half of the maximal velocity for the reaction. When k_2 is smaller than k_{-1}, K_M measures the strength of the ES complex, a low K_M indicates a strong binding whereas a high K_M indicates a weak binding.[5]

1.19. Enzymatic inhibition

The regulation of enzymatic activity is fundamental in order to achieve fine control of the particular flux along a metabolic pathway. There are many factors that control enzymatic activity: pH, temperature, cofactors, compartmentalisation, feedback inhibition and regulatory molecules are among the most important. In particular, molecules that act by slowing enzymatic turnover are known as enzyme inhibitors.

1.19.1. Classification of inhibitors

A compound can decrease the enzymatic activity by binding to the enzyme's active site either in a transient, reversible manner, or *via* an irreversible covalent chemical modification.

Reversible inhibitors are divided into three groups:

Competitive inhibitors compete with the substrate for binding to the active site and once bound they prevent the forward reaction occurring, thus effectively reducing overall enzymatic turnover.

Non-competitive inhibitors do not prevent the binding of the substrate complex to the active site but they will bind to another site of the enzyme (allosteric site) altering the enzyme activity.

Uncompetitive inhibitors bind to and stabilise the enzyme-substrate preventing substrate release from the active site.

Irreversible inhibitors generally modify an enzyme in a covalent manner, such that the enzyme cannot undergo turnover. This inhibition tends to be specific, in that the protein is not destroyed as in the case of extreme variations of temperature or pH (i.e. denaturation of the enzyme); usually the irreversible inhibitor contains reactive fragments that react specifically with residues at the active site, preventing turnover.[5]

1.20. Reversible inhibition

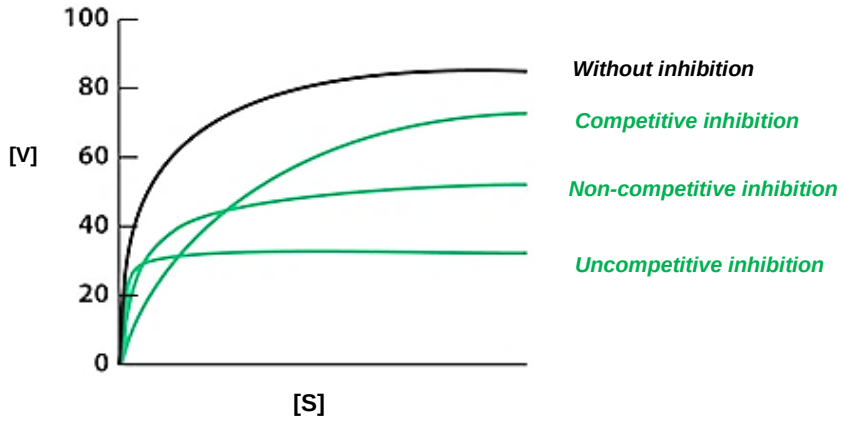

Figure 1.19. Three modes of the reversible inhibition. V = reaction rate, S = substrate concentration.[39]

Competitive inhibitors and non-competitive inhibitors can be distinguished by plotting the reaction rates against the corresponding substrate concentrations, as shown in Figure 19. The curve for a competitive inhibitor shows a reduction in the slope when compared to the inhibitor-free curve, and at saturating substrate concentrations the characteristic V_{max} is maintained. In the case of a non-competitive inhibitor, the initial rate slows, but there is also a decrease in the V_{max}, indicating that the inhibitor does not compete with the substrate for the active site.

1.21. Example of reversible inhibitors

A classic example of a competitive inhibitor is the antibiotic sulfanilamide **160**, which mimics para-aminobenzoic acid (PABA) **154**. PABA is an intermediate in the biosynthetic pathway that leads to folic acid **159**, an important cofactor for various methyltransferase enzymes involved in the biosynthesis of purines and pyrimidines. PABA is converted to dihydropteroic acid by the enzyme dihydropteroate synthase, which in turn is processed to folic acid. Since mammals do not synthesise folic acid and depend upon external sources, the inhibition of the dihydropteroate synthase by sulfanilamide **160** allows for selective treatment of bacterial infections (Scheme 1.13).[39]

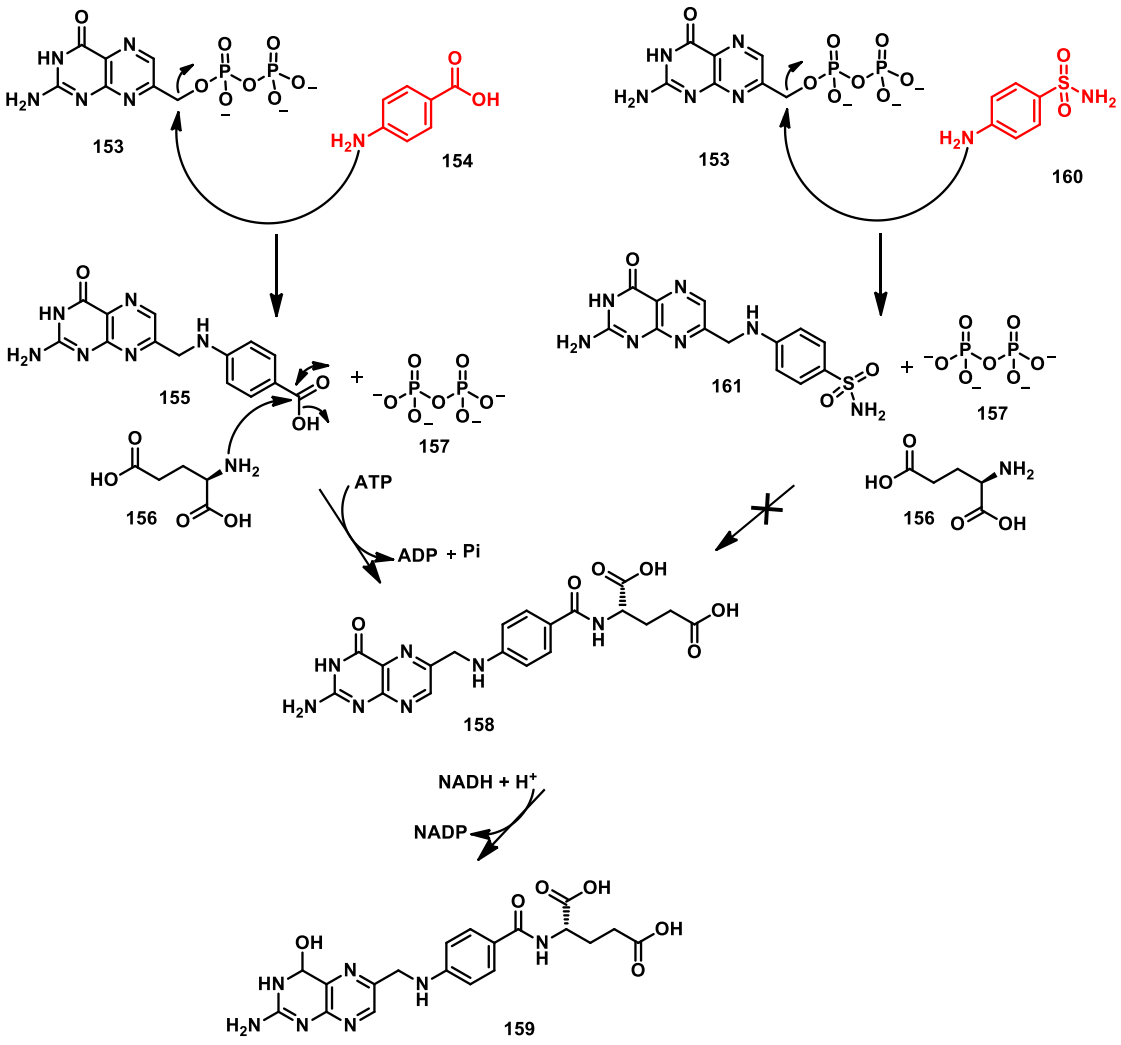

Scheme 1.13. Sulfanilamide **160** as a competitive inhibitor of dihydropteroate synthase.[39]

Tripanavir **163** belongs to the Protease inhibitors (PI) class and it has been approved by the US FDA for the HIV treatment. It is a sulfonamide dihydropyrone derivative and is

the first PI with a non peptidic structure. Tripanavir acts as a competitive inhibitor by binding directly to the active site of HIV aspartyl protease and blocking the hydrolysis of viral polyproteins that are involved in the HIV replication process. The mechanism of action of **163** is still under investigation (Scheme 1.14).[40]

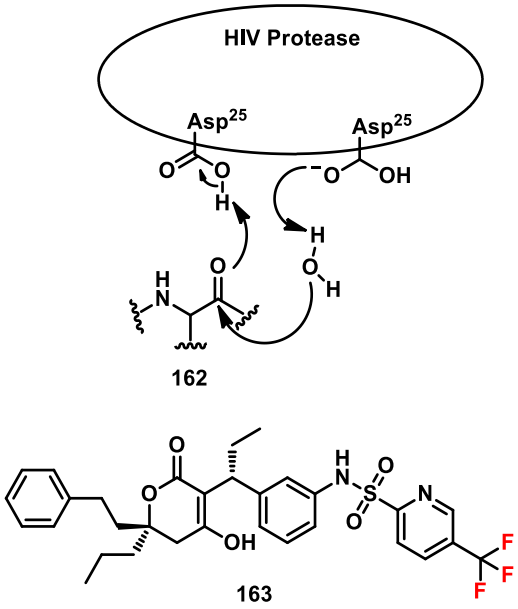

Scheme 1.14. Tripanavir **163** as HIV protease inhibitor.[40]

Most of non-competitive inhibitors can be regarded as allosteric effectors, compounds that bind remote to the active site.

Pyruvate kinase catalyses the final step of glycolysis. The reaction proceeds by transfer of the phosphate group from phosphoenol pyruvate (PEP) **165** to adenosine diphosphate (ADP) **164,** yielding adenosine triphosphate (ATP). The production of ATP is allosterically controlled, amongst other effectors, by ATP itself which binds to an allosteric site on pyruvate kinase and thus inactivates the enzyme (Scheme 1.15).[41]

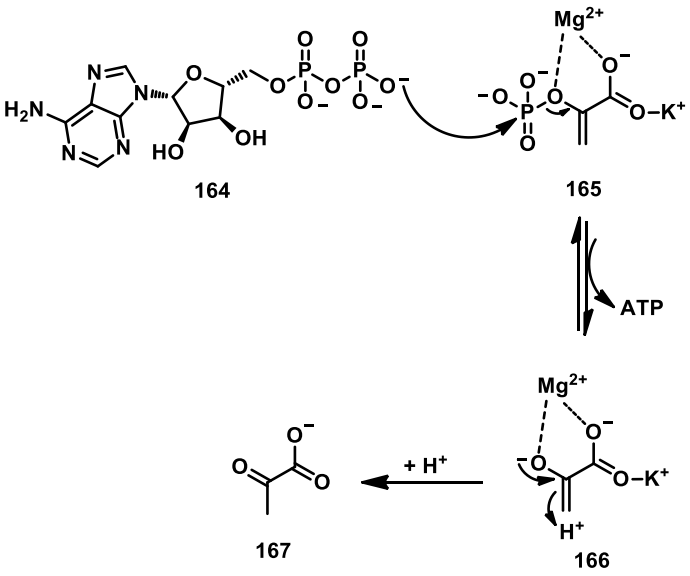

Scheme 1.15. The pyruvate kinase reaction.[41]

Aspartate transcarbamoylase (ATCase) is a cytosolic enzyme that mediates the condensation of aspartate **168** and carbamoyl phosphate **169** to generate N-carbamoylaspartate **170** and orthophosphate **171**. This reaction is the first committed step on pyrimidine nucleotide biosynthesis. ATCase is inhibited by cytidine triphosphate (CTP) **172**, the final product of the enzyme-controlled pathway.

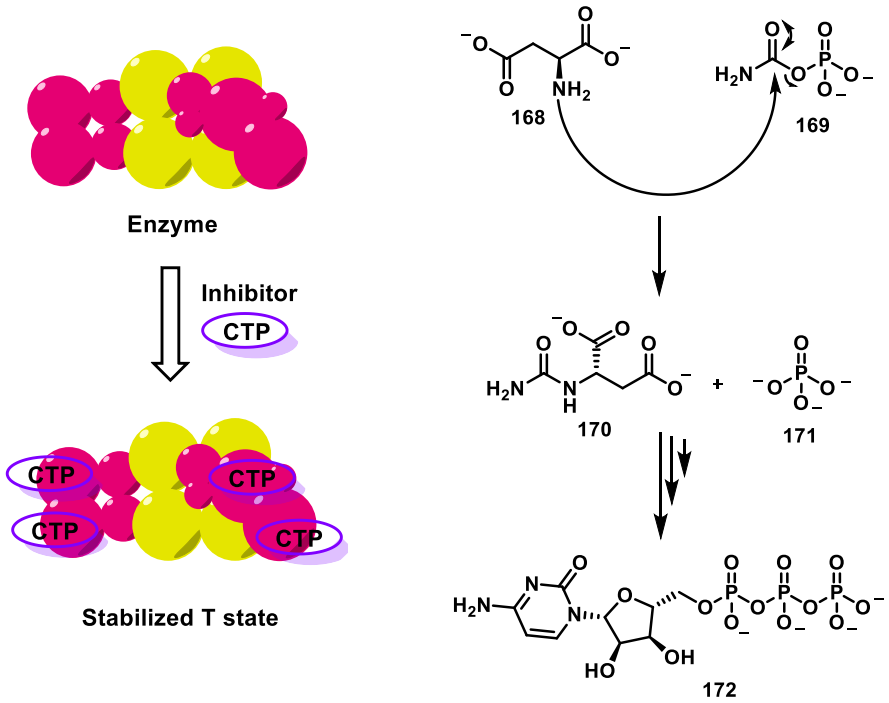

Scheme 1.16. Cytidine triphosphate **172** as an inhibitor of aspartate transcarbamoylase.[42]

The mechanism suggested for the allosteric regulation of the enzyme by CTP, indicates a conformational change of the quaternary structure of the enzyme. The enzyme exists in equilibrium between two conformations: the inactive form termed the tense state (T) and the relaxed one (R). When CTP is bound to the enzyme, it shifts the equilibrium towards the T, decreasing enzyme activity and reducing N-carbamoylaspartate production (Scheme 1.16).[42]

Lansoprazole **173** is an uncompetitive inhibitor of hydrogen/potassium adenosine triphosphatase, an enzyme of the gastric parietal cell membrane that forms part of the proton pump involved in the final step of the acid secretory process. It binds covalently to the parietal cell, modulating the pH of the stomach and inhibiting the secretion of gastric acid. It received FDA approval in 1995 for the treatment of peptic ulcer disease, gastroesophageal reflux and Zollinger-Ellison syndrome (Scheme 1.17).[43]

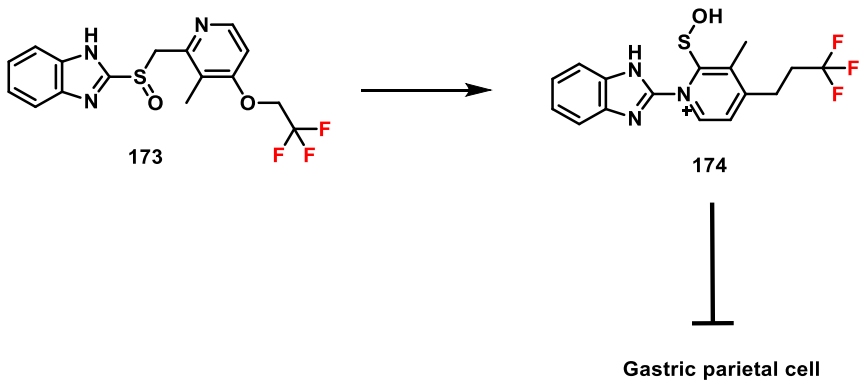

Scheme 1.17. Lansoprazole **173** as proton pump inhibitor.[43]

1.22. Irreversible inhibition

Suicide inhibition is a particular kind of irreversible inhibition; the enzyme binds a substrate analogue which is converted into a reactive intermediate that covalently modifies and binds permanently to the enzyme, forming a stable inhibitor-enzyme complex. The design of a suicide inhibitor requires an understanding of the enzyme mechanism, with the aim of producing a compound that is reasonably inert until triggered by the enzyme.

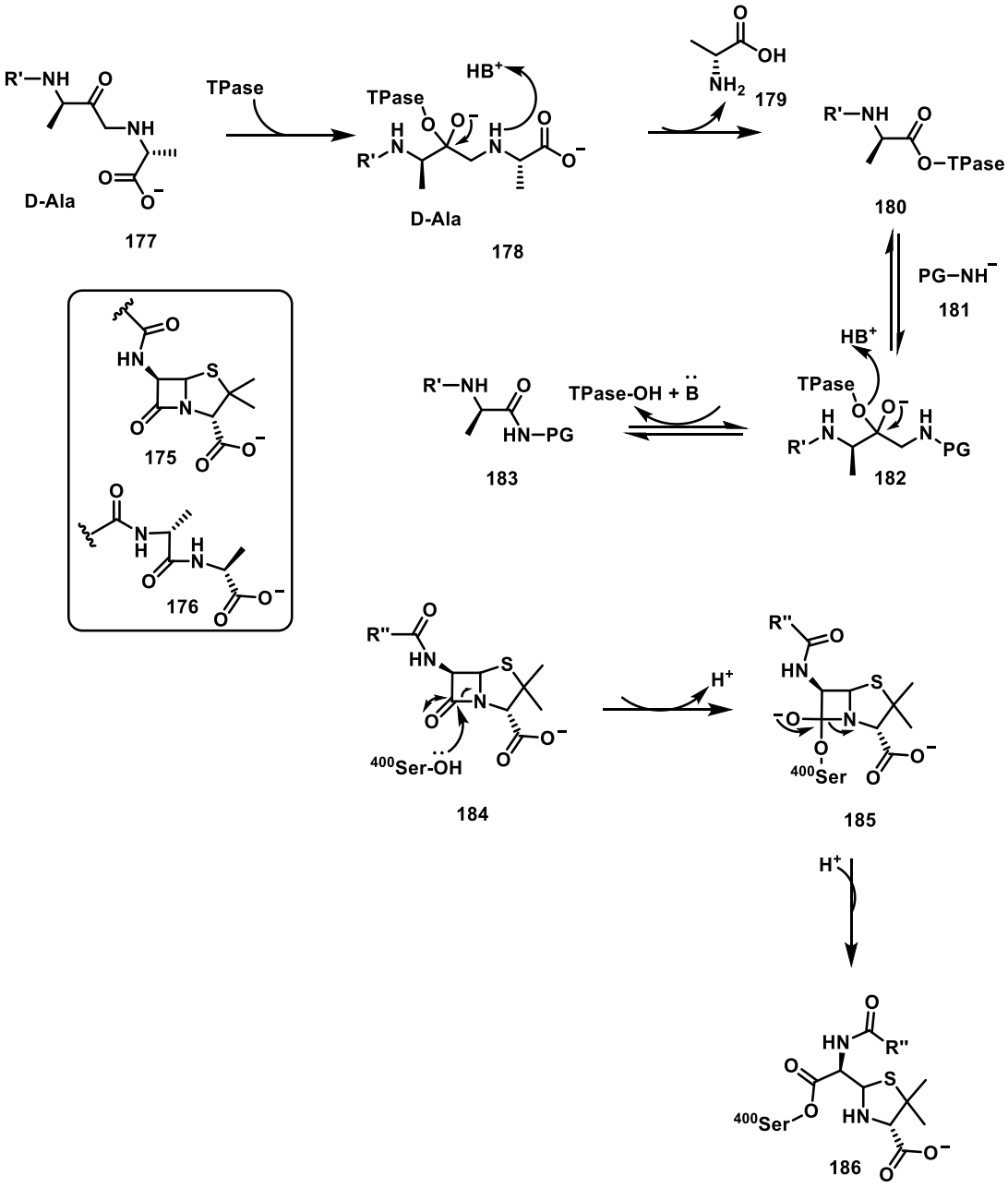

Scheme 1.18. Penicillin **184** as a suicide inhibitor of D,D-transpeptidase (TP), PG = prosthetic group. [44]

Penicillin **184** is a “suicide” inhibitor of D,D-transpeptidase, a fundamental bacterial enzyme involved in the biosynthesis of the bacterial cell wall. The transpeptidation reaction catalysed by this enzyme crosslinks chains of peptidoglycan on the surface of the bacterial wall, forming a 3D network that confers structural integrity to the cell. As shown in Scheme 20, the β-lactam nucleus of **175** mimics the terminal D-Ala-D-Ala sequence of the peptide subunit **176**. Upon binding, the Ser-400 acts as a nucleophile attacking at the β-lactam in **184**, irreversibly acylating Ser-400 and finally disrupting the cell wall synthesis.[44]

α-difluoromethylornithine, known as eflornithine **188**, is a fluorinated analogue of ornithine and acts as suicide inhibitor of ornithine decarboxylase (ODC). ODC catalyses the ornithine **187** decarboxylation to form putrescine.

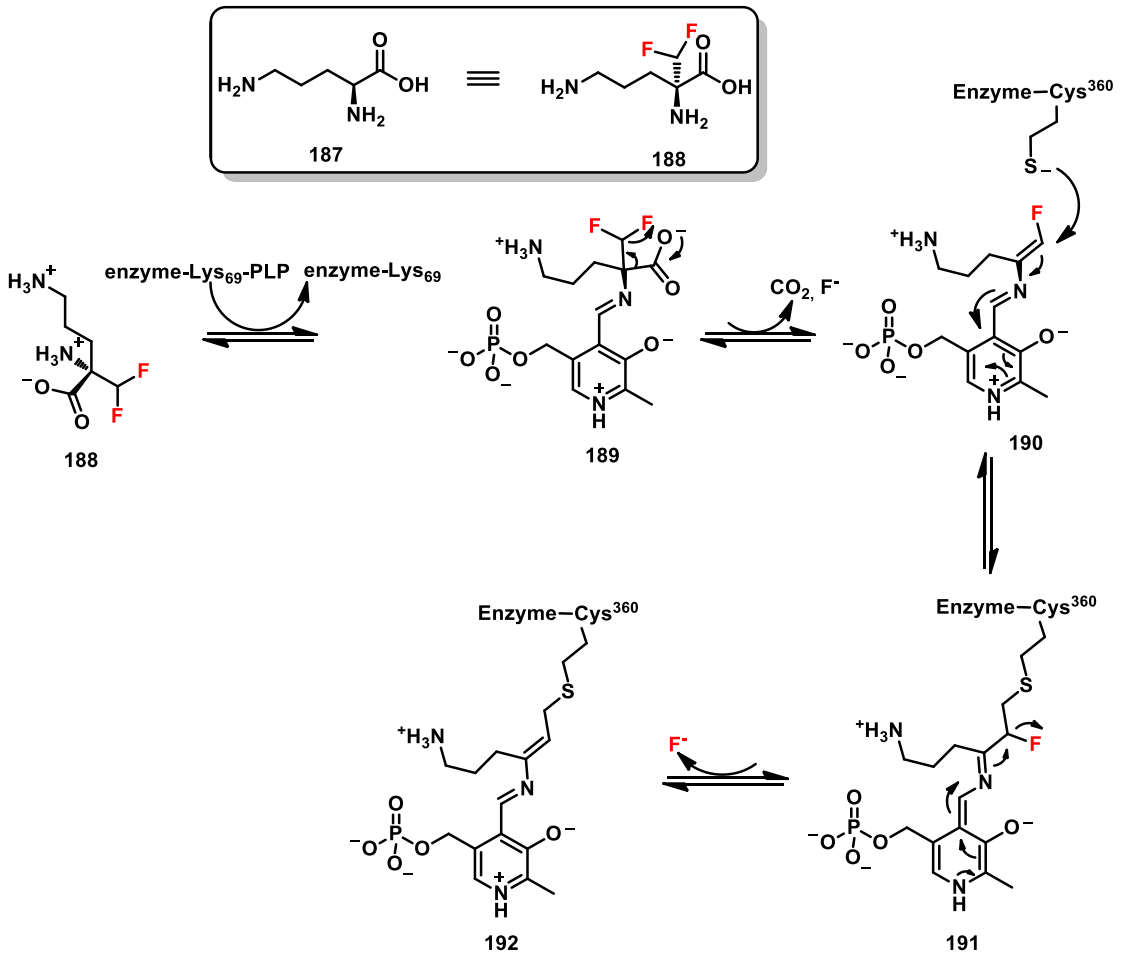

Scheme 1.19. The proposed mechanism of the interaction of eflornithine **188** within OCD active site.

This is the rate limiting step in the biosynthesis of polyamines, essential for all prokaryotic and eukaryotic cells. It is suggested that eflornithine **188** binds directly to the ODC where

it is decarboxylated. It binds to the Cys-360 amino acid residue in the active site thus blocking ornithine from accessing it (Scheme 1.19). The biosynthesis of polyamines is essential for the parasitic replication and survival, hence **188** is used for the treatment of parasitic diseases such as the african sleeping sickness.[12]

1.23. Enzymatic inhibition as tool for the study of enzymatic reactions and for the design of therapeutic targets

Enzymatic inhibition is a spontaneous physiological process in all living organisms. The human pancreas, for instance, produces several proteases, enzymes responsible for the breakdown of proteins and thus potentially dangerous to the organ itself. In order to avoid self-harm, the pancreas produces a potent protease inhibitor called “pancreatic trypsin inhibitor” which can selectively block the digestive action of the pancreatic proteases.

Inhibiting an enzyme can lead to essential information regarding its binding properties, substrate specificity and the types of reactions the enzyme can catalyse. Investigating metabolic pathways with the use of inhibitors as probes allows access to a more detailed understanding of the entire mechanism and its regulation. For example, inhibition of acetyl-CoA carboxylase (ACC) leads to the inhibition of fatty acid synthesis and stimulation of fatty acid oxidation, having the potential to affect a series of cardiovascular risk factors associated with metabolic diseases such as obesity, diabetes, atherosclerosis etc.

Currently, most drug discovery and development efforts are focused on finding and optimising drug candidates that can inhibit specific enzyme targets. A classic example is aspirin **196**, an inhibitor of the cyclooxygenase reaction which is involved in prostaglandins (PGs) **194** synthesis and the inflammation response (swelling, pain and fever). The overall synthesis of prostaglandins is catalysed by prostaglandin H_2 synthase. The substrate for this enzyme is arachidonic acid **193**, a hydrophobic molecule generated from the hydrolysis of membrane lipids. Arachidonic acid **193** is transferred to the active site of the enzyme through a hydrophobic channel in the protein. Aspirin **196** blocks this channel and prevents prostaglandin synthesis by transferring an acetyl group to a serine residue (Ser-530) within the active site of the enzyme (Scheme 1.20).[45]

Enzymes increase the rates of reactions by stabilisation of the transition state to which the enzyme binds with higher affinity. “Transition state analogues” can be ideal inhibitors of specific enzymes and have potential as highly selective drugs. For instance, the inhibition of purine nucleoside phosphorylase (PNP) **199** by a tight binding inhibitor (K_i picomolar) called Immucillin-H (Imm-H) **203** is an instructive example. Genetic deficiency of PNP **200** can lead to significant T cell-mediated immunosuppression, Imm-H **203** mimics the transition state of PNP **202** and selectively inhibits the PNP enzyme, blocking the growth of malignant T cell leukemia lines and inducing apoptosis (cell death) (Scheme 1.20).[46]

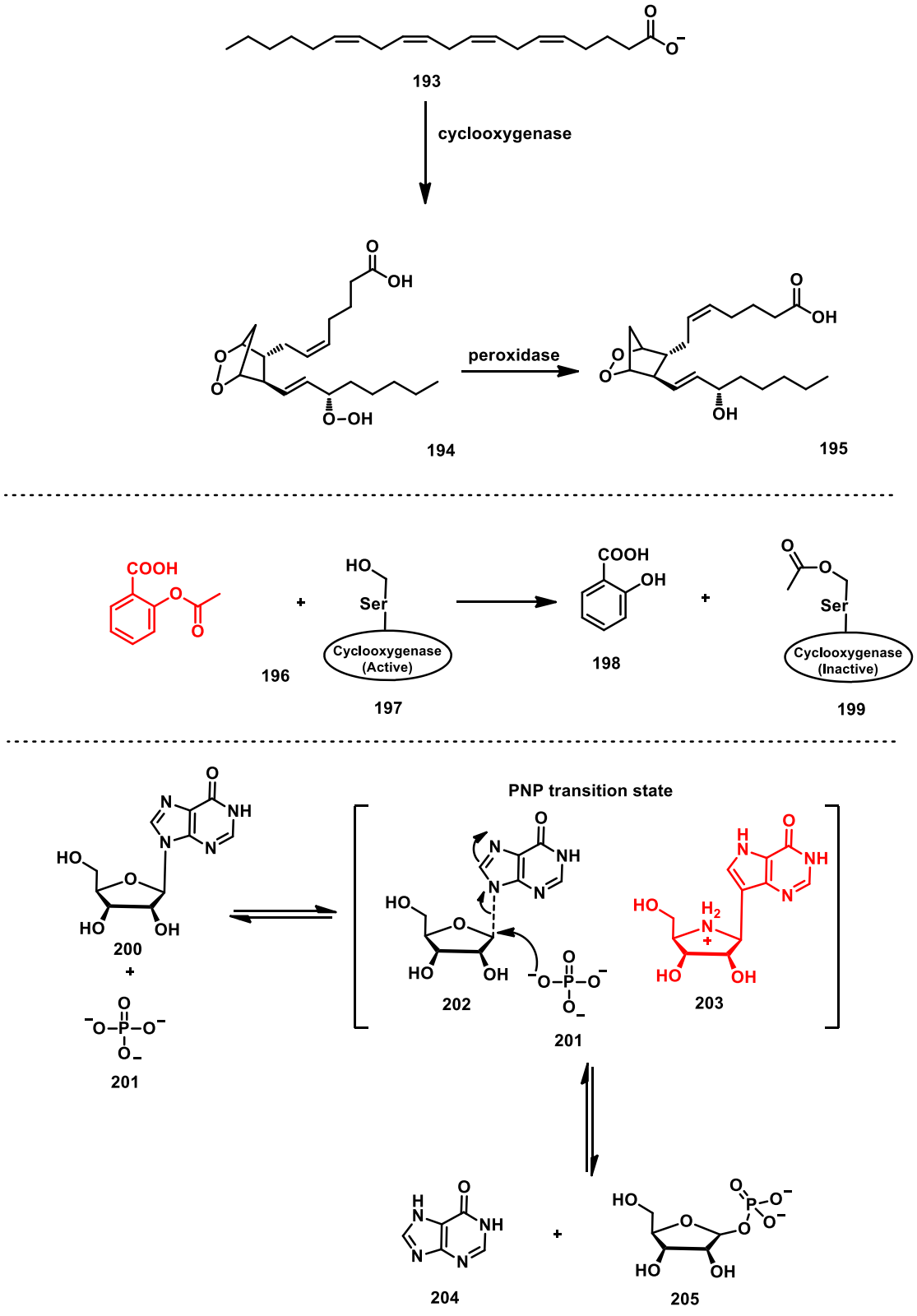

Scheme 1.20. Immucillin H **203** and Aspirin **196**.[45,46]

1.24. Fluorovinyl thioether as stereo-electronic thioester enol/ate mimic: design of an acetyl-CoA analogue

The fluorovinyl moiety has potential as a stereo-electronic mimic of enol/ate intermediates which are involved in many important metabolic pathways. As said previously, thioesters such acyl co-enzymeAs, are central metabolites in many important enzymatic pathways. They can undergo condensation reactions though enols or enolates to form C-C bonds. Acetyl-CoA **2** is a central intermediate in the citric acid cycle and other essential metabolic pathways. In the citric acid cycle, citrate synthase uses acetyl-CoA **2** and catalyses a condensation reaction via enol/ate formation (Scheme 1.21).

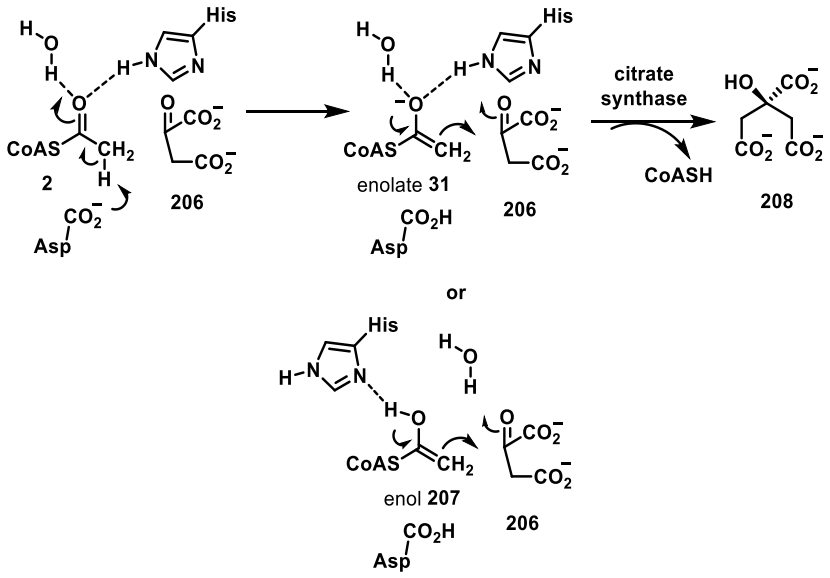

Scheme 1.21: Citrate synthase condensation of acetyl-CoA **2** to citrate **208** via an enol/ate intermediate formation.

α-Fluorovinyl thioethers possess spatial and electrostatic profiles compatible with the potential to mimic these enzyme intermediates. With this concept in mind, a theoretical calculation of the electrostatic profiles and dipole moments of a thioester enol **210** and a fluoro vinyl thioether **211** was performed. This analysis shows a similar stereo-electronic profile between a vinyl fluoride and an enol (Figure 1.20).[47]

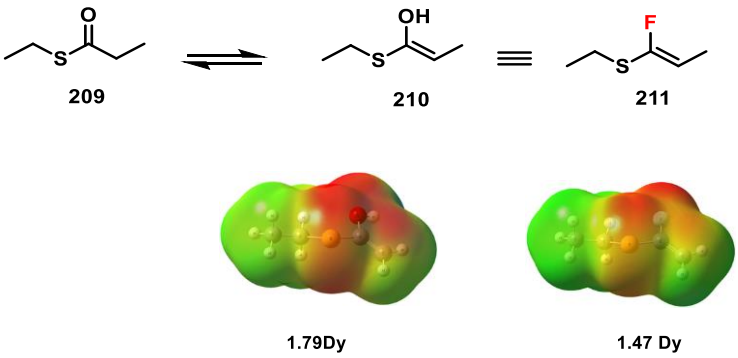

Figure 1.20. Electrostatic profiles and dipole moments of a enol thioester **210** and a fluorovinyl thioether **211**.[47]

Based on these findings, it was envisaged that fluoro vinyl thioether **212** possesses a spatial and electrostatic profile consistent with the potential to mimic the enol/ate intermediate of important thioesters such as acetyl-CoA **2** (Scheme 1.22). It would follow that fluoro vinyl-CoA **212** will mimic the enol/ate of acetyl-CoA and bind through intermolecular interactions with the amino acid residues (Asp-375 and His-274) within the active site of the enzyme. Compound **212** was found to be a low micromolar inhibitor of citrate synthase (see Chapter 2 for further details). In this context, inhibition of citrate synthase, became a focus. Thus, a series of acetyl-CoA analogues, modified on the acyl-CoA fragment, will be synthesised and studied as inhibitors of citrate synthase. [47]

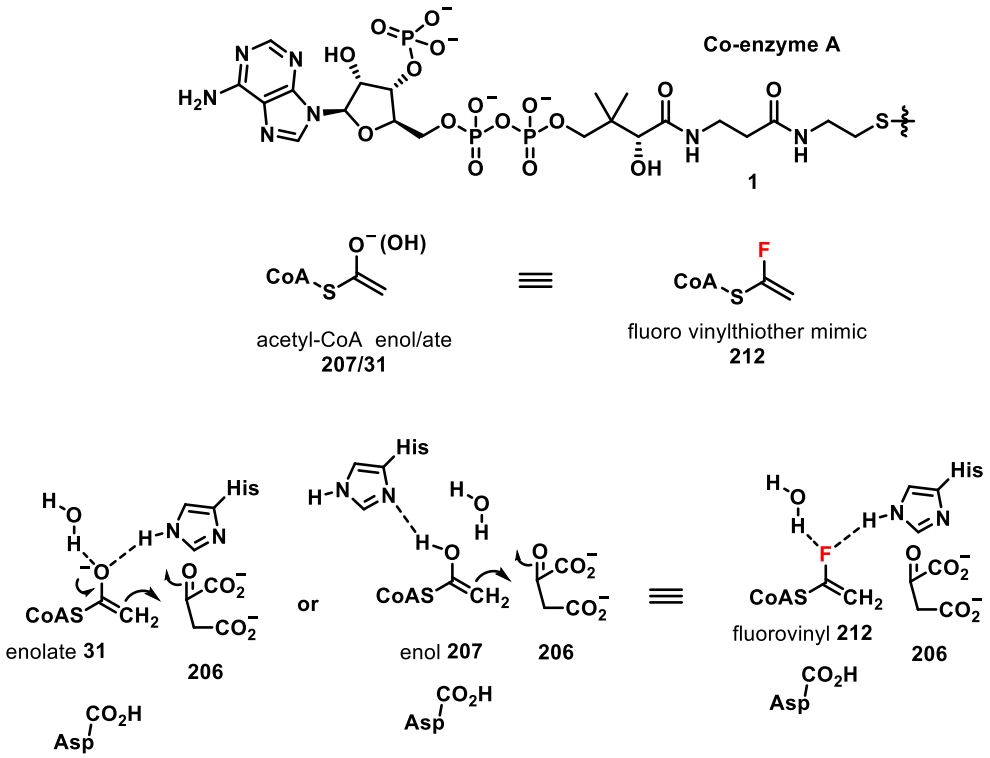

Scheme 1.22. Fluorovinyl thioether **212** designed as an analogue of acetyl-CoA **2**.[47]

1.25. References

1 M. G. Rubanu, D. Bello, N. Bandaranayaka, J. P. Götze, M. Bühl, D. O'Hagan, *ChemBioChem*, **2019**, *20*, 1174-1182.

2 F. Lipmann, *J. Biol. Chem.*, **2005**, *280*, 164–167.

3 P. K. Mishra, D. G. Drueckhammer, *Chem. Rev.*, **2000**, *100*, 3283–3309.

4 D. L. Nelson, M. Cox, *Lenhinger principles of Biochemistry*, 6th edn., **2013**.

5 J. Berg, J. Tymoczko, L. Stryer, *Biochemistry*, **2002**, 5th ed.

6 M. K. Campbell, O. F. Shawn, *Ketone Bodies*, **2006**, 5th ed.

7 K. C. Cheng, J.-N. Liao, P. C. Lyu, *Biochem. J.*, **2012**, *446*, 395–404.

8 L. Tong, *Cell. Mol. Life Sci.*, **2005**, *62*, 1784–1803.

9 P. Von Wettstein-Knowles, J. G. Olsen, K. A. McGuire, A. Henriksen, *FEBS J.*, **2006**, *273,* 695–710.

10 Y. A. Chan, A. M. Podevels, B. M. Kevany, M. G. Thomas, *Nat. Prod. Rep.*, **2009**, *26*, 90–114.

11 B. Shen, *Curr. Opin. Chem. Biol.*, **2003**, *7*, 285–295.

12 P. Kirsch, *Modern Fluoroorganic Chemistry*, **2004**, 3st ed.

13 D. O'Hagan, C. Schaffrath, S. L. Cobb, J. T. G. Hamilton, C. D. Murphy, *Nature*, **2002**, *416*, 279.

14 D. O'Hagan, *Chem. Soc. Rev.*, **2008**, *37*, 308–19.

15 P. Shah, A. D. Westwell, *J. Enzyme Inhib. Med. Chem.*, **2007**, *22*, 527–540.

16 M. B. Van Niel, I. Collins, M. S. Beer, H. B. Broughton, S. K. F. Cheng, S. C. Goodacre, A. Heald, K. L. Locker, A. M. MacLeod, D. Morrison, C. R. Moyes, D. O'Connor, A. Pike, M. Rowley, M. G. N. Russell, B. Sohal, J. A. Stanton, S. Thomas, H. Verrier, A. P. Watt, J. L. Castro, *J. Med. Chem.*, **1999**, *42*, 2087–2104.

17 Y. Kokuryo, K. Kawata, T. Nakatani, A. Kugimiya, Y. Tamura, K. Kawada, M. Matsumoto, R. Suzuki, K. Kuwabara, Y. Hori, M. Ohtani, *J. Med. Chem.*, **1997**, *40*, 3280–3291.

18 H. J. Böhm, D. Banner, S. Bendels, M. Kansy, B. Kuhn, K. Müller, U. Obst-Sander, M. Stahl, *ChemBioChem*, **2004**, *5*, 637–43.

19 B. E. Smart, *J. Fluor. Chem.*, **2001**, *109*, 3–11.

20 D. O'Hagan, H. S. Rzepa, *Chem. Commun.*, **1997**, 645–652.

21 L. Hunter, *Beilstein J. Org. Chem.*, **2010**, *6*, 1–14.

22 P. Shah, A. D. Westwell, *J. Enzyme Inhib. Med. Chem.*, **2007**, *5*, 527–540.

23 D. O'Hagan, *J. Fluor. Chem.*, **2006**, *127*, 1479–1483.

24 P. T. Lowe, S. Dall'Angelo, A. Devine, M. Zanda, D. O'Hagan, *ChemBioChem*, **2018**, *19*, 1969–1978.

25 W. E. Morton, G.O. Lancaster, G.E., Fulmor, W., Meyer, *J. Am. Chem. Soc.*, **1969**, *91*, 1535–1537.

26 C. D. Murphy, C. Schaffrath, D. O'Hagan, *Chemosphere*, **2003**, *52*, 455–461.

27 L. Ma, A. Bartholome, H. Tong, Z. Qin, Y. Yu, *Chem.Sci.*, **2015**, 1414–1419.

28 K. Müller, C. Faeh, F. Diederich, *Science*, **2007**, *317*, 1881–1886.

29 S. Swallow, *Prog. Med. Chem.*, **2015**, *54*, 65–133.

30 C. Isanbor, D. O'Hagan, *J. Fluor. Chem.*, **2006**, *127*, 303–319.

31 R. H. Hesse, D. H. R. Barton, H. T. Toh, M. M. Pechet, *J. Org. Chem.*, **1972**, *37*, 329 –330.

32 C. Y. Kim, J. S. Chang, J. B. Doyon, T. T. Baird, C. A. Fierke, A. Jain, D. W. Christianson, *J. Am. Chem. Soc.*, **2000**, 122, 12125–12134.

33 N. A. Meanwell, *J. Med. Chem.*, **2018**, *61*, 5822–5880.

34 J. M. Domagala, L. D. Hanna, C. L. Heifetz, M. Hutt, T. F. Mich, J. P. Sanchez, M. Solomon, *J. Med. Chem.*, **1986**, *29*, 394–404.

35 J. J. Parlow, R. G. Kurumbail, R. A. Stegeman, A. M. Stevens, W. C. Stallings, M. S. South, *Bioorganic Med. Chem. Lett.*, **2003**, *13*, 3721–3725.

36 E. T. Kool, H. O. Sintim, *Chem. Commun.*, **2006**, 3665–75.

37 J. P. Burkhart, P. M. Weintraub, C. A. Gates, R. J. Resvick, R. J. Vaz, D. Friedrich, M. R. Angelastro, P. Bey, N. P. Peet, *Bioorg.Med.Chem*, **2002**, *10*, 929–934.

38 M. Frederickson, J. R. Coggins, C. Abell, *Chem. Commun.*, **2002**, *2*, 1886–1887.

39 C. Rye, R. Wise, V. Jurukovski, J. DeSaix, J. Choi, A. Yael, *Biology*, **2016**, 1st ed.

40 J. Wang, M. Sánchez-Roselló, J. L. Aceña, C. Del Pozo, A. E. Sorochinsky, S. Fustero, V. A. Soloshonok, H. Liu, *Chem. Rev.*, **2014**, *114*, 2432–2506.

41 G. Valentini, L. Chiarelli, R. Fortini, M. L. Speranza, A. Galizzi, A. Mattevi, *J. Biol. Chem.*, **2000**, *275*, 18145–18152.

42 J. M. Berg, J. Tymoczko, L. Stryer, *Biochemistry*, **2002**, 5th ed.

43 J. Wang, J. Luis, C. Pozo, A. E. Sorochinsky, S. Fustero, V. A. Soloshonok, H. Liu, *Chem Rev*, **2014**, 2432–2506.

44 R. J. Cox, *Introduction to Enzyme and Coenzyme Chemistry*, **2005**, 2nd ed.

45 J. R. Vane, R. M. Botting, *Thromb. Res.*, **2003**, *110*, 255–258.

46 W. F. De Azevedo, F. Canduri, D. M. Dos Santos, J. H. Pereira, M. V. B. Dias, R. G. Silva, M. A. Mendes, L. A. Basso, M. S. Palma, D. S. Santos, *Biochem. Biophys. Res. Commun.*, **2003**, *309*, 917–922.

47 D. Bello, R. A. Cormanich, D. O'Hagan, *Aust. J. Chem.*, **2015**, *68*, 72–79.

2. *DESIGN OF ACETYL-COA ANALOGUES AS INHIBITORS OF CITRATE SYNTHASE*

2.1. Citrate synthase as key enzyme of metabolism

Citrate synthase is present in nearly all living cells capable of oxidative mechanism. It is involved in the condensation of oxaloacetate to form citrate and it is one of a relatively small class of enzymes able to catalyse C-C bond formation without the presence of a metal ion cofactor. It plays a key role in the central metabolic pathway of aerobic organisms, the Krebs cycle, catalysing the irreversible conversion of oxaloacetate **1** and acetyl-CoA **2** to citrate by a condensation reaction. The Krebs cycle, also known as the TCA cycle (tricarboxylic acid cycle) or citric acid cycle, is illustrated in Scheme 1. It represents a central driver for cell respiration: acetyl-CoA **2** is fed through the cycle as a C_2 carrier, in a series of redox reactions. Energy is obtained and stored as chemical potential into NADH, $FADH_2$ and ATP, referred to as reduced electron carriers that in turn transfer their reducing equivalents into the electron transport chain, generating ATP. The Krebs cycle consists of 7 steps, each defined by the specific enzyme catalysing the transformation:[1]

Citrate synthase is the first enzyme involved in the cycle. Pyruvate **3** generated from glycolysis is oxidised to acetyl-CoA **2** by the pyruvate dehydrogenase complex. Acetyl-CoA **2** then enters the citric acid cycle and is converted to citrate **208** by citrate synthase.

Aconitase: Citrate is isomerized into isocitrate **213** by a dehydration-hydration sequence through *cis*-aconitase. The reaction is mediated by aconitase, an iron-sulfur enzyme. Catalytic residues His-101 and Ser-642 are involved respectively in the protonation and deprotonation step.

Isocitrate dehydrogenase: mediates the oxidative decarboxylation of isocitrate **213** to α-ketoglutarate **214**. The reaction proceeds by oxidation of isocitrate **213** to form oxalosuccinate which loses CO_2 and generates α-ketoglutarate **214**.

α-*Ketoglutarate dehydrogenase*: A further oxidative decarboxylation converts α-ketoglutarate **214** into succinyl-CoA **215**, generating NADH.

Succinyl-CoA synthetase: catalyses the conversion of succinyl-CoA **215** to succinate **216**.

Succinate dehydrogenase: mediates the oxidation of succinate **216** to fumarate **217**. The mechanism of the oxidation is not clear but it is believed to proceed by a concerted dehydrogenation reaction with concomitant reduction of FAD^+.

Fumarase: Fumarate **217** undergoes a stereospecific hydration reaction to form L-malate **218**.

Malate dehydrogenase: L-malate **218** is finally oxidised to oxaloacetate **206** with production of NAD^+.

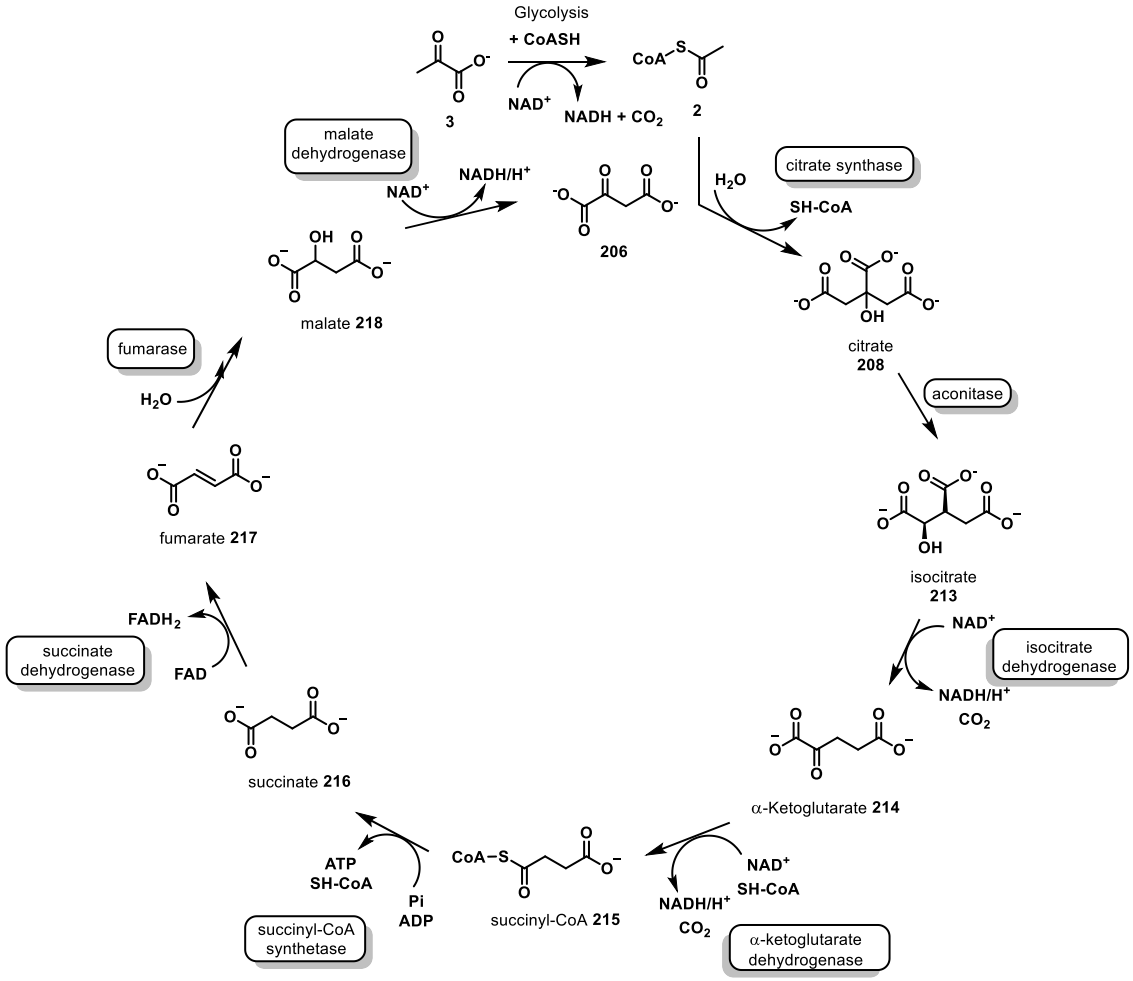

Scheme 2.1. The citric acid cycle.[1]

2.2. Structure and mechanism of porcine citrate synthase

Citrate synthase has been isolated from multiple sources. The most common form is porcine which consists of a homodimer of molecular weight 90-100 kDa; however a tetrameric form with a large subunit molecular weight (about 60 kDa) is found in some prokaryotic organisms.[2,3] Porcine citrate synthase consisting of two identical subunits of 437 amino acids whose structure has been determined by X-ray crystallography.[4] The free enzyme is an open form with two domains forming a cleft that contains the substrate-binding site; on binding oxaloacetate the smallest domain rotates by 18° leading to cleft closure. The existence of an open and closed structure explains the enzyme ordered kinetic sequence. The conformational change generates the acetyl-CoA **2** binding site and closes the oxaloacetate **206** binding site, preventing any interaction between the solvent and the bound substrate. Citrate synthase catalyses the condensation reaction with its open conformation, by bringing the substrates (oxaloacetate and acetyl-CoA) and the amino acid residues closer in the active site. Once citrate is generated, co-enzyme A is released and the enzyme returns to its open form.

The proposed mechanism as described by Remington *et al.*[3] in1986 (Scheme 2.2), involves the participation of three ionisable side chains in the active site for acid-base catalysis: His-274, His-320, Asp-375 .

- *Deprotonation step*: Asp-375 acts as a base removing a proton from the methyl group of acetyl-CoA **2**, forming its enolate **31**. His-274 stabilises the acetyl-CoA intermediate **31** by hydrogen bonding with the enolate oxygen.
- *Condensation reaction*: the enolate of acetyl-CoA **31** acts as nucleophile, attacking the carbonyl group of oxaloacetate **206**; His-320 acts as a general acid, donating a proton to the oxaloacetate **206** carbonyl group in a concerted step with inversion of configuration, forming citryl-CoA **219** bound to the enzyme.
- *Hydrolysis reaction*: in this step, citryl-CoA **219** is hydrolysed to citrate **208** and Co-ASH; it is suggested that residue His-320 deprotonates a nearby water molecule that acts as the nucleophile attacks citryl-CoA **219**. Release of the CoA and citrate **208** involves the switch from the closed to the open conformation of the enzyme (Scheme 2.2)[5].

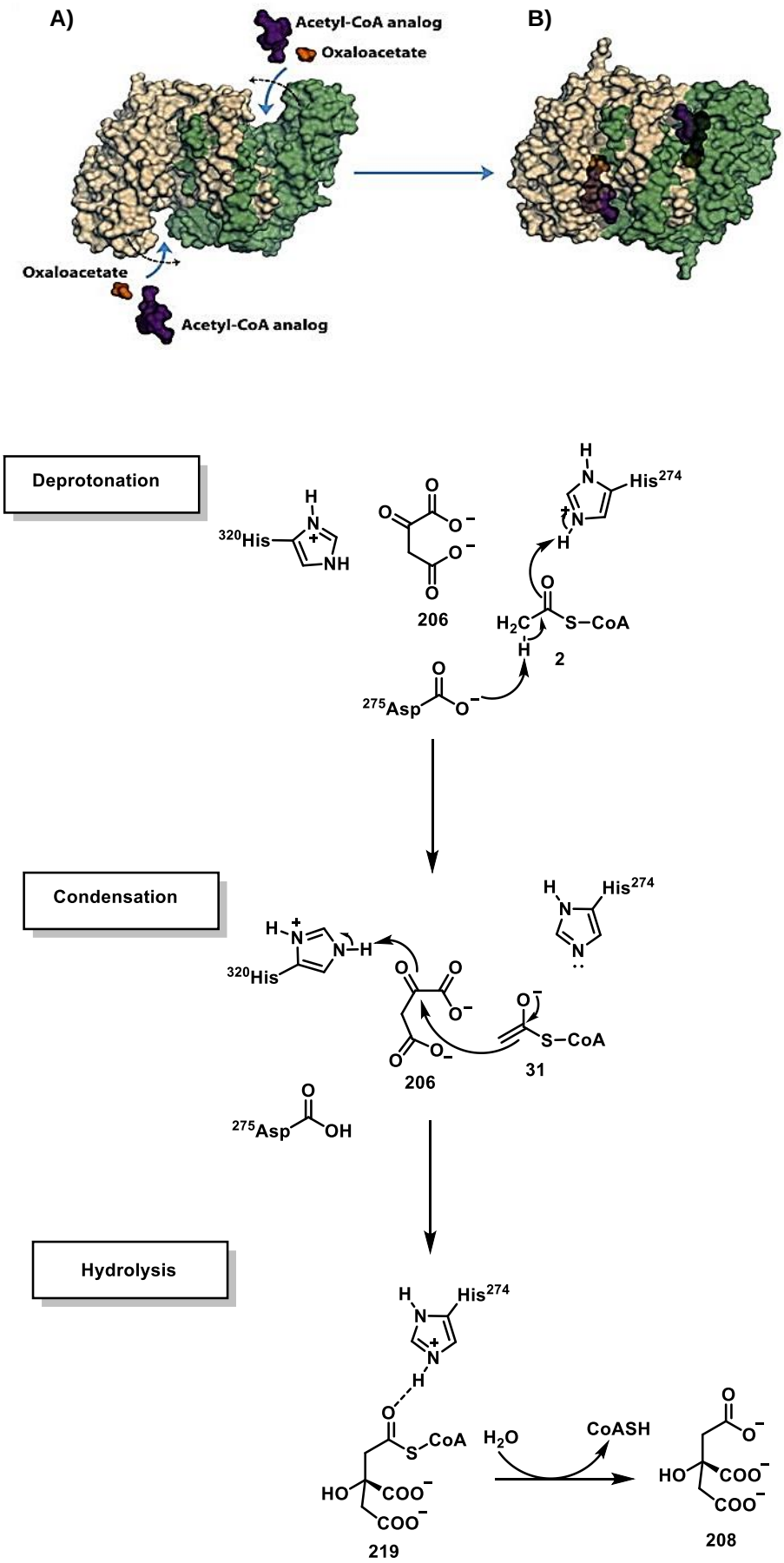

Scheme 2.2. Citrate synthase mechanism. [3,6]

The flexible domain of each subunit of the enzyme undergoes a conformational change on binding oxaloacetate and generating a binding site for acetyl-CoA **2**: **A** is the open form of the enzyme and **B** is closed with oxaloacetate bound.[5,6]

2.3. Citrate synthase inhibition

Mitochondrial citrate synthase from human omental adipose tissue is associated with endocrinal and metabolic abnormalities like obesity and diabetes, suggesting that citrate synthase activity could be used as a biomarker for such diseases. The need to fully understand the structure and mechanism of this enzyme has stimulated the design and synthesis of a series of inhibitors that mimic acetyl-CoA **2** or oxaloacetate **208**.

2.4. The historical debate on the nature of the acetyl-CoA intermediate in the condensation step

Attention has focused on the identification of the nucleophilic intermediate in the citrate synthase-mediated reaction, in order to establish whether the reaction proceeds *via* the enol or enolate form of acetyl-CoA. Karpusas *et al.*[4] proposed a mechanism for the condensation reaction step of citrate synthase in 1990, described in Scheme 2.2. This study was based on the 1.9 Å resolution structure of the ternary complex citrate synthase-oxaloacetate-carboxymethyl-CoA, the latter being a potent inhibitor of citrate synthase.[4] The hydrogen bond angles, calculated from the electronic density map of the ternary complex, indicate that the carboxylate of carboxymethyl-CoA **220** interacts with Asp-375 and His-274 through almost ideal hydrogen bond geometries. This arrangement resembles more closely the configuration of the transition state of acetyl-CoA as shown in Scheme 2.3. The overall mechanism proposed is that reported by Remington *et al*.[3] in Scheme 2.2. The deprotonation of acetyl-CoA by Asp-375 results in the formation of an enol **207** rather than an enolate **31** whose generation would have required a higher energy, incompatible with the observed kinetics. Enol **207** is stabilised by hydrogen bonding to His-274. The mechanism proposed for the condensation step suggests the protonation of the carbonyl oxygen of oxaloacetate **206** by His-320. The nucleophilic attack of the enol **207** to oxaloacetate **206** is controlled by the hydrogen bond to His-274. The X-ray structure obtained for the ternary complex of citrate synthase with L-malate and acetyl-CoA at 2.2 Å also supports the hypothesis that His-274 acted as a general acid in the enolization step while Asp-375 acted as a general base.[4]

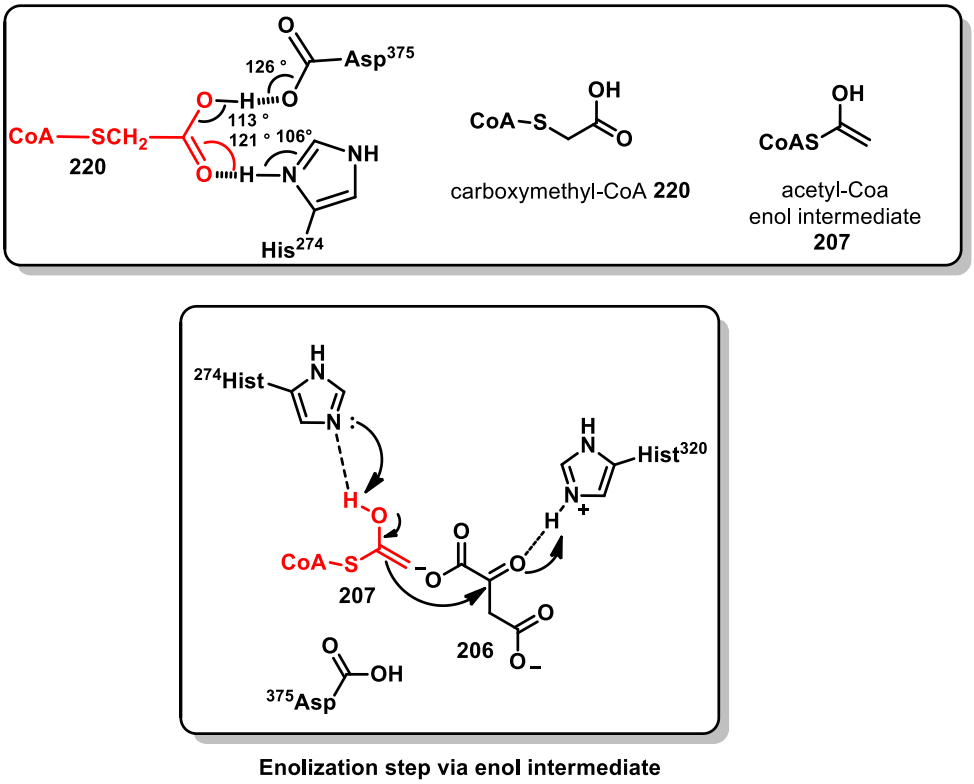

Scheme 2.3. Study of the deprotonation step via enol intermediate by Karpusas *et al*.[4]

Enol formation was also supported by an early theory study (1994) by O'Hagan and Rzepa [7] investigating the stereospecific control of the conversion of fluoroacetyl-CoA **221** to (*2R*,*3R*)-fluorocitrate **224** by citrate synthase (Scheme 2.4). In the condensation step, citrate synthase appears to be highly selective favouring the abstraction of the 2-*pro*-S hydrogen atom over the 2-*pro*-R; the condensation thus effectively proceeds with inversion of configuration at the prochiral centre, resulting in the attack onto the *Si*-face of the α-carbonyl of oxaloacetate **206**. Kinetic isotope data for citrate synthase[8] indicated that the rate-limiting step is the deprotonation step. Consequently, the selective discrimination of fluoroacetyl-CoA **221** prochiral hydrogens appears to be related to the relative energies of the *syn* or *anti* orientation of the C-F bond with respect to the oxygen atom of the newly formed neutral enol or enolate intermediates. A computational study[7] evaluated the relative energies of the two isomers enol/enolate and suggested that the *E*- configuration **222** was lower in energy than the *Z*- configuration **225** suggesting an enol rather than an enolate intermediate.

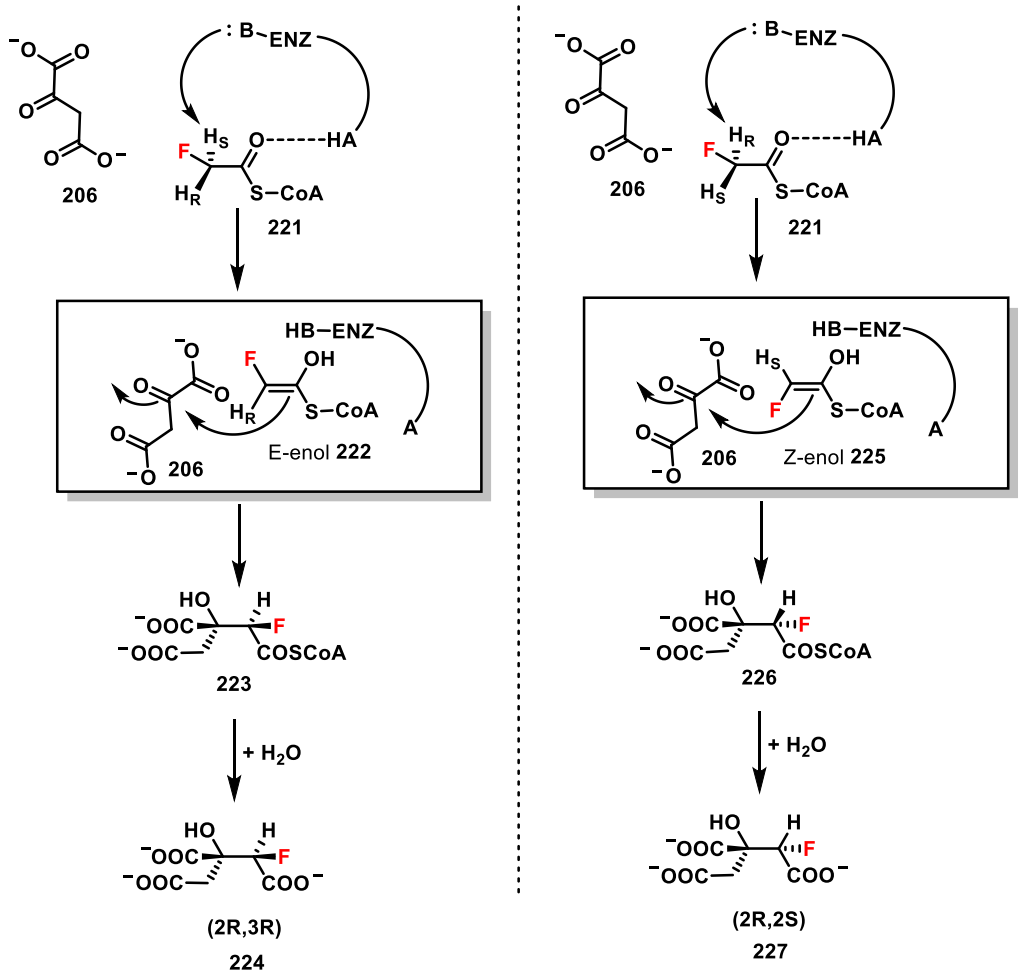

Scheme 2.4. Theory study of the stereospecific control of citrate synthase catalysed condensation reaction of fluoroacetyl-CoA **221** as mimic of acetyl-CoA.[7]

In contrast, the work of Mulholland *et al.*[7] supported the idea that the nucleophilic intermediate involved in the condensation step is indeed an enolate.[7] In their work published in 1998, they reported a quantum mechanical/molecular mechanical (QM/MM) study of the enolization step of acetyl-CoA within the active site. Calculations were based on the 1.9 Å resolution structure of the ternary complex of chicken citrate synthase (closed conformation) with acetyl-CoA **2** and *R*-malate bound to the enzyme in the same conformation as oxaloacetate **206**.[4] It appears that His-274 and His-320, both being neutral, are fundamental for the stabilization of the enolate **31**. As shown in Scheme 2.5, the carbonyl oxygen of acetyl-CoA **2** is stabilised at the active site by hydrogen bonding with His-274; after enolate **31** formation, this bond is further strengthened by the interaction with the negative charge on the enolate oxygen **31**. Calculations of the activation energies reported for the citrate synthase reaction indicate that enolate **31** is stabilised relative to the substrate by ΔG = 11.5 - 15 kcal / mol. This stabilisation is crucial

to the catalytic strategy of citrate synthase, explaining the fastest step being associated with deprotonation. The enolate **31**, being a good nucleophile, should react faster than an enol **207**.[9]

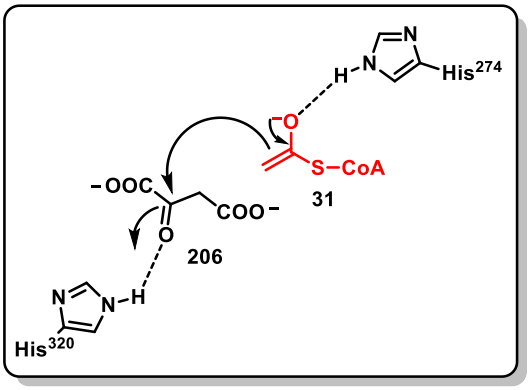

Scheme 2.5. Enolization step catalysed by citrate synthase via acetyl-CoA enolate **31** intermediate.[9]

Van der Kamp and Mulholland [10] also investigated the enantioselective conversion of fluoroacetyl-CoA to fluorocitrate described in Scheme 2.4. The QM/MM energy profiles obtained for the *E*- and *Z*-isomers, showed that the enantioselectivity emerges mostly from the energy difference between the *E*- and *Z*-enolates**,** hence favouring the *E*-configuration**,** and to a lesser extent, interactions with the enzyme active site. These findings also suggests that the rate limiting step is the formation of citryl-CoA rather than the deprotonation step as previous suggested.[10]

2.5. *Acetyl-CoA analogues as inhibitors of citrate synthase: insights into the structure and the catalytic mechanism*

In 1974, Johansson and Petersson reported a kinetic study on the inhibition of citrate synthase by adenosine triphosphate (ATP), propionyl-CoA and 2-oxoglutarate. Propionyl-CoA was a competitive inhibitor showing a similar binding affinity to acetyl-CoA. The affinity of acetyl-CoA and propionyl-CoA with the enzyme seems to increase significantly with oxaloacetate bound. This increased binding affinity, appears to be associated with the interaction of enzyme-bound oxaloacetate and the acyl groups of acetyl-CoA and propionyl-CoA in the correct orientation for reaction. ATP and oxoglutarate are both competitive inhibitors of citrate synthase both binding equally strongly to the free enzyme or when it is bound to the other substrates. The kinetic study showed a cooperativity between the substrate binding sites that could explain the ordered nature of the reaction mechanism and the high specificity of the enzyme.[10]

In 1981, Bayer *et al.*[11] provided evidence on the conformational changes of citrate synthase during the catalytic cycle (Scheme 2.2). They reported the synthesis of five analogues of acetyl-CoA described in Figure 2.1. Carboxymethyl-CoA **220**, a transition state analogue of acetyl-CoA, is the most powerful non-competitive inhibitor (K_i = 0.47 µM). Carboxylate **220** has a formal negative charge as does the enolate of acetyl-CoA. Malonyl-CoA **230**, carboxyethyl-CoA **229** and ethyl-CoA **231** are poor inhibitors of the enzyme, presumably not satisfying the structural requirements for analogues of any intermediate state. Amide **228** displays a good inhibitory potency (Ki = 2 µM) towards the enzyme. The increased affinity of the analogues after oxaloacetate **206** is bound, is consistent with the conformational change on binding oxaloacetate described previously.

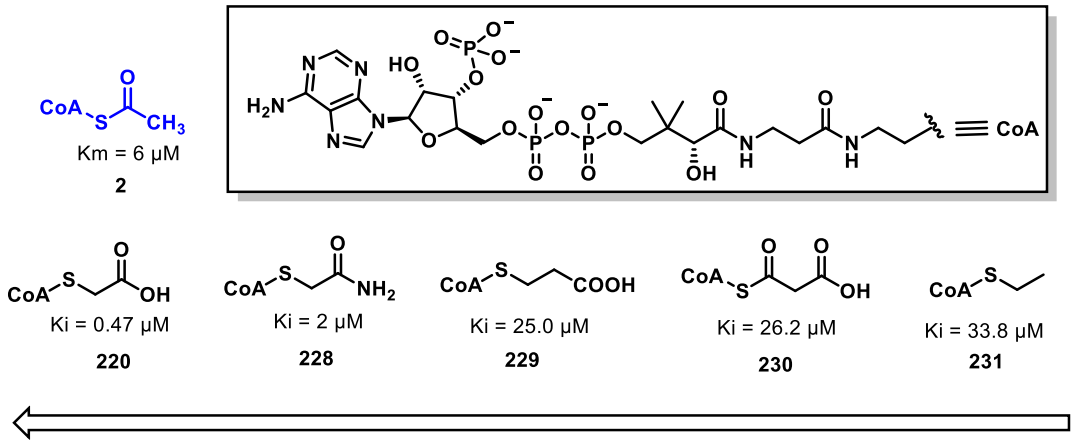

Figure 2.1. Inhibition studies for conformational changes of citrate synthase.[11]

Martin *et al.*[12] have reported a combined chemical and enzymatic synthesis of a series of dethia analogues of acetyl-CoA, replacing the sulfur atom with a methylene group (Scheme 2.6).[12]

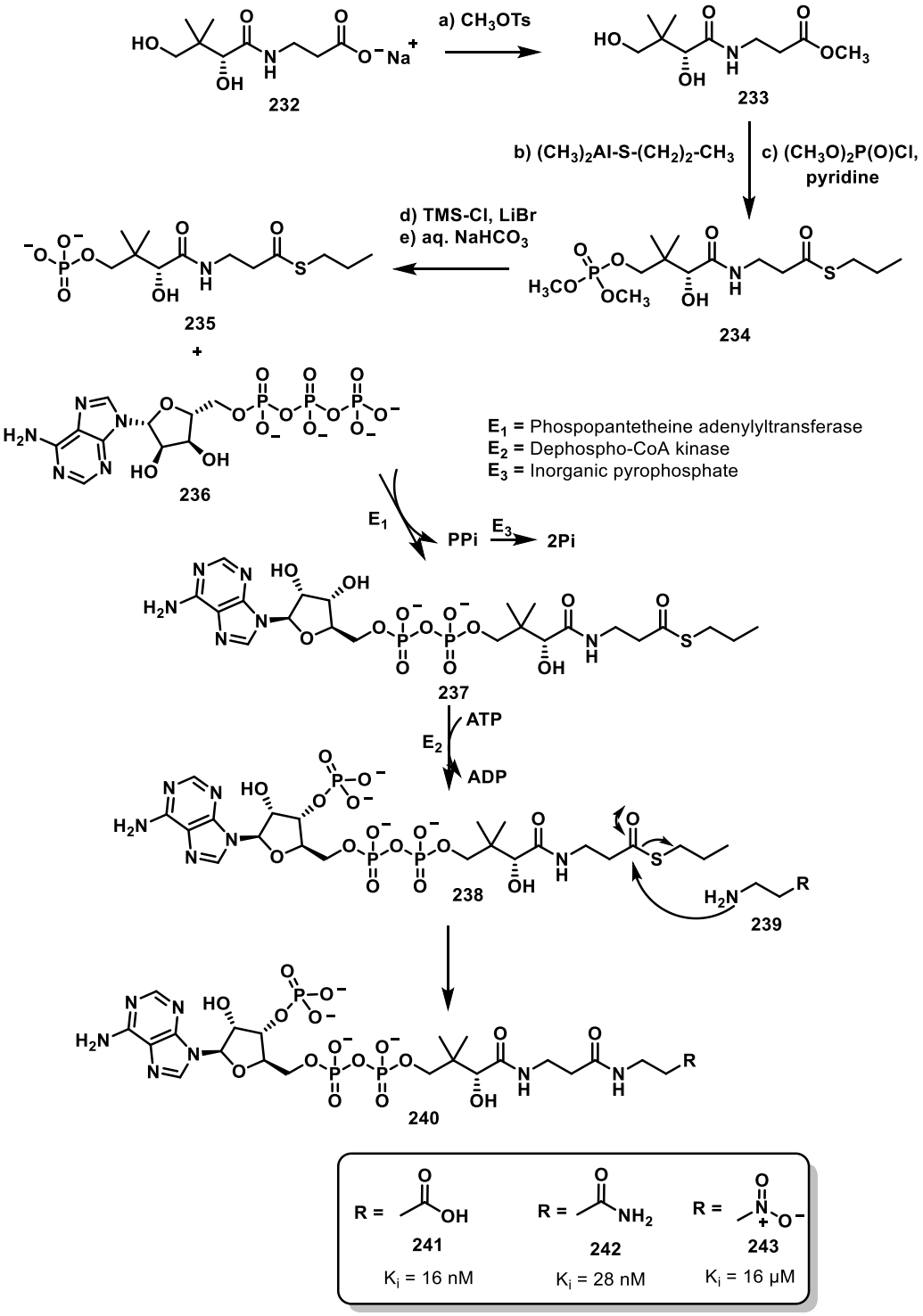

Scheme 2.6. Chemoenzymatic synthesis of dethia acetyl-CoA analogues by Martin *et al*.[12]

Tosylation of sodium pantothenate **232** generated the methyl thioester **233** which was converted to the propyl thioester by treatment with dimethyl-(propylthio)-aluminium reagent. Subsequent phosphorylation generated the dimethyl phosphate **234**, which was in turn treated with trimethylsilyl chloride and lithium bromide furnishing phosphate **235**. This compound was then incubated with ATP and phosphopantetheine adenylyl transferase to generate **237** which was phosphorylated by incubation with ATP and dephospho-CoA kinase, yielding thioester **238**. The corresponding amines **239** were reacted with **238** to give the acetyl-CoA analogues **241**, **242** and **243**.

Carboxylate **241** was found to be a potent competitive inhibitor of citrate synthase (*K*i = 16 nM); the negative-charged oxygen of the carboxylate is spatially located to bind the site of the oxygen of the enolate of acetyl-CoA **2**, thus approximating the latter both electronically and sterically.

A strong binding affinity to citrate synthase was also observed for the amide analogue **242**, with a *K*i = 28 nM. The amide group is both a good hydrogen bonding donor and acceptor with a polarised carbonyl and provides good binding to the enzyme with a good spatial positioning with respect to acetyl-CoA or its enolate. The nitro alkyl derivative **243** exhibits a much lower affinity for citrate synthase, with a *K*i = 16 µM. This is clearly a less ideal mimic of the enol/ate intermediate compared to the previous two substrates **241** and **242**, with nitro not being a good hydrogen bond acceptor.

With respect to the work reported by Martin *et al*.[12] for the synthesis of the potent inhibitors **241** and **242**, Usher *et al.* [13] carried out a crystallography study on the hydrogen bond strength variation in the enzyme-inhibitor complexes. They found that the hydrogen bonds between the carboxylate oxygen of compound **241** and the carboxylate oxygen of Asp-375 are uncommonly short (Figure 2.2). Compound **242** displays a longer hydrogen bond (2.38 Å) than that of compound **241** (2.49 Å) but it also appears to be still unusually short. This experimental evidence suggests strong binding.

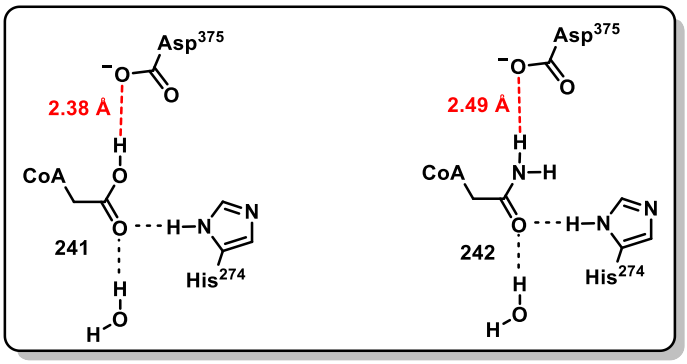

Figure 2.2. Hydrogen bonding patterns of analogues **241** and **242**. [13]

The proposed role of short hydrogen bonding in enzyme catalysis is believed to be correlated to the pKa match between the enzymatic residues at the active site and the substrate. In 1995, Swartz *et al.* [14] explored the *α*-fluoro analogues of the potent inhibitors **244** and **245**, with the aim of probing their inhibitory potency towards citrate synthase and to investigate the effect of pKa matching on binding affinity and hydrogen bond length of **241** and **242** (Figure 2.3). Fluorinated analogues **244** and **245** were less potent inhibitors than **241** and **242**. The decreased binding affinity is believed to be associated with the larger fluorine causing unwanted steric interactions with the amino acid residues in the active site. Also, the possibility of fluorine being freely solvated could affect its interactions in the active site.

The data based on the crystal structures of citrate synthase with **244** and **245** showed that for **244**, the hydrogen bond with Asp-375 was similar (2.3 Å to 2.6 Å) with respect to that calculated for the system **241**-Asp-375 (2.4 Å), whereas for **245** only one stereoisomer was observed to bind, with a calculated hydrogen bonding distance also similar (2.51 Å) to that of **242** (2.49 Å). The results obtained did not support any correlation between hydrogen bond strength and hydrogen bond length in the enzyme-inhibitor complexes.

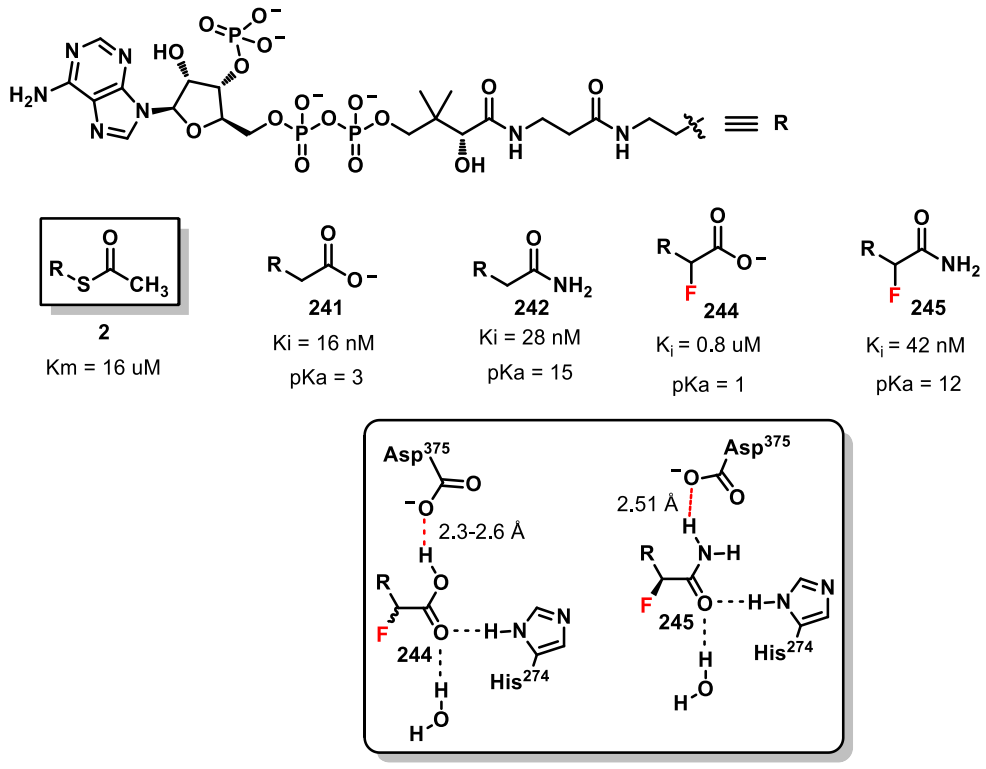

Figure 2.3. α-Fluoro acid **244** and *α*-fluoro amide **245** analogues of acetyl-CoA.[14]

Vogel *et al.* [15] described a modification of the method previously used for the synthesis of Co-A analogues (described in scheme 2.6);[12] by preparing intermediate **248**. Acyl-CoA **248** was prepared by nucleophilic acyl substitution of **238** with amine **246**. Acidic hydrolysis of tris-thio-ortho ester analogue **247** gave CoA analogue **248**.

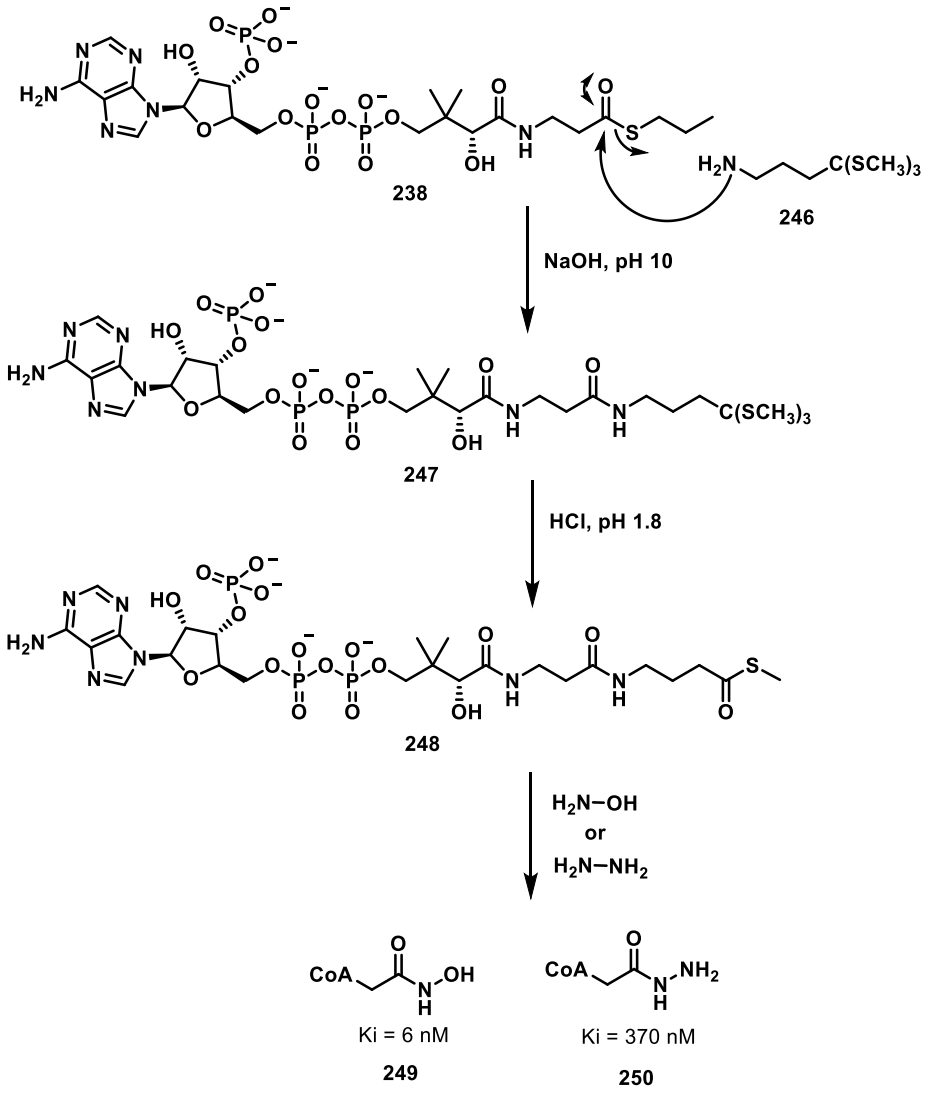

Scheme 2.7. Synthesis of hydroxamate **249** and hydrazide **250**.[15]

Hydroxamate **249** and hydrazide **250**, were prepared by nucleophilic acyl substitution of **248** with hydroxylamine and hydrazine, respectively. Hydroxamate **249** turned to be the most potent competitive inhibitor of citrate synthase reported to date, with a K_i of 6 nM, slightly better than compounds **241** and **242** described in Scheme 2.6. Hydrazide **250** was also found to be a good competitive inhibitor; although with a K_i = 370 nM two order of magnitude less potent (Scheme 2.7).

2.6. *Project background: Design of a fluorovinyl thioether analogue of the enol/ate form of acetyl-CoA*

This project aimed to explore the stereo-electronic compatibility between a fluorovinyl thioether and an enol/ate thioester motif. The fluorovinyl thioether mimics the enol/ate motif where fluorine replaces the oxygen on the enolate. Oxygen and fluorine have similar electronegativity (F = 3.98 versus O = 3.44) and Van der waals radii values (F = 1.47Å versus O = 1.52Å) sharing a similar steric and electronic profile.

As described previously in Chapter 1, it was found a clear spacial and electronic similarity between thioester enol **210** and fluorovinyl thioether **211**.[10]

Given the close steric and electronic profiles of these motifs, our group became interested in designing a fluorovinyl thioether motif as a mimetic of the enol/ate form of acetyl-CoA **2**. Thus fluorovinyl-CoA (FV-CoA) **212** was evaluated as an inhibitor of pig heart citrate synthase. Analogue **212** emerged to be a low micromolar inhibitor with a Ki of 4.4 μM and with a higher affinity for the enzyme than acetyl-CoA **2** (Km = 5.8 μM) (Figure 2.4).

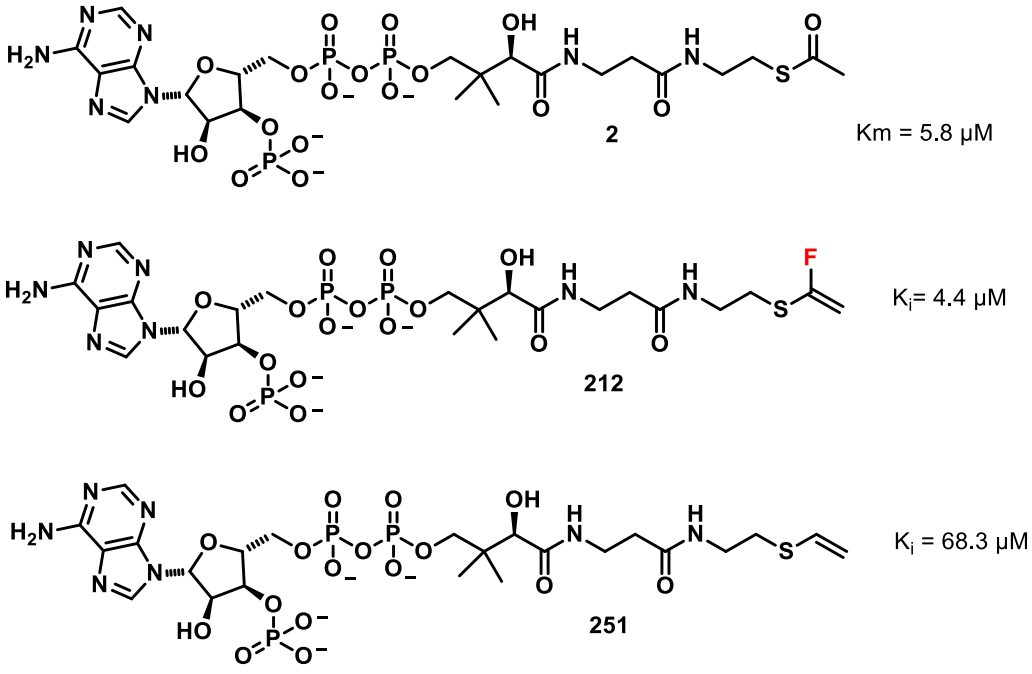

Figure 2.4. Fluorovinyl thioether **212** and defluoro hydrate **251** analogues of acetyl-CoA.

The vinyl thioether **251** (K_i^{app}= 68.3 μM) was also synthesized as a control. By comparing **212** and **251** a clear "fluorine effect" was demonstrated. This was supported by QM computational studies that calculated that fluorovinyl thioether-CoA binds more strongly then vinylthioether-CoA, as evidenced through shorter hydrogen bond distances (2.02 Å

F…H-His & 2.00 Å F…H-water). This is consistent with fluorine participating in hydrogen bonding interactions in the pre-organised active site and it also indicates that compound **212** mimics an enolate rather than an enol intermediate.[16]

2.7. Synthetic approaches to acetyl-CoA analogues

Different strategies have been developed for the synthesis of acetyl-CoA analogues in the past. As described previously in Scheme 2.6, Martin *et al.*[12] reported a combined chemical and enzymatic synthesis of potent inhibitors **241** and **242**. A modified version of this method was also used by Vogel *et al.*[15] to generate **249** and **250** reported in Scheme 2.7. Acetyl-CoA analogues can be also prepared from the appropriately modified pantothenyl motif using the protocol reported by Wright *et al.*[17] using the recombinant CoA enzymes. PanK (pantothenate kinase), PPAT (phosphate adenylate kinase) and DPCK (dephospho coenzyme-A kinase) to generate the acetyl-CoA derivative. A modified procedure using the three *Escherichia coli* enzymes was used by Tosin *et al.*[18] for the synthesis of dethiamalonyl-CoA analogues **256** (Scheme 2.8).[18]

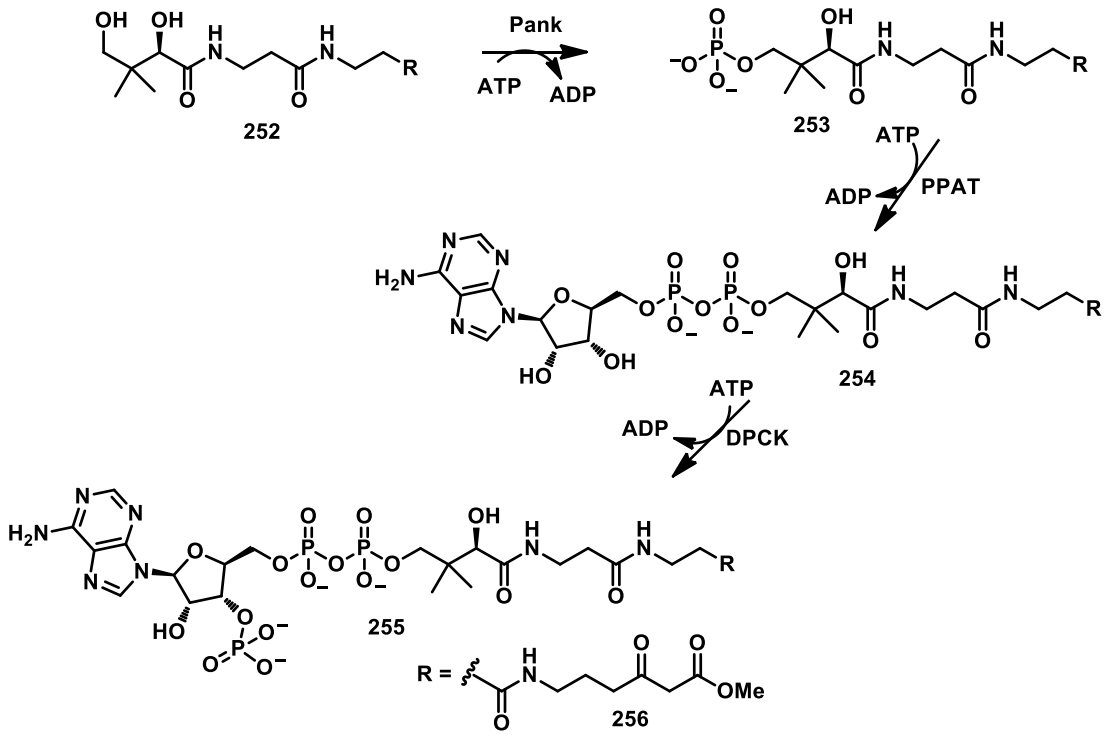

Scheme 2.8. Preparation of acetyl-CoA analogues by Wright *et al.*[17,18]

Recently, Sanichar *et al.*[19] explored a boric acid mediated one-step transamidation reaction with a suitable amine under mild conditions, leading to useful CoA analogues from CoASH in reasonable yields and good conversions (Scheme 2.9).

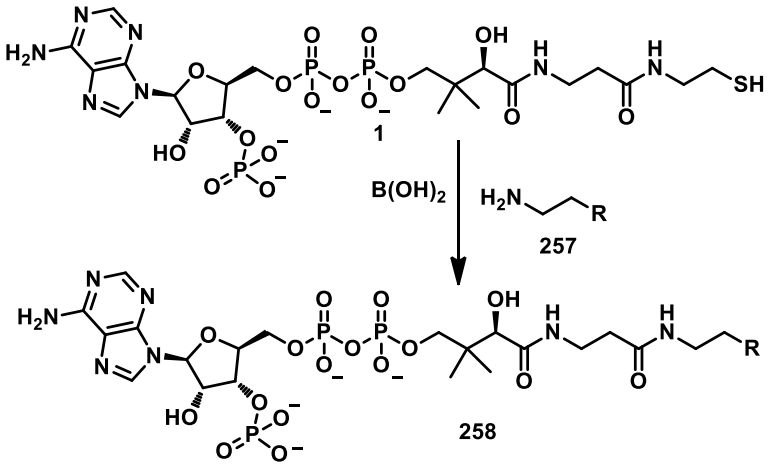

Scheme 2.9. Synthesis of acetyl-CoA derivatives via transamidation.[19]

2.8. Design of dethia fluoro vinyl-CoA 261 and analogue 262

Following from the recent inhibition of citrate synthase by fluorovinyl thioether analogue **212** in the St Andrews laboratory,[16] a dethia fluorovinyl-CoA analogue **261** was envisaged as a target. An acetyl-CoA-analogue can be synthesised from the appropriately modified pantothenyl motif using the protocol reported by Wright *et al.*[17] (Scheme 2.10) The synthesis of compound **260**, as a non-fluorinated control, was also envisaged to assess any fluorine effect associated with inhibition.

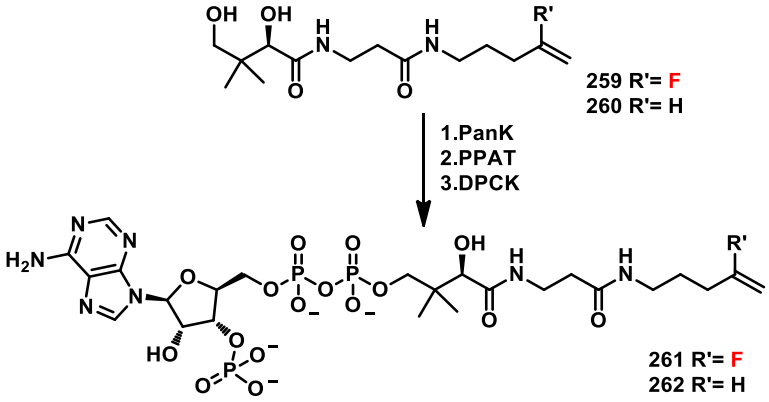

Scheme 2.10. Synthesis of dethia analogue of acetyl-CoA **261** and **262**.[16,17]

2.9. Cloning of PanK, PPAT and DPCK proteins

The cloning and the over-expression of Pank, PPAT and DPCK enzymes were carried out by Dr Nouchali Bandaranayaka at the University of St Andrews, following previously published procedures.[17]

In order to prepare the coenzyme-A analogues, the three enzymes involved in the biotransformation required to be over expressed. PanK and PPAT were cloned into pET29b and DPCK cloned into pET20b (+) plasmids by using modified primers (see Chapter 5, Experimental Part). These plasmids were gifted by Dr Manuela Tosin from the University of Warwick.[18] Due to overexpression inconsistencies DPCK gene was PCR amplified using DPCKFP and DPCKRP and cloned into pEHISTEV plasmid.[20] PanK and PPAT recombinant plasmids were transformed into BL21 gold (DE3) cells (Agilent) and DPCK-pEHISTEV was transformed into BL21-codonPlus (Agilent) for over expression of the respective proteins according to previously published procedures.[16,17]

2.10. Over-expression and purification of PanK, PPAT and DPCK proteins

Luria Broth LB (20 mL) supplemented was inoculated with kanamycin (100µg/ml for PanK and PPAT) or ampicillin (100µg/ml for DPCK) and incubated at 30℃ for 16h. Baffled shake flasks (2L) containing LB media (1L) and kanamycin (100 µg/mL) antibiotic (Pank, PPAT) or ampicillin (DPCK) and 1mL of the overnight inoculated culture (LB inoculated with kanamycin or ampicillin) were cultured and incubated at 37°C until the optical density reached (OD_{600}) 0.6. The cultures were induced by addition of IPTG and incubated at 25°C with shaking for 20h before harvesting by centrifugation. The cells were disrupted after addition of deoxyribonuclease I from bovine pancreas and 2 tablets of Mini protease inhibitor cocktail. The lysate was filtrated and centrifuged. The protein (Pank/PPAT/DPCK) was purified by affinity chromatography using a Ni^{2+} Sepharose column. Bound protein was washed (50mM HEPES pH 7.5, 500mM NaCl+ 30mM imidazole pH 7.5) four times and eluted (50mM HEPES pH 7.5, 500mM NaCl+ 250 mM imidazole pH 7.5) three times. SDS-page analysis of all the fractions showed the elution fractions were freed of other proteins, thus they were pooled and dialysed against 4 L of buffer (50mM HEPES pH 7.5 + 100mM NaCl) to remove imidazole and other salts from the protein. The dialysed protein was then concentrated by filter centrifugation until the desired concentration (10mg/mL) was achieved.

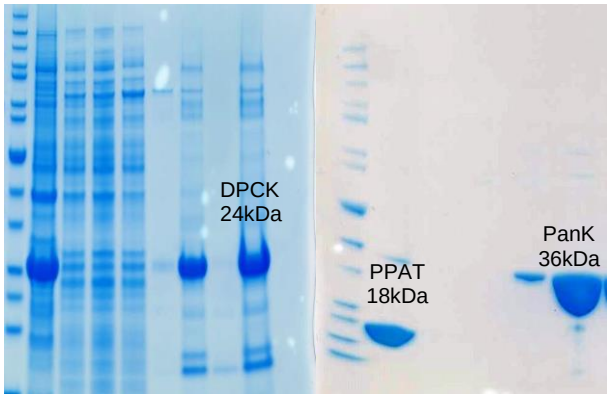

Figure 2.5. SDS-page gel of purified PanK, PPAT and DPCK proteins. [16–18]

2.11. Synthetic approaches to fluoroalkenes

Several methods have been developed for the synthesis of fluoroalkenes but most of the common approaches give mixtures of *E*/*Z* diastereoisomers which can be challenging to separate. One of the common synthetic approaches reported for the synthesis of fluoroalkenes is to start from a fluoro bromo alkene **267**. These can be synthetised via Wittig chemistry promoted by a diethyl zinc **266**, with aldehydes and ketones **263**. The first step of the reaction involves the formation of phosphonium salt **268** generated by the reaction between triphenylphosphine **265** and tribromofluoromethane **264** as illustrated in Scheme 2.11. Debromination of phosphonium salt **269**, to give the key ylide intermediate **270**, is promoted by phosphine **265** or activated zinc **271**. The aldehyde or ketone **263** acts as a trapping agent shifting the equilibrium from the phosphonium salt **269** towards the ylide **270**.[21] The reaction generally gives good yields of the *E*/*Z* products **267** but moderate stereoselectivity.

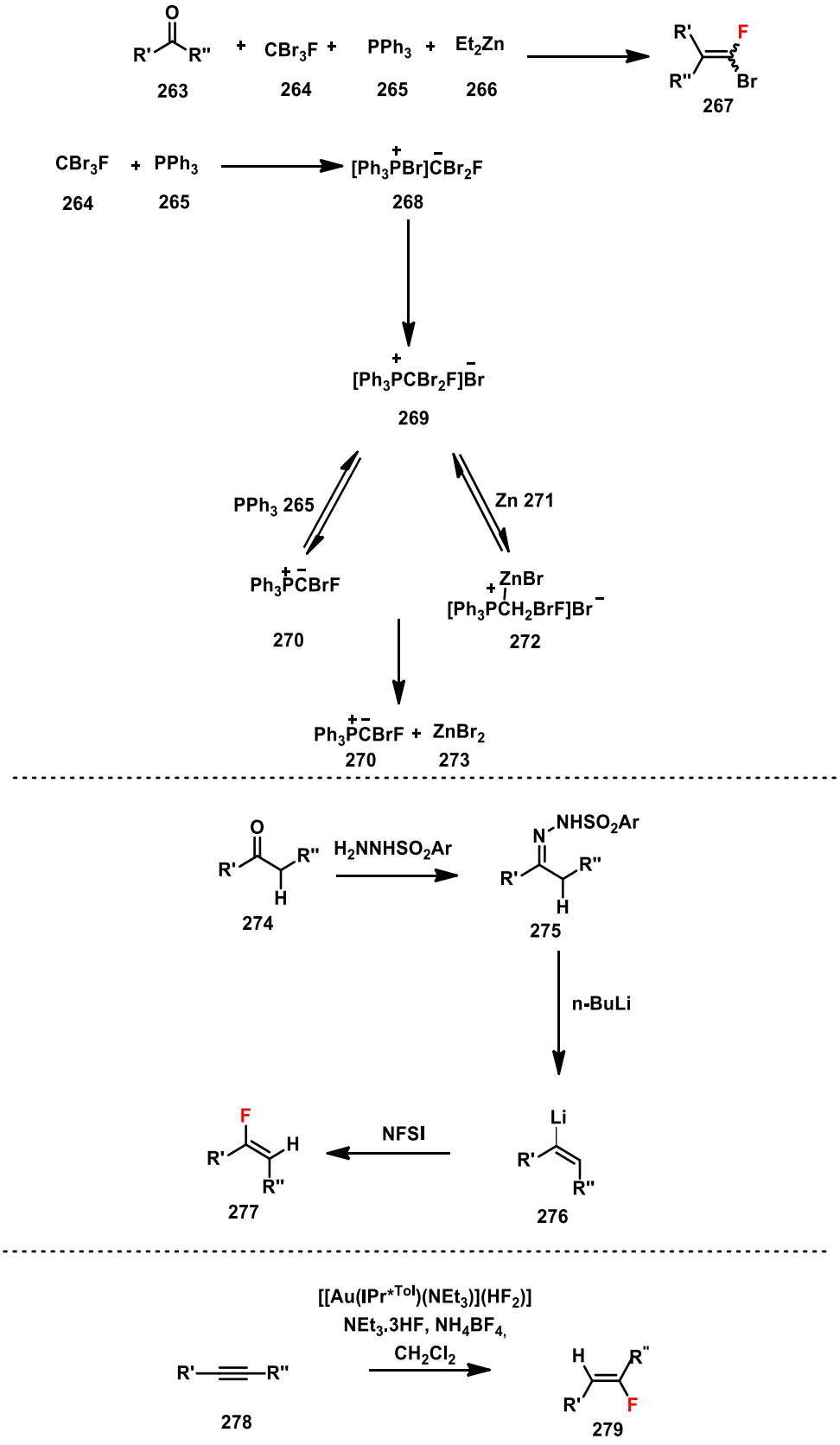

Scheme 2.11. Previous synthetic approaches to fluoroalkenes.[21–23]

A stereoselective synthesis of fluoroalkenes **277** has been developed by Yang *et al.*[22] This is a Shapiro fluorination that involves the condensation of a N-sulfonyl hydrazine with a ketone, to give a N-sulfonyl hydrazone **275**. An n-butyllithium promoted elimination generates vinyllitihum **276**, that reacts with N-fluorobenzenesulfonimide (NFSI) to give fluoro olefins **277** in high stereoselectivity. This can be *E* or *Z* accordingly to the nature of the ketone used. The method has been used to access new fluorinated analogues of natural products including steroids.

High regioselectivity for the synthesis of fluoroalkene motifs was also achieved by N-heterocyclic carbene gold mediated hydrofluorination of alkynes **278**,[23] yielding just the *Z* isomer **279** (Scheme 2.11).

2.12. Synthetic approach to vinylfluoride 259

It was envisaged that pantothenyl precursor **259** could be prepared from fluoro vinyl amine **281** which itself could derive from phthalimide **282** as illustrated in Scheme 2.12.[16]

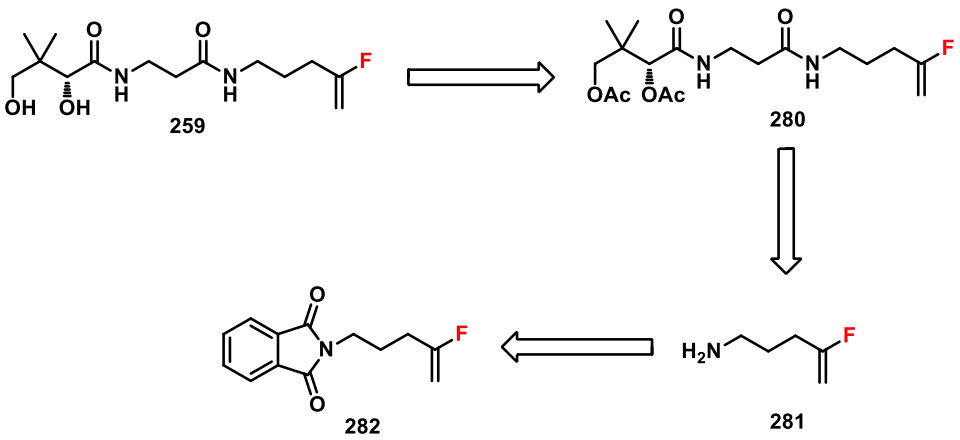

Scheme 2.12. Retrosynthetic approach to the synthesis of pantothenyl **259**.[16]

The first synthetic method in the literature for the synthesis of phthalimide **282** progressed via fluoro-bromination using N-bromo succinimide and triethylamine hydrogenfluoride to generate the bromo-fluoro regioisomers **285**.[24] The mechanism presumably proceeds via bromonium intermediate **284** followed by a nucleophilic substitution to give the two isomers (Scheme 2.13). However, the reaction was poor with low conversion and only a trace of the desired bromo fluoro alkene was generated.

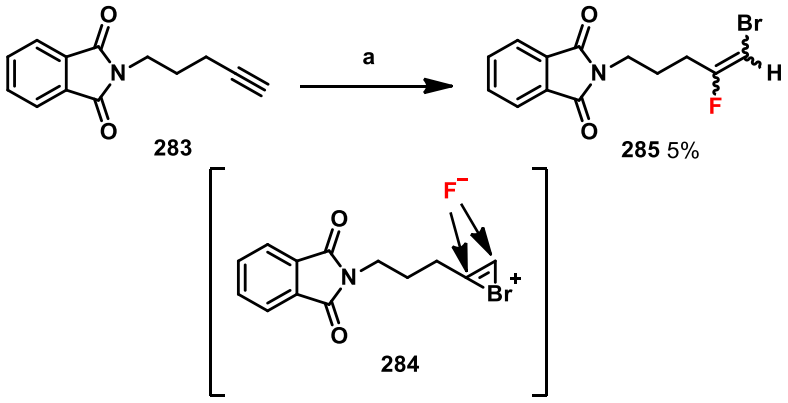

Scheme 2.13. Bromo-fluorination of alkyne **283**: a) NBS, Et_3N HF, DCM, RT.[24]

The only other method previously described for the synthesis of **282** is illustrated in Scheme 2.14. It involved gold catalyzed hydrofluorination of alkynes [23] using the DMPU-HF complex as the source of hydrogen fluoride. 1,3-Dimethyl-3,4,5,6-tetrahydro-2(1H)-pyrimidinone (DMPU) is a better hydrogen bond acceptor (pK_{BHX}= 2.82) than pyridine (pK_{BHX}= 1.86) or triethylamine (pK_{BHX}= 1.98). This makes DMPU-HF complex more acidic than the Et_3N-HF and Py-HF complexes. The gold phthalimide-complex [25] **286** promotes the hydrofluorination and no reaction is observed without this catalyst. Terminal and internal alkynes were successfully monofluorinated with high control of regioselectivity and in excellent yields.

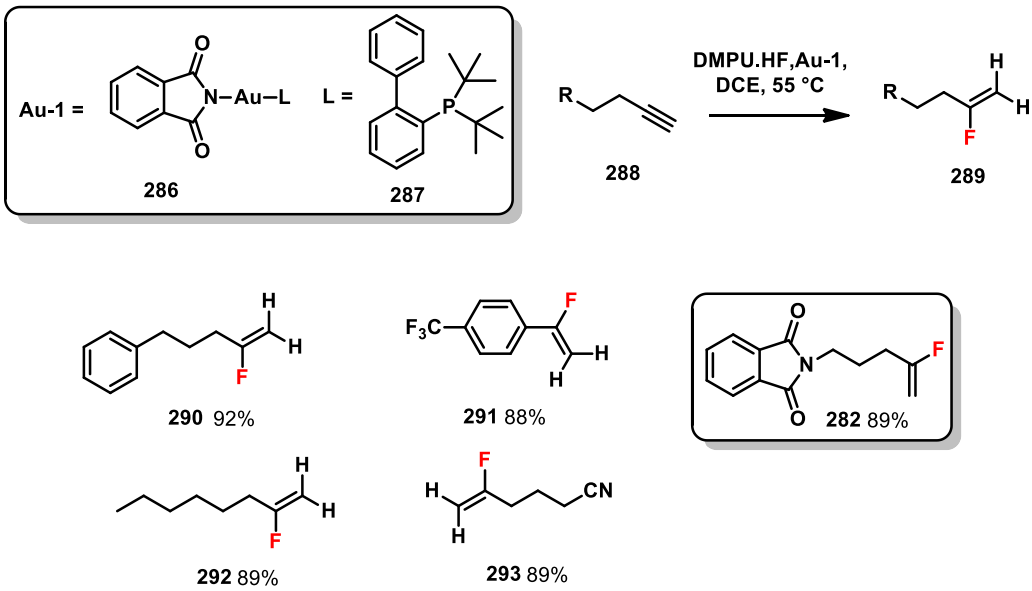

Scheme 2.14. Gold catalyst monofluorination of functionalized alkynes .[19-21,25]

Thus, **282** was synthesised by hydrofluorination of N-(4-pentynyl)-phthalimide **283** with DMPU-HF and the catalyst **286** in high yield (84%), using $CHCl_3$ instead of DCE as previously reported.[26] This was then treated with hydrazine monohydrate to generate the required fluorovinyl amine **281**. This amine could be precipitated in ethanol with hydrochloric acid (5M) to remove any excess of hydrazine monohydrate. After solvent removal the crude was freeze dried. Treatment with 5M sodium hydroxide allowed the aqueous phase to be extracted with dichloromethane. The mixture was carefully concentrated under vacuum due to the high volatility of amine **281**. The solution of **281** in dichloromethane was used directly for the amide coupling step with pantothenic acid diacetylester **294**.[14,19-27] This gave amide **280** in moderate yield. Finally, the acetate group was hydrolysed under basic conditions to give the desired diol **259** (Scheme 2.15).

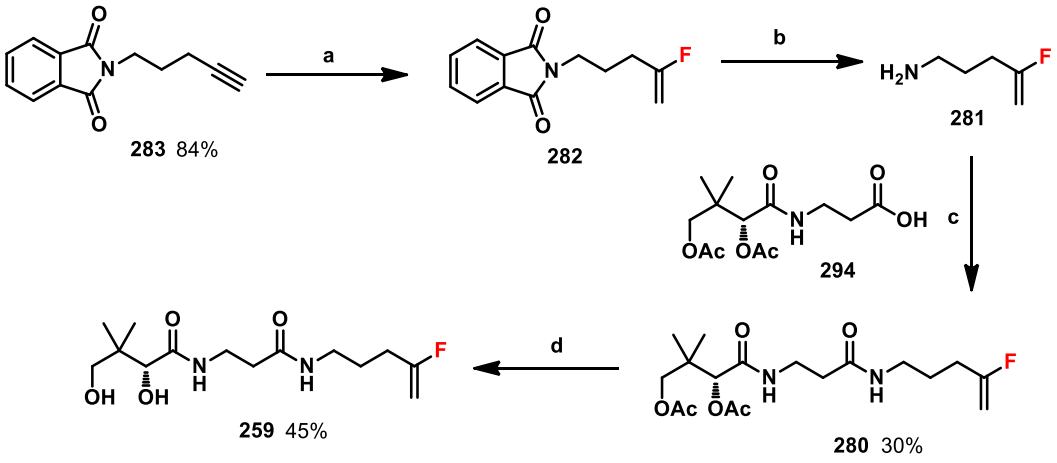

Scheme 2.15. Synthesis of N-(4-fluoropent-4-en-1-yl)-D-pantothenamide **259**: a) DMPU-HF, Au-1 **286**, dry $CHCl_3$; b) hydrazine monohydrate, EtOH ; c) HOBt, EDCI, Et_3N, CH_2Cl_2, d) NaOMe (5.4 M in methanol), MeOH.[16,23-27]

The desired compound **259** was successfully prepared in moderate yield as an important building block for this study. It was now progressed by the three-step biotransformation, to generate the co-enzyme A analogue.

2.13. Synthesis of fluorovinyl-dethia-CoA 261

The synthesis of the co-enzyme A derivative **261** was carried out enzymatically according to the procedure used for FV-CoA analogue **212** (Scheme 2.16).[16]

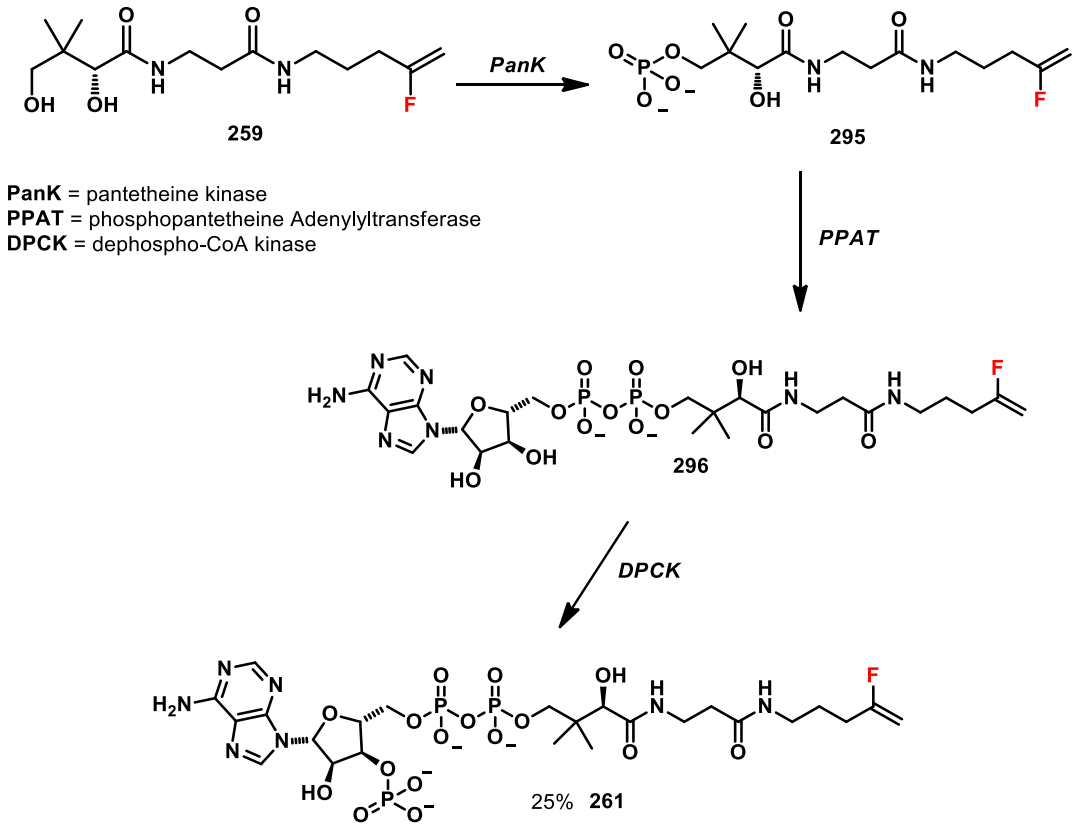

Scheme 2.16. Biotransformation approach to fluorovinyl-dethia-CoA **261**, the yield reported is over 3 steps.[16]

Intermediate **261** was prepared in a one pot/ two-step enzymatic reaction. PanK mediated phosphorylation was followed by a PPAT addition of the adenine monophosphate. HPLC purified intermediate **296** was then progressed to its final form **261** by DPCK mediated further phosphorylation.

The enzymatic biotransformation was monitored by HPLC. After 16 h, the starting material **259** (red) (retention time = 20.1 min) was fully converted to the PanK product **295** (retention time = 17.6 min). The PPAT catalyzed step was slower (24 h) and did not progress completely to intermediate **296** (retention time = 16.4 min). Unreacted **295** was recovered by HPLC and could be re-used in subsequent bio-transformations for the synthesis of **296** (Figure 2.6).The corresponding products are highlighted in the chromatogram shown below, **261** highlighted in purple is the most polar with the shortest retention time, then **296** (green) and then **261** (blue).

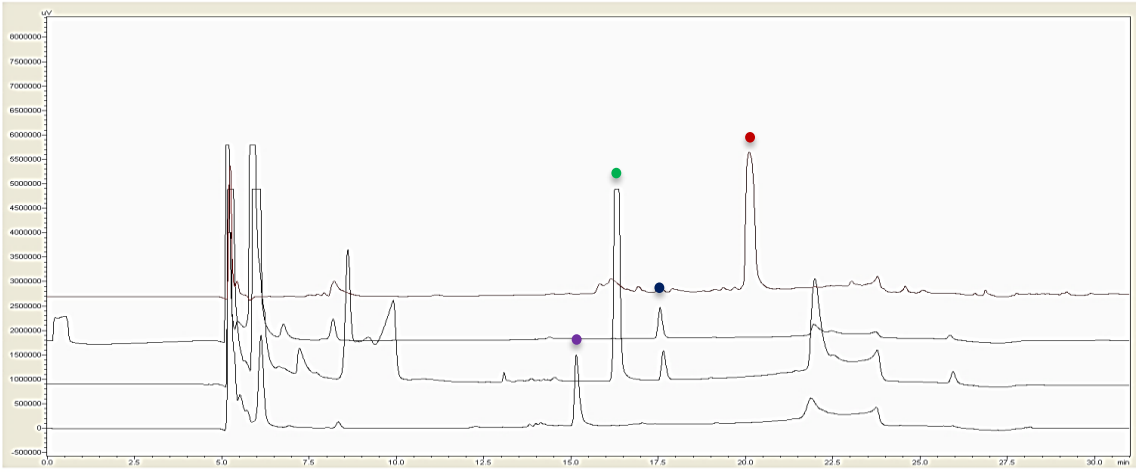

Figure 2.6. The HPLC profile of the three enzymatic reactions of N-(4-fluoropent-4-en-1-yl)-D-pantothenamide **259**.

Intermediate **296** was finally purified by semi-preparative HPLC and its constitution was confirmed by mass spectrometry. The ^{1}H NMR spectrum was assigned by a Double Quantum Filter COSY 2D experiment (DQF-COSY) as illustrated in Figure 2.7. C2 and C8 protons of the heterocyclic purine (H2, H8) and C1', C4' protons of the nucleoside (H1', H4') are characteristic of the adenosine moiety. The C2' protons signal (H2') is partially hidden by the solvent peak and the C3' proton (H3') is overlapping with the $C23_{cis}$ proton ($H23_{cis}$) as shown in Figure 2.7A. $C23_{cis}$ (J = 18.5, 3.0 Hz) and $C23_{trans}$ (J = 50.0, 3.0 Hz) protons of the fluorovinyl moiety ($H23_{cis}$, $H23_{trans}$) have been identified by their corresponding coupling constants. The ^{19}F NMR spectrum shows a singlet at -75 ppm that belongs to trifluoro acetic acid (used as HPLC mobile phase acidic modifier) and a multiplet that relates to the fluoro vinyl motif coupled with C23 protons ($H23_{cis}$, $H23_{trans}$).

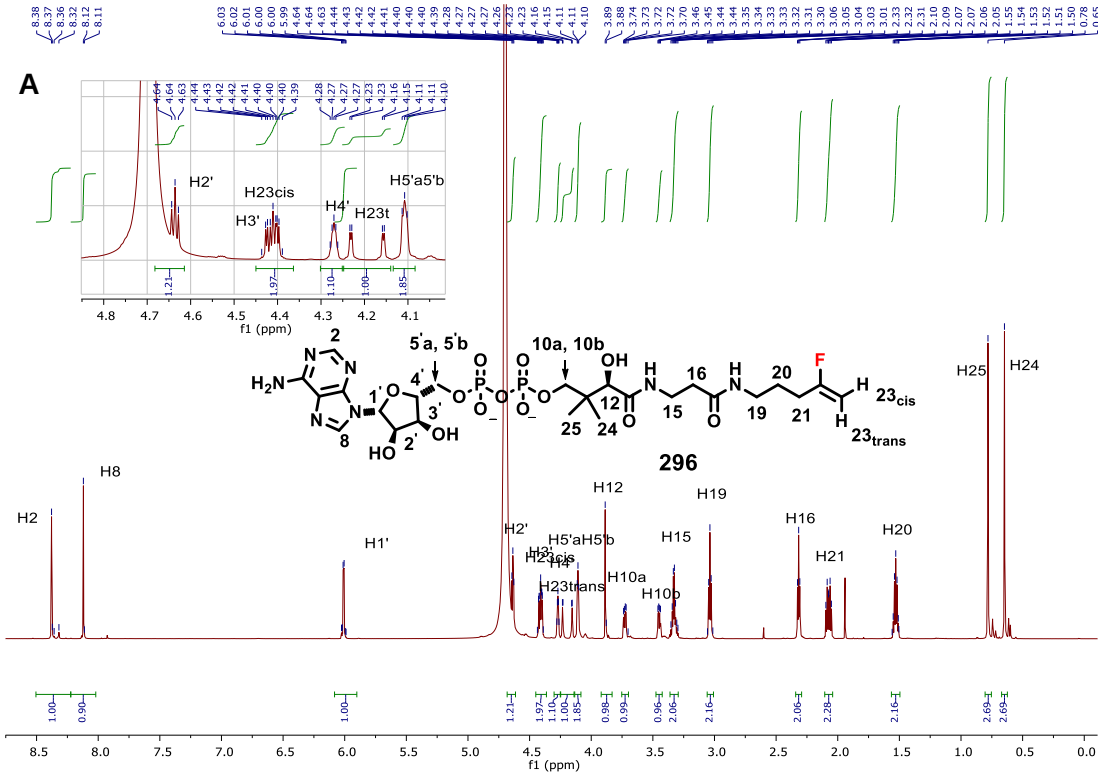
A
H2'
H23cis
H3'
H4'
H23t
H5'a5'b
f1 (ppm)
5'a, 5'b
10a, 10b
296
H8
H2
H1'
H12
H19
H2'
H5'aH5'b
H15
H16
H20
H21
H23trans
H10a
H10b
H25
H24
f1 (ppm)

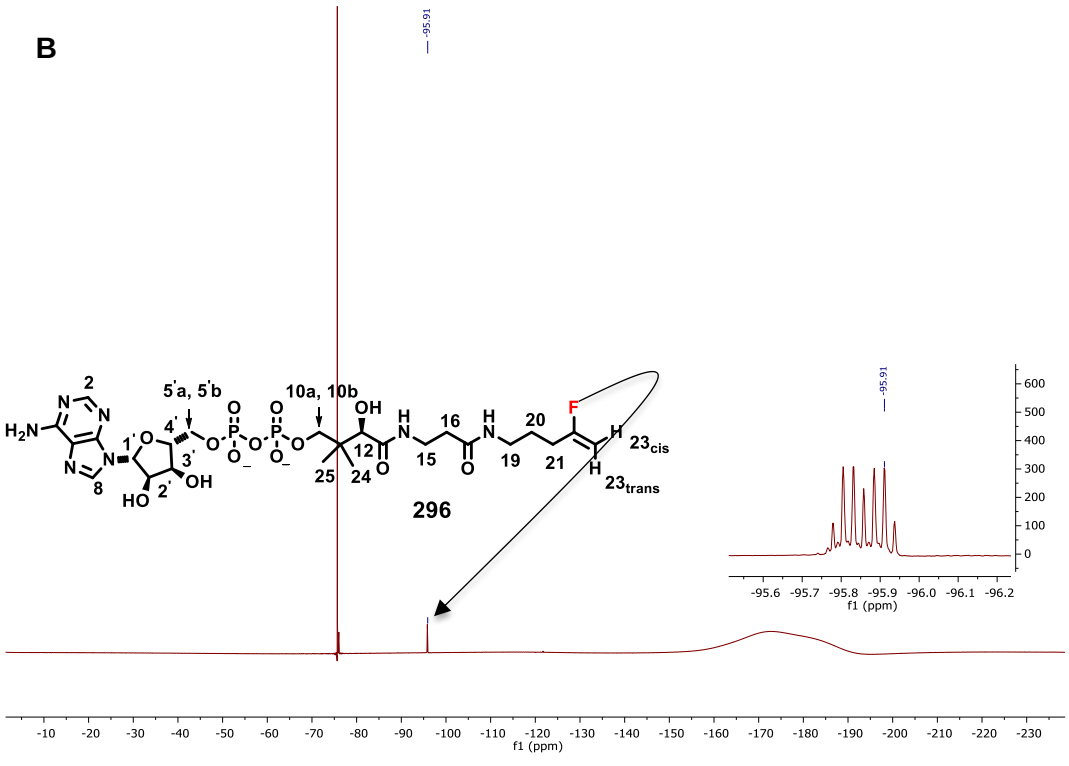
B
-95.91
5'a, 5'b
10a, 10b
296
f1 (ppm)

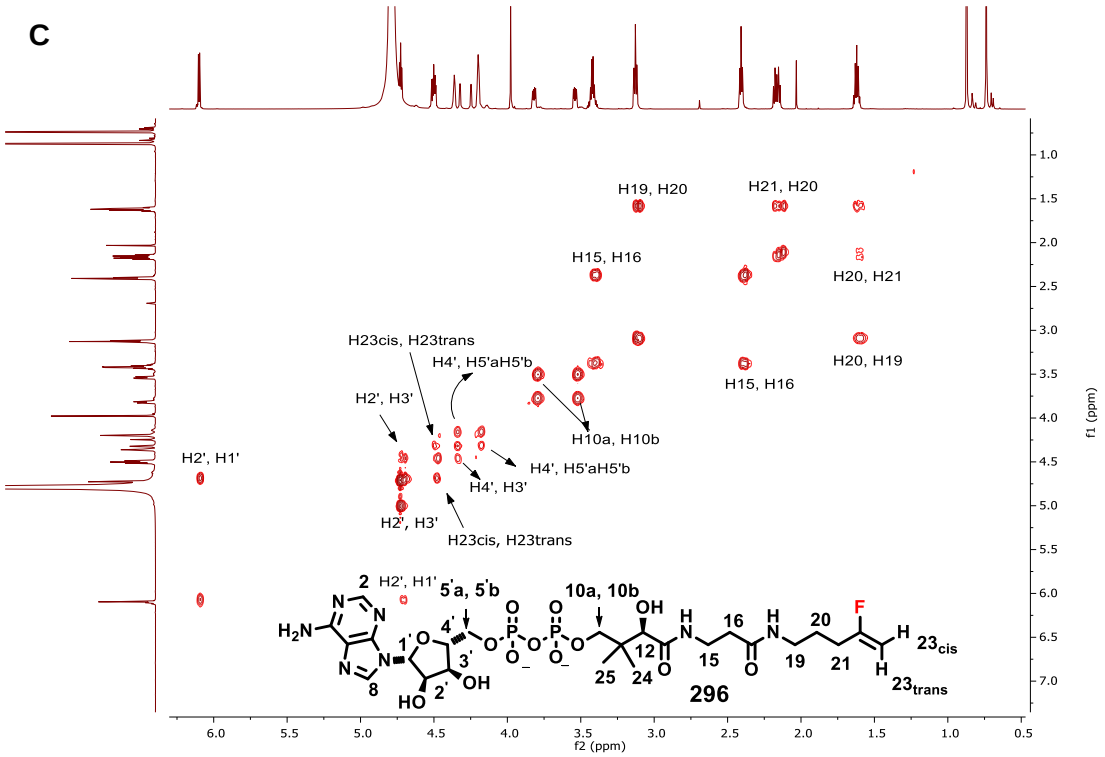

Figure 2.7. NMR spectra of PPAT intermediate **296**: compound **296** has been characterised by A) ^{1}H NMR, B) ^{19}F NMR and C) ^{1}H-^{1}H-2D-COSY NMR.

Intermediate **296** was then progressed to the final coenzyme-A derivative **261**, by a further phosphorylation mediated by DPCK. A comparison of the PPAT and DPCK products by ^{1}H NMR in Figure 2.8 shows that C3', C2', C4' protons of the final product (H3', H2', H4') **261** are shifted downfield. This is consistent with phosphorylation at O-3' in **261**.

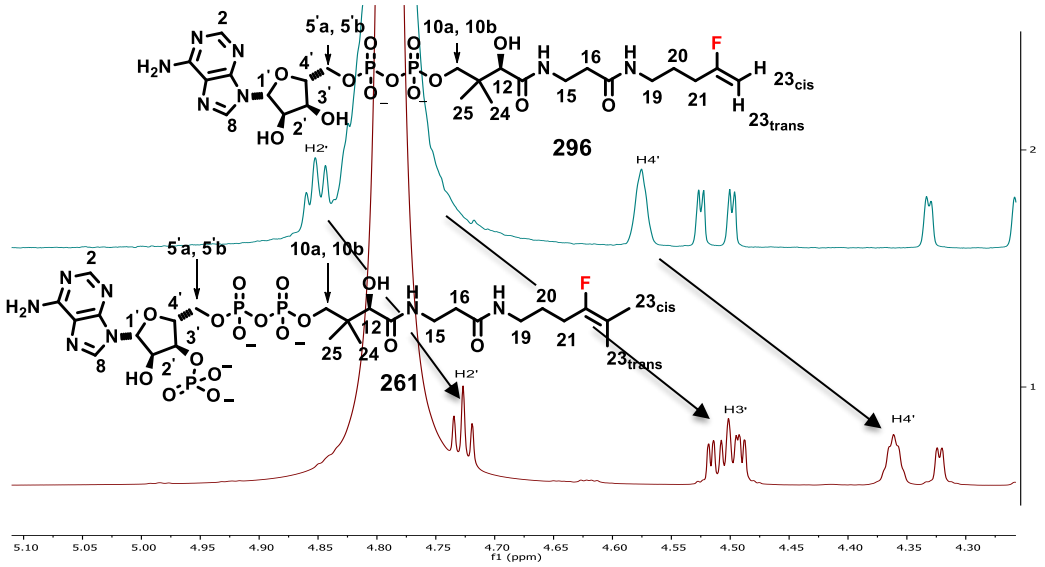

Figure 2.8. A comparison of PPAT **296** and DPCK **261** products after HPLC purification.

The required product **261** was also purified by semi-preparative HPLC chromatography and 5 mg was isolated. Figure 2.9 shows the relevant NMR spectra for **261**. All of the ^{1}H-NMR peaks were assigned by using Double Quantum Filter COSY 2D experiment (DQF-COSY) by comparison with F-CoA compound **212**.[16]

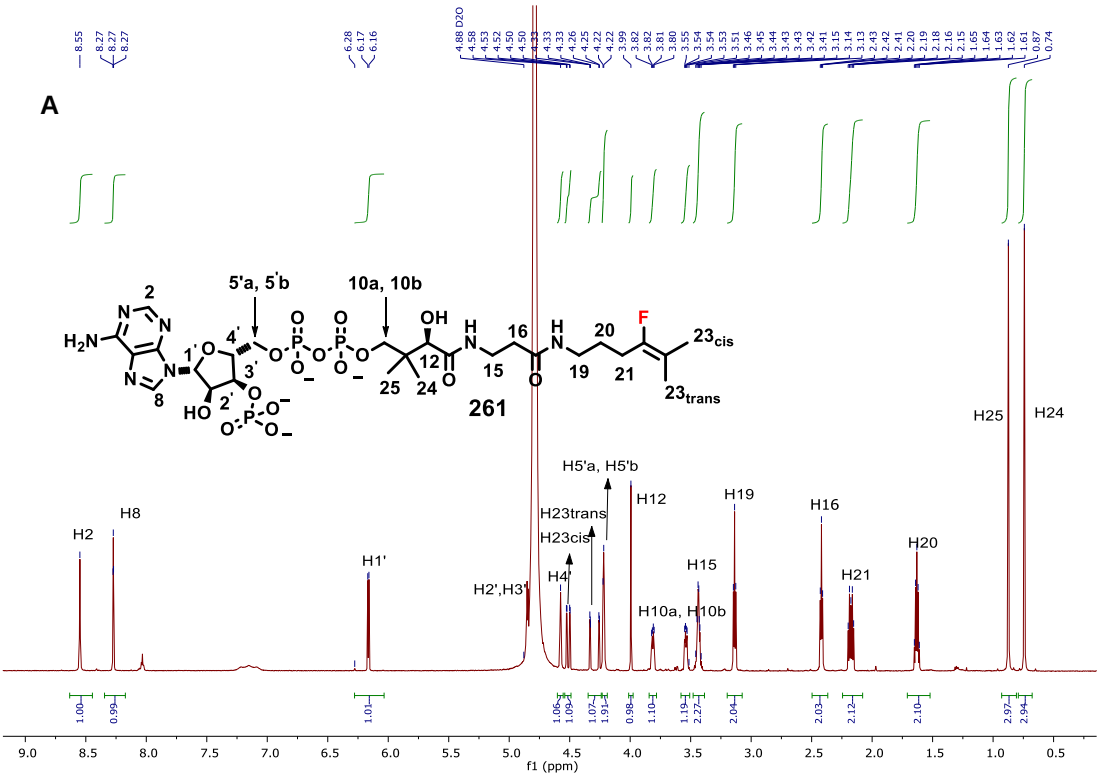

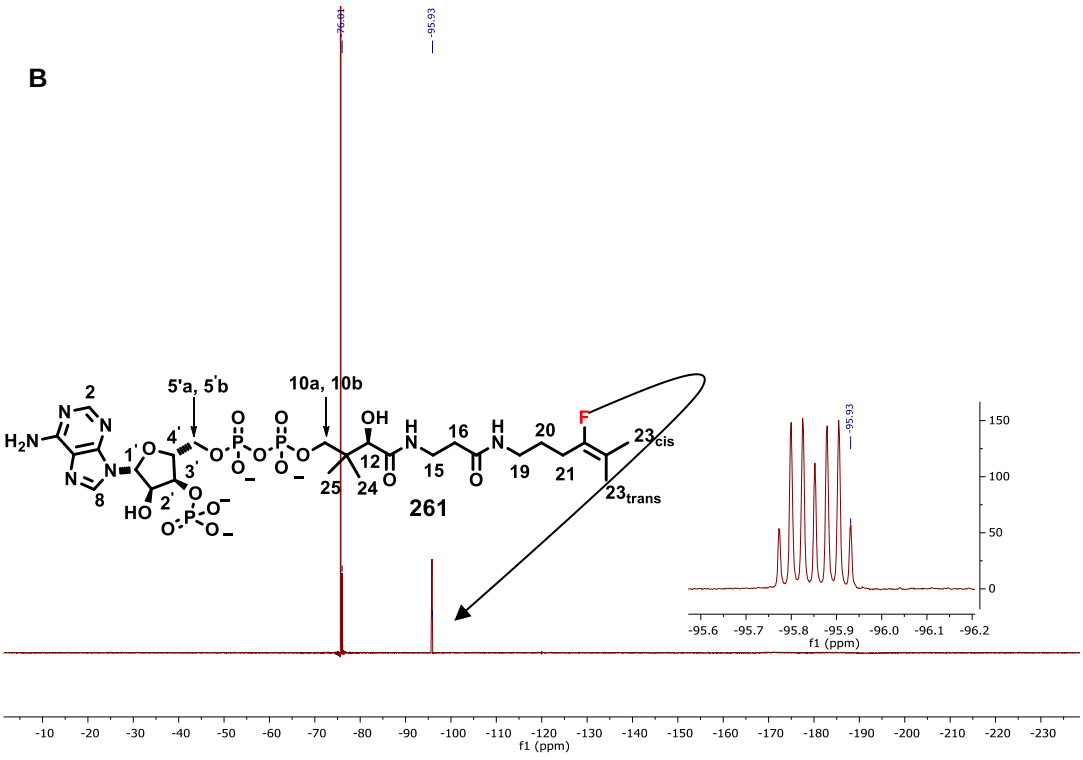

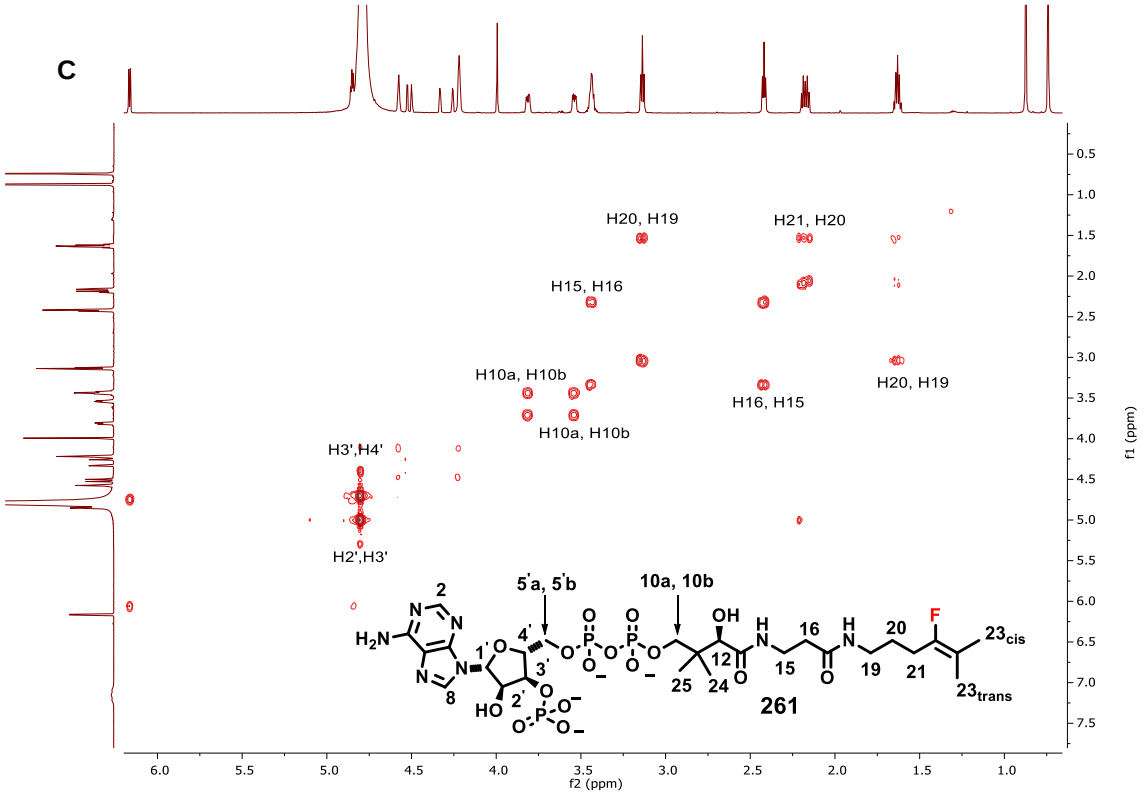

Figure 2.9. A) ^{1}H-NMR, B) ^{19}F-NMR and C) ^{1}H-^{1}H-2D-COSY NMR data for fluorovinyldethiaCoA **261**.[16]

2.14. Synthesis of the vinyl dethia analogue (V-CoA) 262

In order to conduct a comparative inhibition study, defluoro analogue **262** was designed as control compound relative to fluoro-vinyl **261**. This would allow any fluorine effect to be evaluated. In order to achieve this, pent-4-enyl-N-phthalimide **298** was prepared. This was made by a nucleophilic substitution of potassium phthalimide **297** with 4-bromo-1-pentene.[28]

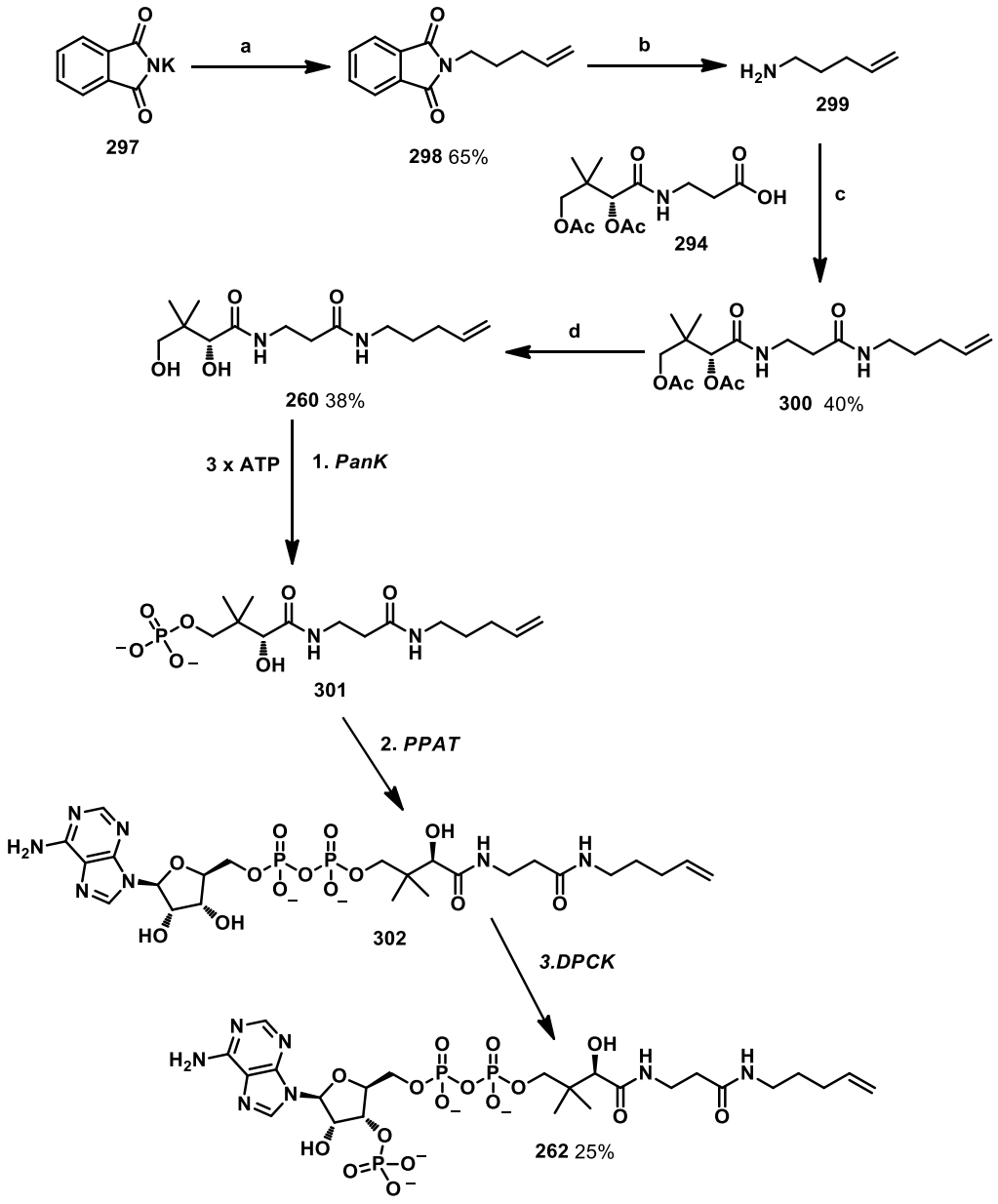

Scheme 2.17. Synthesis of vinyl-dethia-CoA **262**: a) DMF, 4-bromo-1-pentene, reflux ; b) hydrazine monohydrate, EtOH; c) HOBt, Et_3N, EDCI, CH_2Cl_2; d) MeONa, MeOH.[16,18,28–30]

Phthalimide **298** was then treated with hydrazine monohydrate to generate pentenylamine **299**,[30] using the same work up conditions described for the fluoro analogue **281**. Amine **299** was isolated as a solution in dichloromethane without further purification due its high volatility. Amide coupling then gave the diacetylated derivative **300**. Finally basic hydrolysis of **300** allowed access to diol derivative **260** which was progressed to the acetyl-CoA analogue **262** by the three step biotransformation, as illustrated in Scheme 2.17.[16,18,28–30]

The HPLC profile illustrated in Figure 2.10, shows the three enzymatic products. Phosphorylated pantetheine **301** (retention time = 17.70 min) was converted to intermediate **302** (retention time = 16.30 min) but without complete consumption of **301**. This sluggishness was also previously observed for the vinyl fluoride **296**. Intermediate **302** then was purified by HPLC and progressed to its final coenzyme-A form **262** after phosphorylation with DPCK (retention time = 15.10 min). The corresponding products are highlighted in the chromatogram shown below, **262** highlighted in purple is the most polar with the shorter retention time, then **302** (green) and then **301** (blue).[16]

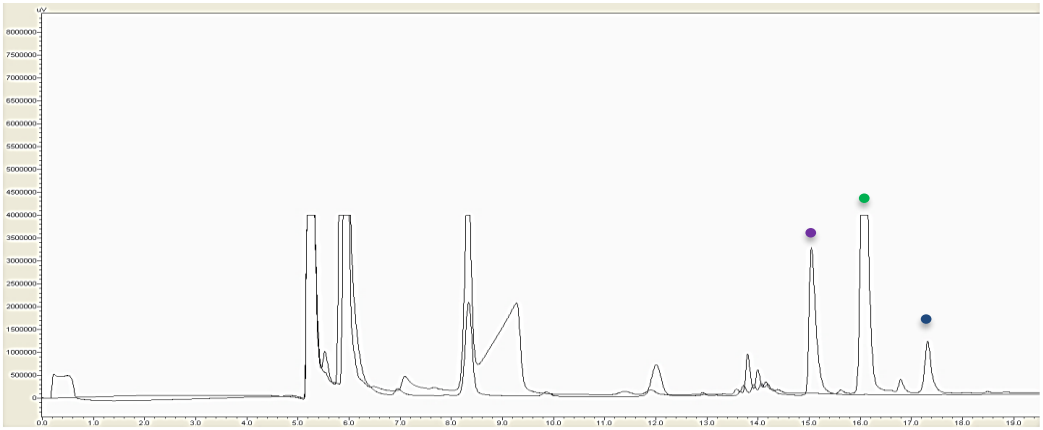

Figure 2.10. The HPLC profile of the three enzymatic reactions required to generate vinyl-dethia-CoA analogue **262**.[16]

Vinyldethia-CoA ^{1}H NMR signals were assigned using a Double Quantum Filter COSY 2D experiment (DQF-COSY) as shown in Figure 2.11 and by comparison with the fluorinated dethia analogue **261** (Figure 2.9). C22 (H22) and C23 protons (H23) correspond to the vinyl protons with C22 proton (H22) shifted downfield. The adenine C2 and C8 proton signals (H2, H8) and C1', C2', C3', C4', C5' protons of the nucleoside (H1', H2', H3', H4', H5') were also identified by ^{1}H NMR and 2D-COSY. High resolution mass spectrometry analysis gave a further confirmation of vinyldethia-CoA structure **262**.[16]

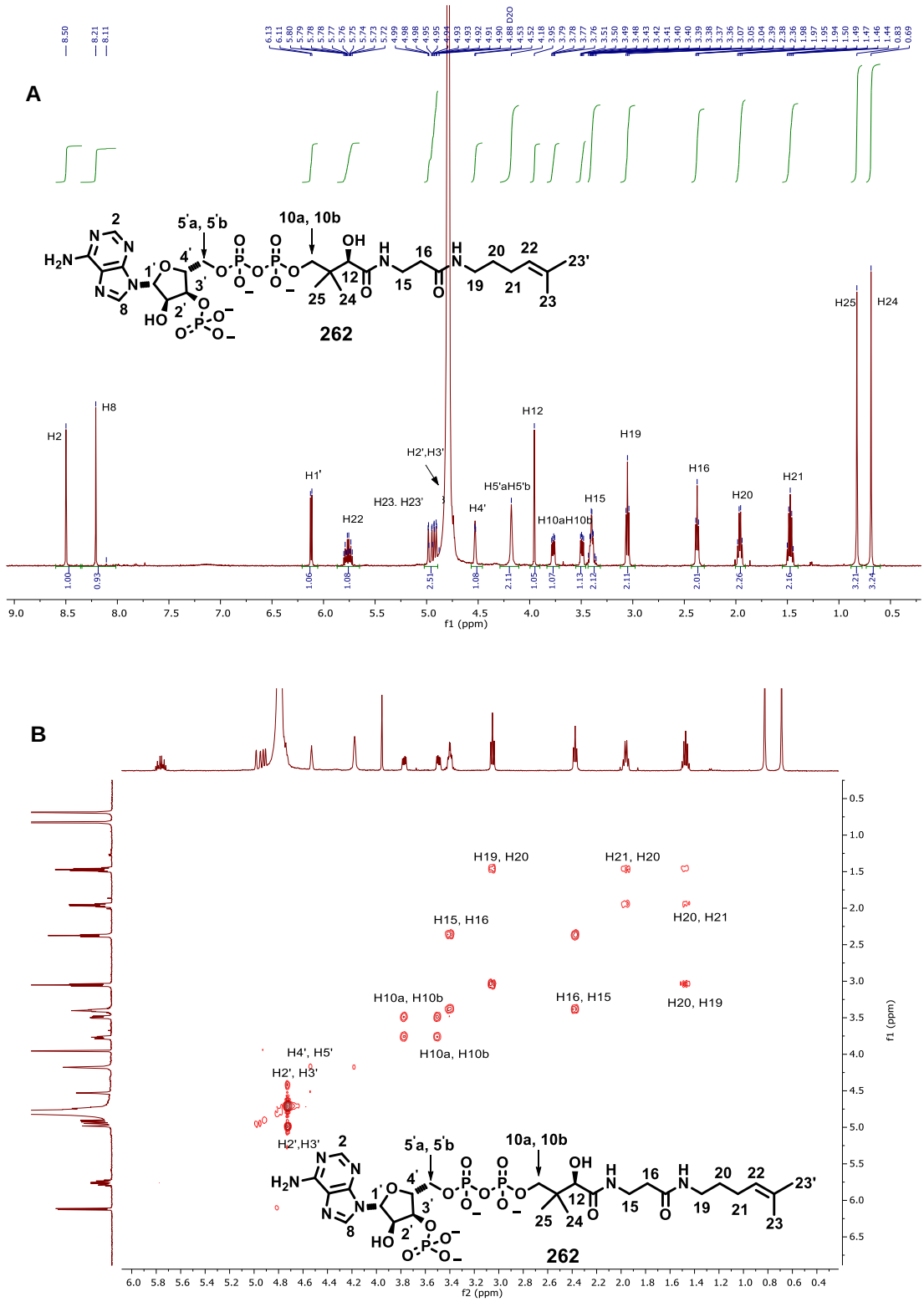

Figure 2.11. Fully assigned A) ^{1}H-NMR and B) ^{1}H-^{1}H-2D-COSY NMR analysis of vinyl-dethia-CoA **262**.[16]

2.15. Determination of Km for acetyl-CoA for porcine citrate synthase

In the first instance a Km value was established for acetyl-CoA. This was achieved by the Ellman's reagent-based spectrophotometric assay as previously described for quantitative CoASH release.[31,32]The UV assay measures the consumption of acetyl-CoA by quantifying the formation of a yellow complex produced by reaction of DTNB with CoA-SH which is released during enzymatic turnover.

The enzymatic activity against acetyl-CoA was determined by the calculation of the Michaelis-Menten constant Km. The Km was obtained by measuring the Ellman's reagent-based spectrophotometric assay described above.[33,32]

Thus, solutions containing OAA (250 µM), DTNB (250 µM) and increasing amount of acetyl-CoA (3.12 µM, 6.25 µM, 12.5 µM, 25 µM, 50 µM, 75 µM and 100 µM, respectively) in TRIS buffer (50 µM, pH = 8.0) were loaded in 400 µL quartz cuvettes, blanks were taken and the reaction were then started by adding and thoroughly mixing in a 4 µL of the previously prepared stock solution of citrate synthase in TRIS buffer (200 nM, pH= 7.8) in order to achieve a final concentration of 2.7 nM (final reaction volume = 400 µL). The appearance of the coloured anion TNB^-, obtained by cleavage of DTNB, was recorded by measuring the absorbance at 412 nm versus time (sampling every 2 second, maximum measuring time 200 seconds). The measurements were carried out in two repeats for each acetyl-CoA concentration. The data obtained were converted to concentration vs time by using the Lambert-Beer law (ε_{415} DTNB = 14150 M^{-1} cm^{-1}) and plotted to XY graphs for each acetyl-CoA concentration in order to extrapolate the linear portions (initial velocities) of the curves. The chosen data points for each repeated measurement were then processed using linear regression with Graphpad® Prism to get the initial velocities values (µM/s). These values were finally plotted against the corresponding acetyl-CoA concentration using the nonlinear Michaelis-Menten enzyme kinetics method in Graphpad® Prism yielding the graph and values reported below:

K_m = 5.8 (± 0.3) µM

V_{max} = 0.25 µM/s (±0.003) µM/s

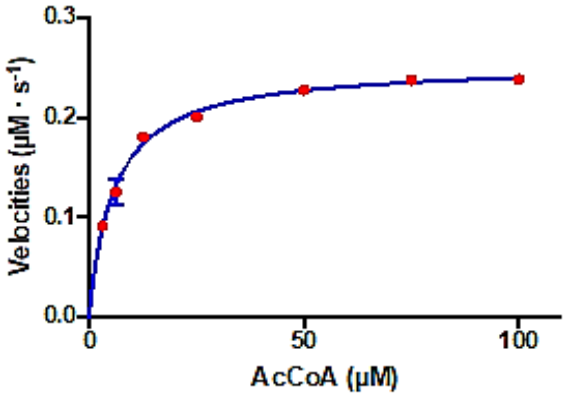

Figure 2.12. The Km value for acetyl-CoA **2**

The Km value found for acetyl-CoA is 5.8 µM. This value agrees with the value reported previously by Johansson *et al.* (Km = 6 µM)[34] at 26.5 °C in 0.1 M Tris buffer (pH = 8.2), 250 µM of DTNB, 0.2 nM of the enzyme, fixed concentration of oxaloacetate and varying the acetyl-CoA concentration from 0 to 60 µM. The same value of Km for acetyl-CoA was obtained by Bayer *et al.*[11] working at 25 °C in Tris-HCl (100 µM), oxaloacetate (0.5 µM), DTNB, citrate synthase and oxaloacetate (0.2 µM) modulating the acetyl-CoA concentration.[11,34,35]

2.16. General procedure for determining IC_{50} and inhibition constants of inhibitors

The inhibitory activity of the acetyl-coA analogues described in this chapter were assessed by calculating the IC_{50} and K_i parameters. IC_{50} represents the concentration of the inhibitor needed to reduce the rate of enzymatic activity by half. IC_{50} were then converted to K_i (measures the binding affinity of the target inhibitor with the enzyme). Control experiments were carried out to assess the enzyme activity, without the presence of the inhibitor and varying other parameters such as substrates concentrations.

Several initial velocities were measured for each compound maintaining a fixed concentration of acetyl-CoA and increasing the inhibitor concentration. Solutions containing OAA (250 µM), DTNB (250 µM), acetyl-CoA (25 µM) and with increasing concentrations of compounds **261**, **262** in Milli-Q water, were placed in 400 µL quartz cuvettes. Blanks were taken and the reactions were started by thoroughly mixing 4 µL of the stock solution of citrate synthase (3nM). The appearance of the coloured complex was recorded measuring absorbance at 412 nm versus time (sampling every 2 seconds for 200 seconds). Two repeats at each concentration were carried out for both compounds tested. The data obtained were converted to concentrations applying the Lambert-Beer equation and plotted to XY graphs for each concentration of inhibitor to extrapolate the linear gradients (initial velocities) of the curves.

The resultant values were converted to % of response and plotted against the logarithm of the inhibitor concentration. The obtained values (%) were plotted against the logarithm of the test compound concentration using Prism Graphpad®. Estimation of the corresponding logarithm of the inhibitors at 50 % response gave the IC_{50} for that compound (Figure 2.13). [16]

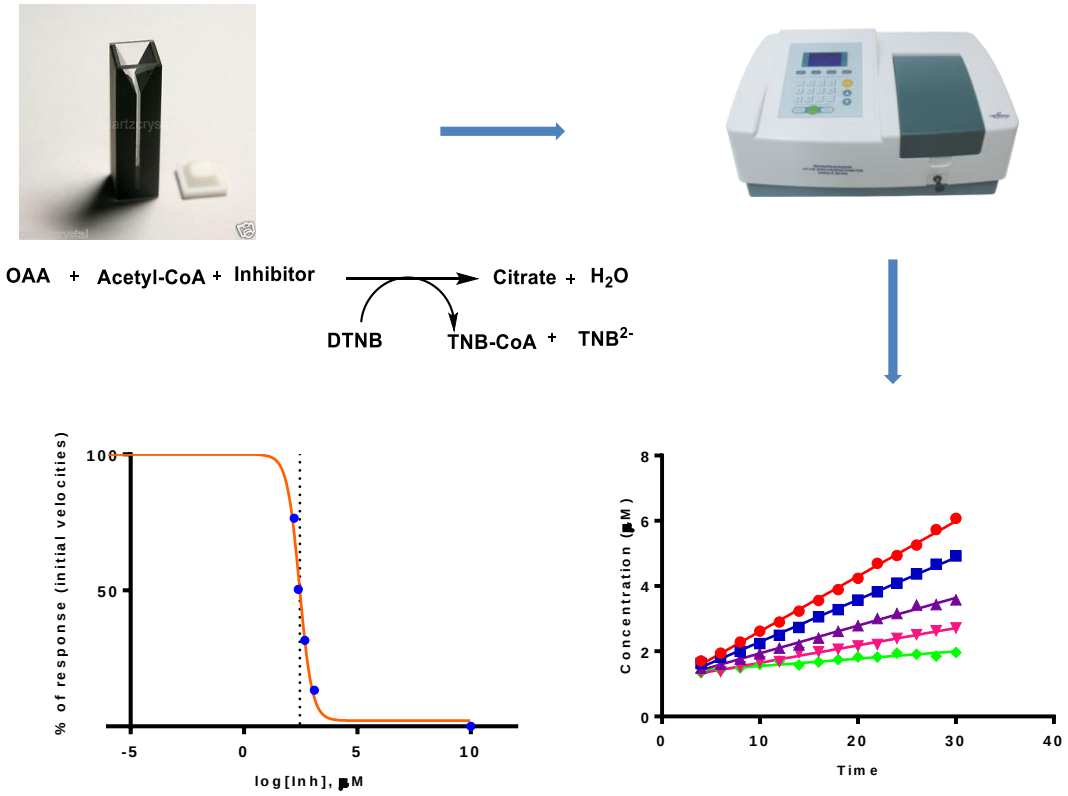

Figure 2.13. General procedure for the determination of IC_{50} values: the image above illustrates the main steps of the IC_{50} and Ki determination of inhibitors of citrate synthase.[16]

With these values, the apparent inhibition constants K_i^{app} (the binding affinity of the test compound for the enzyme) for each of the test compounds could be calculated using a web application based on the Cheng-Prussof equation shown in Figure 2.14. [36]

$$K_i = \frac{IC_{50}}{(S/K_m + 1)} \begin{cases} if\ S = K_m, & K_i = IC_{50}/2 \\ if\ S >> K_m, & K_i << IC_{50} \\ if\ S << K_m & K_i \cong IC_{50} \end{cases}$$

Figure 2.14. The Cheng-Prussof equation used for the calculation of K_i values for the inhibitors.[36]

2.17. Inhibition values of fluoro dethia-CoA 261 and vinyl-dethia-CoA 262

Coenzyme-A analogues **261** and **262** were investigated as inhibitors of citrate synthase. As shown in Figure 2.15, the dethia fluorovinyl inhibitor **261** was a poor inhibitor of citrate synthase with a K_i^{app} (44.8 µM) 10 times less than the fluoro vinyl thioether analogue **212** (K_i^{app} =.4.3 µM). The poorer inhibition capacity of compound **261** is clearly related to the replacement of the sulfur of the thioether with the CH_2 moiety. The comparison of **261** with the non-fluorinated analogue **262** (K_i^{app} = 53.1 µM) has highlighted a modest fluorine effect for compound **261**.[14]

IC_{50} = 238.8 (± 47.9) µM

K_i^{app} = 44.8 (± 9.2) µM

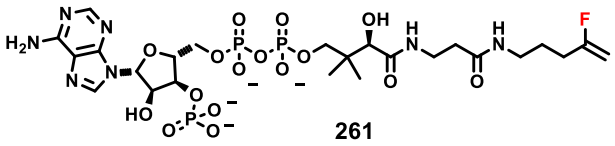

261

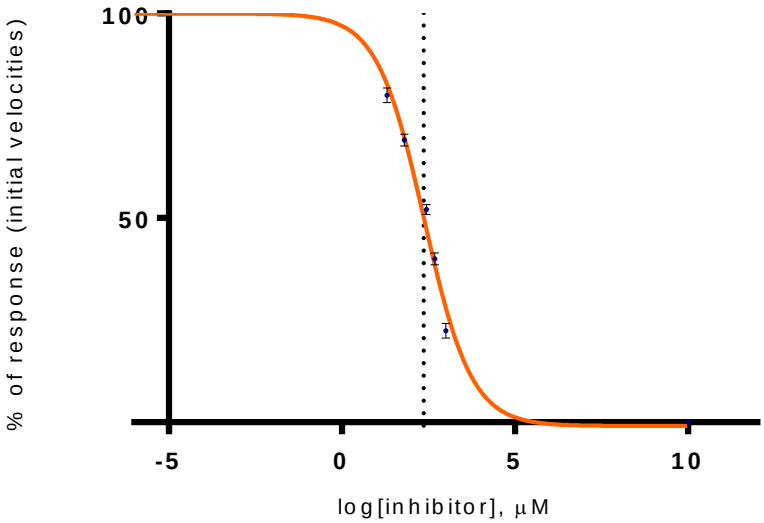

IC_{50} = 281.9 (± 32.4) µM

K_i^{app} = 53.1 (± 6.5) µM

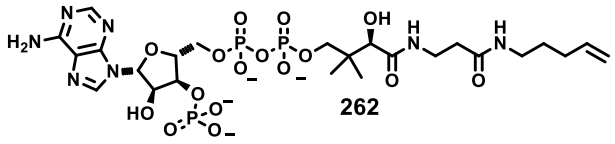

262

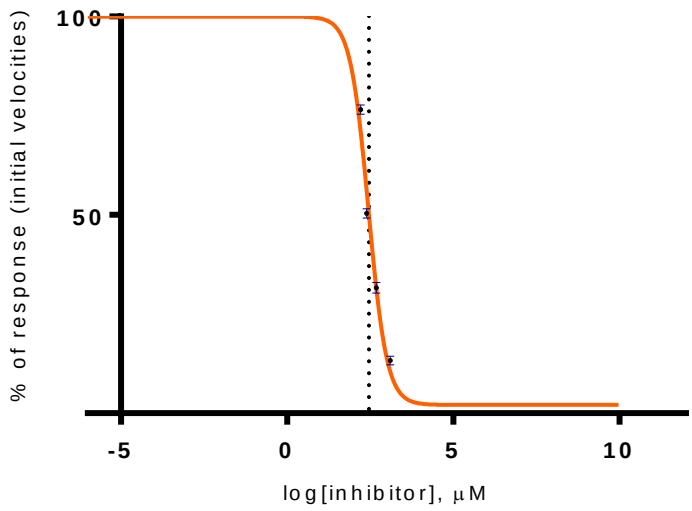

Figure 2.15. $K_{i\ app}$ and IC_{50} values for **261** and **262**.[14]

2.18. Historical sulfoxide investigated as an inhibitor of citrate synthase

Sulfoxide **305** was previously synthesised in 1994 as a mixture of diastereomers where it was investigated as an inhibitor of chloramphenicol transferase as shown in Scheme 2.18.[12] It was designed as a mimic of the tetrahedral intermediate or transition state in the acyl transferase reaction. It was found to have a lower binding affinity than acetyl-CoA but it was never studied as an inhibitor of citrate synthase. In this case the sulfonyl group is located to replace the carbonyl group of acetyl-CoA, with the polarized oxygen located at the enolate site of the enzyme.

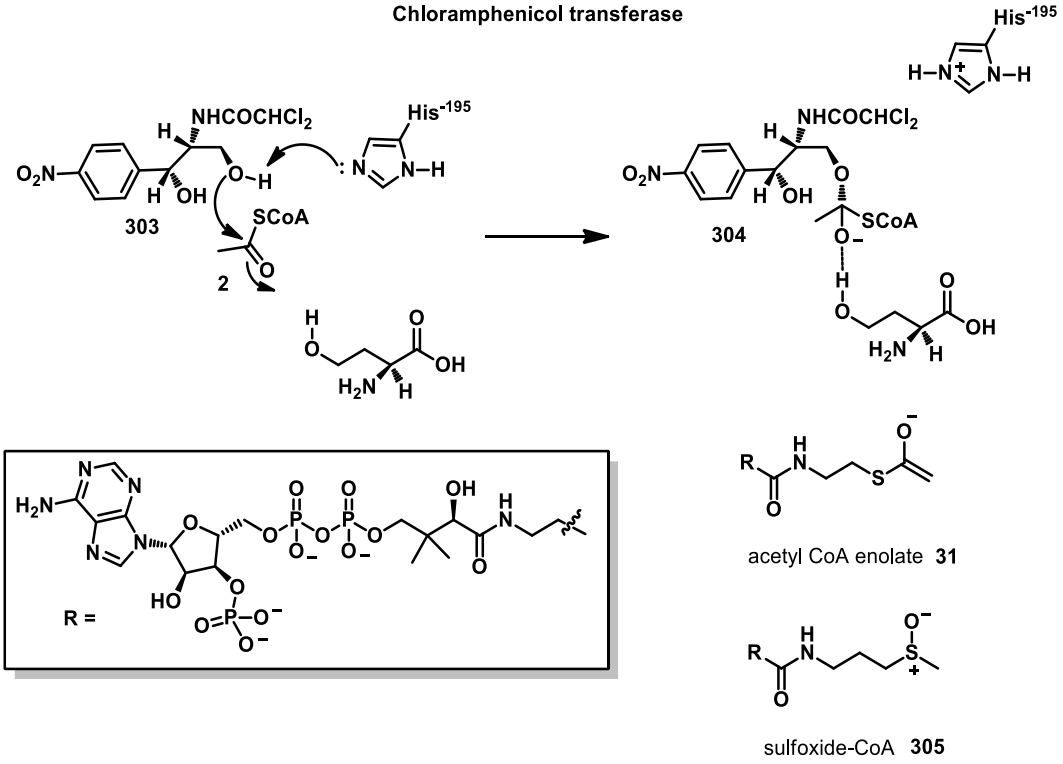

Scheme 2.18. Study of sulfoxide-CoA **305** as an inhibitor of chloramphenicol transferase.[12]

The reported synthesis involved amide formation of amine **308** with the analogue of co-enzyme A **238**. The synthesis of **238** has been reported previously in Scheme 2.6**.** In coenzyme A analogue **238**, the thioester bond and the methyl group are respectively replacing the amide bond and the thiol of CoA-SH **1**. Sulfoxide amine **308** was prepared by oxidation of methylthio-propyl-phthalimide **306** followed by deprotection to generate amine **308**. Since the sulfoxide amine **308** was racemic, the corresponding CoA analogue **305** is necessarily obtained as a mixture of epimers (Scheme 2.19).

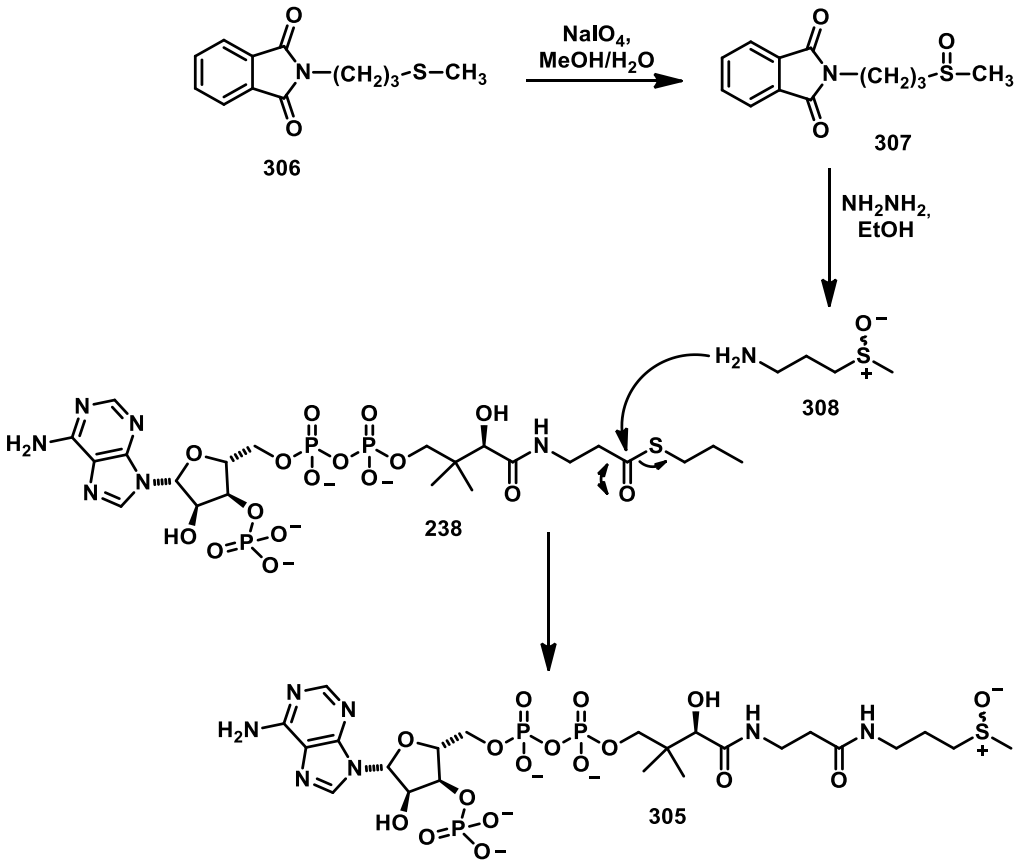

Scheme 2.19. Previous synthesis of sulfoxide-CoA **305** as an epimeric mixture.[12]

2.19. Synthetic approach of sulfoxide CoA 305

In our case we developed a different route to **305**. Pantothenyl sulfoxide **312** was prepared by synthesis and then progressed through the biotransformation to **305**. Accordingly, 3-methylthiopropylamine **309** was coupled with diacetyl pantothenic acid **294** to give the thiomethyl pantothenyl diacetate **310**. Finally, oxidation of sulfide **310** with mCPBA gave the mixture of diastereomers **311**. Hydrolysis under basic conditions of diacetate **311**, led to the desired compound **312** (Scheme 2.20).[16]

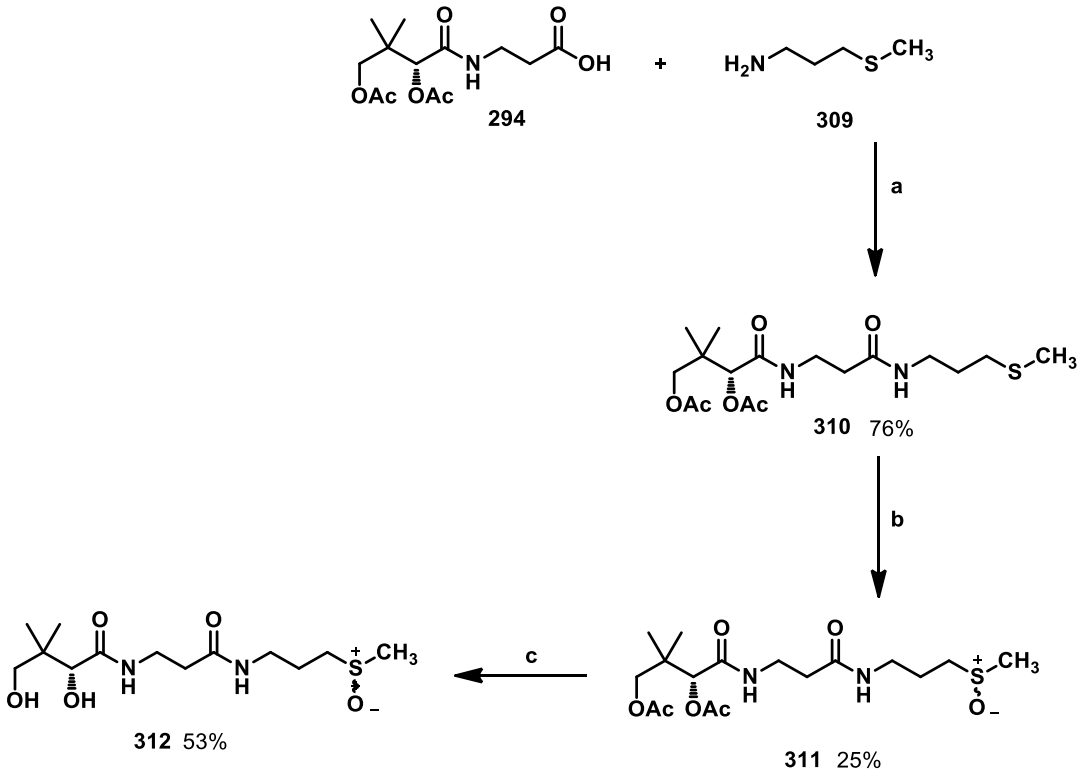

Scheme 2.20. Synthesis of sulfoxide **312**: a) HOBt, Et_3N, EDCI, CH_2Cl_2; b) mCPBA, CH_2Cl_2; c) EtONa (5M in EtOH), EtOH.[16,17,18]

The oxidation of thiomethyl pantetheine diacetyl **310** was monitored by thin-layer chromatography and just one equivalent of mCPBA was added to avoid sulfone formation. Pantetheine **310** was treated with mCPBA to give sulfoxide **311** as a mixture of stereoisomers. The ^{1}H NMR ($CDCl_3$) analysis of **311** is illustrated in Figure 2.16. It can be assumed that the ratio is 1:1. Comparison of the ^{1}H NMR spectra of compound **310** and **311** in $CDCl_3$ suggests the generation of the isomer mixture with the two signals associated with the C12 proton (H12) in **311** that occurs as singlet in **310**. The same duplicity pattern was observed for the C1 proton (H1) signal in **311**.

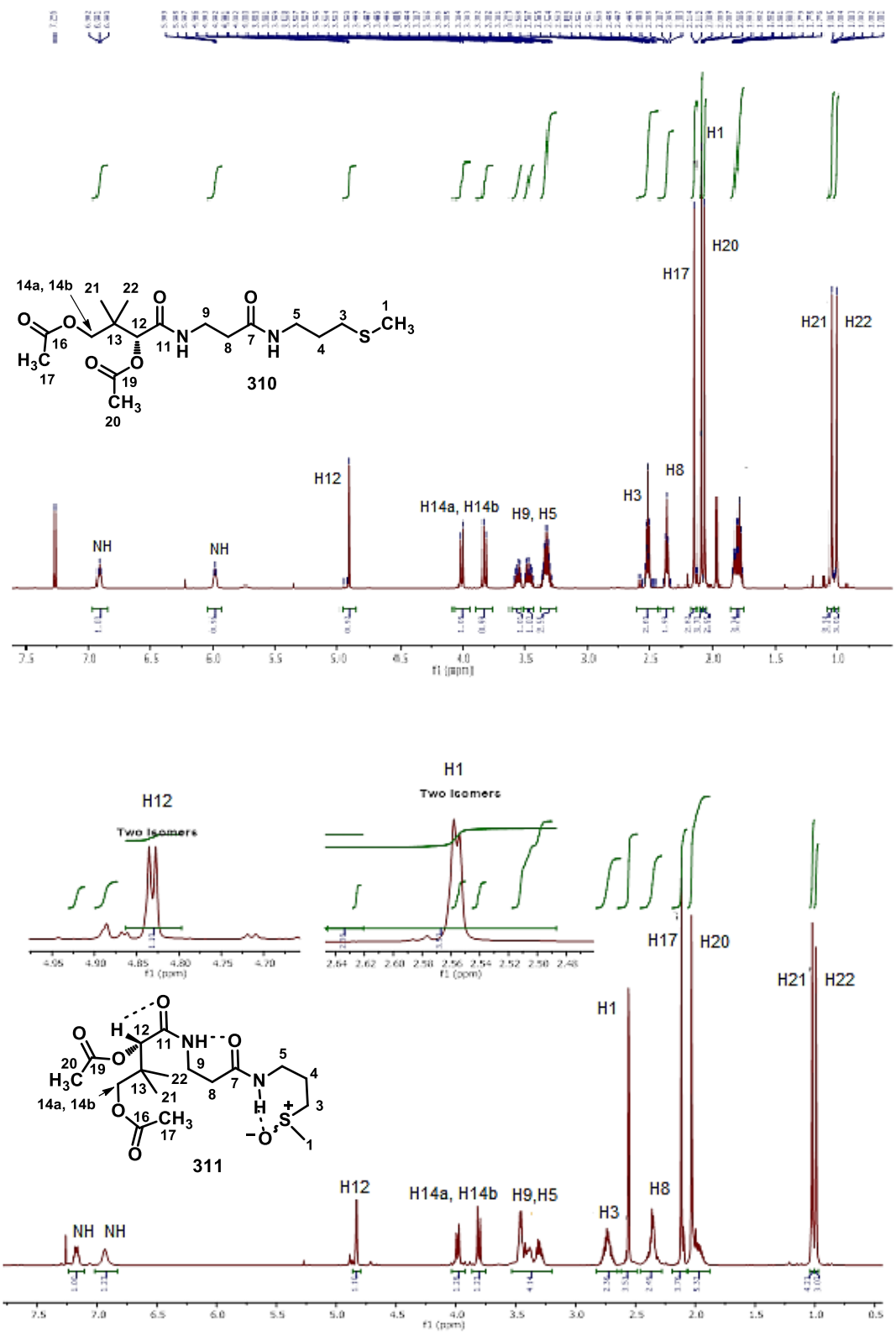

Figure 2.16. ^{1}H NMR comparison of sulfonyl **310** and sulfoxide **311**

The isomerism for **311** shows up in $CDCl_3$ through the duplicity of C12 and C1 protons (H12, H1) signals. This could be explained by H bonding interactions in **311** as shown in Figure 2.16.

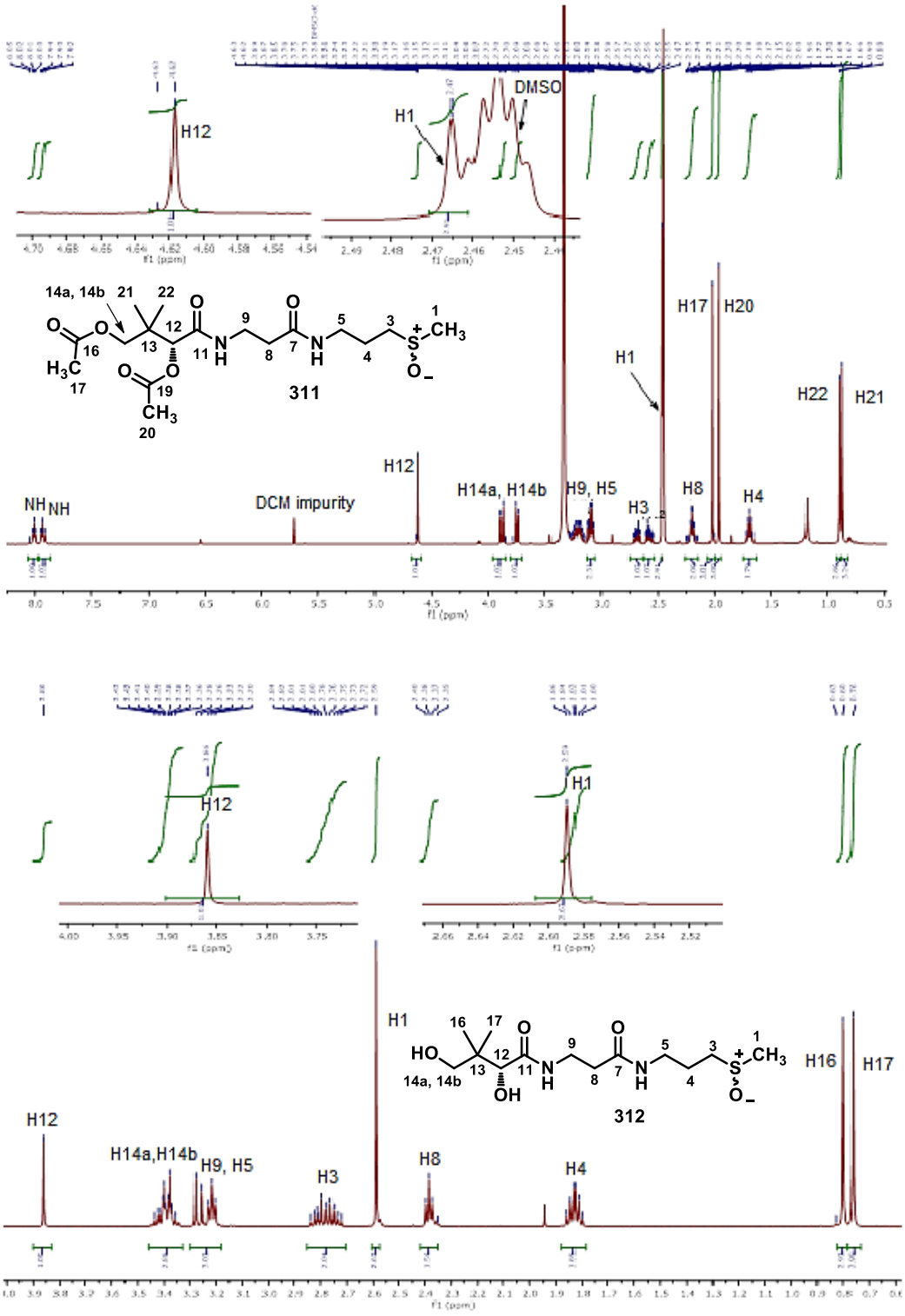

Figure 2.17. ^{1}H NMR of **311** and **312** in CD_3SO and D_2O: the duplicity of C1 and C12 protons (H1, H12) observed in Figure 2.16 for $CDCl_3$, is absent in more polar solvents.

The duplicity is suppressed in more polar solvents such as CD_3SO (for **311**) and D_2O (for **312**) that are capable of H bonding interactions themselves (Figure 2.17).

In the attempt to prepare a single sulfoxide isomer, an asymmetric approach for the oxidation reaction was tentatively explored. Catalytic asymmetric oxidation of sulfides to sulfoxides has been investigated for many years as chiral sulfoxides are useful synthons.[37] The method chosen here was a modified Sharpless oxidation as developed by Kagan and Modena using diethyl tartrate (DET) as the chiral agent, titanium tetraisopropoxide [$Ti(OiPr)_4$] as a coordination catalyst and cuprene hydroperoxide (CHP) or tert-butyl-hydroperoxide (TBHP) as the oxidant. This method has been shown to give high enantioselectivity with certain substrates as illustrated in Scheme 2.21.[37–40]

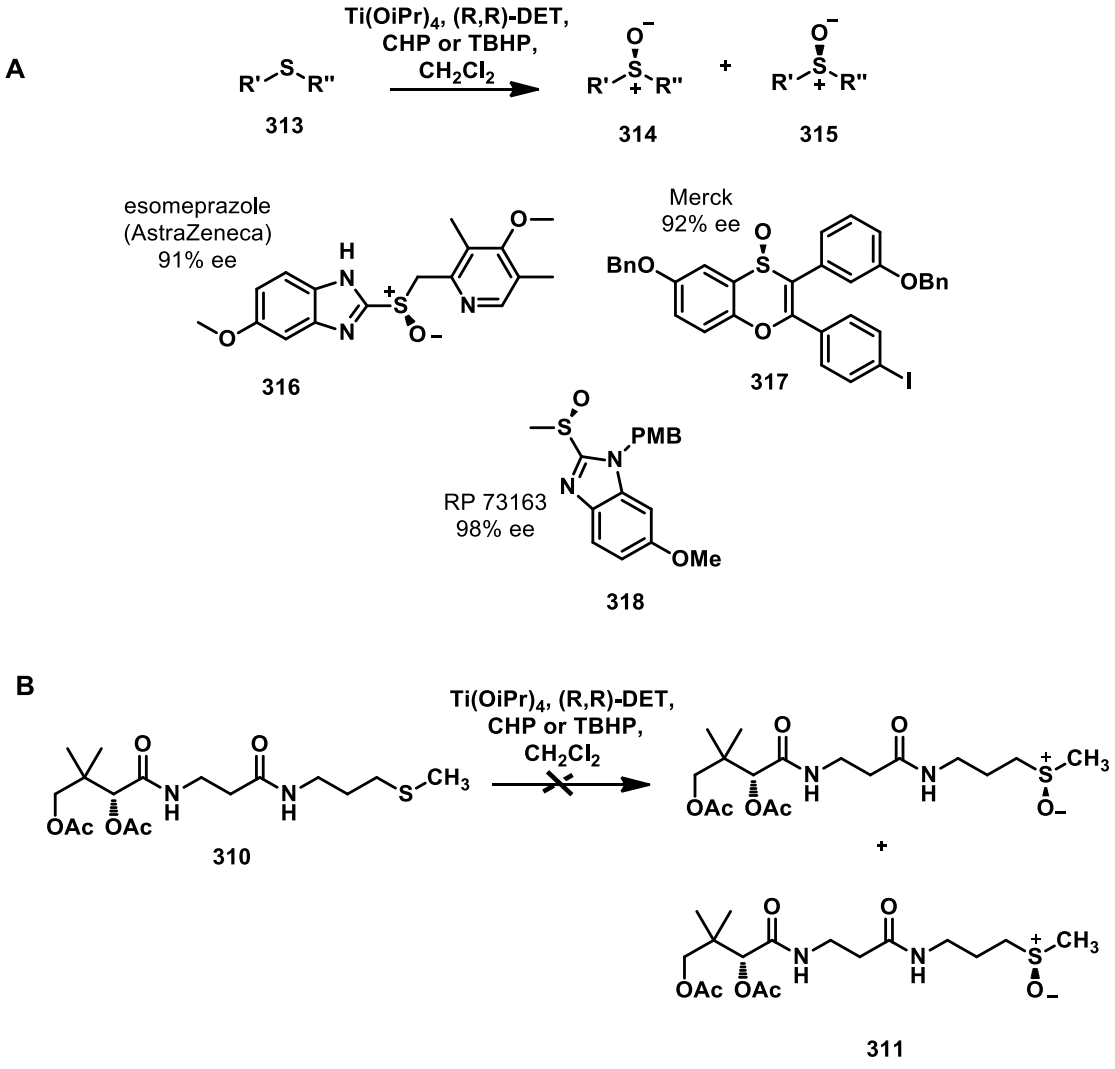

Scheme 2.21. A) Enantioselective oxidation of sulfides to sulfoxides, B) attempted stereoselective oxidation of **310**.[37–40]

In the event, oxidation of sulfide **310** under Kagan's conditions gave poor conversion to the sulfoxide **311** mixture after 16 h with no change of the ratio (1:1). This outcome could be related to the more complex structure of substrate **310** when compared to the aryl or alkyl sulfide reported with this procedure (Scheme 2.21A). The asymmetric approach was not explored any further.

Sulfoxides **311** was hydrolyzed under basic conditions as shown in Scheme 2.20 and progressed to substrate **312** for the biotransformation. Compound **312** was converted into sulfoxide-CoA **305** following the same procedure described for acetyl-CoA analogues **260** and **261**. The three-step biotransformation was monitored by HPLC and the DPCK mediated product (retention time = 13.6 min) **305** was purified and its identity confirmed by mass spectrometry, ^{1}H NMR and ^{1}H-^{1}H-COSY 2D NMR experiments.[16]

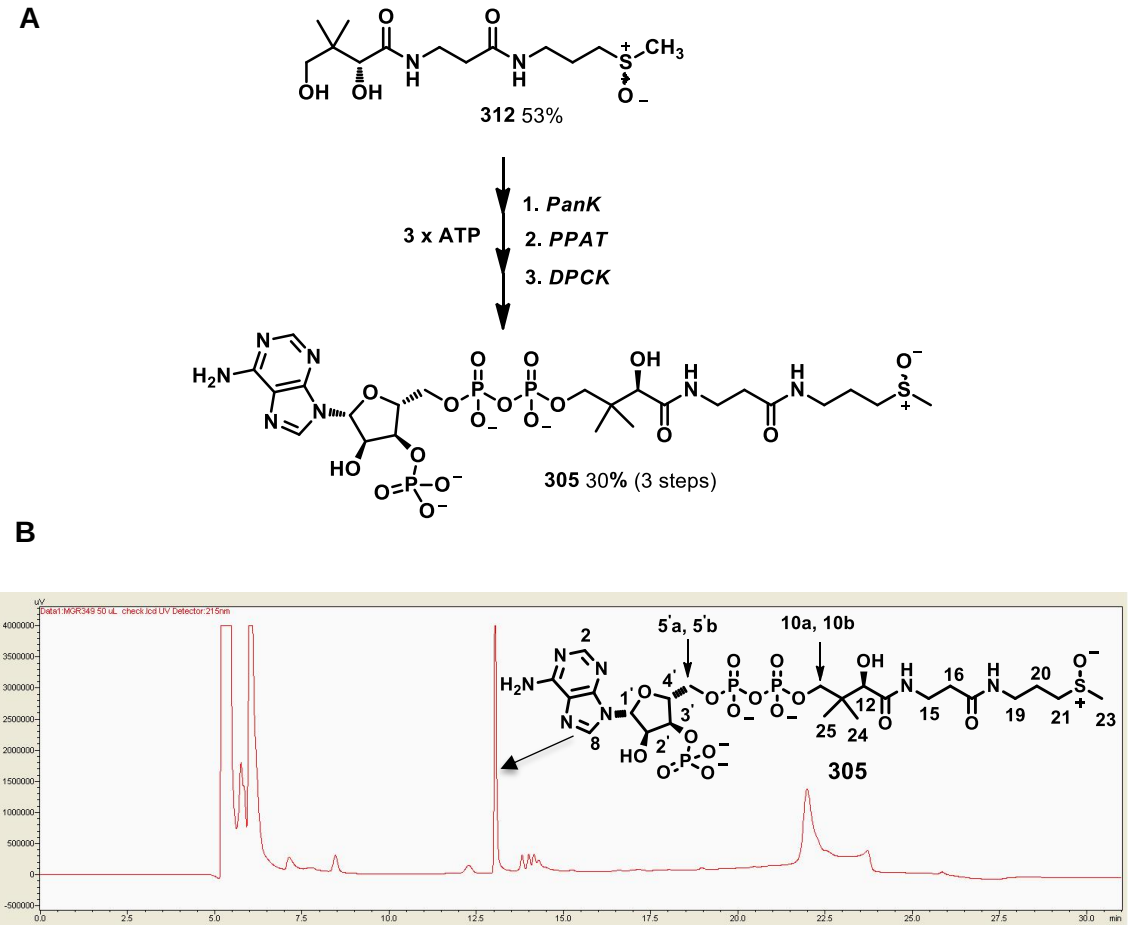

Scheme 2.22. A) The biotransformation pathway and B) the HPLC profile of **305**.[16]

The ^{1}H NMR spectrum was assigned using a Double Quantum Filter COSY 2D experiment (DQF-COSY) and by comparison with the fluorinated dethia analogue **260**.

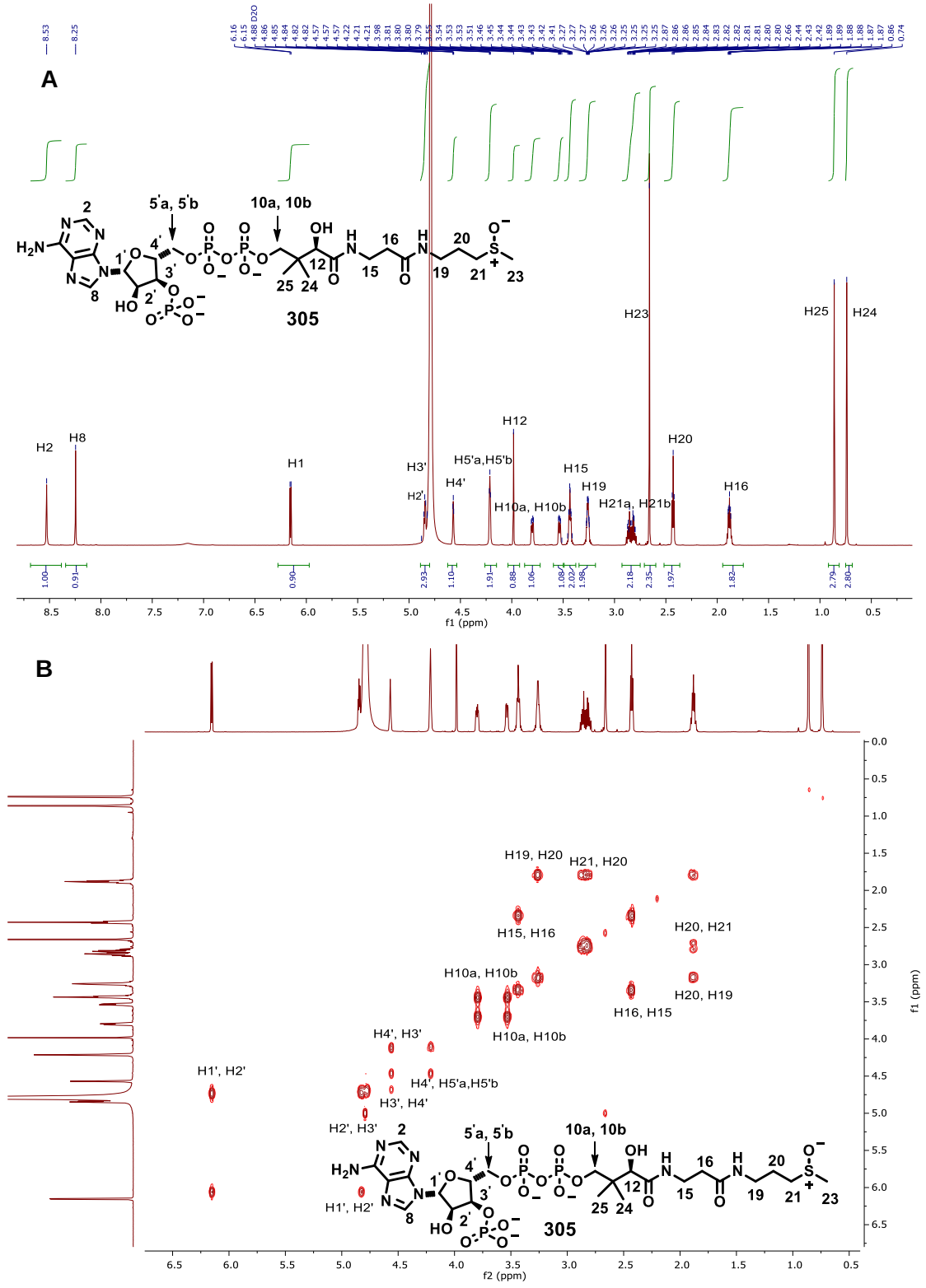

Figure 2.18. A) ^{1}H NMR and B) 2D COSY characterization of compound Sulfoxide-CoA **305**: ^{1}HNMR signals were assigned by 2D COSY and by comparison with fluorinated dethia analogue **260**.[14]

As observed for **260** and **261**, the adenosine moiety of coenzyme A analogue **305** is identified by the C2, C8 protons of the adenine (H2, H8) and the C1', C2', C3', C4' protons of the nucleoside (H1', H2', H3', H4'). The sulfoxide presence is confirmed by the C23 methyl proton at 2.7 ppm (H23) directly attached to sulfur (Figure 2.18). Product **305** structure was also supported by HR-MS.[16]

2.20. Inhibition studies of citrate synthase

Sulfoxide-CoA **305** was assayed with citrate synthase. It showed a relatively good inhibitory activity towards citrate synthase with a K_i of 11.1 µM, a value higher than the Km of acetyl-CoA (5.8 µM). The $^{+}S\text{-}O^{-}$ bond is polarized with a partial negative charge located on the oxygen atom, displaying a better hydrogen bond acceptor capacity than the inhibitors bearing alkylnitrate **243** or malate **230** groups (Figure 2.1), as also **260** and **261**.

$\mathbf{K_i^{app}}$ = 11.1 (± 0.9) µM

$\mathbf{IC_{50}}$ = 59.18 (± 4.4) µM

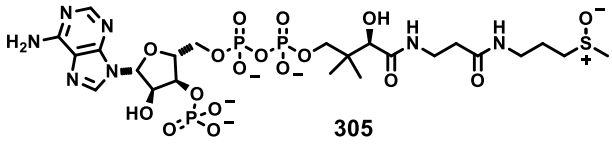

305

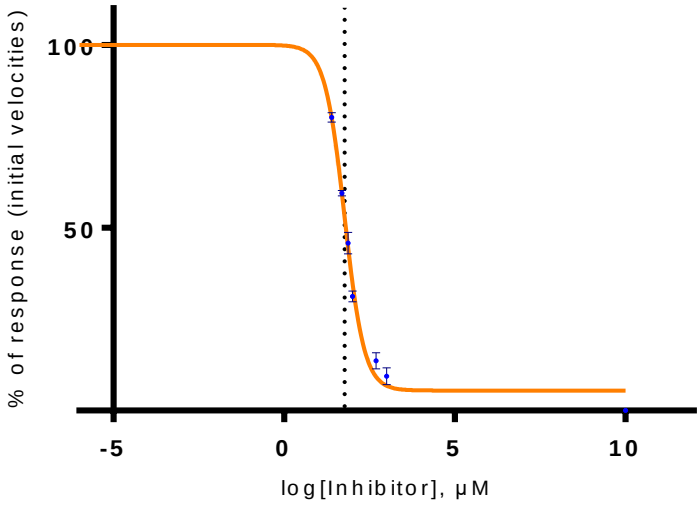

Figure 2.19. IC_{50} and K_i^{app} values for sulfoxide-CoA **305**.[14]

2.21. *Crystallization of sulfoxide-CoA 305 -citrate synthase complexes*

The porcine citrate synthase crystallization and soaking process were performed by Dr. Nouchali Bandaranayaka from the University of Saint Andrews:

Pig heart citrate synthase was crystallized from a small-molecule cocktail containing cystamine dihydrochloride, aspartame and benzamidine hydrochloride according to Larson *et al.* procedure. [41]

Pig heart citrate synthase was purchased from Sigma (UK) as an ammonium sulfate suspension and was dialyzed against water to a concentration of 10 mg ml^{-1}. The dialysis procedure resulted in the formation of a substantial amount of precipitate, which was removed by centrifugation. The protein was concentrated with Vivaspin (Germany). The crystals were grown by vapor diffusion at room temperature in 96-well Intelli-Plates (Hampton Research, Aliso Viejo, California, USA) with 90 µl reservoirs of 25%(w/v) PEG 3350+ 0.1 M MES pH 6.5/7.5 and 1mM of sulfoxide compound. The protein droplets were of 4 µl volume at 13.5mg/ml and consisted of two parts of the stock protein solution and one part each of the 'cocktail' of small molecules and the reservoir solution. All solutions were buffered to pH 7.8 with 0.1 M Tris–HCl. The 'cocktail' was made to concentrations of approximately 1%(w/v) of each of the small molecules, namely aspartame, benzamidine hydrochloride and cystamine dihydrochloride. The concentrations of the small molecules in the crystallization drop were approximately 5-10 mM. Crystals appeared and grew to full size within one to two weeks**.**

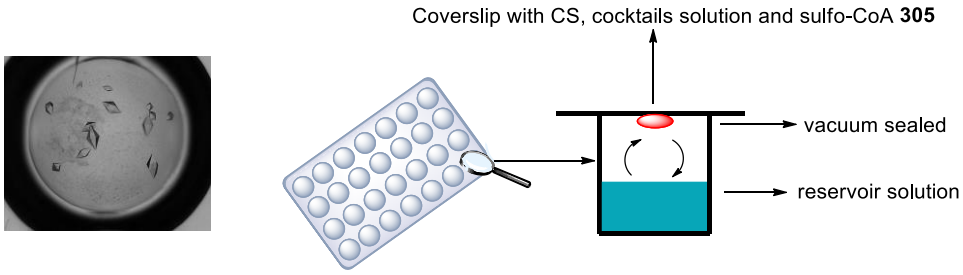

Figure 2.20. Sitting drop crystallization: the drop is on a pedestal separated from the reservoir with a high sealing of the environment for the equilibration between the drop and the reservoir to occur

Crystals were shot by Dr Magnus Stephen Alphey (University of St Andrews) in house at 100K on a Rigaku 007 HFM rotating anode X-ray generator with a Saturn 944 CCD detector. The data set obtained showed strong electron density for the adenine moiety bound to the enzyme however the pantothenyl chain of **305** was not visible due to

disorder. Several crystals were shot, however all of them resulted in the same outcome and it was not possible to get any information on binding of the sulfoxide to the active site.

2.22. *Conjugated (Z)-319 and (E)-320 thioalkenes*

The *Z* and *E* conjugated thioacrylates **319** and **320** became targets: it was envisaged that the electrostatic nature of carboxylate group would enhance binding and that two geometries could be explored. The closest known inhibitor to **319** and **320** is carboxy ethyl-CoA **229**, which has a Ki of 26 μM. [11,14]

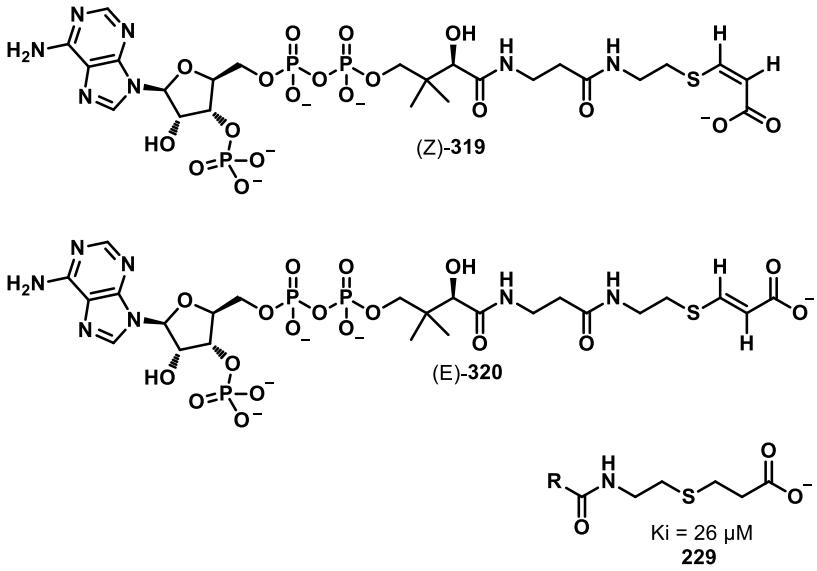

Figure 2.21. Candidate inhibitors (Z)-**319** and (E)-**320**.[14]

2.23. *Previous approaches to conjugated E- and Z-thioalkenes isomers*

The synthesis of alkylthio acrylate motifs has been reported. One of the procedures involved a nucleophilic substitution of *E*-β-tosylacrylic derivatives **323** by the corresponding thiols **322** in the presence of sodium hydride.[42] The reaction takes place at the β position with retention of configuration and with high *E*-regioselectivity. A water mediated thiolation of ethyl propiolate **324** has been explored by Randive et al.[43] affording the desired product in good yield and high regio- and stereo- selectivity in favour of the *Z* isomer **326**. They observed an increase of the yield with increased polarity of the solvent, whereas raising the temperature led to a change of the *E*/*Z* ratio towards the E-isomer **327**. Another synthetic approach involved a Michael addition of thiols to electron deficient alkynes **328** bearing an acetylenic ketone using boron trifluoride diethyl etherate as a coordinating and activating agent for conjugated addition. Terminal alkynes reacted with the thiol yielding mainly the *Z*-isomers **329** of the resultant vinyl thioether, while internal alkynes gave the *E*-isomers **330** (Scheme 2.23)[44]

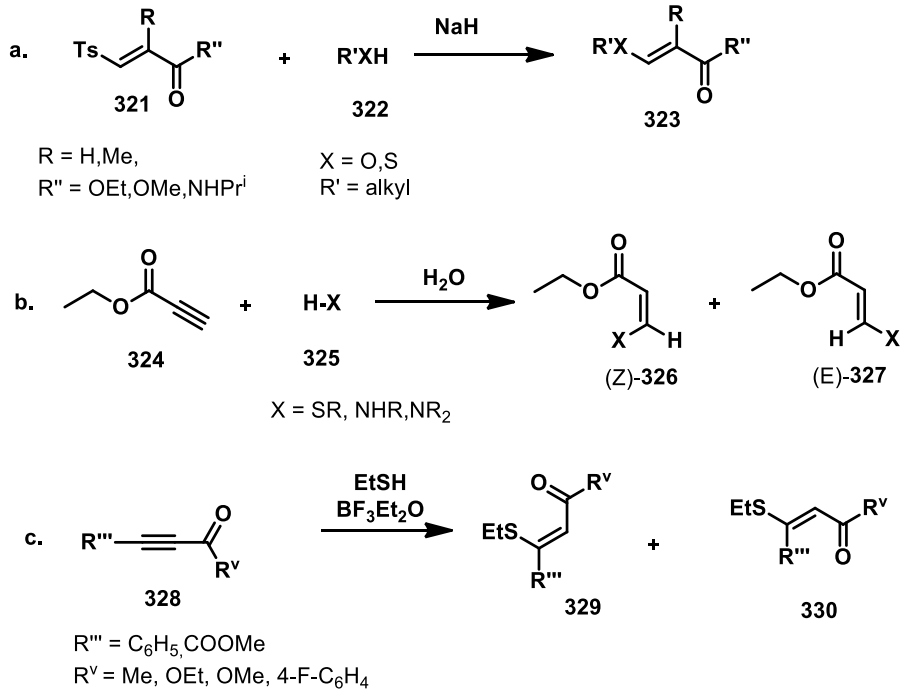

Scheme 2.23. Previous synthesis of E-and Z- thioacrylates: a) a nucleophilic substitution of tosyl-acrylates derivatives with functionalised thiols,[36] b) a thiolation mediated by water,[37] and c) $BF_3.Et_2O$ activated Michael addition. [38,45]

2.24. Synthesis of (E)-320 and (Z)-319 thioacrylate-CoA

In view of the previous protocols, it was contemplated to start from the diacetyl pantothenic acid **294**.[16,27] This involved a mediated coupling with cysteamine to generate the protected pantetheine **331** which was then conjugated to methyl propiolate. This gave the mixture of isomers *(Z)*-**332** and *(E)*-**333** (Scheme 2.24). [46]

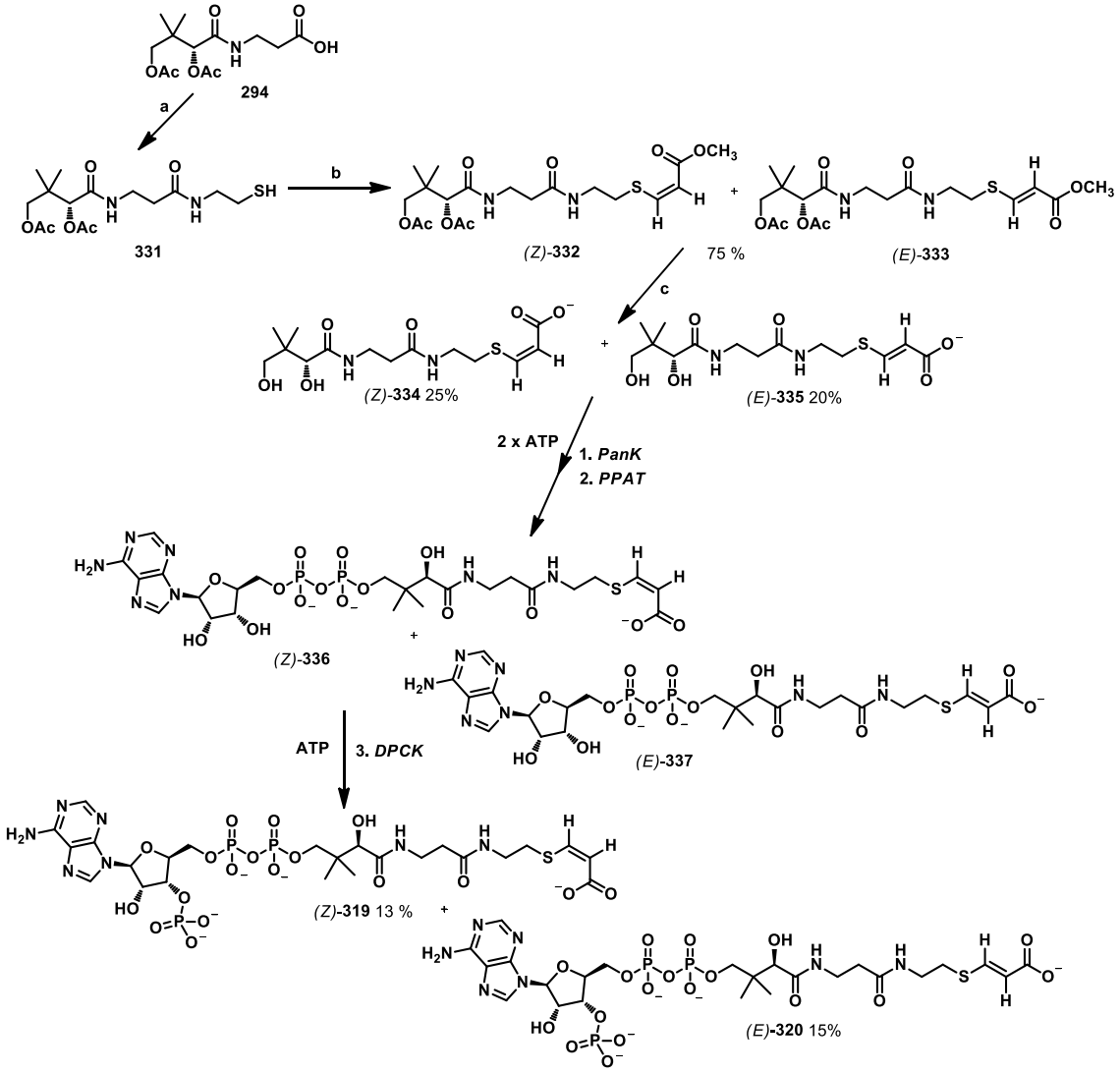

Scheme 2.24. Chemo enzymatic synthesis of *(Z)*-**319** and *(E)*-**320** thioacrylate-CoA: a) 1,1'-dicarbonyldiimidazole, cysteamine-HCl, THF, reflux b) DBU, methyl propiolate, THF; c) LiOH, THF/H_2O, 0°C. [16,27,46]

^{1}H NMR analysis indicated a 60:40 ratio with *Z* isomer **332** as the major product. The isomers could be separated by HPLC but it proved most convenient at this stage to take them as a mixture through the biotransformation protocol and separate them after the

second enzymatic step. Given the close retention time between the two isomers shown in Figure 2.22 (Z isomer **336** retention time = 14.8 min, E isomer **337** retention time = 15.1 min), different parameters were varied to develop the best gradient HPLC method for their separation. Finally, the intermediate products were separated using a linear gradient of acetonitrile/water in 0.05% of trifluoro acetic acid (0 to 20% acetonitrile in 10 min, then 20% acetonitrile for 10 min, then from 20% to 60% acetonitrile in 5 min to wash the column, then from 60% to 0% acetonitrile in 5 minutes, and 0% acetonitrile for 10 min to re-equilibrate the column). Low volume injections (100-200 µL) were performed in order to achieve the best separation.

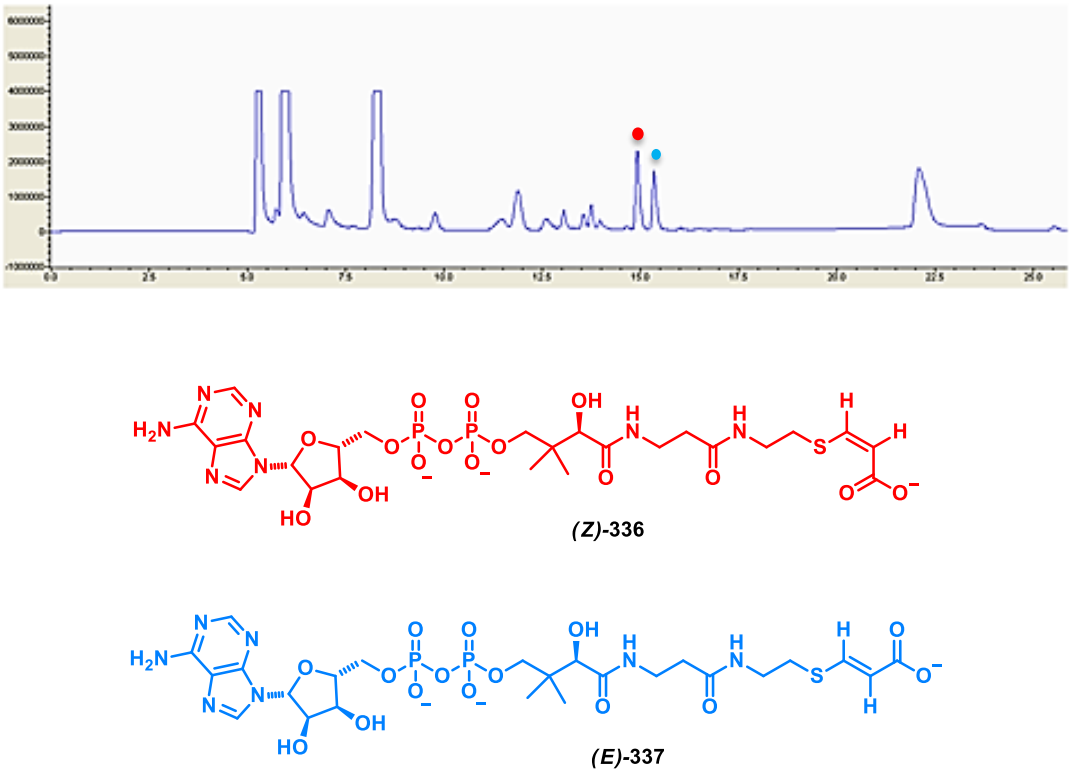

Figure 2.22. The HPLC profiles of intermediate (Z)-**336** and (E)-**337**.

Finally, (*Z*)-**336** and (*E*)-**337** were separately converted to (*Z*)-**319** and (*E*)-**320** and purified by HPLC.[16] The DPCK products (*Z*)-**319** and (*E*)-**320** were individually characterised by ^{1}H NMR and ^{1}H-^{1}H-2D COSY NMR.[16] Figure 2.23 shows the ^{1}H NMR of (*Z*)-**319** and (*E*)-**320** where (*E*)-**320** has a larger coupling constant (J = 15.0 Hz) than (*Z*)-**319** (J = 10.0 Hz).[16]

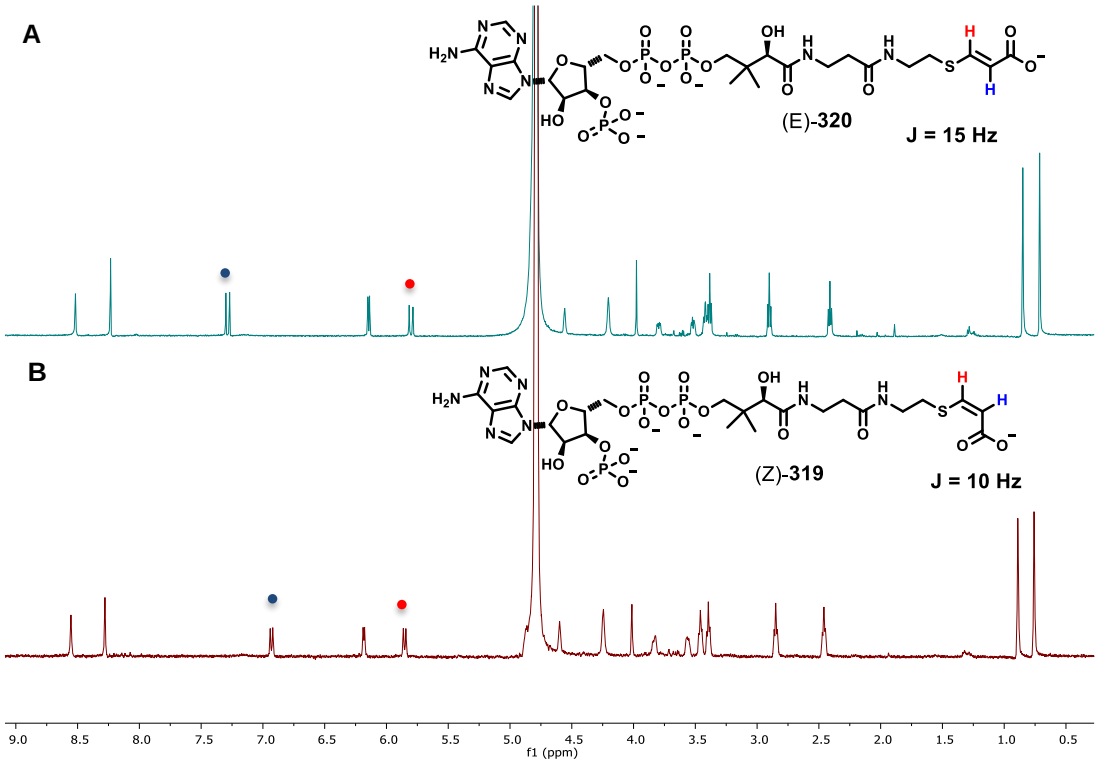

Figure 2.23. ^{1}H NMR spectra of A) *(E)*-**320** and B) *(Z)*-**319**.[16]

All of the ^{1}H NMR signals of (Z)-**319** and (E)-**320** isomers were assigned using Double quantum Filter COSY 2D experiment (DFQ-COSY) as illustrated in Figure 2.24 and Figure 2.25.[16] Of significance was the identification of C22, C21 protons (H22, H21) of the conjugated thioester moiety, and the C2, C8, C1', C2', C3', C4', C5' protons of the adenine fragment (H2, H8, H1', H2', H3', H4', H5') for both (Z)-**319** and (E)-**320,** whose constitution was also confirmed by HR-MS.[16]

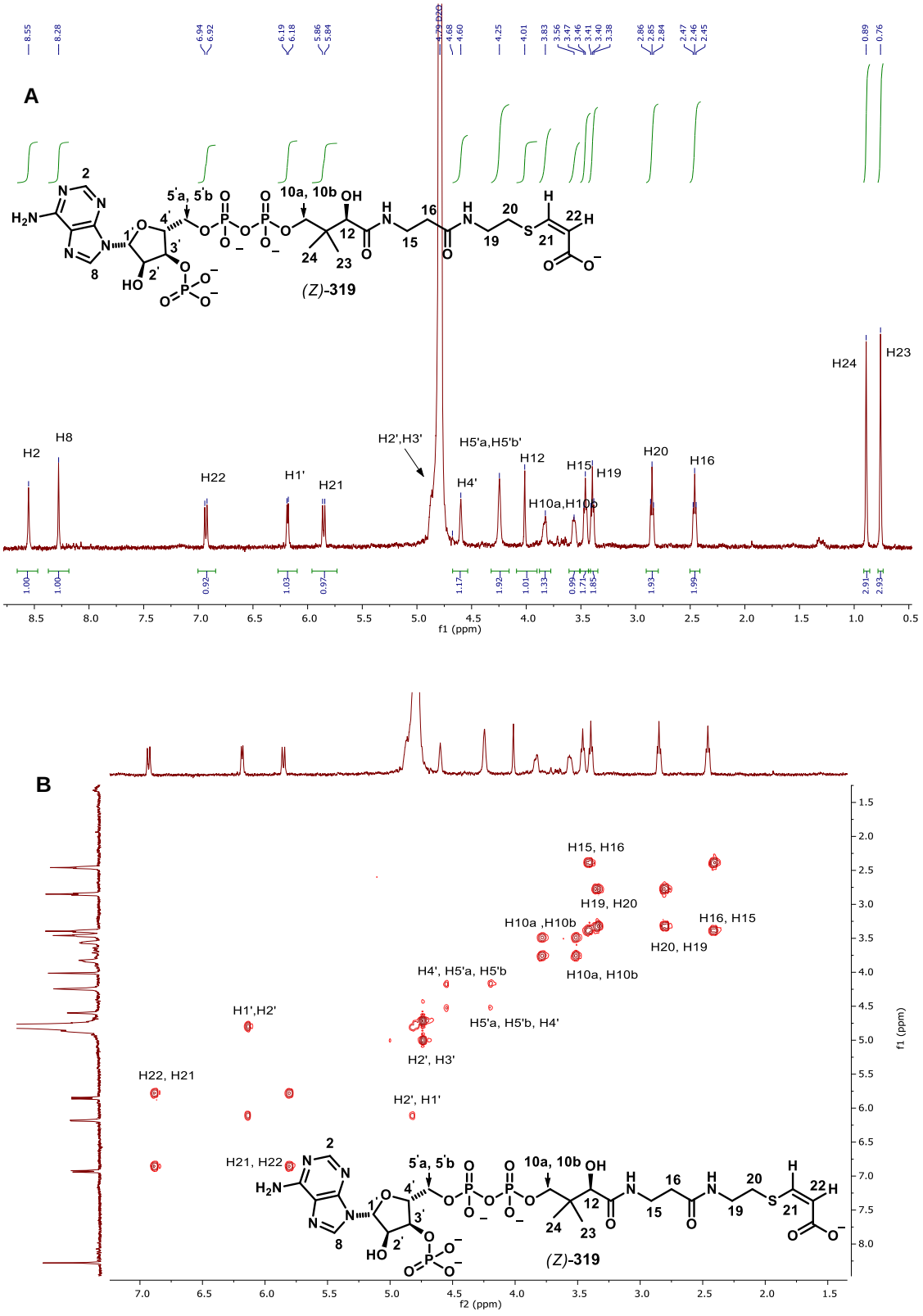

Figure 2.24. A) ^{1}H NMR characterization of *S*-(*Z*-propenoic-3-yl)-coenzyme A **319**: ^{1}HNMR signals were assigned by B) ^{1}H-^{1}H-2D COSY NMR and by comparison with fluorinated dethia analogue **260**.[16]

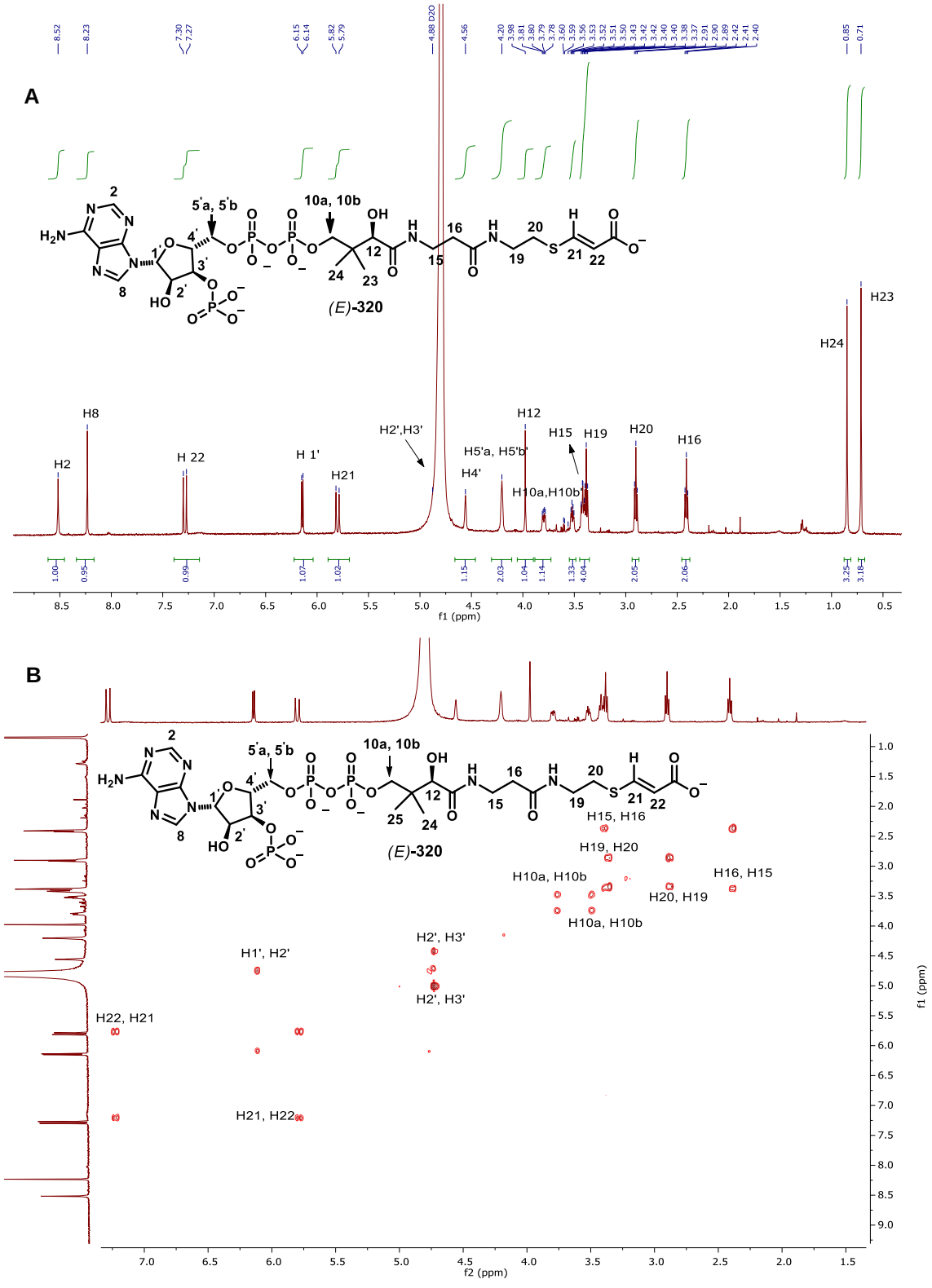

Figure 2.25. ^{1}H NMR characterization of *S*-(*E*-propenoic-3-yl)-coenzyme A **320**: ^{1}HNMR signals were assigned by ^{1}H-^{1}H-2D COSY NMR and by comparison with fluorinated dethia analogue **260**.[16]

2.25. *Inhibition studies of (Z)-319 and (E)-320 isomers towards citrate synthase*

Compounds *(Z)*-**319** and *(E)*-**320** were separately assayed against citrate synthase, using the protocol described previously. However, they did not show any meaningful inhibition of citrate synthase. The constrained geometric isomers do not appear to access any relevant conformation on binding to the enzyme (Table 2.1).[16]

	IC_{50}	K_i^{app}
(Z)-**319**	≥ 3 mM	≥ 500 µM
(E)-**320**	≥ 3 mM	≥ 500 µM

Table 2.1. Inhibition studies of *(Z)*-**319** and *(E)*-**320**.[16]

2.26. Conclusions

Following the encouraging results of the micromolar inhibition of citrate synthase by fluorovinyl thioether (FV-CoA) **212** in this study, five additional analogues of acetyl-CoA (**261, 262, 305,** *(Z)*-**319,** *(E)*-**320**) were successfully synthesised and investigated as inhibitors of porcine citrate synthase. Acetyl-CoA analogues **261, 262, 305,** *(Z)*-**319,** *(E)*-**320** were made by synthesis of the appropriate pre-pantothenyl moieties and assembling the co-enzyme A structure with the three-step biotransformation protocol. Fluorovinyl dethia CoA **261** was prepared as an analogue of FV-CoA **212** to verify if the replacement of the sulfur atom with a methylene moiety would affect the binding affinity. In the event, the affinity was reduced by an order of magnitude. In this case, fluorine is replacing the oxygen atom of an enolate. Both fluorine and oxygen display high electronegativity (F = 3.98 versus O = 3.44) and are isosteric with close van der Waals radii (F = 1.47 Å versus O = 1.52 Å). They also have similar electronic profiles being next to each other on the Periodic Table. Vinyl thioether **262** was synthesised as a control to explore any fluorine effect in the citrate synthase assays. Sulfoxide-CoA **305** has previously been investigated as an inhibitor of acyl transferase enzymes but not for citrate synthase. Sulfoxide-CoA **305** has the sulfoxide methyl moiety replacing the enolate of acetyl-CoA **31**. Finally, two conjugated esters isomers *(Z)*-**319** and *(E)*-**320** were also prepared and explored as inhibitors of citrate synthase. The carboxylate group was anticipated to be a good replacement for a citrate carboxylate as it had the potential to locate into a carboxylate binding site. *(Z)*-**319** and *(E)*-**320** can be compared spatially to historical inhibitor carboxy ethyl-CoA **229**. However being conformationally constrained, they had the potential to access two different conformation in the binding site of the enzymes (Figure 2.26).[16]

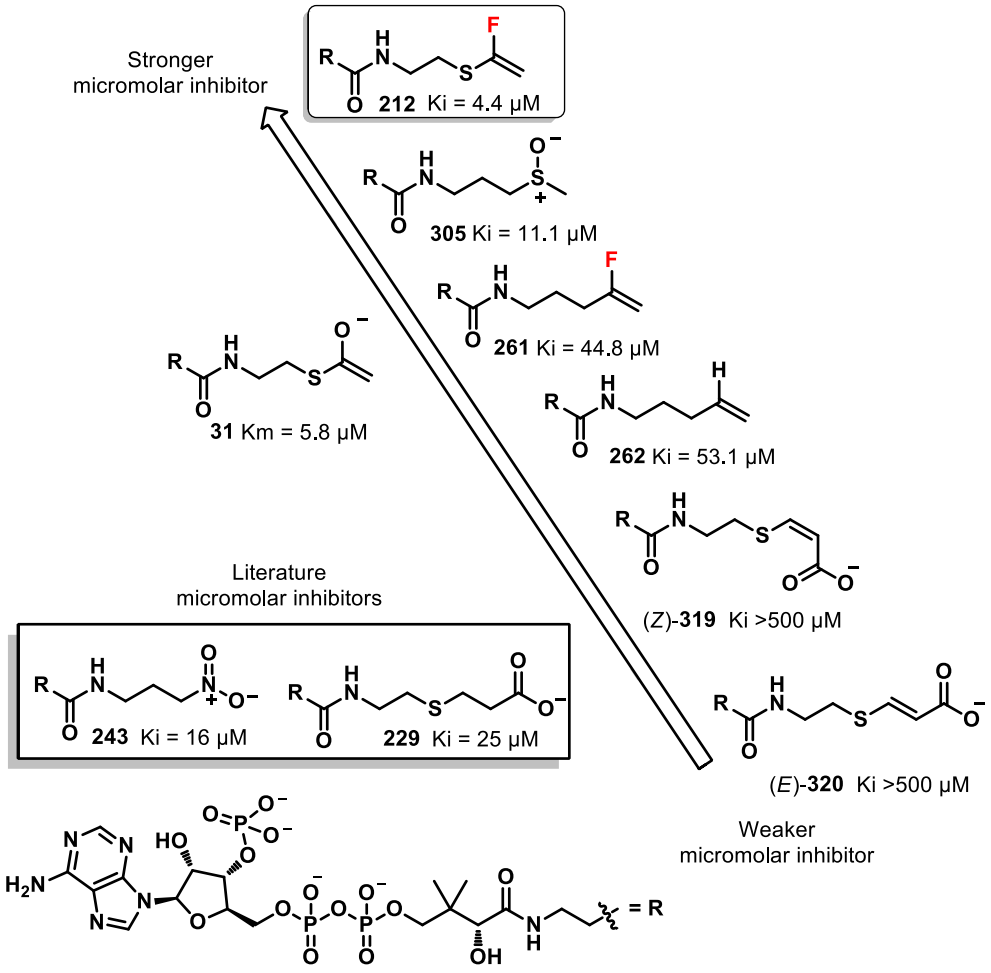

Figure 2.26. Acetyl-CoA analogues as inhibitors of porcine citrate synthase.[16]

With these compounds in hand, they were all explored as inhibitors of citrate synthase monitoring co-enzyme A release from acetyl-CoA. The inhibition data are illustrated in Figure 2.26 and are reported as K_i values. Fluorovinyl-dethia-CoA **261** was found to be a poor inhibitor of citrate synthase with a K_i value (K_i = 44.8 µM), one order higher than the Ki value found for micromolar inhibitor fluorovinyl-thioether CoA **212** (K_i = 4.4 µM). The poor inhibition potency of **261** compared to **212**, suggests that the sulfur atom replacement with a methylene group in **261** negatively affects the binding affinity for the enzyme. It is believed that this replacement could lead to the disruption of the electronic density in **261**, thus making this compound a less suitable analogue of acetyl-CoA than **212**. The inhibition studies on the hydrated vinyl-CoA **262** which was designed as a control for **261**, indicated a residual fluorine effect (Ki **262** = 53.1 µM versus Ki **261** = 44.8 µM). Sulfoxide **305** was a relatively good low micromolar inhibitor (Ki = 11.1 µM). The polarised S^+-O^- bond seems to exert a better hydrogen bond acceptor capacity than the literature inhibitors nitro-alkyl **243** and malate **229**. Sulfoxide **305** was investigated

as mixture of diastereoisomers, thus the inhibition data is an average of the two perhaps indicating that one isomer might bind more tightly to the enzyme than the other. Unfortunately, the X-ray analysis of co-crystallized complexes of **305** with citrate synthase did not give any useful information about the binding. Conjugated thioacrylate isomers *(E)*-**320** and *(Z)*-**319** were finally explored as inhibitors of citrate synthase, however, they did not show any meaningful inhibition. The two geometries of *(E)*-**320** and *(Z)*-**319**, which relate spatially to known low micromolar inhibitor carboxy-ethyl **229**, do not seem to access any relevant conformation on binding or access the carboxylate sites.[16] Although they possess a carboxylate group bearing a located negative charge as well as acetyl-CoA enolate **31**, the isomers do not probably fit into the enzyme cleft. Future work will be focused on investigating these substrates as inhibitors of other acetyl-CoA utilising enzymes such as malate synthase whose mechanism of action is still under study. This enzyme pathway is crucial for understanding plant, animal and human pathogenesis such as *M. tuberculosis*. Malate synthase regulation could lead to its reduced growth in macrophages. Computational studies should be carried out to assess the fitting of the potential inhibitors into the targeted enzyme active site. Furthermore, *(E)*-**320** and *(Z)*-**319** have potential as malonate analogues and they could be studied as inhibitors of acetyl-CoA carboxylase (ACC) that is involved in fatty acids biosynthesis. Regarding the sulfoxide mixture **305**, different stereoselective approaches should be investigated to get the two isomers separated, thus they could be assessed separately as inhibitors of citrate synthase and other acyl-CoA utilizing enzymes.

2.27. References

1 C. Rye, R. Wise, V. Jurukovski, J. DeSaix, J. Choi, A. Yael, *Biology*, **2016**, 1st ed.

2 D. P. Bloxham, D. C. Parmelee, S. Kumar, R. D. Wade, L. H. Ericsson, H. Neurath, K. A. Walsh, K. Titani, *Proc. Natl. Acad. Sci.*, **1981**, *78*, 5381–5385.

3 C. T. Evans, L. C. Kurz, S. J. Remington, P. A. Srere, *Biochemistry*, **1996**, *35*, 10661–10672.

4 M. Karpusas, B. Branchaud, S. J. Remington, *Biochemistry*, **1990**, *29*, 2213–2219.

5 G. Wiegand, S. J. Remington, *Ann.Rev.Biophys.Chem.*, **1986**, *15*, 97–117.

6 D. L. Cox, M. Nelson, *Leningher principles of biochemistry*, **2013**, 3rd ed.

7 D. O'Hagan, H. S. Rzepa, *J. Chem. Soc., Chem. Commun.*, **1994**, 2029.

8 H. Lenz, W. Buckel, P. Wunderwald, G. Biedermann, V. Buschmeier, H. Egqerer, J. W. Cornforth, J. W. Redmond, R. Mallaby, *Eur. J. Biochem.*, **1971**, *24*, 207–215.

9 A. J. Mulholland, W. G. Richards, *J. Mol. Struct.*, **1998**, *427*, 175–184.

10 D. Bello, R. A. Cormanich, D. O'Hagan, *Aust. J. Chem.*, **2015**, *68*, 72–79.

11 E. Bayer, B. Bauer, H. Eggerer, *Eur. J. Biochem.*, **1981**, *120*, 155–160.

12 D. P. Martin, R. T. Bibart, D. G. Drueckhammer, *J. Am. Chem. Soc.*, **1994**, *116*, 4660–4668.

13 K. C. Usher, S. J. Remington, D. P. Martin, D. G. Drueckhammer, *Biochemistry*, **1994**, *33*, 7753–7759.

14 B. Schwartz, D. G. Drueckhammer, K. C. Usher, S. J. Remington, *Biochemistry*, **1995**, *34*, 15459–15466.

15 K. W. Vogel, D. G. Drueckhammer, *J. Am. Chem. Soc.*, **1998**, *120*, 3275–3283.

16 D. Bello, M. G. Rubanu, N. Bandaranayaka, J. Götze, M. Bühl, D. O' Hagan, *ChemBioChem*, 2019, **20**, 1174–1182.

17 I. Nazi, K. P. Koteva, G. D. Wright, *Anal. Biochem.*, **2004**, *324*, 100–105.

18 M. Tosin, D. Spiteller, J. B. Spencer, *ChemBioChem*, **2009**, *10*, 1714–1723.

19 R. Sanichar, J. C. Vederas, *Org. Lett.*, **2017**, *19*, 1950–1953.

20 H.Liu, J.H. Naismith, *Protein Expr Purif.*, **2009**, *63*, 102–111.

21 X. Lei, G. Dutheuil, X. Pannecoucke, J. C. Quirion, *Org. Lett.*, **2004**, *6*, 2101–2104.

22 M. H. Yang, S. S. Matikonda, R. A. Altman, *Org. Lett.*, **2013**, *15*, 3894–3897.

23 F. Nahra, S. R. Patrick, D. Bello, M. Brill, A. Obled, D. B. Cordes, A. M. Z. Slawin, D. O'Hagan, S. P. Nolan, *ChemCatChem*, **2015**, *7,* 240–244.

24 M. Lubke, R. Skupin, H. Gunter, *J. Fluor. Chem.*, **2000**, *102*, 125–133.

25 J. Han, N. Shimizu, Z. Lu, H. Amii, G. B. Hammond, B. Xu, *Org. Lett.*, **2014**, *16*,

3500–3503.

26 O. E. Okoromoba, J. Han, G. B. Hammond, B. Xu, *J. Am. Chem. Soc.*, **2014**, *136*, 14381–14384.

27 D. Bello, D. O'Hagan, *Beilstein J. Org. Chem.*, **2015**, *11*, 1902–1909.

28 X. Qi, F. Yu, P. Chen, G. Liu, *Angew. Chem. Int. Ed.*, **2017**, *19*, 316-319.

29 D. P. Martin, D. G. Drueckhammer, *J. Am. Chem. Soc.*, **1992**, *114*, 7287–7288.

30 W. Du, Q. Gu, Y. Li, Z. Lin, D. Yang, *Org. Lett.*, **2017**, *19*, 316–319.

31 P. A. Srere, L. Gonen, H. Brazil, Acta *Chem.Scand.*, **1963**, *17,* 129–134.

32 V. M. Anoop, Basu.U, M. T. McCammon, L. McAlister-Henn and G. J. Taylor, *Plant Physiol.*, **2003**, *132*, 2205–2217.

33 P. A. Srere, *Biochem. Biophys. Res. Commun.*, **1965**, *1*, 87-90.

34 C.J. Johansson, A.Mahlén, *Biochim. Acta*, **1973**, *309*, 466–472.

35 P. A. Srere, *Methods Enzymol.*, **1969**, *13*, 3–11.

36 R. Z. Cer, U. Mudunuri, R. Stephens, F. J. Lebeda, *Nucleic Acids Res.*, **2009**, *37*, 441–445.

37 E. Wojaczynka, J. Wojaczynk, *Chem. rev.,***2009**, *65*, 2000-2009.

38 T. Torn, C. Bolm, *Organicsulfur Chemistry in Asymmetric synthesis,* **2008**, 1-29.

39 G. E. O'Mahony, A. Ford, A. R. Maguire, *J. Sulfur Chem.*, **2013**, *34*, 301–341.

40 C. Cardellicchio, G. Fracchiolla, F. Naso, P. Tortorella, *Tetrahedron*, **1999**, *55*, 525–532.

41 S. B. Larson, J. S. Day, C. Nguyen, R. Cudney, A. McPherson, *Acta Crystallogr. Sect. F Struct. Biol. Cryst. Commun.*, **2009**, *65,* 430–434.

42 S. Blaya, R. Chinchilla, C. Nájera, *Tetrahedron*, **1995**, *51*, 3617–3626.

43 N. A. Randive, V. Kumar, V. A. Nair, *Monatsh. Chem.*, **2010**, *141*, 1329–1332.

44 Q. F. Zhou, X. P. Chu, S. Zhao, T. Lu, W. F. Tang, *Chin. Chem. Lett.*, **2012**, *23*, 639–642.

45 S.K. Jarchow-Choy, E. Sjuvarsson, H. O. Sintim, S. Eriksson, E.T. Tool, *J.Am.Chem.Soc.*, **2009**, *131*, 5488–5494.

46 Carney et al., *US Patent No.4*, **1989**, 5488-5494.

3. *TOWARDS THE SYNTHESIS OF AN ACETYL-COA CARBOXYLASE INHIBITOR*

3.1. Acetyl-CoA carboxylase: enzyme structure and mechanism of action

Acetyl-CoA carboxylase is a biotin dependent enzyme, involved in the synthesis and oxidation of fatty acids. It mediates the irreversible carboxylation of acetyl-CoA **2** to form malonyl-CoA **33**, the rate determining step of fatty acid biosynthesis. Its structure consists of three functional domains. These domains are:

The biotin carboxylase domain (BC) mediates the ATP dependent N -1' carboxylation of biotin **340** to form carboxy-biotin **32**. The BC structure contains three domains A, B and C. The active site is located at the interface between the B and the A, C domains. The B domain undergoes a conformational change. The closed conformation may be significant for the catalysis process whereas the open one appears to be associated with substrate binding and product release.

The carboxyl transferase domain (CT) catalyses the carboxylation of acetyl-CoA **2** to form malonyl-CoA **33**. The CT structure contains two central domains, the N (amino terminus) and the C (carboxyl terminus). It shows a dimeric structure with a head-to-tail arrangement such that the N domain of one monomer is connected to the C domain of the other.

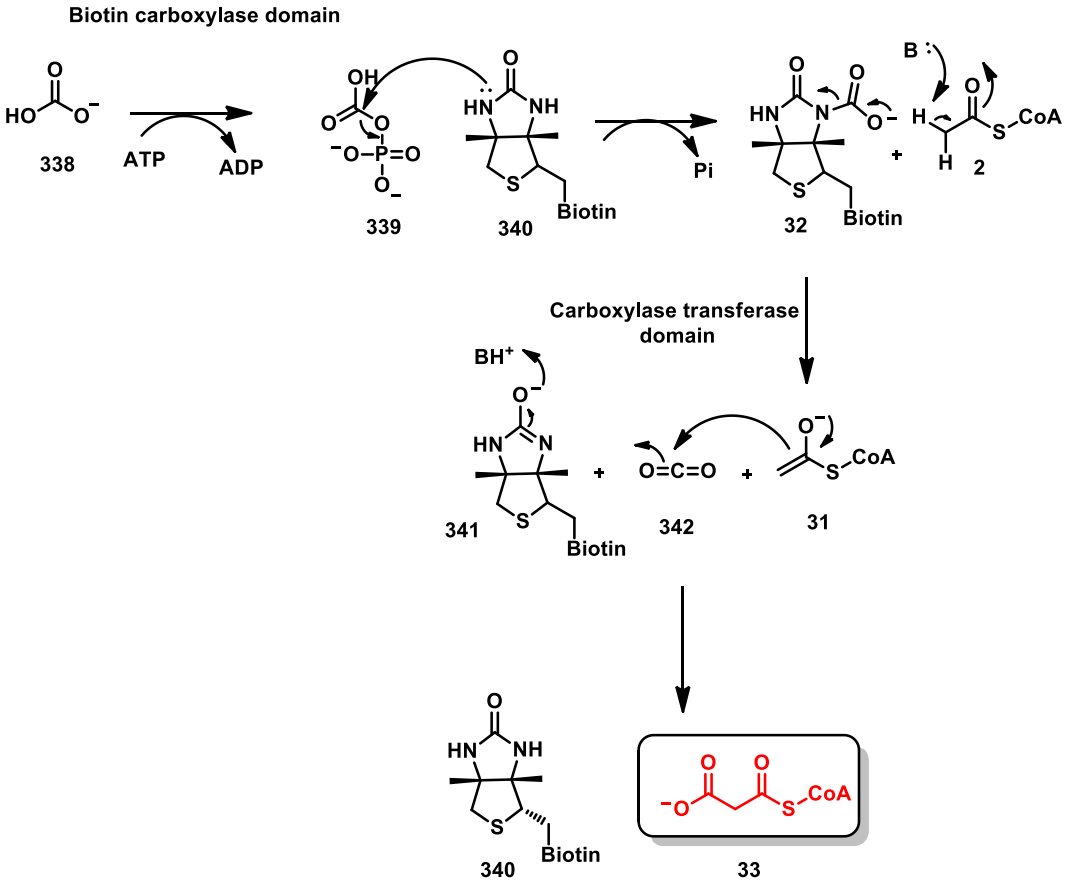

Scheme 3.1: Acetyl-CoA carboxylase mediates the first step of fatty acid biosynthesis.[1,2]

The biotin carboxyl carrier protein (BCC) carries the biotin covalently bound to the Ɛ-nitrogen of a lysine residue from the carboxyl terminus.[1]

Two main isoforms of ACC are present in mammals, ACC1 and ACC2 which differ in tissue distribution and function. ACC1 is found in the cytoplasm of all living cells monitoring the regulation of fatty acid synthesis, whereas ACC2 is present in oxidative tissues and mostly regulates fatty acid oxidation (Scheme 3.1).[2]

3.2. Malonyl-CoA as central metabolite

Malonyl-CoA **33** is produced within the mitochondria, peroxisomes and cytosol of mammalian cells. It is generated by the irreversible carboxylation of acetyl-CoA **2** mediated by acetyl-CoA carboxylase and it is an intermediate of fatty acid biosynthesis and fatty acid elongation (Scheme 3.1).

3.3. The role of malonyl-CoA in fatty acid biosynthesis

Fatty acid biosynthesis: All the reactions in the fatty biosynthesis process are catalysed by a multienzyme complex, the fatty acid synthase (FAS) that carries out the chain elongation process from acetyl-CoA **2** and malonyl-CoA **33**. Fatty acid synthase exists in two forms, Type I and Type II. Type I is a multifunctional polypeptide enzyme commonly found in both animals and fungi, whereas, Type II consists of associated monofunctional enzymes and is found in archea and bacteria.

Mammalian fatty acid synthase is a dimer of two 260-kD subunits. Each subunit is folded into three domains connected by flexible regions. *Domain 1* represents the substrate entry and condensation unit and consists of acetyl-transferase, malonyl-transferase and β-ketoacyl synthase that mediates the condensation step. *Domain 2* is the reduction unit and contains the acyl carrier protein (ACP), β-ketoacyl reductase, dehydratase and enoyl reductase. *Domain 3* serves as the product release unit and accommodates the thioesterase. This multienzyme complex, consisting of covalently connected enzymes, is highly stable and it allows the transfer of the intermediate products from one active site to an another without leaving the assembly.

Before the elongation of the fatty acids chain process starts, acetyl-CoA **2** and malonyl-CoA **33** are loaded onto the fatty acid synthase. The acetyl group of acetyl-CoA **2** is transferred to a pantothenate group of the acyl carrier protein (ACP), a small peptide located in *Domain 1* of FAS. The second transfer is from the pantothenate moiety to a cysteine thiol (-SH) on FAS. Malonyl-CoA **33** is also transferred in a similar manner to acetyl-CoA **2**.

Condensation step: The acetyl **35** and malonyl **34** thioester undergo a condensation reaction producing an aceto-acetyl moiety **36** which is bound to the ACP with loss of carbon dioxide. In the process, the acetyl-group is transferred to the malonate bound to thiol of ACP, forming the aceto-acetyl ACP **36**. In each condensation step the acyl chain is extended by two carbon atoms.

Reduction step: The aceto-acetyl moiety **36** generated in the condensation step, undergoes a reduction at the keto carbonyl group to form D-β-hydroxybutyryl-ACP **37**, this reaction is mediated by β-ketoacyl-ACP reductase with hydride donated from NADPH.

Dehydration step: β-Hydroxyacyl-ACP dehydratase catalyses the elimination of water from D-β-hydroxybutyryl-ACP **37** to yield crotonyl-ACP **38**.

Reduction step: Butyryl-ACP **39** is generated after reduction of the double bond of crotonyl-ACP **38** catalysed by enol-ACP reductase with NADPH as the hydride donor. These four reactions, are representative of the first cycle of chain lengthening during

fatty acid assembly. The FAS complex operates a series of decarboxylative Claisen condensations, extending the C-C backbone for the production of C_{16} – C_{18} chain fatty acids such as palmitoyl-CoA **343** and linoleoyl-CoA **344**.[1,3]

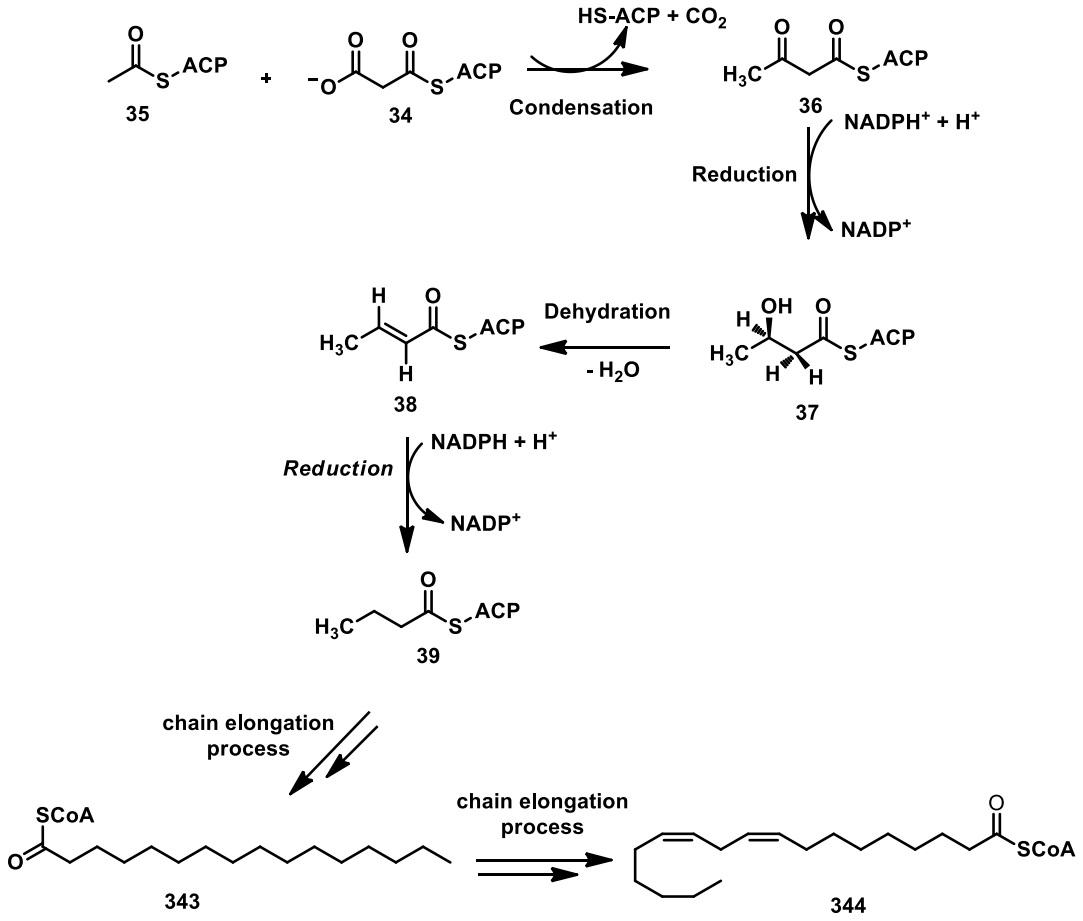

Scheme 3.2: An overview of fatty acid biosynthesis.[1,3]

3.3.1. Carnitine acyl transferase regulation: β-oxidation of fatty acids

Carnitine acyl transferase is a mitochondrial enzyme whose function is to facilitate the transport of fatty acids across the mitochondrial membrane by converting them to carnitine esters. The acyl group is transferred from the acyl-CoA **345** to the hydroxyl group of carnitine **346** to generate acyl carnitine **347**, which is transferred to the inner membrane and converted back to the CoA esters by carnitine palmitoyl transferase II. These Co-A esters participate in β-oxidation process of fatty acids, described in Chapter 1, paragraph 1.2., to generate acetyl-CoA **2**.[1,4]

A

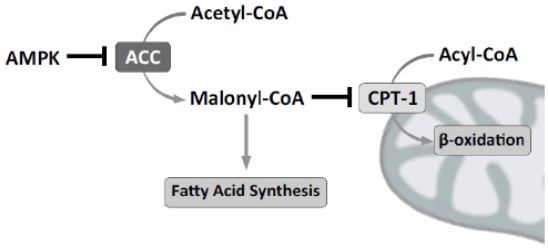

B

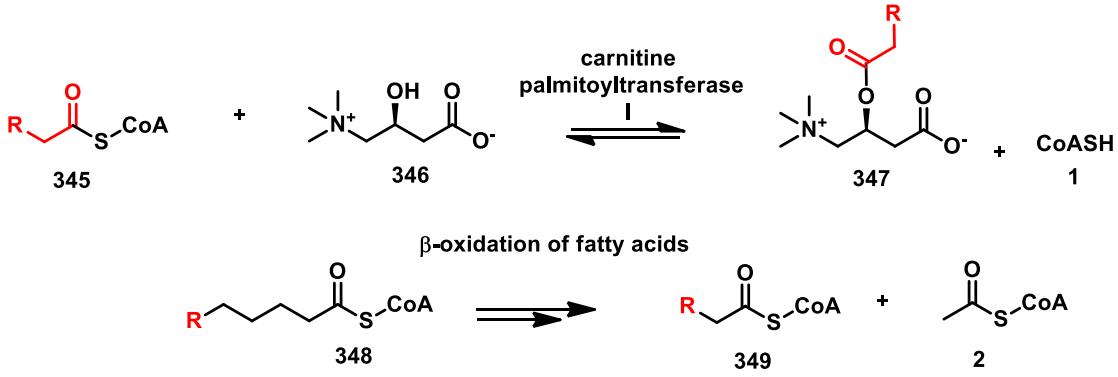

Scheme 3.3. The degradation of fatty acids: long chain fatty acids broken down into fatty acyl- and acetyl-CoA molecules.[1,4]

Fatty acid synthesis and degradation are simultaneously regulated so they are not active at the same time. Acetyl-CoA carboxylase plays a central role in the regulation of fatty degradation. Malonyl-CoA **33**, reaches high concentration levels and inhibits carnitine acyl-transferase preventing access of fatty acyl-CoA to the mitochondrial matrix. Since there are not any crystal structures of carnitine acyl-transferase available, its mechanism of action is still unclear. Studies are focused on the identification of the residues responsible for the inhibition of carnitine acyltransferase by malonyl-CoA **33** in order to gain further insight into the control of the oxidation process. Understanding the

mechanism of regulation of CPTI by malonyl-CoA is significant in drug development for controlling excessive fatty acid oxidation associated to metabolic diseases such as diabetes mellitus or cardiovascular diseases.[4]

3.3.2. Malonyl-CoA decarboxylase deficiency

Malonyl-CoA decarboxylase, found in bacteria and humans, is one of the enzymes responsible for the regulation of malonyl-CoA **33**. It mediates the conversion of malonyl-CoA **33** to acetyl-CoA **2** and carbon dioxide in fatty acid biosynthesis. The exact localization of malonyl-CoA decarboxylase remains unclear, whether it resides in the mitochondria, the peroxisomes or in the cytosol. Malonyl-CoA decarboxylase is a tetramer, each monomer consists of two domains:

The amino terminus is involved in the oligomerization and possesses a helical structure. *The carboxyl terminus* is where malonyl-CoA catalysis takes place.[1,5,6]

The enzyme plays central role in the regulation of fatty acid oxidation as well as in fatty acid metabolism. It is believed that the increase of malonyl-CoA decarboxylase activity alters malonyl-CoA levels. Variations result in an increase in fatty acid oxidation as is observed in diabetes and other metabolic and cardiovascular abnormalities. Dyck *et al.*[5] have reported the synthesis of two potent inhibitors of cardiac malonyl-CoA decarboxylase, CBM-300864 **350** and CBM-301940 **351**. Data showed that MCD inhibitors led to an increase of myocardial malonyl-CoA levels and a decrease of fatty acid oxidation in both *ex vivo* rat hearts and pig hearts (Scheme 3.4).

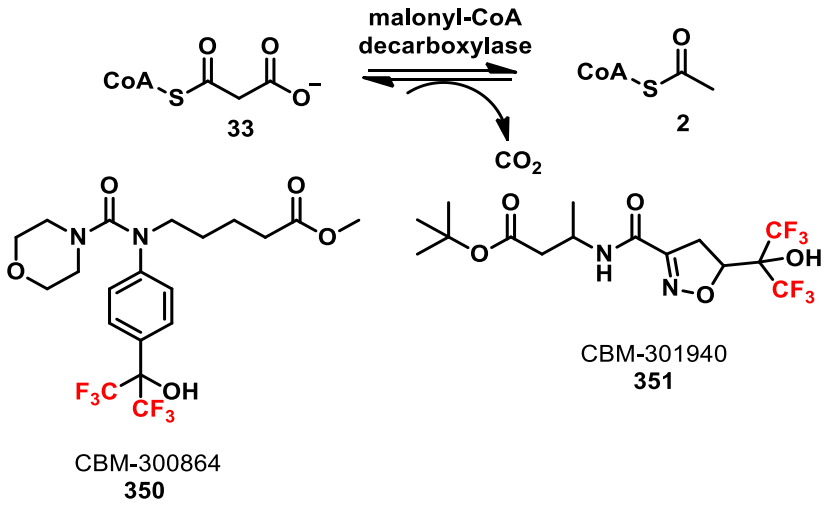

Scheme 3.4. Malonyl-CoA decarboxylase inhibitors designed for treatment of ischemic heart disease.[1,3,5,6]

These results suggested that the pharmacological inhibition of malonyl-CoA decarboxylase could limit fatty acid oxidation. This in turn leads to an increase of glucose oxidation associated with an improvement in the functional recovery of the heart, for diseases such as ischemia (Scheme 3.4).[5]

3.4. Acetyl-CoA carboxylase inhibition

Compound CP-640186 **352** is a bipiperidinylcarboxamide analogue which has emerged as an important inhibitor (IC_{50} = 55 nM) of both isoform of mammalian acetyl-CoA carboxylases. Computational and kinetic studies of the inhibitor-enzyme complex suggested that CP-640186 **352** is probably located in the biotin active site and it is classified as a non-competitive inhibitor. In cell cultures, as well in animal models, CP-640186 **352** seems to reduce malonyl-CoA levels, fatty acids biosynthesis and it stimulates fatty acid oxidation. Furthermore, it can reduce body fat mass and body weight improving insulin sensitivity. This highlights the potential applications of acetyl-CoA carboxylases inhibitors as antiobesity and antidiabetic drugs.[7–9]

Acetyl-CoA carboxylase inhibitors also find applications as antibacterial agents, controlling the production of infecting organisms that are related to lipid synthesis for proliferation. Haloxyfop **353** is used as pre- and post- emergency herbicide in broad leafs crops, targeting the CT domain of ACC and shutting down the fatty acid biosynthesis. It is an aryloxyphenoxypropionate bearing a characteristic lactate moiety and only the (R)-isomer is active as herbicide. Crystal structures of yeast ACC with Haloxyfop **353** show that binds to the active site, at the interface of the dimer of the CT domain. One of the oxygens of the carboxylate group interacts through hydrogen bonding with the amide groups of Ala-1627 and Ile-1735 residues. The binding of herbicide **353** leads to a conformational change of several residues at the interface, generating a hydrophobic pocket and disrupting the domain structure (Figure 3.1).[10,11]

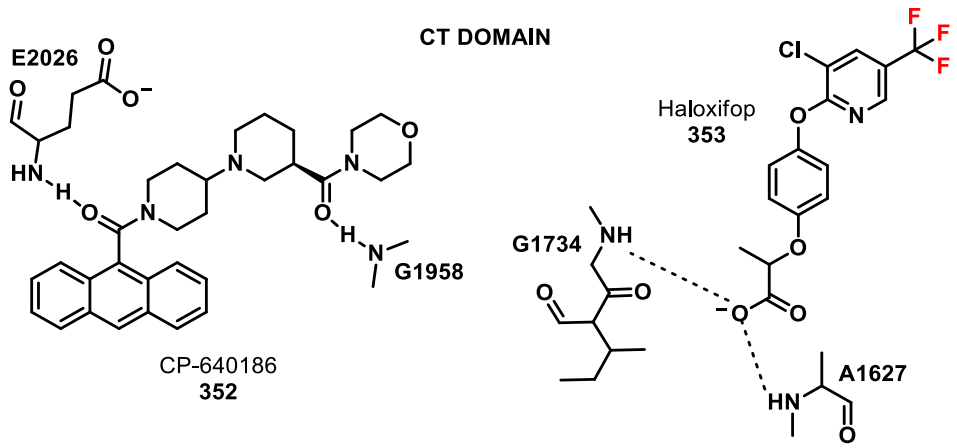

Figure 3.1: Inhibitor CP-640186 **352** and Haloxifop **353** targeting the CT domain. [7–11]

Mimics of long chain fatty acids have also been designed as inhibitors of the carboxyl transferase component of acetyl-CoA carboxylase, mimicking palmitoyl-CoA. A chloro acetylated biotin derivative (CABI) **354** was found to inhibit ACC animal and reduce lipidic accumulation. It was suggested that, once inside the cell, CABI reacts with endogenous co-enzyme A to form analogue CABI-CoA **355** that inhibits the cytosolic isoform of acetyl-CoA carboxylase. The potential of CABI-CoA **355** to minimise the lipidic accumulation makes acetyl-CoA carboxylase an attractive target for the development of anti-obesity agents (Figure 3.2).[12] Soraphen A **356** is a macrocyclic polyketide natural product isolated from the culture broth of *Sorangium cellulosum*, a soil-dwelling myxobacterium. Soraphen A **356** acts as a potent inhibitor of Hepatitis C inhibiting acetyl-CoA carboxylase activity by disabling the polymerisation process, targeting the BC domain. The inhibitor binds at the interface of the A and C domains of the biotin carboxylase component of ACC. X-Ray studies reveal that the oxygens of the methoxy groups are hydrogen bonded to the side chain of Arg-276 residue whereas the hydroxyl group interacts with the Ser-77 residue.[9,13,14]

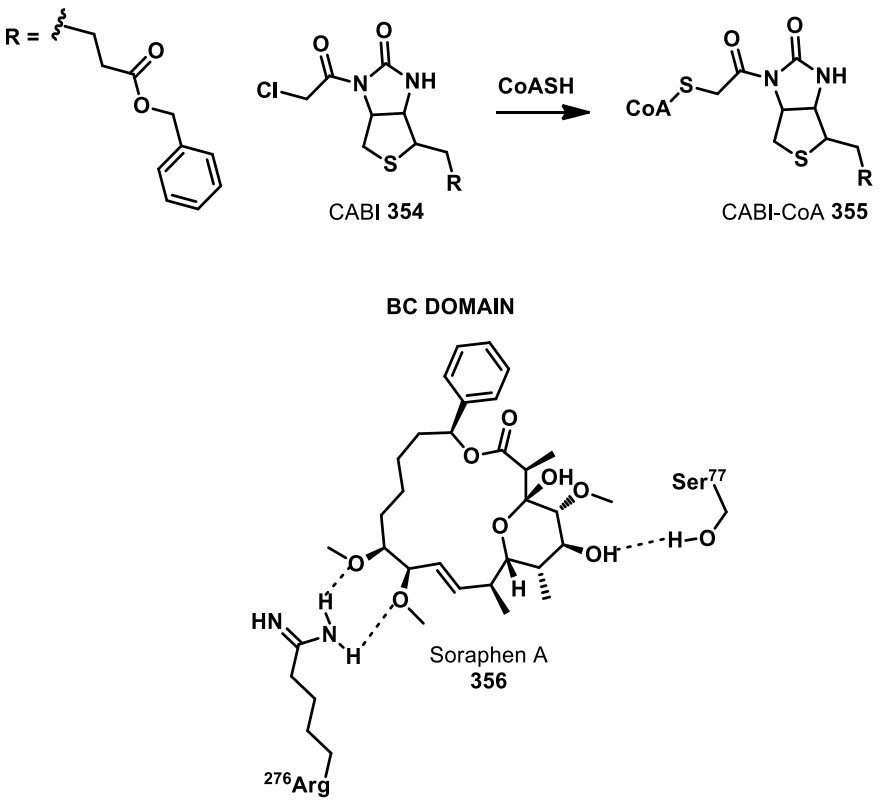

Figure 3.2: Acetyl-CoA carboxylase inhibitors CABI-CoA **355** and Soraphen **356**.[9,12–14]

3.5. Design of an acetyl-CoA carboxylase inhibitor

On the basis of our previous findings on the inhibition of citrate synthase by fluorovinylthioether analogue of acetyl-CoA,[15] the β-fluoroacrylate thioether analogue **357** was envisaged as a mimetic of the enolic form of malonyl-CoA **33**. Compound **357** has a close stereo and electronic profile to **33** (Figure 3.3).

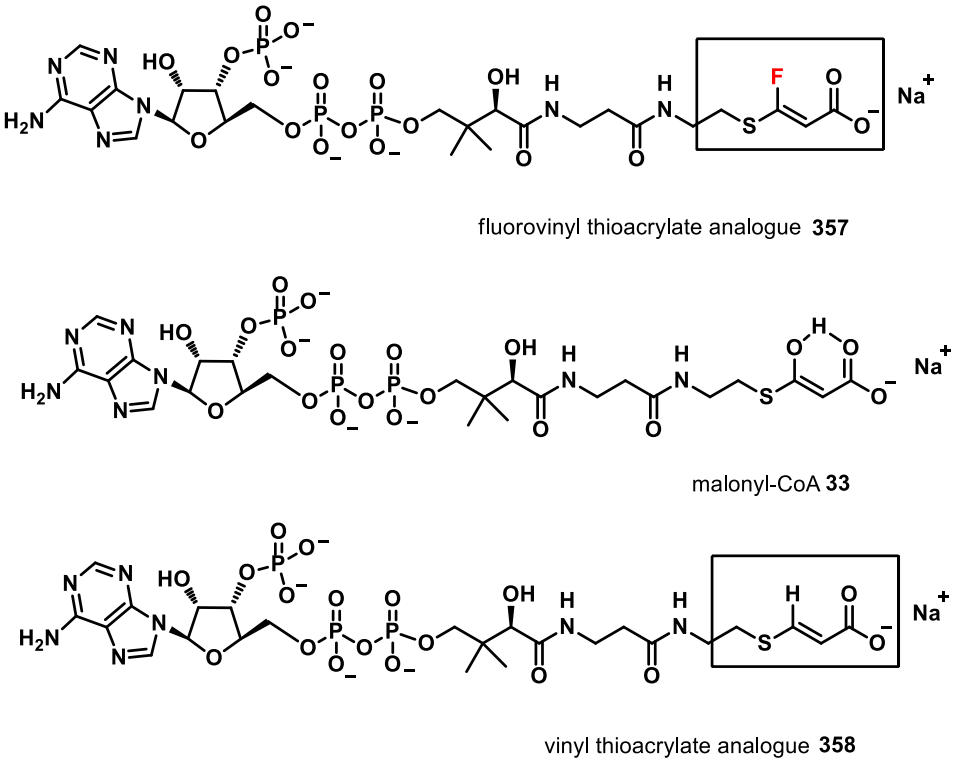

Figure 3.3: Malonyl-CoA analogue **357** developed as acetyl-CoA carboxylase inhibitor.

Following the strategy outlined previously[15,16], it was envisaged that β-fluoroacrylate thioether **359** could then be progressed to the full analogue **357** by the three-step biotransformation (Scheme 3.5). Soaking crystals of protein-inhibitor complexes will be carried out to investigate the inhibitor-protein binding. A non-fluorinated analogue **358** will also be synthesised as a control compound relative to **357** to assess the "fluorine effect" on the binding affinity to the enzyme.

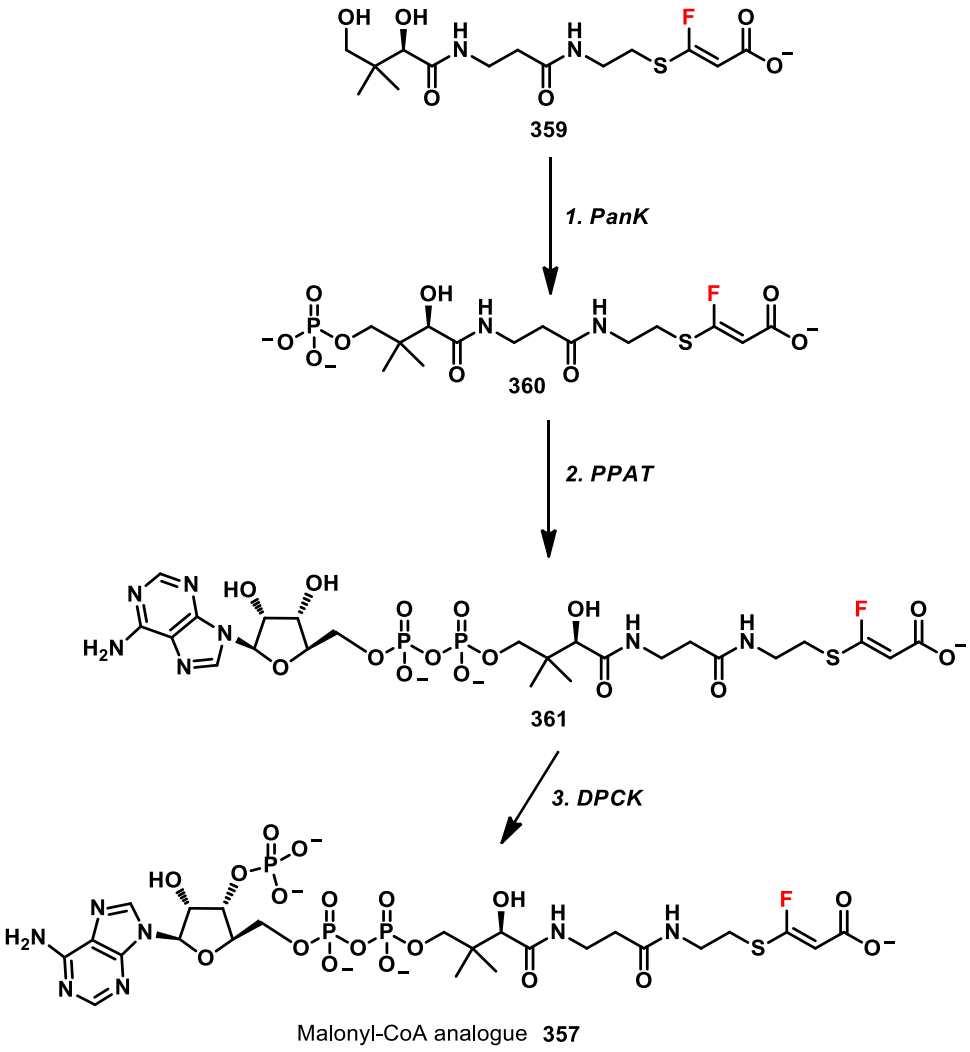

Scheme 3.5: Biosynthetic approach for malonyl-CoA analogue **357**.[15,16]

3.6. Results and discussion: approach to the fluoro vinyl thioacrylate 359

It was envisaged that fluorovinyl thioacrylate **362** could be accessed by a silver/iodide promoted fluorination of the *E*:*Z* mixture of conjugated thioalkenes *(E)*-**333** and *(Z)*-**332**. The diacetylated conjugated esters *(E)*-**333** and *(Z)*-**332** were prepared by Michael addition of pantetheine diacetate **331** with ethyl propiolate giving a mixture of the two isomers *(E)*-**333** and *(Z)*-**332** (40:60) in good yield. [17] However, the fluorination of the conjugated alkenes with silver fluoride/iodine and triethylamine, did not generate any fluorinated product. This is probably due to the electron deficient double bond affecting its reactivity towards the silver/iodide promoted fluorination. This can be contrasted with diacetyl thioacetylene **363** as a substrate which generated diacetylated fluorovinyl derivative **364** on AgF treatment (Scheme 3.6). Compound **364** was synthesised as , intermediate for the synthesis of F-CoA **212** (Chapter 2, Figure 2.4). [15]

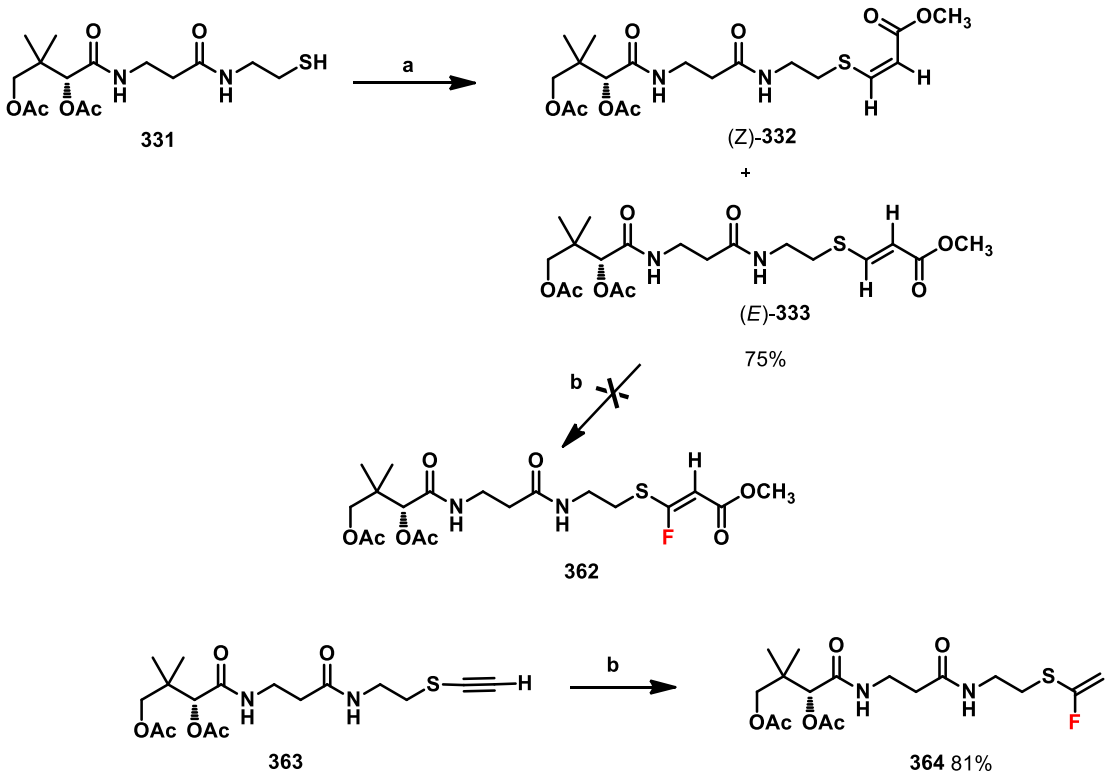

Scheme 3.6: The synthetic approach of fluorovinyl thioacrylate **362** from conjugated esters *(E)*-**333** and *(Z)*-**332** a) methyl propiolate, DBU, THF; b) AgF, I_2, Et_3N, MeCN. [15,17]

3.6.1. Synthetic approach to fluorovinyl thioacrylate 359 from thioester precursor 365

As an alternative approach, it was anticipated that pantothenyl thioether **359** could be prepared from thioester **365**. Fluorination of **365** followed by a basic hydrolysis could offer access to **359** (Scheme 3.7). Due to the instability of the fluoro vinylthioether moiety in acidic conditions,[15] an acetate protection of the diol group was used rather than the common acetal approach. Thus, acetate groups can be removed under basic conditions without compromising the stability of the vinyl fluoride in **359**.

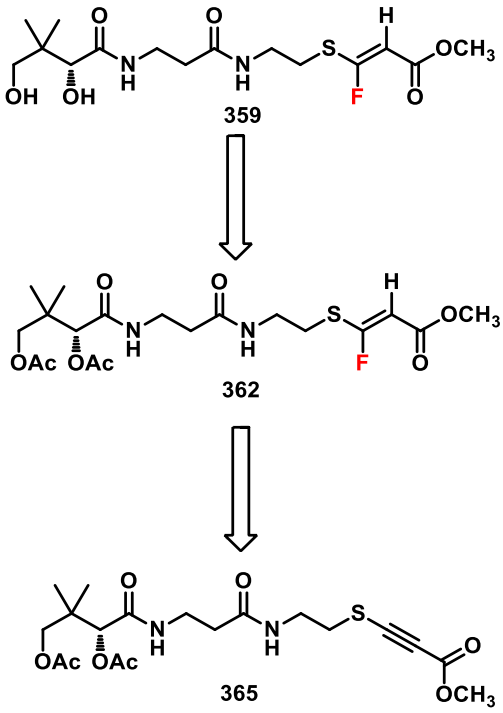

Scheme 3.7. Retrosynthetic approach of fluorovinyl thioacrylate **359**.[15]

The target alkynyl thioester **365** was successfully synthesised from diacetyl thio-alkyne **363**. This acetylene was prepared via electrophilic alkynylation of diacetylated pantetheine thiol **331** with 1-[(trimethylsilyl)ethynyl]-1,2-benziodoxol-3(1*H*)-one **366** as developed by Waser *et al.*[18] The pantetheine **331** was prepared from **294** with cysteamine (Scheme 3.8).

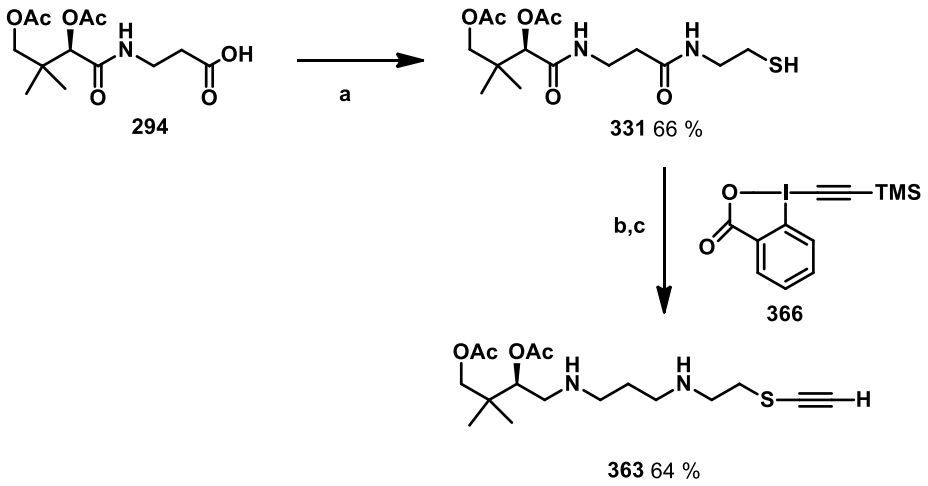

Scheme 3.8. Synthetic procedure of thioacetylene **363:** a) Cysteamine, HOBt, dry THF, reflux, b) TBD, THF, 25 °C, c) TBAF.H_2O, THF, 25 °C.[18]

Several attempts were made to prepare the desired alkyne thioester **365** starting from thioacetylene **363**.

The first approach involved an electrophilic acylation of thioacetylene **363**. Acetylide formation with n-butyllithium was followed by addition of methyl chloroformate. This afforded a complex and inseparable mixture of products. A copper promoted acylation of **363** offered milder conditions, but there was no obvious formation of the desired ester **365** (Scheme 3.9).

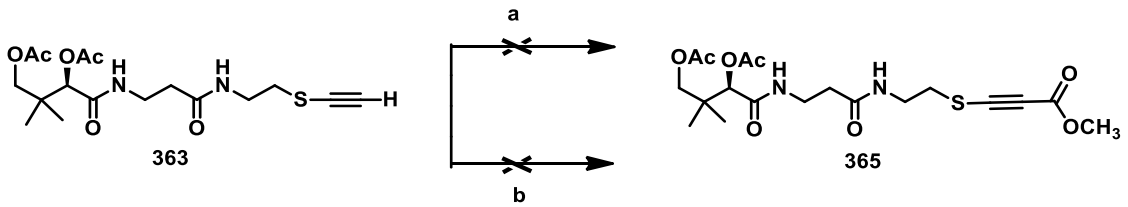

Scheme 3.9. Routes to thioester **365**: a) n-BuLi, MeCOCl, THF, -78 °C, b) Cu(II)I, MeCOCl, Et_3N, THF, 25 °C.

3.6.2. Palladium chloride oxidative carbonylation of the thioalkene derivative

An alternative carboxylation method to the electrophilic acylation was explored and it involved a Pd mediated oxidative carbonylation catalysed by palladium chloride (II). Oxidative carbonylation involves the reduction of Pd (II) to Pd (0) followed by the addition of an oxidant $CuCl_2$ to re-oxidise the Pd (0) to Pd (II) and rendering the reaction catalytic. A base is required to quench the carboxylic acid product. The first step involves the formation of copper acetylide **368** followed by insertion of palladium which leads to intermediate **369**. Treatment of **369** in the presence of carbon monoxide should generate **370**. Methanolysis then generates ester **371**(Scheme 3.10).[19,20]

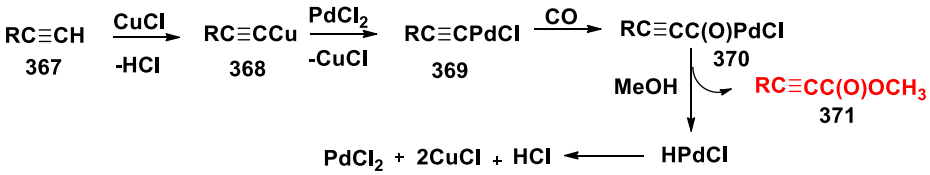

Scheme 3.10. General mechanism of the oxidative carbonylation.[19,20]

Thioacetylene **363** was converted to ester **365** under an atmospheric pressure of carbon monoxide at 0°C and at the atmosphere pressure. This used catalytic $Pd(II)Cl_2$ and an equivalent of $Cu(II)Cl_2$ (Scheme 3.11 A). An Eglington coupling to form diacetylene **372** resulted in a significant side product. The mechanism involves the generation of a copper (II) alkynyl complex **374**, which undergoes dimerization generating **372**. The Eglington coupling seems to prevail over the oxidative carbonylation affording **372** as the major product (Scheme 3.11B).[19,20,21]

A)

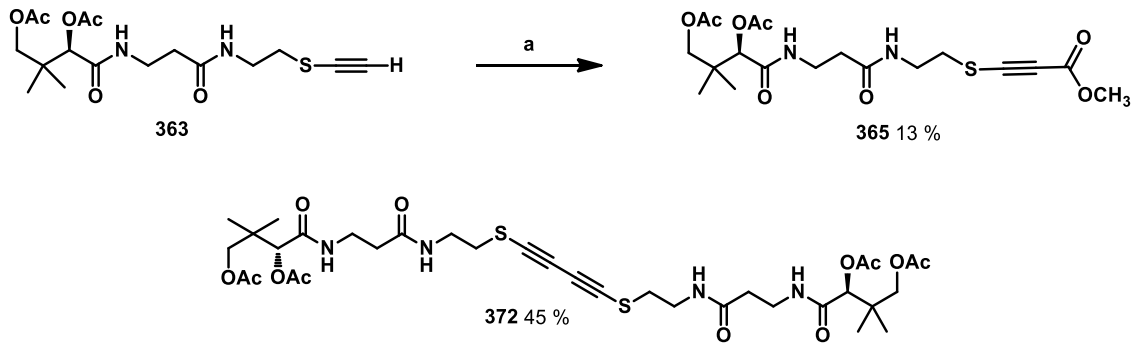

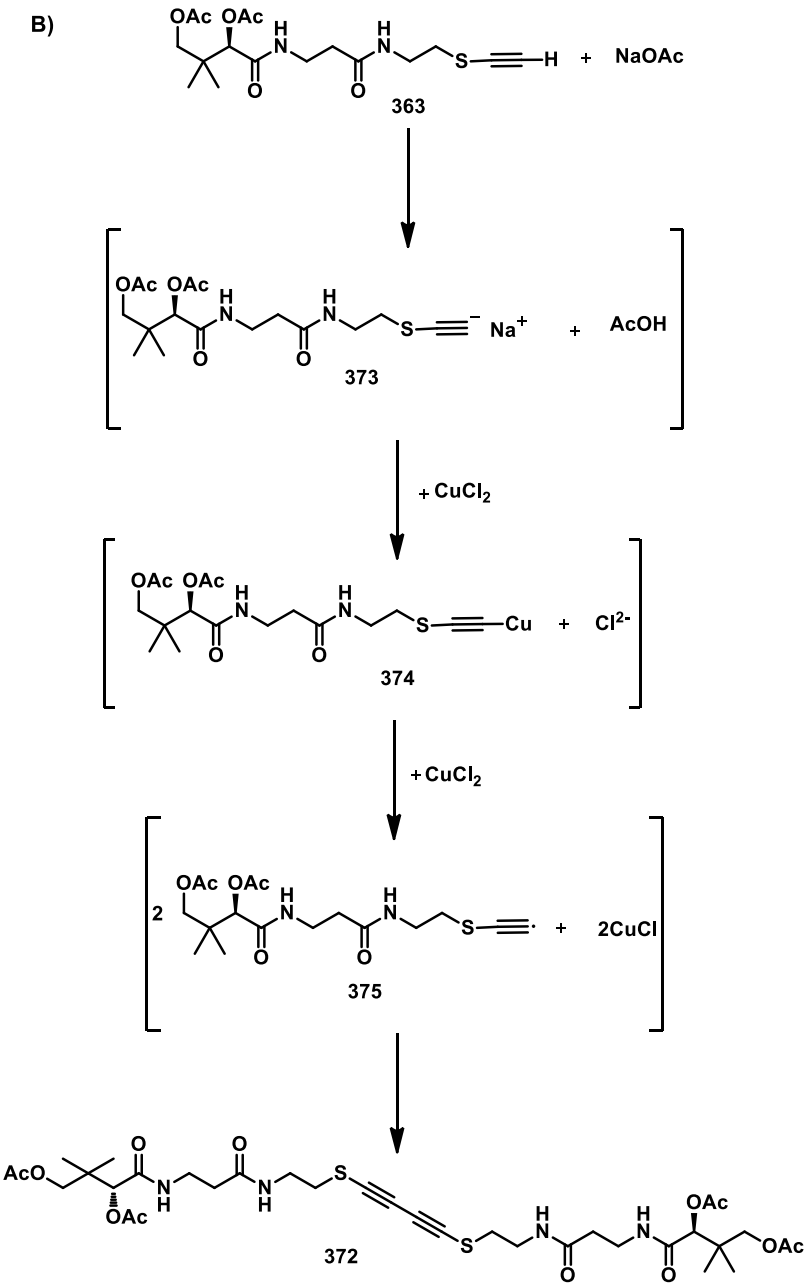

Scheme 3.11. A) Palladium chloride(II) mediated oxidative carbonylation of **363** a) $Pd(II)Cl_2$, $Cu(II)Cl_2$, CO (1 bar) , NaOAc, MeOH, 0 °C. B) Eglington coupling mechanism.[19,20,21]

Dimer **372** could be readily distinguished from monomer **365** by ^1H NMR as shown in Figure 3.4 and particularly from the chemical shift of C3, C3' (H3, H3') protons of **372** versus C6 proton (H6) in **365**, and the disappearance of methyl group C1 protons (H1) in **372** (Figure 3.4).

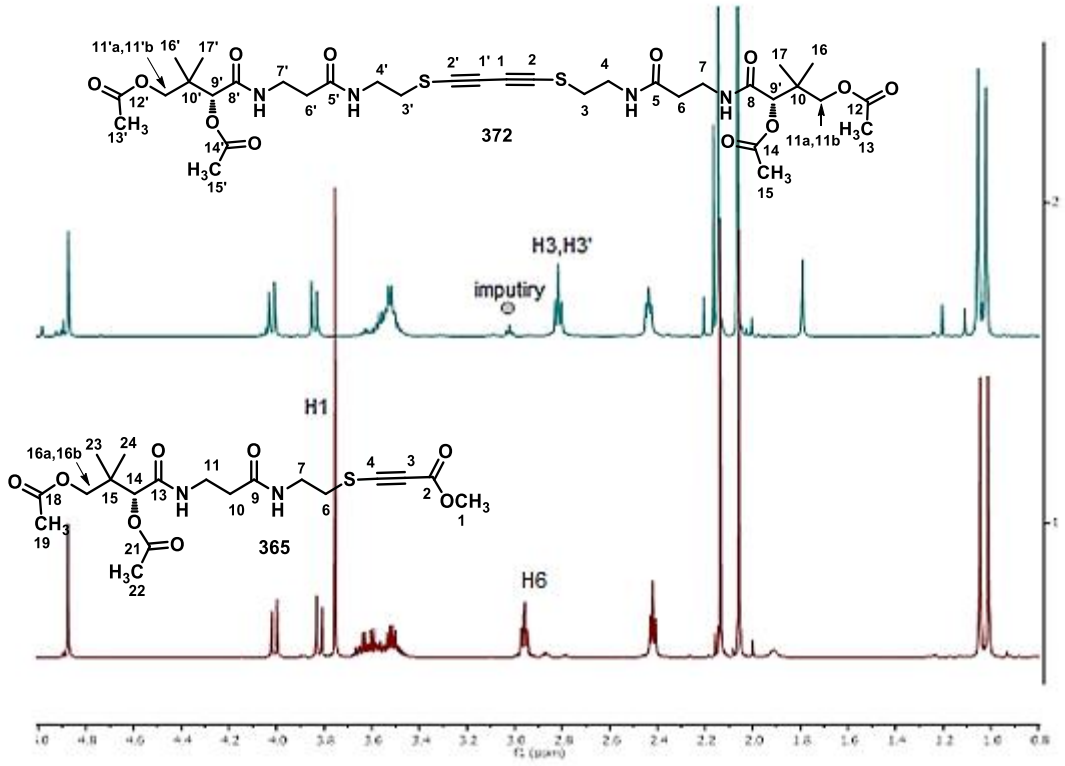

Figure 3.4. ^{1}H NMR of (A) **372** and (B) **365**.

In order to find the optimal conditions to favour a carbonylation over a dimerization process, different reaction parameters were varied (Table 3.1). All the reactions were monitored by ^{1}H NMR for 18 h. The product: dimer ratio was calculated by ^{1}H NMR. High pressures of carbon monoxide were used in order to increase the amount of gas dissolved in the reaction mixture and to promote oxidation over the dimerization. At 50 bars, the formation of additional unidentified side products was observed, thus further reducing the overall product yield.

The temperature seems to play a key role as the ratio between diacetylated thioester **365** and dimer **372** changes significantly in favour of **372** at higher temperatures (0 °C to RT). It appears that the formation of dimer **372** can be minimised by carrying out the reaction at lower temperatures (-10 to -40 ºC) (Table 3.1). However, the reaction proved to be very sluggish at lower temperatures, failing to go to completion and only affording the desired product in low yields (13%).

Entry	Pressure (atm)	Temp	Ratio (365:372) [+]	Time
1	1	-36 °C	15:85	18 h
2	1	-10°C	35:65	18 h
3	1	0°C	50:50	18 h
4	50	0°C	32:68	18 h

Table 3.1. Study of the oxidative carbonylation of **363** to generate **365** modulating the pressure and the temperature parameters. [+]The ratio of **365**:**372** were calculated by ^{1}H NMR.

Further investigation was carried out by changing the oxidant, the base, and the catalyst (Table 3.2). For example, when triethylamine replaced sodium acetate only dimer **372** was obtained. The same result was observed when $PdCl_2(PPh_3)_2$ was used in place of $PdCl_2$. Most positively replacement of $CuCl_2$ with benzoquinone as the oxidant, afforded a 1:1 mixture of 46:54.

Entry	Base	Catalyst	Additive	Solvent	Temp/Time	Ratio (365:372)
1	TEA	$PdCl_2$	$CuCl_2$	MeOH	0°C/ 18h	0:100
2	AcONa	$PdCl_2(PPh_3)$	$CuCl_2$	MeOH	0°C/ 18h	0:100
3	AcONa	$PdCl_2$	Benzoquinone	MeOH	0°C/ 18h	46:54

Table 3.2. Investigation of the oxidative carbonylation of **363** to generate **365** varying base and additive.

Despite these efforts to improve the outcome of the oxidative carbonylation, the reaction was neither predictable or reproducible and the yields of **365** were not considered useful for synthetic purposes.

3.6.3. *Synthesis of ethyl ester via imidazolium sulfurane electrophilic alkynylation*

An alternative synthetic procedure involved an electrophilic alkynylation of thiols using an alkynyl imidazolium sulfurane **382** as described by Alcarazo *et al.*[22,23] These interesting reagents have been investigated in electrophilic group transfer reaction such as electrophilic cyanation. Generally yields are good (Scheme 3.12).[22,23]

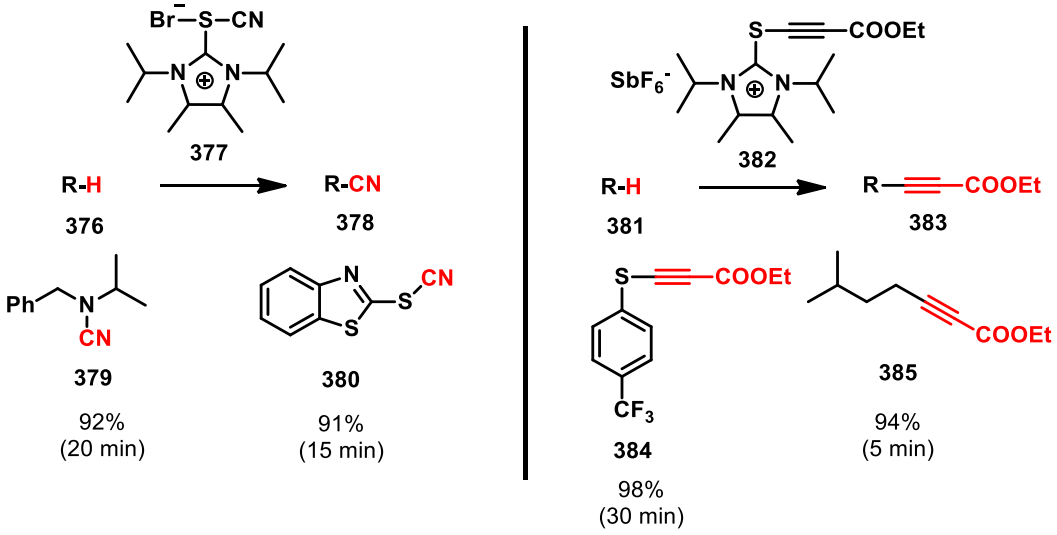

Scheme 3.12. Study of imidazolium sulfuranes as electrophilic group transfer reagents.[22,23]

Given the similarity in electronic structure between cyanides and alkynes bearing electron withdrawing substituents, imidazolium thioesters were also studied as electrophilic group transfer reagents. The imidazolium sulfurane **382** mediated electrophilic alkynylation of different sulfides, bearing electron rich and electron poor substituents also gave good results.

The mechanism suggested for this reaction, is an electrophilic substitution process as described by Frei *et al.*[18,24] for the hypervalent iodine reagent. The reaction is believed to proceed via a triangular atomic arrangement between thiol sulfur thiolate **388**, the iodine of the hypervalent reagent (I (III)) **386** and the α-carbon atom of the protected acetylene derivative **387**. Nucleophilic addition of the anion sulfide in **388** to the α-carbon atom of the acetylene derivative in **387** with concomitant cleavage of the S(imidazolium)-C bond, generates thioacetylene **391** (Scheme 3.13).

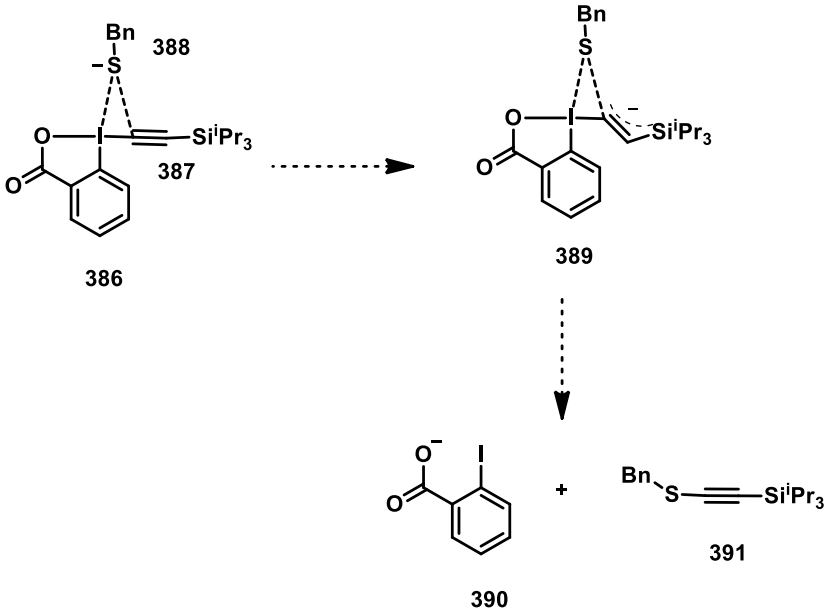

Scheme 3.13. Mechanism of the hypervalent iodine agent (TMS-EBX) with a thiol as reported by Frei *et al.*[18,22–24]

The alkynyl imidazolium sulfurane **382** described by Alcarazo *et al.*,[22] was prepared from diisopropylthiourea **392** and acetoin **393** to generate **394**. When treated with bromine this gave dibromide **395**.

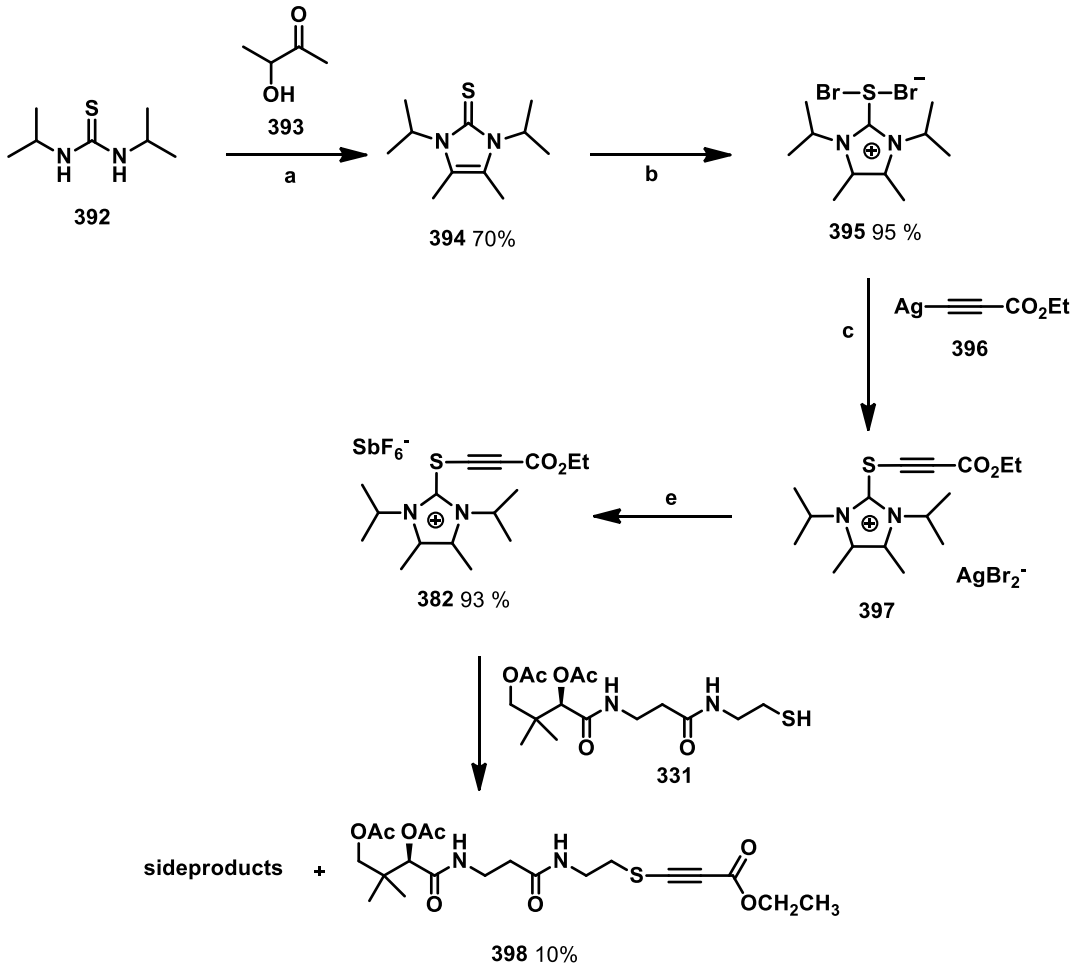

Scheme 3.14. Route to ethyl thioester **398** using imidazolium **382**: a) 1,3-diisopropyl-2-thiourea **393**, 1-hexanol, 158 °C b) Br_2, dry DCM, 0°C, c) and d) silver ethyl propiolate **396**, silver hexafluoro antimonate, dry DCM, 25 °C, e) DIPEA, 25 °C.[22,23]

Silver propiolate **396** was added to a solution of **395** in dichloromethane which led to the alkynylated imidazolium **397** as a dibromo-argentate salt**,** which in the presence of $AgSbF_6^-$ afforded **382**. Treatment of the diacetylated pantetheine **331** with **382** resulted in a rapid conversion of the starting material over 10 min yielding product **398** although in low yield (10%), along with a complex mixture of by-products which proved hard to be separated and identify. ^{1}H NMR analysis indicated that the ratio of product **398** : by-products was roughly 15:85 (Scheme 3.14).[22]

Screening of different bases and solvents was performed to optimize the yield of the reaction and to minimize side reactions.

Entry	Base	Temp.	Time	Solvent	Ratio (398: side-products)
1	Pyridine	RT	30 min	DCM	13:87
2	NaHCO3	RT	30 min	Dioxane	10:90
3	DBU	RT	30 min	DCM	0:100
4	DIPEA	-78 °C	30 min	DCM	0:100
5	DIPEA	0 °C	30 min	DCM	16:84
6	DIPEA	40 °C	30 min	DCM	0:100

Table 3.3. Exploring different bases and solvents for the preparation of **398**

As shown in Table 3 (Entry 1-3), modulation of base strength did not improve the product ratio, indicating that the best base was DIPEA. Also varying the temperature did not seem to affect the ratio significantly (Entry 4-6). Furthermore, scale up of the reaction seemed to significantly decrease the yield of the product with the promotion of the side reactions. Therefore, due to this problem and the lack of reproducibility, this synthetic procedure was not developed any further. The sulfide substrates reported by Alcarazo *et al*.[23] are generally aryl-substituted except for **385** reported in Scheme 3.12, thus the low yield with pantetheine **331** could be related to its more complex and acyclic structure.

3.7. Preparation of fluorovinyl acrylate 362

The fluorination of alkyl thioester **365** was investigated analytically due to the limited amount of material available.

Thus, compound **362** was prepared by conjugate addition of hydrogen fluoride to ester **365** as reported by Li *et al.* [25] using silver fluoride (AgF) in a mixture of water and acetonitrile. This gave the (*E*)-stereoisomer **362** only in moderate yield. The E-stereoisomer was identified by ^{1}H NMR (C3 proton, J = 33.6 Hz) , ^{19}F NMR (*with proton decoupled* -70.51 ppm) and High-Resolution electron spray ionisation mass spectrometry (HR-ESI-MS). The molecular ion (M^{+}) peak found for **362** is 487.1507 which corresponds to [M + Na] $^{+}$ equal to $C_{19}H_{29}O_8N_2FNSNa$ (Scheme 3.15). The ability of silver fluoride to introduce a fluorine atom into compound **365**, lies mostly within the electrophilic character of the alkynyl ester moiety, which reacts as a Michael acceptor and allows the reaction to occur even in the presence of water, which lowers the nucleophilicity of fluoride anion; however silver fluoride could be acting as a Lewis acid, activating the alkyne and therefore increasing its reactivity.

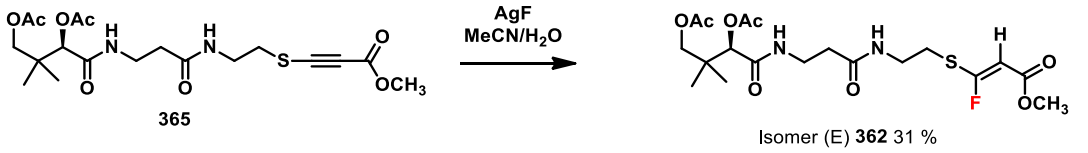

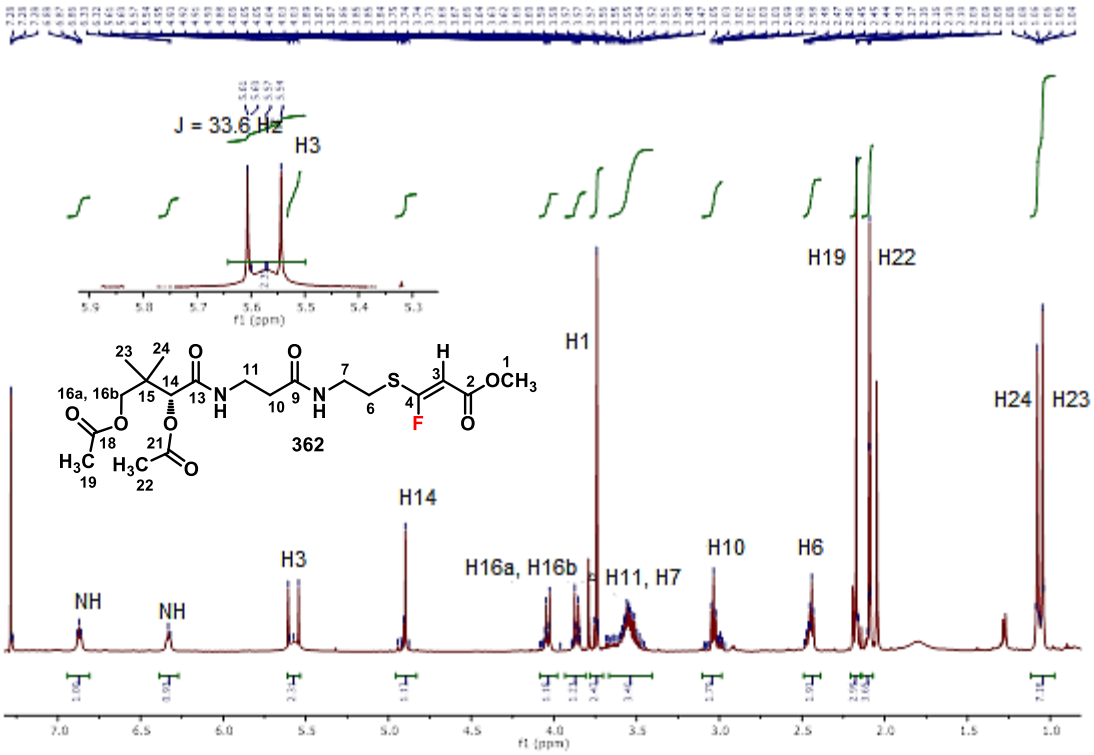

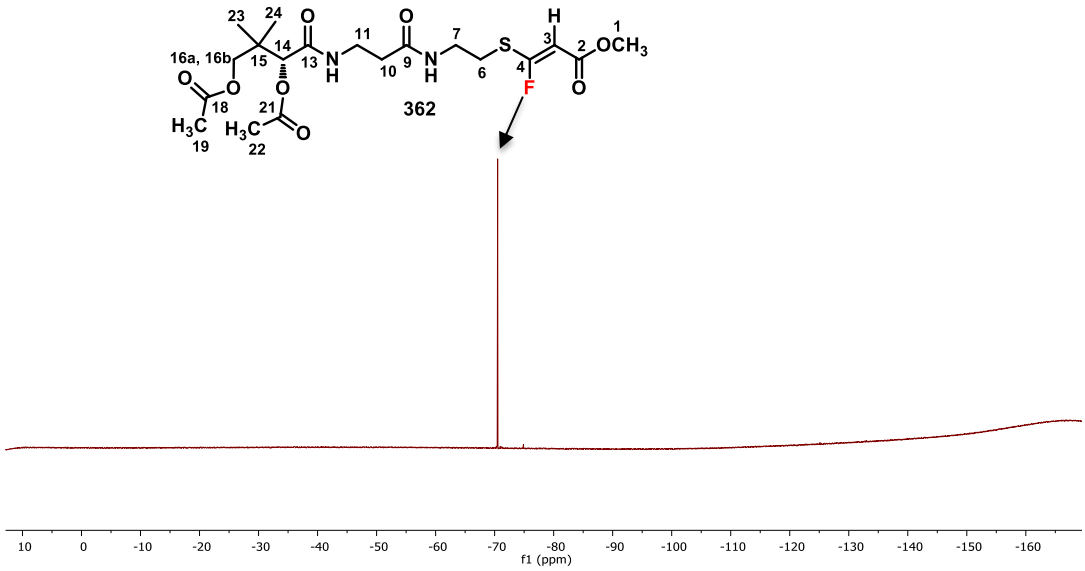

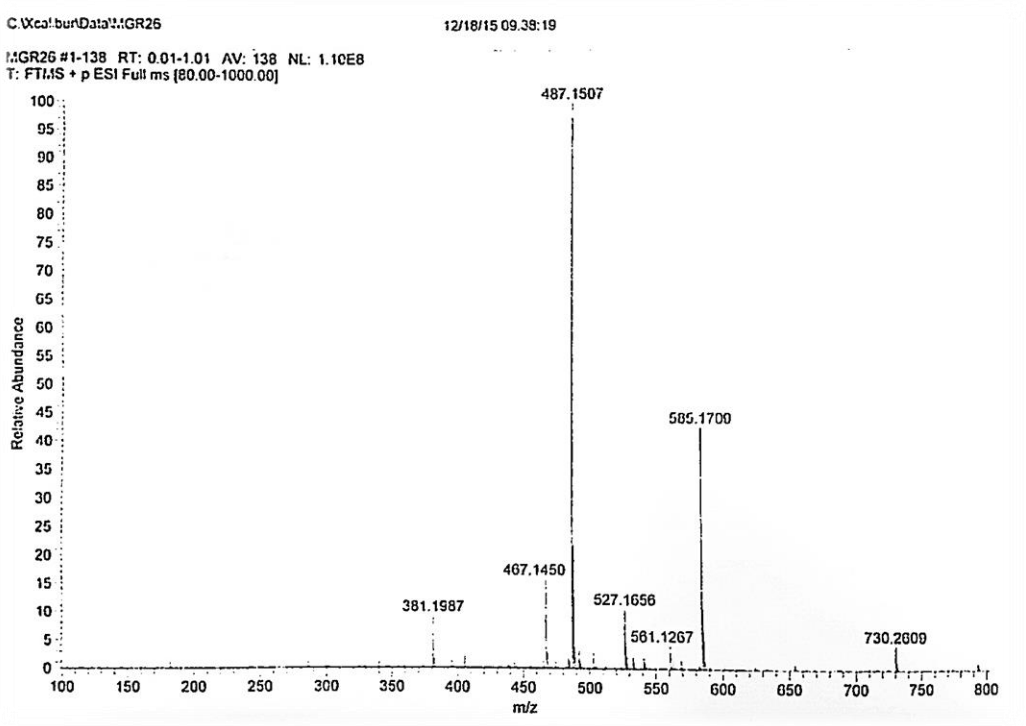

Scheme 3.15. The A) ^{1}H NMR, B) ^{19}F NMR and HR-ESI-MS spectra of fluorovinyl thioacrylate **362**.[25]

Treatment of compound **362** with lithium hydroxide in methanol gave methyl ester **399** as a result of an addition/elimination reaction. (Scheme 3.16).[26] Compound **399** was detected by HR-MS (the molecular ion peak (M^+) found is equal to 415.1509 which corresponds to [$C_{16}H_{28}O_7N_2NaS$]). A THF/H_2O mixture, as used for the hydrolysis of *(Z)*-**332** and *(E)*-**333** in Chapter 2, instead of MeOH as solvent may overcome the addition-elimination reaction.

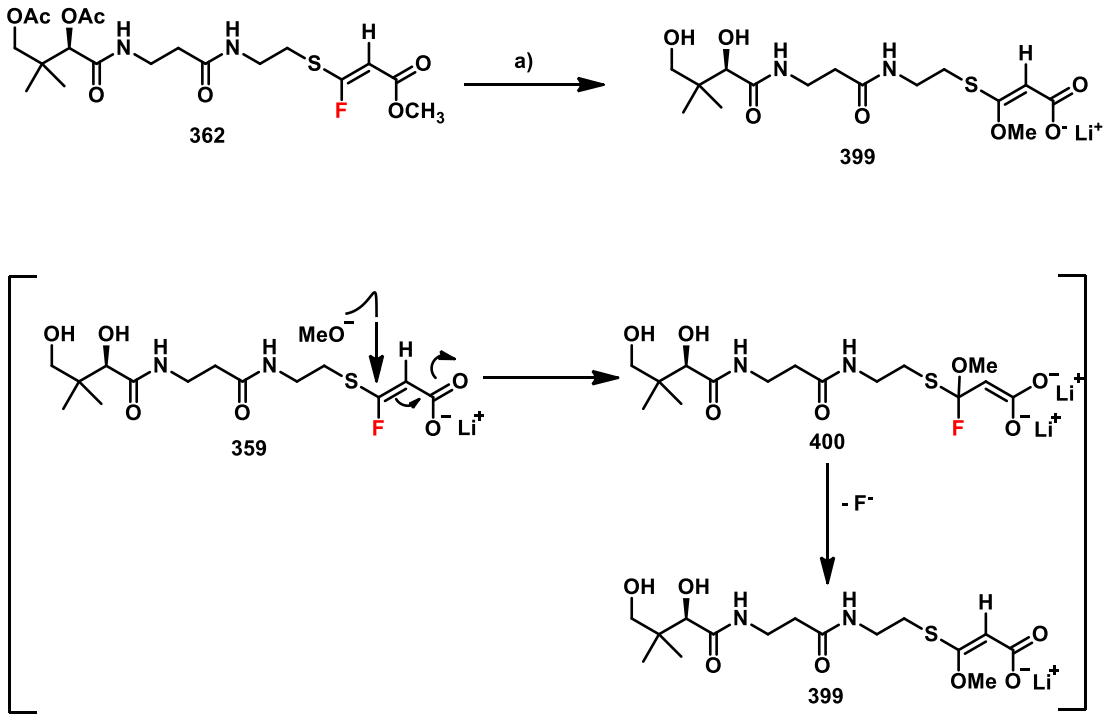

Scheme 3.16. Addition-elimination reaction of **359**: a) LiOH 2M, MeOH, 25 °C.[26]

Access to acetylenic ester **365** and **398** proved to be challenging. The synthetic approaches reported gave the desired product in low yield and lacked reproducibility. Consequently, these synthetic methods were not useful for scale up. Fluorovinyl thioacrylate **362** was prepared analytically but could not be hydrolysed to **359** and consequently it could not be progressed to the desired malonyl-CoA analogue **357**.

3.8. Conclusions

Chapter 3 focused on the attempted synthesis of fluorovinyl thio-acrylate-CoA **357** as an analogue of malonyl-CoA **33**. It was envisaged that fluorovinyl thio-acrylate-CoA **357** could be accessed from hydroxylated pantothenyl precursor **359**.

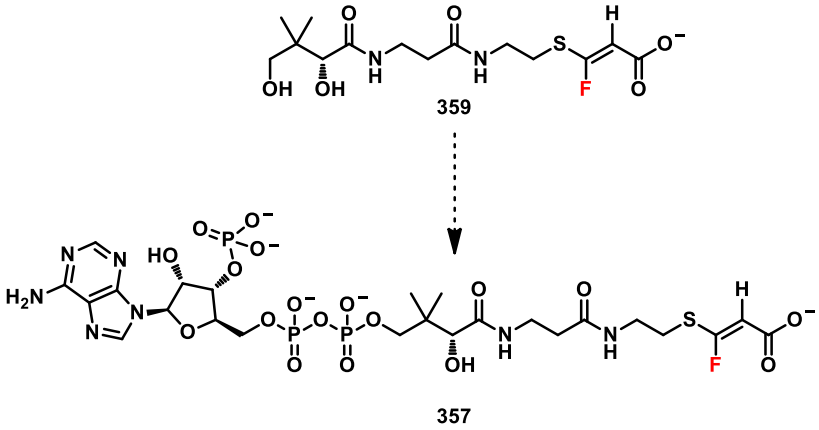

Scheme 3.17. Design of a malonyl-CoA analogue as inhibitor of acetyl-CoA carboxylase

A silver mediated fluorination of conjugated thioesters *(E)*-**333** and *(Z)*-**332** mixture, precursors of acetyl-CoA *(E)*-**320** and *(Z)*-**319** analogues reported in Chapter 2, did not give the desired products and not side products were detected. The starting material proved to be unreactive under these conditions. The presence of an electron withdrawing group such as an ester moiety in *(E)*-**333** and *(Z)*-**332** may affect the electrophilic addition on the alkenyl moiety, limiting silver activation of the double bond.

Then, it was anticipated that target **362** could be also accessed from thioester **365**. Three main synthetic approaches were attempted to access thioester **365**.

The first synthesis was an electrophilic acylation of thioacetylene **363** which did not generate the desired thioester **365**.

The second approach chosen involved a palladium catalysed oxidative carbonylation of acetylene **363**. The reaction gave thioester **365** in low yield and also dimer **372** as the major product.[20,21,22] Dimerization was minimized by working at a higher pressure of carbon monoxide. These results were however not reproducible and did not prove useful for a reliable synthesis. Finally a synthesis of thioester **365** was explored involving electrophilic alkylation of pantetheine **331** with imidazolium sulfurane **382** which was used as an electrophilic transfer reagent.[22,23] The alkynylation gave thioester **398** however in poor yield and as a mixture of side products which could not be identified. A wide range of parameters were varied to optimize the yield of the product and minimize

the side reactions. However, the attempted scale up of the product led to a poor outcome and the method was not pursued.

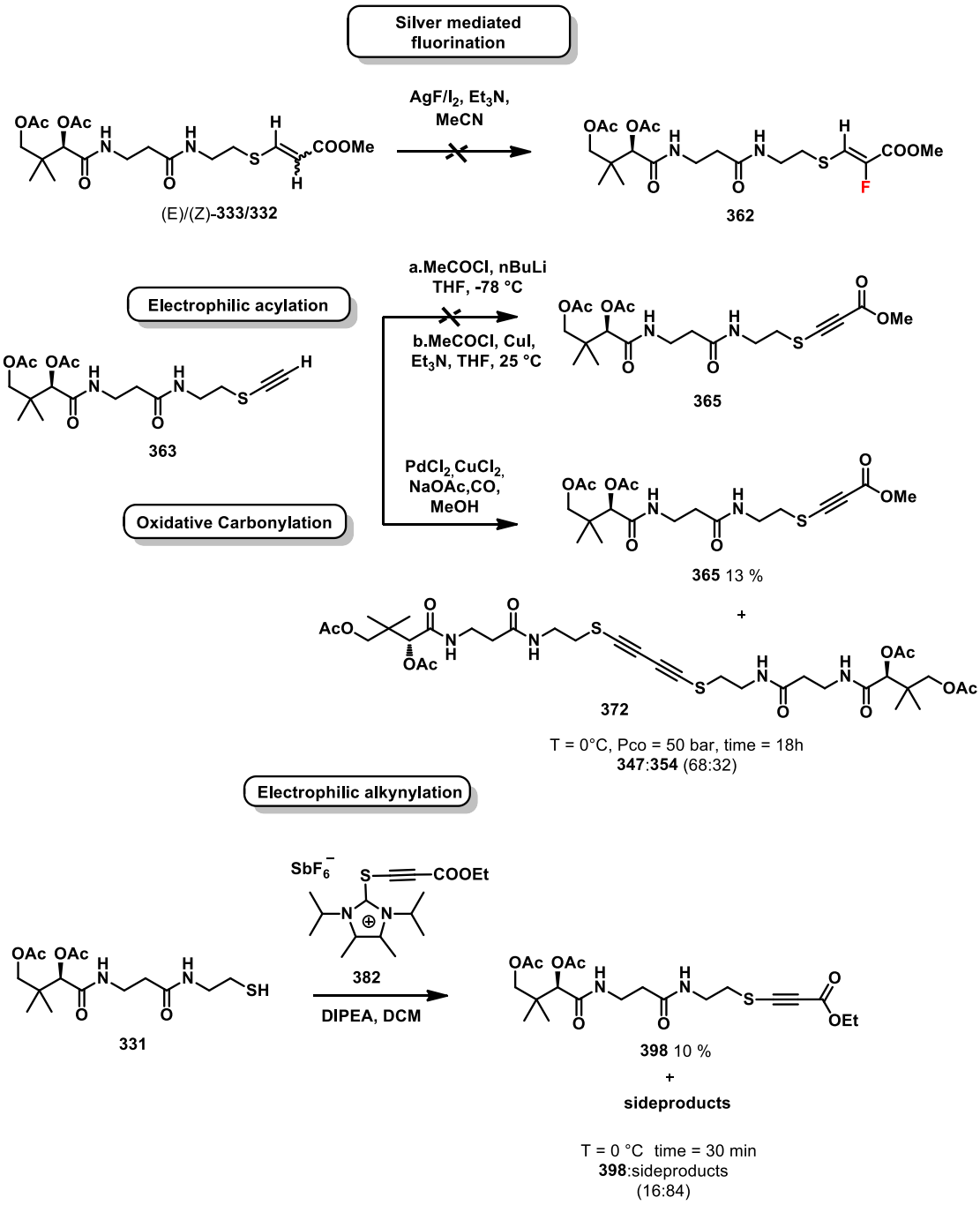

Scheme 3.18. Attempted synthesis of diacetyl thioester precursor **365** and **398**.[20-24]

Fluorovinyl thioacrylate **362** was synthesised in analytical scale by silver mediated fluorination of diacetylated thioester **365**. *E*-fluorovinyl thioacrylate **362** [25] was identified and characterized by NMR and mass spectrometry. The attempted hydrolysis of *E*-fluorovinyl thioacrylate **362** with sodium methoxide in methanol however did not give the

desired compound **359**, but **399** as a result of a nucleophilic attack by methoxide followed by fluoride elimination. (Scheme 3.19)

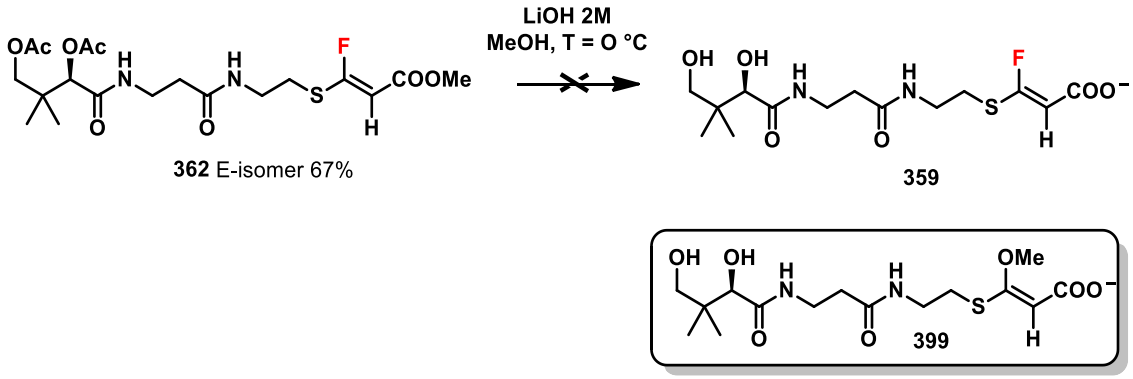

Scheme 3.19. The analytical scale investigation of the fluorination and the hydrolysis step for the synthesis of derivative **359**.

The synthesis of thioester **365** and **398** proved to be challenging. The synthetic approaches adopted gave **365** and **398** in low yields and lacked reproducibility despite the optimization efforts. Thus, fluorovinyl thioacrylate could not be progressed to its coenzyme-A form **358**. Further work should be focused on the optimization and reproducibility of the oxidative carbonylation reaction. A parameter that has not been investigated is the concentration of the solution, thus working with more diluted concentrations might overcome the dimerization. A different synthetic approach could be used for the synthesis of **365**. The thioester could be accessed from the coupling reaction of **294** and amine **402** to generate **403**. Finally, deprotection of **403** should give the desired product **365**. The protection of the ester in **402**, should overcome any potential cyclization from the reduction of azide **401** to amine **402** (Scheme 3.20).

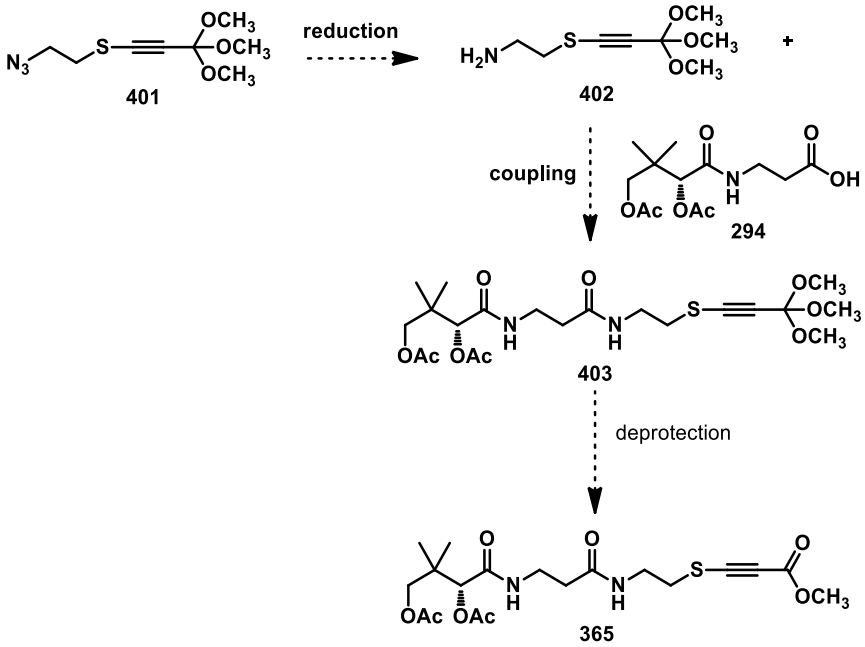

Scheme 3.20. The proposed alternative synthetic route to **365**.

3.9. References

1 J. M. Berg, J. Tymoczko, L. Stryer, *Biochemistry*, **2002**, 5th ed.

2 F. Pietrocola, L. Galluzzi, J. M. Bravo-San Pedro, F. Madeo, G. Kroemer, *Cell Metab.*, **2015**, *21*, 805–821.

3 D. L. Cox, M. Nelson, *Leningher principles of biochemistry*, **2013**, 3rd ed.

4 E. Lo, A. Bentebibel, C. Gurunathan, **2007**, *282*, 18212–18224.

5 J. R. B. Dyck, J. Cheng, W. C. Stanley, R. Barr, M. P. Chandler, S. Brown, D. Wallace, T. Arrhenius, C. Harmon, G. Yang, A. M. Nadzan, G. D. Lopaschuk, *Circ. Res.*, **2004**, 2020.

6 K. D. Cuthbert, J. R. B. Dyck, *Curr. Hypertens rep.*, **2005**, *7*, 407-411.

7 M. P. Bourbeau, M. D. Bartberger, *J. Med. Chem.*, **2015**, *58*, 525–536.

8 H. Zhang, B. Tweel, J. Li, L. Tong, *Structure*, **2004**, *12*, 1683–1691.

9 L. Tong, *Cell. Mol. Life Sci.*, **2005**, *62*, 1784–1803.

10 H. Zhang, Y. Zhiru, Y. Shen, L. Tong, *Science*, 2003, **299**, 2064–7.

11 H. Zhang, B. Tweel, L. Tong, *PNAS*, **2004**, *16*, 5910-5915.

12 K. L. Levert, G. L. Waldrop, J. M. Stephens, *J. Biol. Chem.*, **2002**, *277*, 16347–16350.

13 Y. Shen, S. L. Volrath, S. C. Weatherly, T. D. Elich, L. Tong, N. Carolina, **2004**, *16*, 881–891.

14 R. K. Lyn, R. Mu, D. M. Jones, R. S. Russell, J. P. Pezacki, *ACS Infect. Dis.*, **2015**, *1*, 130-134.

15 D. Bello, M. G. Rubanu, N. Bandaranayaka, J.P. Götze, M. Bühl, D. O' Hagan, *ChemBioChem*, **2019**, *20*, 1174–1182.

16 I. Nazi, K. P. Koteva, G. D. Wright, *Anal. Biochem.*, 2004, **324**, 100–105.

17 Carney et al., *US Patent No.4*, **1989**, 5488-5494.

18 R. Frei, J. Waser, *J. Am. Chem. Soc.*, **2013**, *135*, 9620–9623.

19 V. R. Khabibulin, V. Kulik, I. V. Oshanina, L. G. Bruk, O. N. Temkin, V. M. Nosova, Y. Ustynyuk, V. K. Bel'skii, I. Stash, K. Lysenko, M. Y. Antipin, *Kinet. Catal.*, **2007**, *48*, 228–244.

20 J. Tsuji, M. Takahashi, T. Takahashi, *Tetrahedron Lett.*, **1980**, *21*, 849–850.

21 J. Jover, *J. Chem*, **2015**, *1*, 1-8.

22 J. Peça, G. Talavera, B. Waldecker, M. Alcarazo, *Chem. Eur.J.*, **2017**, *23*, 75–78.

23 G. Talavera, J. Peña, M. Alcarazo, *J. Am. Chem. Soc.*, **2015**, *137*, 8704–8707.

24 R. Frei, M. D. Wodrich, D. P. Hari, P. Borin, *J Am.Chem.Soc.*, **2014**, *136*, 16563–16573.

25 Y. Li, X. Liu, D. Ma, B. Liu, H. Jiang, *Adv. Synth. Catal.*, **2012**, *354*, 2683–2688.

26 D. Bello, R. A. Cormanich, D. O'Hagan, *Aust. J. Chem.*, **2015**, *68*, 72–79.

4. *SELECTIVELY FLUORINATED ANALOGUES OF ACETYL-COA*

4.1. The CF_2 motif as a bioisostere of the carbonyl group

The difluoromethylene moiety has been explored as a bio isostere of the carbonyl group in a wide range of bioactive molecules. It was found to be an effective mimic of a ketone when incorporated into inhibitors of the FKBP proteins, belonging to the immunophilin family. FKBP is a prolyl isomerase which catalyses the interconversion between *cis* and *trans* isomers of peptide bonds at the amino acid proline and it assists the folding of these proteins. Due to their properties, FKBP has been associated with many inflammatory diseases such as atherosclerosis, arthritis and viral infections. Tacrolimus **404** is an immune suppressive drug that inhibits prolyl isomerase activity by binding FKBP12 and promoting the production of T-cells stimulating for the body's immune response. Immunosuppressive inhibitors GPI-1046 **405** and V-10367 **406** were also designed as FKBP12 inhibitors. These are analogues of tacrolimus **404**, replacing the macrolide moiety with a pyrrolidine ring in **405** and a piperidine ring in **408**. The replacement of the α-ketone in derivatives **405** and **408** with a CF_2 moiety led to the synthesis of derivatives **406** and **407** which are more potent inhibitors of FKBP12 than **407** and **408**. 2-Aryl-2,2-difluoroacetamide **407** was designed as mimic of the inhibitor V-10367 **408** of FKB12. The X-ray studies of the crystal structure of the protein with inhibitor **407** indicated that one of the fluorine atoms mimics the hydrogen bonding interaction of the ketone in **408** with the hydroxyl of Tyr-26 on the enzyme, whereas the other fluorine atom interacts with a *meta* hydrogen of Phe-36 (Figure 4.1).[1]

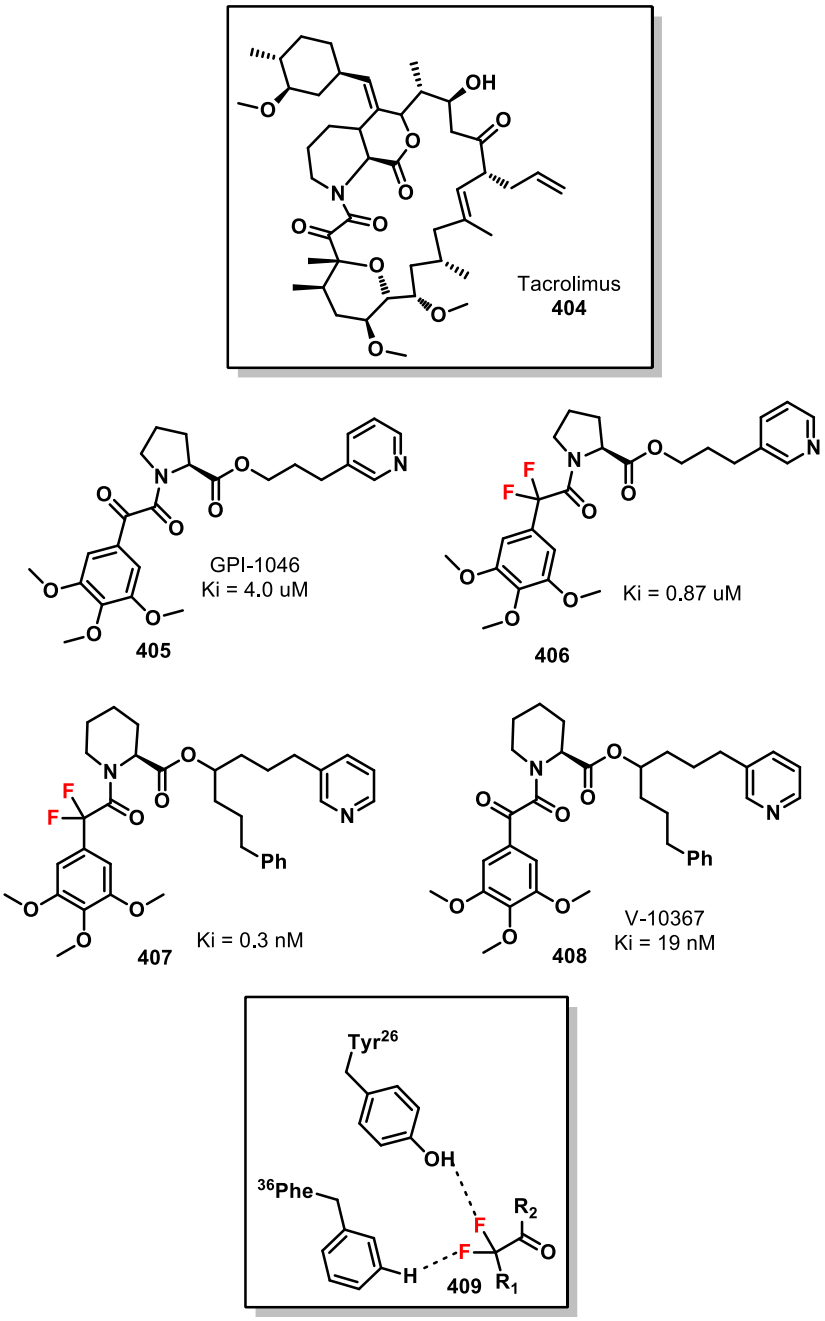

Figure 4.1. Difluoromethylene analogues of the non-immunosuppressive inhibitors of FKBP binding proteins.[1]

CF_2 incorporation has also found applications in the development of inhibitors targeting the ɣ-secretase as shown in Figure 4.2. ɣ-secretase is a multi-subunit protease complex responsible for the cleavage of the transmembrane domain of the amyloid-β-protein precursor into the amyloid β-protein (Aβ), the main component of the amyloid plaques found in Alzheimer patients. The design of ɣ-secretase inhibitors failed due to their side effects such as skin cancer and they seemed to be related to the inhibition of NOTCH

processing activity. The NOTCH receptor is a transmembrane protein vital for many cellular systems, its inhibition is usually associated with a wide range of disorders and malignancies. The introduction of a difluoro moiety in **410**, as a replacement for the carbonyl group, enhanced metabolic stability over **411** to cytochrome P450 3A4 enzymatic oxidation. [2,3]

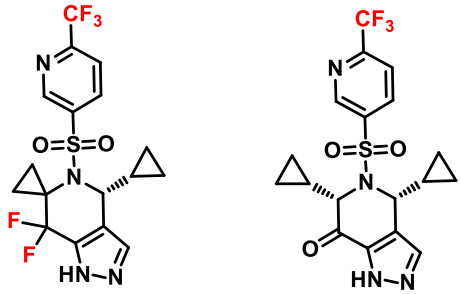

Figure 4.2. Increase of the metabolic stability of γ-secretase inhibitors by incorporation of the difluoro methyl moiety.[2,3]

Xiamuxi *et al.*[4] reported the study of tetrahydropyridomidinone derivatives as potential antipsychotics bearing an arylpiperidine ring, as D_2, 5-HT_{1A}, 5-HT_{2A} receptors antagonists. Compound **412** was prepared as a derivative of **413** with a difluoro moiety replacing C=O; it showed higher agonist activity than ketone **413** (Figure 4.3).

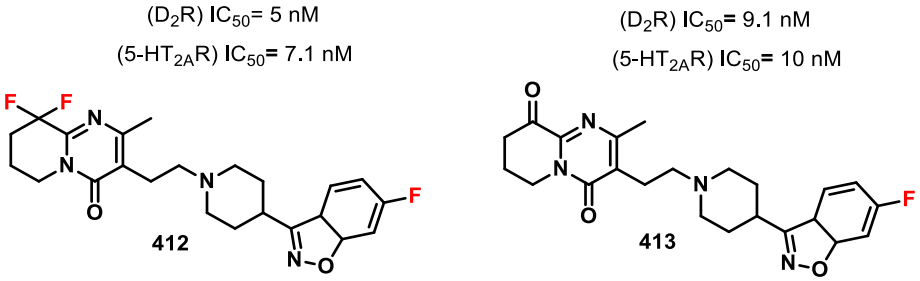

Figure 4.3. The higher potency of difluoro **412** as D_2 and 5HAT_{2A} receptor antagonist than ketone **413**.[4]

4.2. *Design of a difluoro-CoA analogue of acetyl-CoA as potential inhibitor of citrate synthase: CF_2 moiety replacing C=O of acetyl-CoA*

The difluoro ethyl thioether motif possesses a methyl group bound to a carbon bearing two strong electron withdrawing fluorine atoms. Consequently, the methyl group hydrogens are highly polarised and can act as hydrogen bond donor, although more lipophilic than hydroxyl or amine. The incorporation of this motif into a molecule can impact its chemical and biological activity. Based on the encouraging results obtained for the inhibition of citrate synthase by FV-CoA **212**,[5] a α,α-difluoroethyl-CoA analogue of acetyl-CoA **414** became a target to assess the electronic interaction within the active site of the enzyme. It was envisaged that the α,α,-difluoroethyl-CoA analogue **414** could be accessed from difluoroethyl thioether **415** by the three-step biotransformation used for the synthesis of previous Co-A analogues (Scheme 4.1).[16]

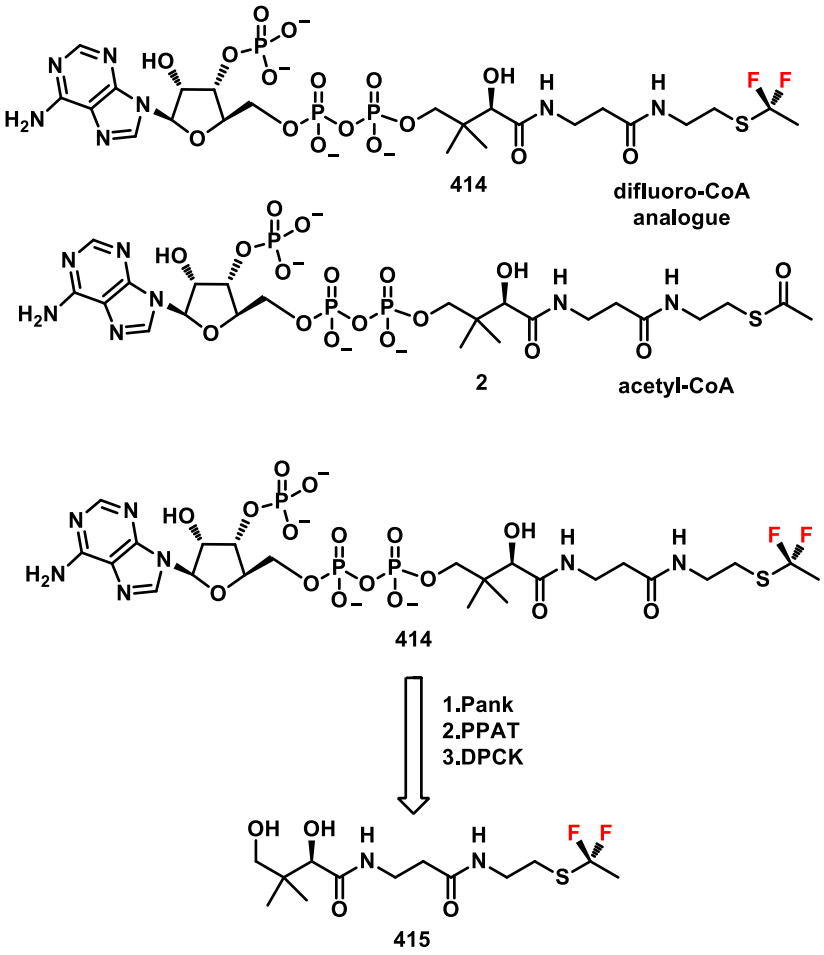

Scheme 4.1. Design of a difluoroethyl thioether-CoA **414** analogue of acetyl-CoA.

4.3. *Previous synthesis approaches to the difluoromethylene moiety*

One of the most common strategies for gem-difluorination, is the conversion of aldehydes and ketones **416** with nucleophilic fluorinating agents such as diethylaminosulfur trifluoride (DAST) or Deoxo-fluor. A DAST mediated nucleophilic substitution has also been applied to the synthesis of β,β-difluoro-α-keto esters **419** as serine protease inhibitors by Parisi *et al.* [32] The β,β-difluoro-α-keto esters derivatives can generate difluoro hemiacetals **418** that mimic intermediate **420** in the serine protease inhibition process (Scheme 4.2).[6,7]

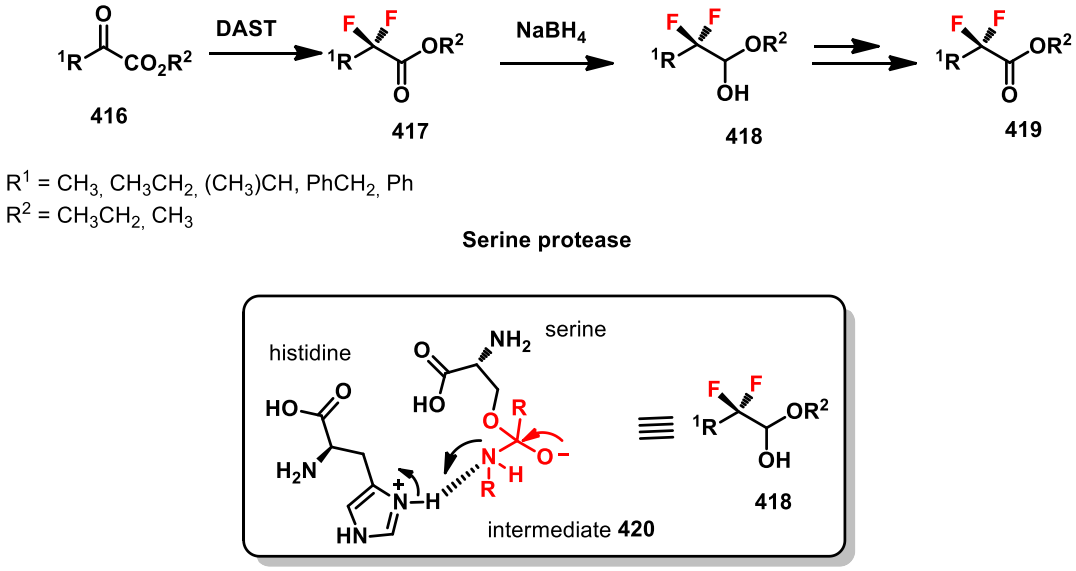

Scheme 4.2. Difluoromethylene motif as serine protease inhibitors.[6,7]

Another synthetic approach to difluoromethylene motifs involves electrophilic fluorination of activated methylene groups bearing electron withdrawing groups such as β-keto esters or amide **421**. The most common fluorinating agents are Selectfluor **428**, N-fluoro benzensulfonimide (NFSI) **427** and *N*-fluoro-*o*-benzenedisulfonimide (NFOBS) **426**. [6] Umemoto *et al* [35] has achieved 2,2-difluorination of malonate derivative **422** with the N-fluoro pyridinium reagent **423** in the presence of a strong Lewis acid catalyst such as aluminium trichloride (Scheme 4.3).[8]

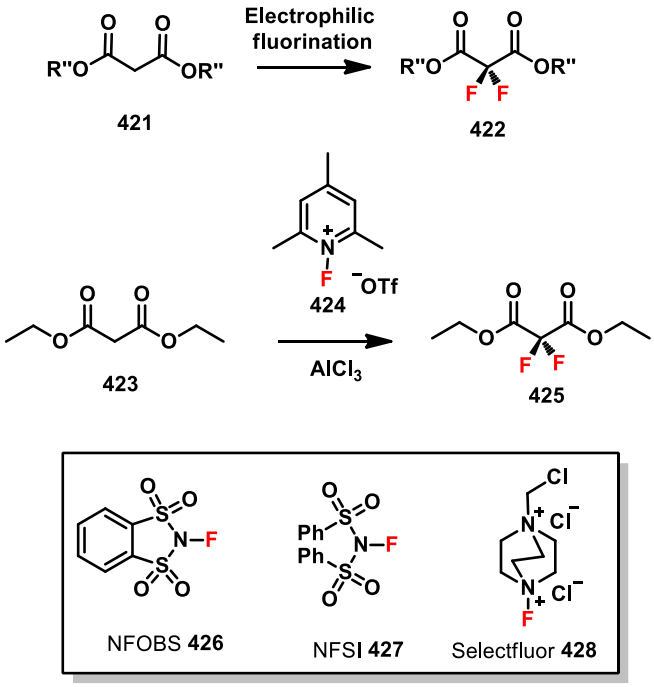

Scheme 4.3. Difluoromethylene formation from carbonyl from β-keto esters.[6]

Prakash *et al.*[9] have reported the reaction of 2,2-diaryl-1,3-dithiolanes **429** with Selectfluor and pyridinium polyhydrogen fluoride (PPHF) under mild condition to give the *gem*-difluoro compounds **430** in good yields (Scheme 4.4).

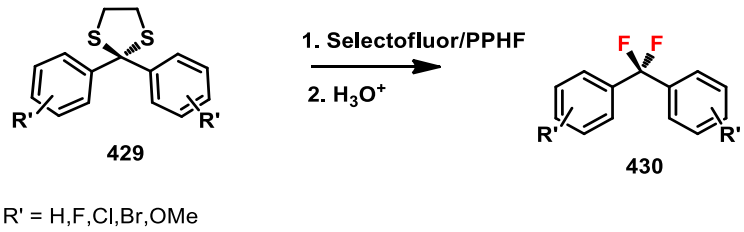

Scheme 4.4. The difluorination reaction of dithiolanes with Selectfluor/PPHF.[9]

4.4. *Results and discussion: Retrosynthetic approach to difluoroethyl thioether 415*

Bello *et al.*[10] reported that the treatment of substituted alkenyl sulfide derivatives **431** with an excess of Olah's reagent promotes difluorination over monofluorination. Thus, it was considered that difluoro ethyl thioether **415** could be accessed by difluorination of thioacetylene **363** followed by basic hydrolysis (Scheme 4.5).

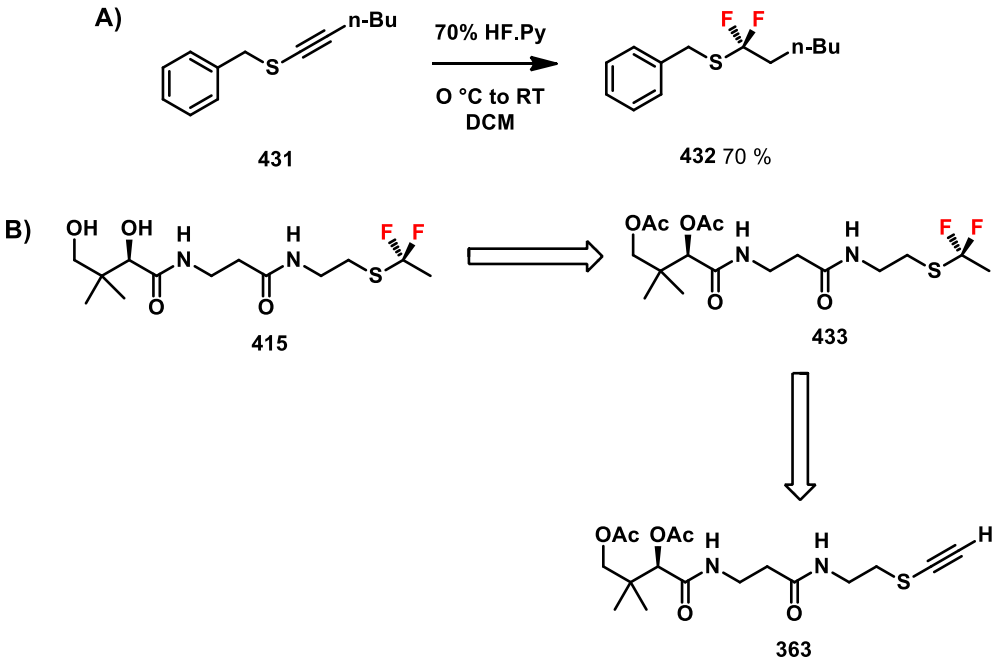

Scheme 4.5. A) Olah's reagent mediated fluorination,[10] B) approach to the synthesis of **415**

4.5. Synthesis of the difluoro methylene pantethenyl moiety

α,α,-Difluoroethyl thioether **415** was prepared by hydrofluorination of thioacetylene **363**. This synthesis was achieved by reaction of **363** with Olah's reagent (70 % Hydrogen fluoride pyridine).[11] Using an excess of HF pyridine, double addition to **363** generated the difluoro ethyl ether **433**. A side product of the reaction is suggested to be the thioester **434** due to the instability of the difluoro moiety under the acidic conditions. The mixture could not be separated by column chromatography due to their closer retention times. However, purification could be achieved by HPLC (reverse phase). Difluoroethyl thioether **433** was hydrolysed under basic conditions generating diol **415** in good yield (69%) (Scheme 4.6).[11]

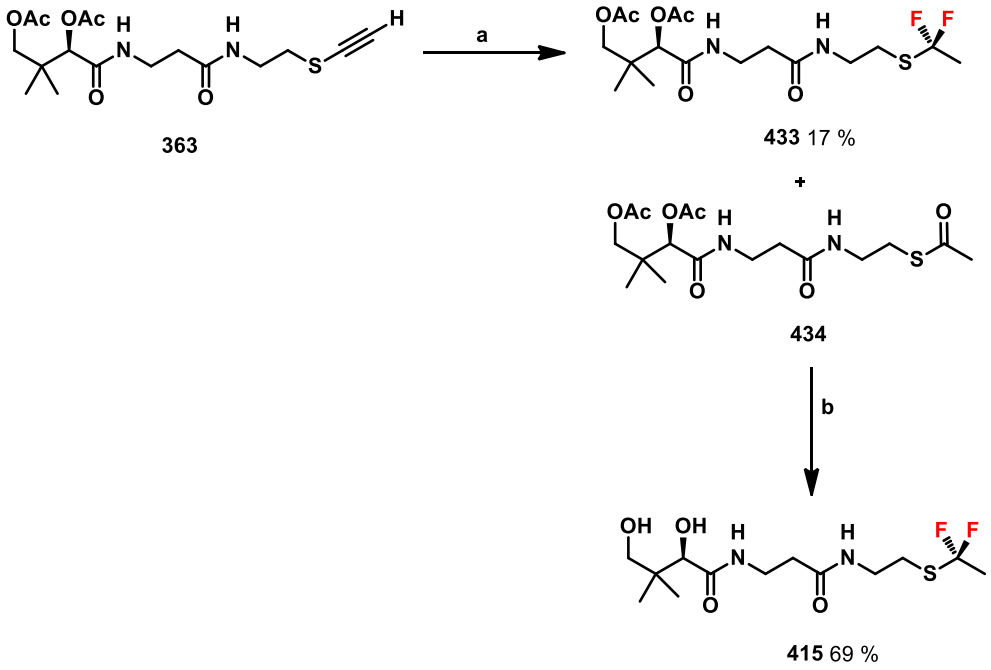

Scheme 4.6. Synthesis of **415**. a) Olah's reagent (70 % HF pyridine, dry CH_2Cl_2, 25 °C, b) MeONa (5.4 M in MeOH), MeOH, 0 °C.[11]

4.6. Attempted biotransformation of the difluoroethyl thioether 415

Difluoroethyl thioether **415** was incubated with the ATP dependent enzymes, PanK and PPAT, respectively to achieve the first and second steps of the biotransformation to the CoA analogue **414**.[5] However, no fluorine signal could be detected by ^{19}F NMR after 16 h of this incubation (Scheme 4.7).

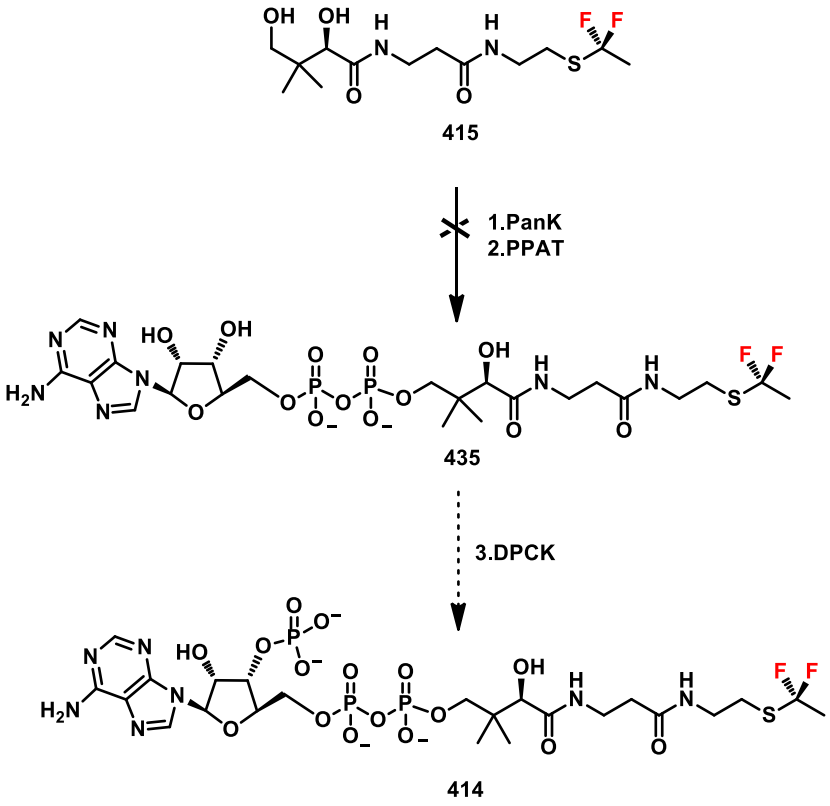

Scheme 4.7. Attempted progression of compound **415** to co-enzyme-A form **414** by the three-step biotransformation.

The loss of the fluorines in **415**, is presumably related to the instability of the difluoroethyl moiety in the buffer solution used (pH 7-8) or to its vulnerability in the enzymatic environment. In order to investigate this, two experiments were set up and monitored by ^{19}F NMR:

Compound **415** was incubated in buffer at pH 7-8 with ATP and $MgCl_2$ (essential for ATP activation) and the solution was monitored for 16 h. In the second experiment, **415** was incubated with buffer (pH 7-8), ATP, $MgCl_2$ and pantothenate kinase (PanK), the first enzyme involved in the biosynthetic pathway of acetyl-CoA. The reaction was also monitored for 16 h. As illustrated in Figure 4.4, the ^{19}F NMR spectra of both solutions show the gradual disappearance of the organic fluorine signal.

Experiment 1: compound **415** + ATP + $MgCl_2$ + Tris-HCl + water, incubation at 37 °C

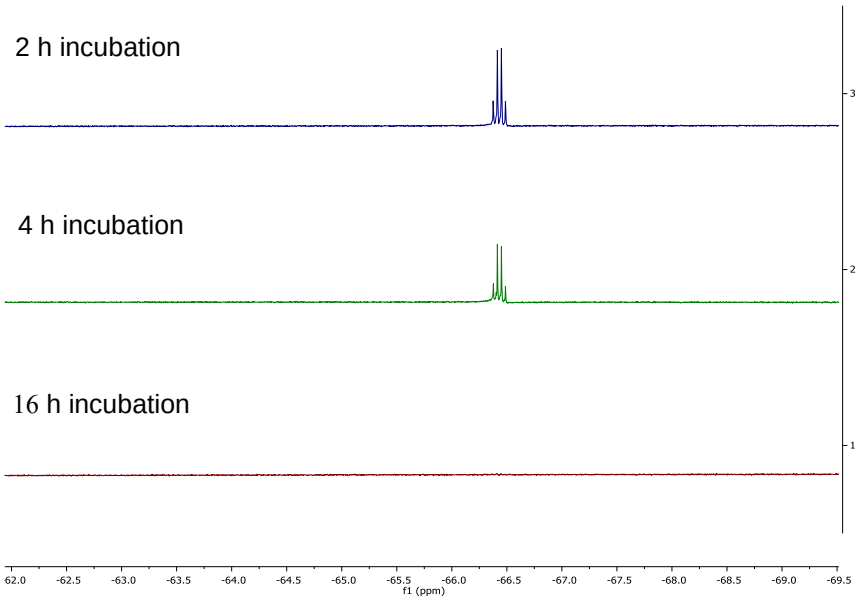

Experiment 2: compound **415** + ATP + $MgCl_2$ + Tris-HCl + PanK + water, incubation at 37 °C

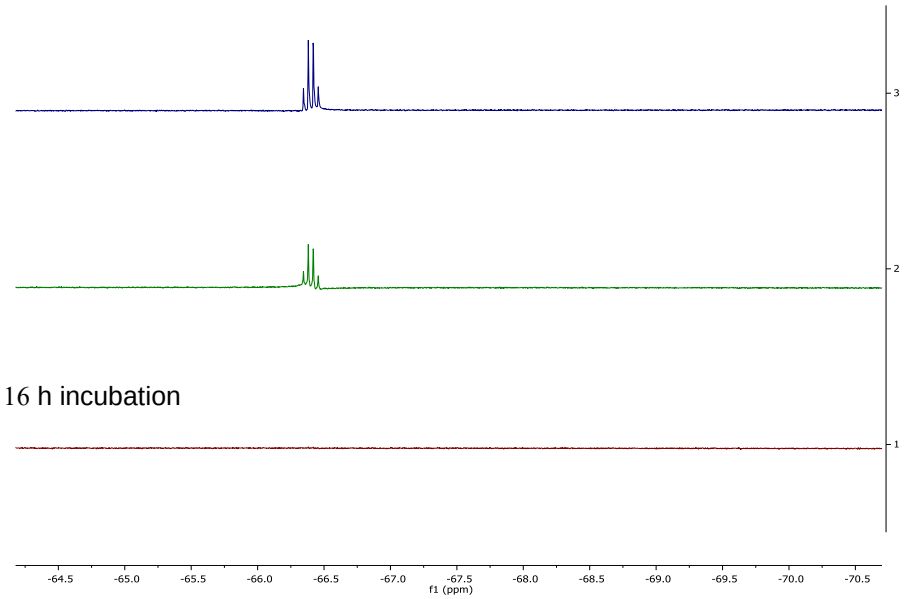

Figure 4.4. The ^{19}F NMR study of difluoro ethyl thioether **415** stability.

It can be assumed that the α,α-difluoroethyl thioether moiety **415** is not stable in the buffer solution at pH 7-8 and that the instability of **415** under these conditions leads to fluorine loss, hence it cannot be progressed to its coenzyme-A analogue **414**.

4.7. A Fluorinated cyclopropane motif

Cyclopropane has a ring strain due to the 60°C bond angle. It also possesses significant torsional strain due to the eclipsing of its hydrogen atoms.[12]

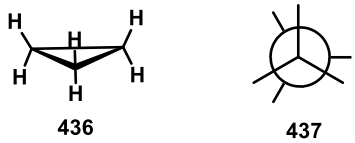

436

437

Eclipsed conformation

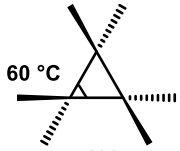

438

Figure 4.5. The cyclopropane structure.[12]

Cyclopropane is the smallest and most conformationally constrained cycloalkane. A motif that is present in a wide range of natural products and biomolecules. The incorporation of a cyclopropane ring offers rigidity and hydrophobicity as a motif for the development of drugs. The introduction of fluorine into a cyclopropane, combining the unique properties of the cyclopropane ring and the fluorine atom, can offer new scaffolds for the synthesis of bioactive molecules. Lemonnier *et al.*[13] have reported the synthesis of monofluorinated cyclopropanes as analogues of glutamic acid **439** and tested these as antagonists mGluR4 receptor. mGluR4 belongs to the family of the metabotropic glutamate receptors in which glutamate is an excitatory transmitter.

They feedback by inhibiting the production of cyclic adenosine monophosphate (cAMP) by adenylyl cyclase, minimizing glutamate release in the synapse whose excessive production is associated with many neurodegenerative disorders such as Parkinson's disease. Cyclopropane (±) (Z)-FAP4 **440** displayed an antagonist activity towards mGluR4 with an EC_{50} of 340 nM (Figure 4.6).[13]

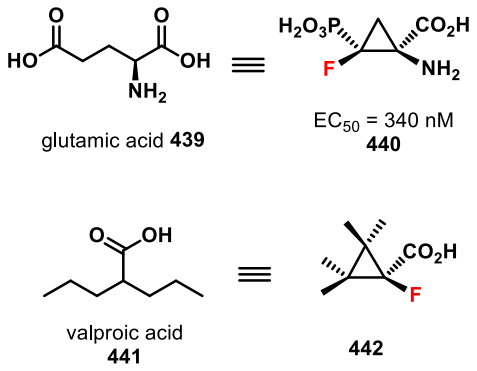

Figure 4.6. Applications of monofluorinated cyclopropane motifs in drug development.[13,14]

Furthermore, the fluorinated cyclopropane **442** was designed as a valproic acid analogue **441** to compensate the teratogenicity and hepatotoxicity associated with this anticonvulsant drug. This analogue presented no teratogenic effect and the two quaternary carbons at the β position of the carboxyl group block its degradation to hepatotoxic metabolites.[14]

4.8. The aryl α,β,β-trifluoro cyclopropane motif

The selective introduction of fluorine into a molecule will increase its polarity and modulate its lipophilicity. [14] The synthesis of aryl *α, α, β*-trifluoro cyclopropane derivatives was investigated by Thomson *et al.*[15] at the University of Saint Andrews as potential building blocks in drug design.

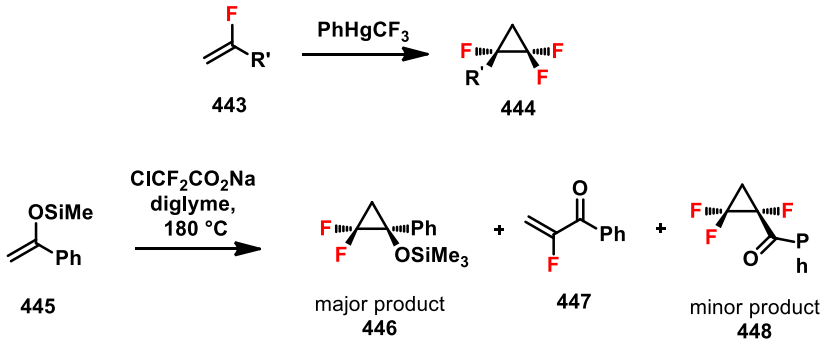

Scheme 4.8. Previous synthesis of trifluoro cyclopropane derivatives.[38,39,40]

Two syntheses of this motifs were reported so far. Oshiro *et al.*[16] described the preparation of trifluoro cyclopropane **448** as minor product after the addition of difluorocarbene to silyl enol ethers to generate **448**. The second synthetic approach involved the addition of phenyl(trifluoromethyl)mercury to vinyl fluorides **443** to generate **444**,[17] however the toxicity of mercury reagents makes this approach less attractive (Scheme 4.8).

The St Andrews group reported the synthesis of aryl *α,β,β*-trifluoro cyclopropane derivatives **452** from α-fluoro styrenes **449** bearing different functionalities in the *para*-position of the phenyl ring. Bromo-fluorination of styrene **449** followed by dehydro-bromination gave access to the α-fluoro styrenes **451**. Reaction then with difluorocarbenes, generated from the Ruppert-Prakash reagent, to vinyl fluorides offered a good route to the *α,α,β*-trifluoro cyclopropane derivatives **452**. These cyclopropanes are robust enough to be derivatised in palladium (III) coupling reactions (Scheme 4.9).[15]

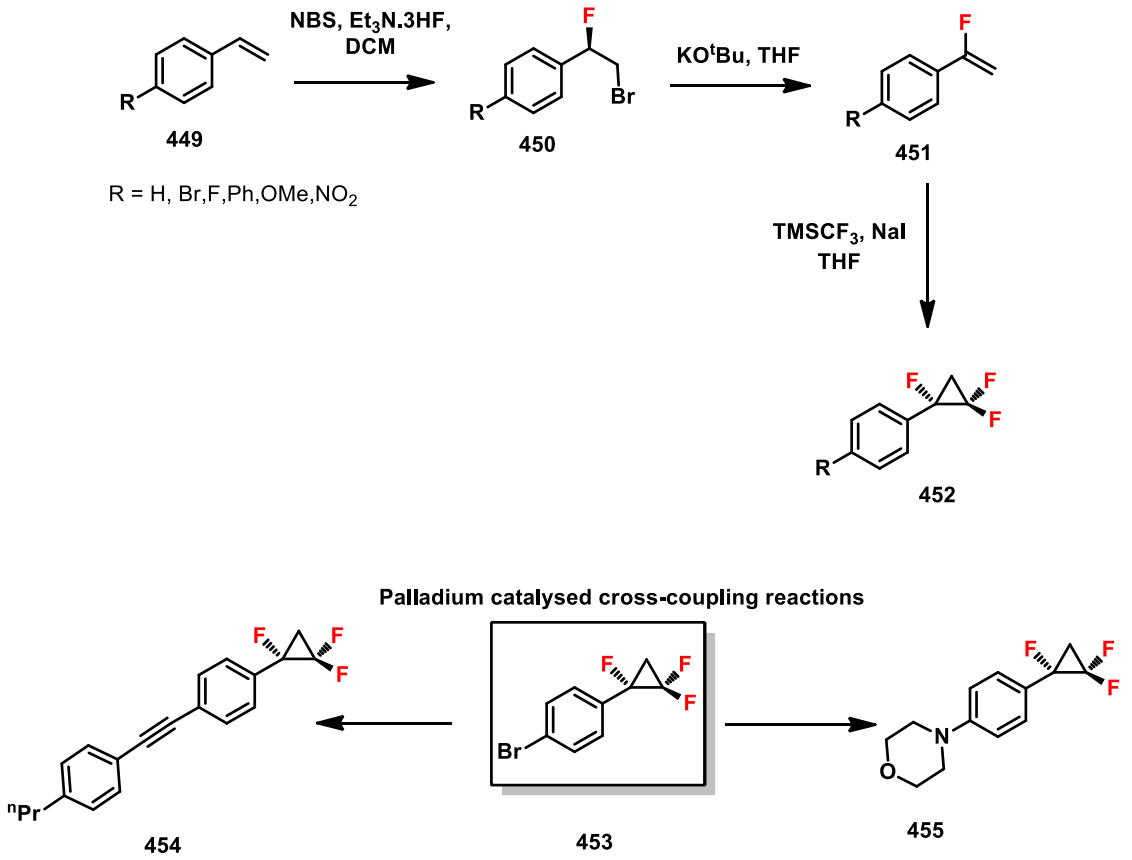

Scheme 4.9. Synthesis and reactivity of the aryl *α,α,β*-trifluoro cyclopropane derivatives.[15]

$RuCl_3/NaIO_4$ mediated aryl oxidation generated the corresponding *α,β,β*-trifluorocyclopropane carboxylic acid **457**, which was used to prepare a wide range of amides **458** (Scheme 4.10A). Amide **458** were found to undergo an elimination-addition reaction with phenols and thiophenols as nucleophiles presumably through the formation of intermediate **459** although this cyclopropane intermediate was not observed. This reactivity is believed to be associated with the polar nature of the *α,β,β*-trifluorocyclopropyl ring conferring reactivity and offers potential for the design of suicide inhibitors with nucleophiles on enzyme active sites (Scheme 4.10B).[15]

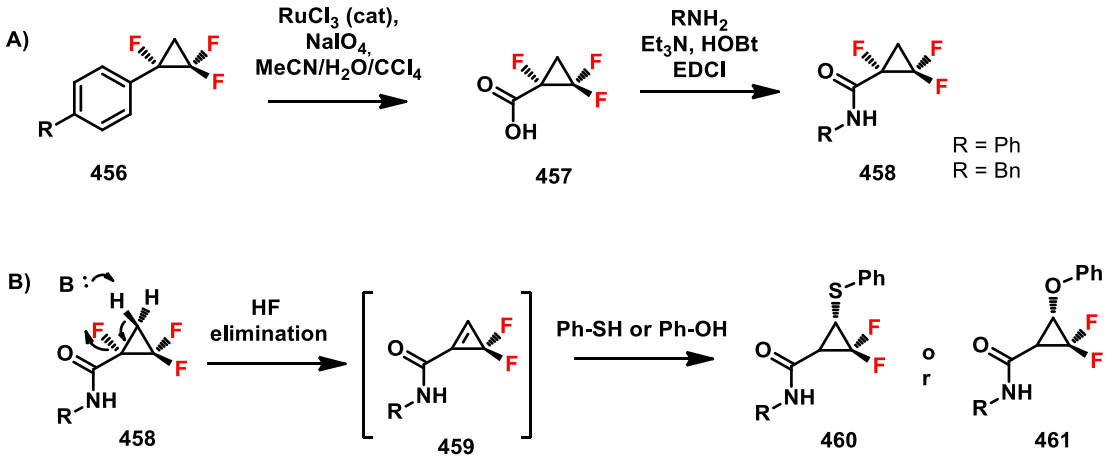

Scheme 4.10. A) The synthesis of the *α,β,β*-trifluorocyclopropane carboxylic acid by $RuCl_3/NaIO_4$ mediated oxidation and investigation of its reactivity. B) the study of the amide derivatives reactivity with thiols and alcohols.[15]

4.9. α,β,β-Trifluorocyclopropane motif in citrate synthase inhibition?

It was anticipated that the *α,β,β*-trifluoro-cyclopropane motif could be introduced as acetyl-CoA analogue **462** where the sulfur atom is replaced by an amide bond. This substrate will then be investigated as an inhibitor of citrate synthase. It has the potential to act as a mechanism based covalent inhibitor (Scheme 4.11).

α,β,β-Trifluorocyclopropane is polar due to the presence of the three fluorine atoms on the ring and it is already demonstrated to be reactive towards alcoholates and thiolates.

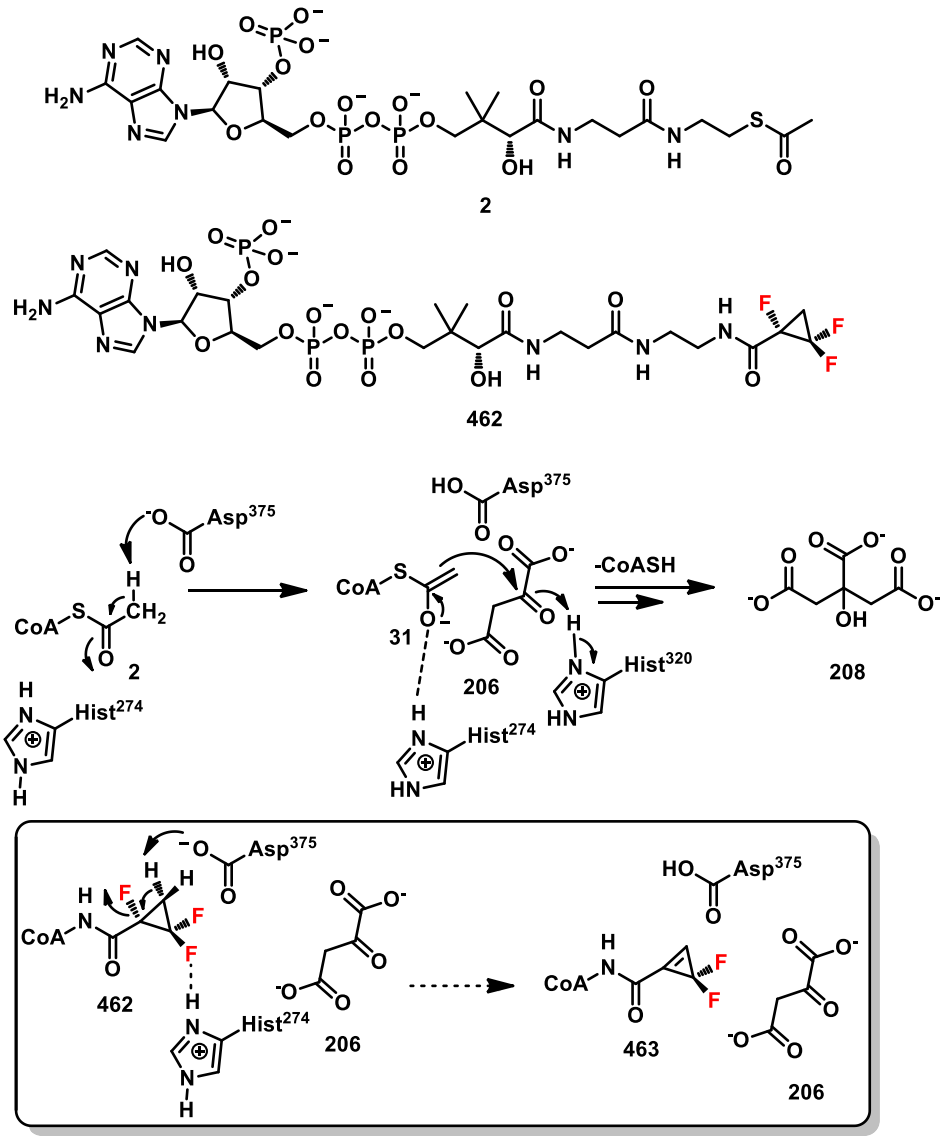

Scheme 4.11. Design of *α,β,β*-trifluorocyclopropane-CoA **462** as an analogue of acetyl-CoA.

4.10. Cyclopropyl-CoA analogues of acyl-CoA thioesters

Cyclopropyl analogues of acyl-CoA have been reported in the past. Hypoglicin A **464** is found in mature ackee fruit which causes Jamaican vomiting sickness and it is identified as (+)-α-amino-2-methylenecyclopropaepropionoic acid **464**. Hypoglycin A **464** is converted to methylenecyclopropanepyruvic acid by transamination followed by an oxidative decarboxylation to give highly toxic *(R)*-2-methylenecyclopropaneacetic acid (MCPA) **465**. The coenzyme ester MCPA **466** interacts irreversibly with the FAD cofactor of pig kidney acyl-CoA dehydrogenase, generating a complex that inactivates the enzyme.

Medium chain acyl-CoA dehydrogenase is involved in the first step of the β-oxidation of fatty acids. It catalyses the first dehydrogenation reaction to generate a *α,β*-unsaturated double bond. Medium chain acyl-CoA dehydrogenase deficiency is associated with the inability of the body to carry out fatty acid degradation. This deficiency is usually associated with hypoglycemia (low blood sugar) and to sudden death.

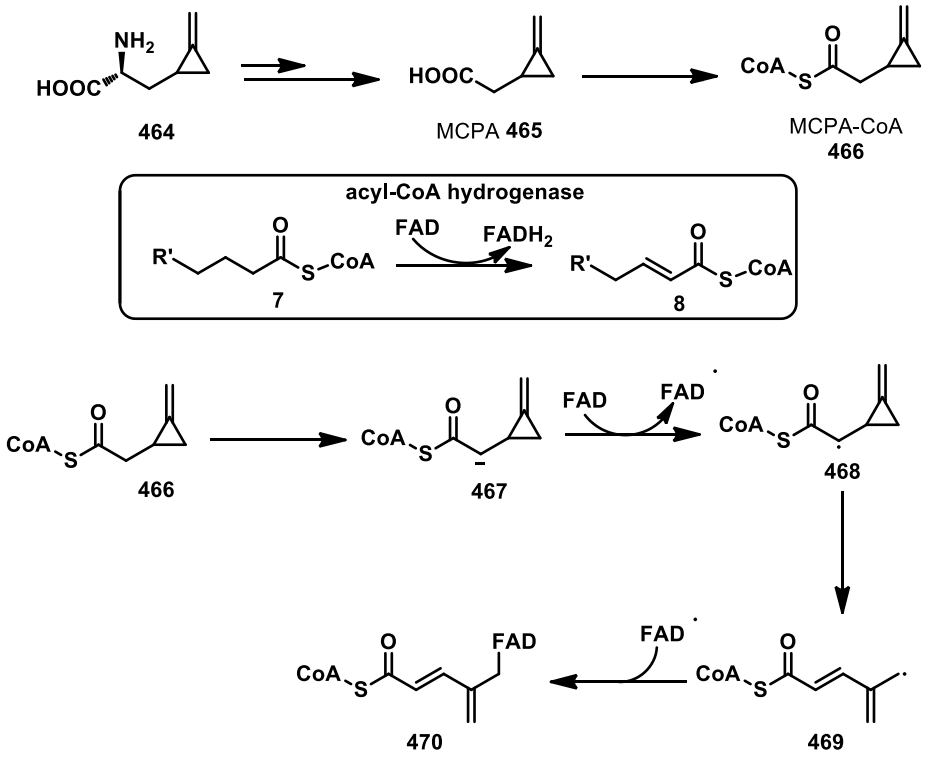

Scheme 4.12. Inhibition of acyl-CoA dehydrogenase by MCPA-CoA.[19]

The inhibition of the enzyme by exo-methylene cyclopropene **466** has been investigated. Baldwin *et al.*[18] reported that inhibitor **466** reacts with the flavin co-factor rather than amino acid residues of the active site. Wenz *et al.*[19] proposed an initial α-deprotonation

of the cyclopropane of **466** followed by ring opening to give intermediate enolate radical **469**. The reaction of **469** with the active site flavin then generates adduct **470** (Scheme 4.12).

In 1996, Li *et al.*[10] reported that methylenecyclopropylformyl-CoA (MCPF-CoA) **472** inhibits irreversibly enoyl-CoA hydratase (Chapter 1), from bovine liver, which is involved in the β-oxidation of fatty acids and in the catabolism of branched chain amino acids (BCAA). It was suggested that methylenecyclopropylglycine (MCPG) **471**, extracted from litchi fruits, is converted to toxic metabolite MCPF-CoA **472**, blocking the *β*-oxidation process. The proposed mechanism for the inactivation of enoyl-CoA hydratase by MCPF-CoA **472** may involve a nucleophilic attack on the electrophilic cyclopropyl moiety of MCPF-CoA, bearing electron-withdrawing groups, followed by a ring-opening reaction (Scheme 4.13).

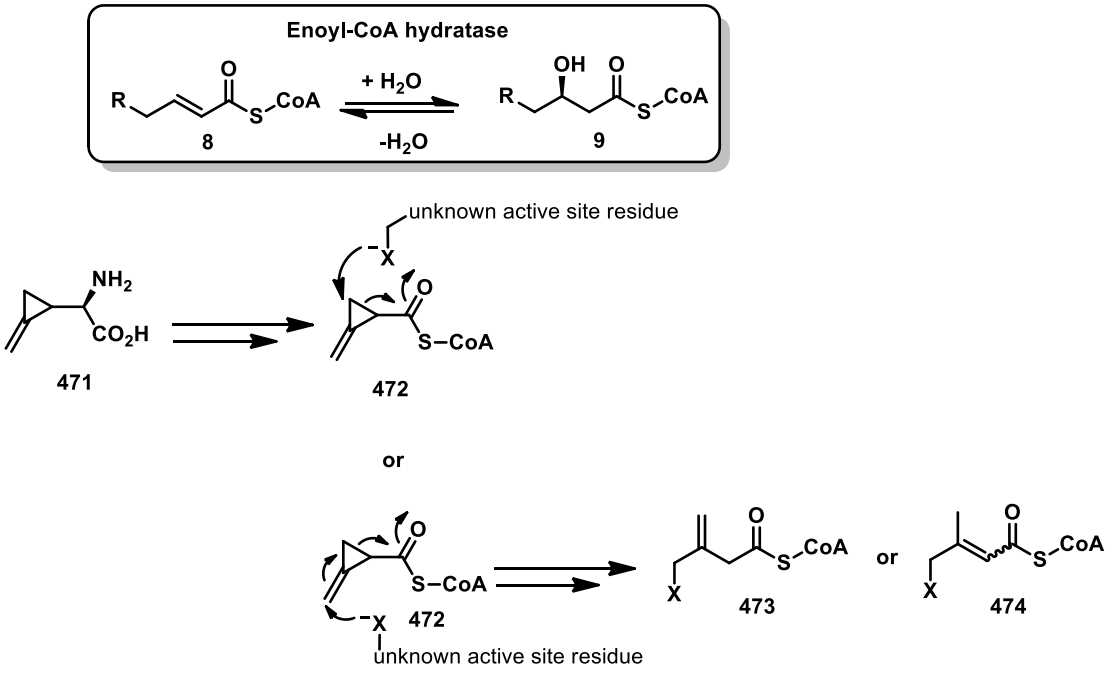

Scheme 4.13. MCPF-CoA **472** as an irreversible and covalent inhibitor of enoyl-CoA hydratase.[10]

4.11. Synthetic approach to the trifluorocyclopropane-CoA 462

Trifluoro-cyclopropane-CoA **462** was prepared from the hydroxylated precursor **479** by the three-step protocol described previously for the synthesis of the other analogues of acetyl-CoA. The synthetic approach chosen for the preparation of **479** involved amide coupling using *α,β,β*-trifluorocyclopropane carboxylic acid **457** (prepared by Dr Q.Zhang from the University of St Andrews) [15] and Boc-protected amine **475** to generate the corresponding amide **476**. Amide **476** was then treated with an excess of trifluoro acetic acid in dichloromethane to give amine **477** as a salt. Excess trifluoroacetic acid in the product was reduced by co-evaporation with toluene under high pressure followed by a C-18 cartridge purification.

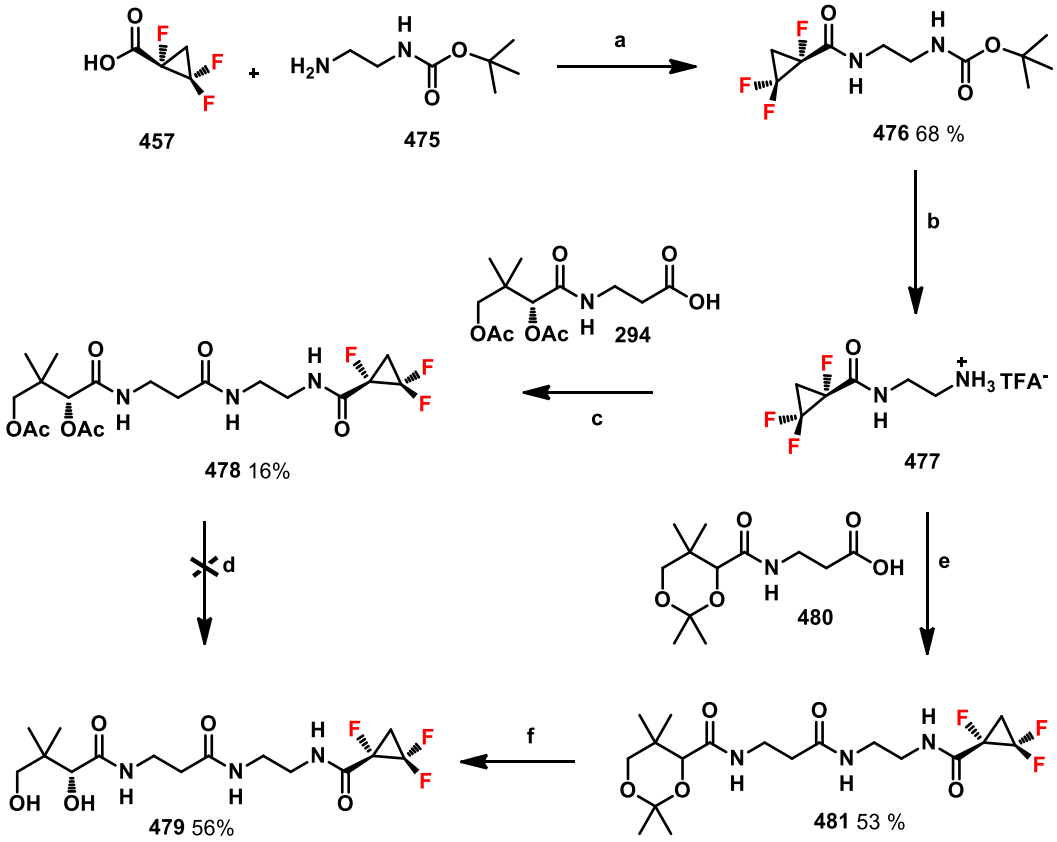

Scheme 4.14. Synthesis of hydroxylated trifluoro cyclopropane derivative **479**: a) HOBt, EDCI, Et_3N, DMF, 0 ° to 25 °C, b) TFA excess, DCM, 25 °C, c) HOBt, EDCI, Et_3N, DCM, 0° to 25 °C, d) AcONa (5.4 M in MeOH), MeOH, 0°C, e) HOBt, EDCI, Et_3N, DMF, 0° to 25 °C, f) pTsOH, THF:H_2O, 0 °.

The next step involved the coupling of amine **477** with pantothenic acid derivative **294** to generate the resulting amide **478**. This was achieved but in low yield. It was found that the trifluorocyclopropane moiety is unstable under basic conditions while it is relatively stable under acidic conditions. Thus, a derivative of pantothenic acid bearing the acetonide moiety as the protecting group **480**, was used for the coupling reaction with amine **477**.[20] The acetonide protecting group was then removed under acidic hydrolysis conditions without compromising the integrity of the fluorinated cyclopropane. Thus, treatment of compound **481** with pTsOH, gave the free diol **479** in good yield (Scheme 4.14).

Cyclopropane **479** was finally progressed to its co-enzyme A analogue **462** by the three-step biotransformation described by Wright *et al.*[5,21] Pank and PPAT mediated enzymatic reactions gave intermediate **483**, which was isolated by HPLC and identified by the ^{1}H NMR and ^{19}F NMR spectra reported in Figure 4.7.

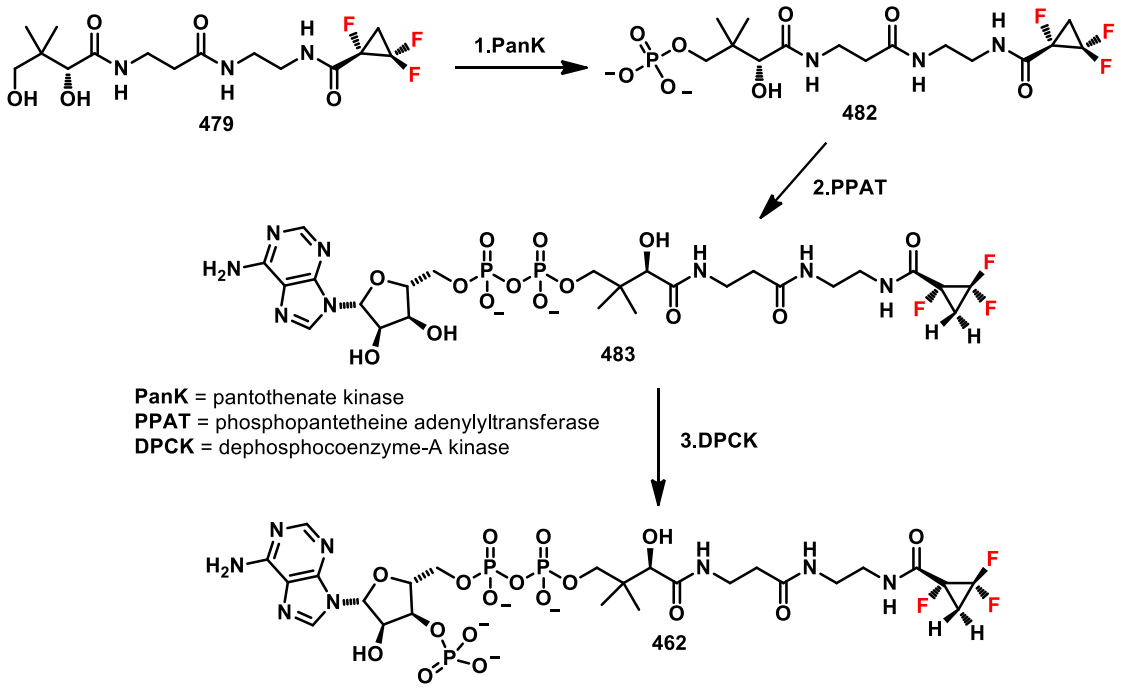

479 482 483 462

Scheme 4.15. The three-step biotransformation to **462**

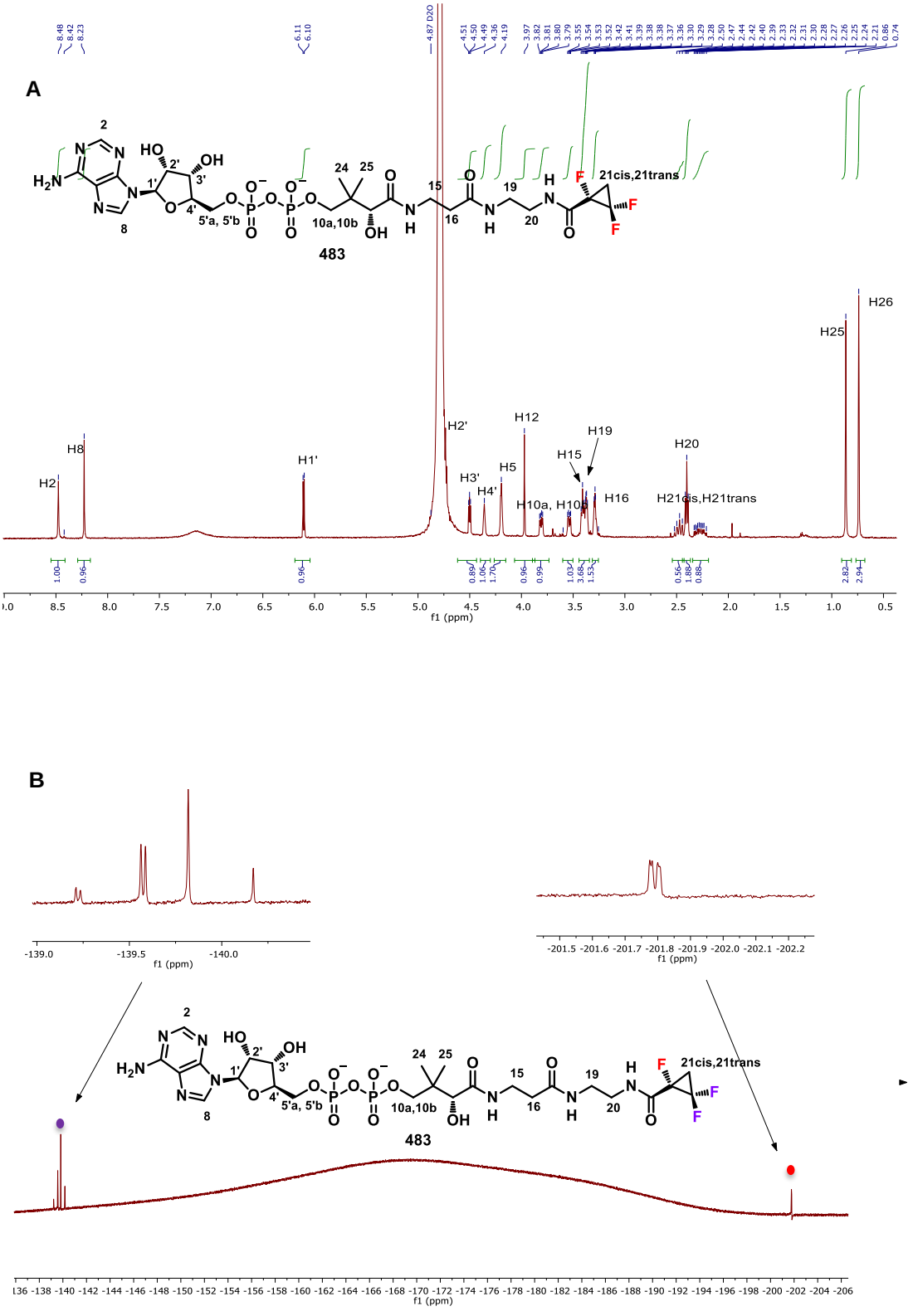

Figure 4.7. A) The ^{1}H NMR and B) ^{19}F NMR spectra of **483**.

The ^{1}H NMR spectra of **483** shows the characteristic signals of the two non-equivalent cyclopropyl ring $C21_{cis}$, $C21_{trans}$ protons ($H21_{cis}$, $H21_{trans}$) and of the adenosine moiety

protons with C2, C8 protons (H2, H8) belonging to adenine and C1', C2',C3',C4' and C5' protons (H1', H2', H3', H4', H5') to the nucleoside. ^{19}F NMR (*with proton decoupled*) shows the non-equivalent CF_2 and CF signals of the cyclopropyl ring. The ABX pattern at -140 ppm belongs to the CF_2 ($^{2}J_{FF}$ = 165.1 Hz, $^{3}J_{FFcis}$ = 11.5 Hz) whereas the doublet of doublets at -200 ppm relates to the CF ($^{3}J_{FFcis}$ = 11.0 Hz, $^{3}J_{FFtrans}$ = 3.0 Hz).

Intermediate **483** underwent a DPCK mediated phosphorylation at the 3'-hydroxyl group to successfully generate *α,β,β*-trifluorocyclopropyl-CoA **462**.This compound (3 mg) was purified by HPLC (retention time =16.20 min). The ^{1}H NMR of *α,β,β*-trifluorocyclopropyl-CoA **462** illustrated in Figure 12 shows that C2',C3' protons (H2', H3') are shifted downfield compared to C2',C3' protons (H2', H3') in the H^{1} NMR spectra relative to precursor **483** (Figure 4.7). The downfield shift for C2, C3' protons for compound **462** is associated with the further phosphorylation on the hydroxyl group (O3') of the ribose ring.

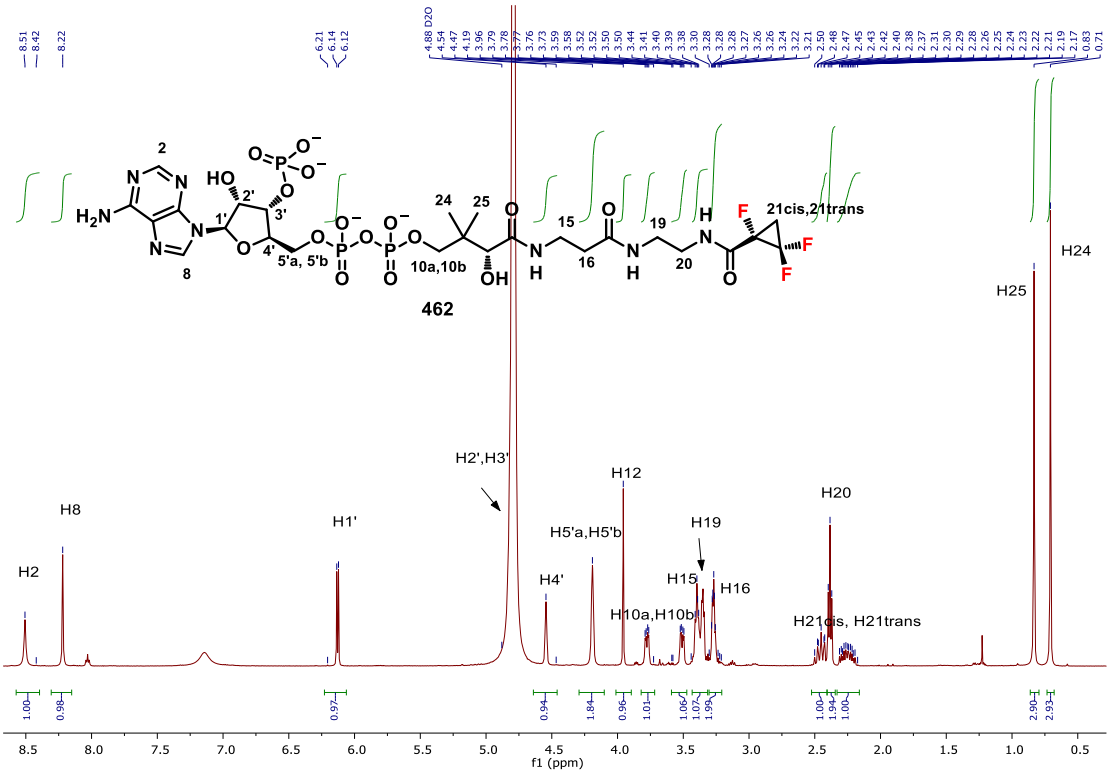

Figure 4.8. ^{1}H NMR spectra of **462**

All the peaks relative to **462** were assigned by ^{1}H NMR, ^{1}H-^{1}H-2D-COSY NMR spectra and by comparison with dethia fluorovinyl-CoA. As for **483**, the non-equivalent protons of the cyclopropyl were significant for the identification of **462**. The ^{19}F NMR (*with proton coupled*) spectra, shown in Figure 4.9B, confirms the ABX pattern at – 140 ppm for the

CF_2 and the quintet for CF due to the coupling with $C21_{cis}$ and $C21_{trans}$ protons ($H21_{cis}$, $H21_{trans}$).

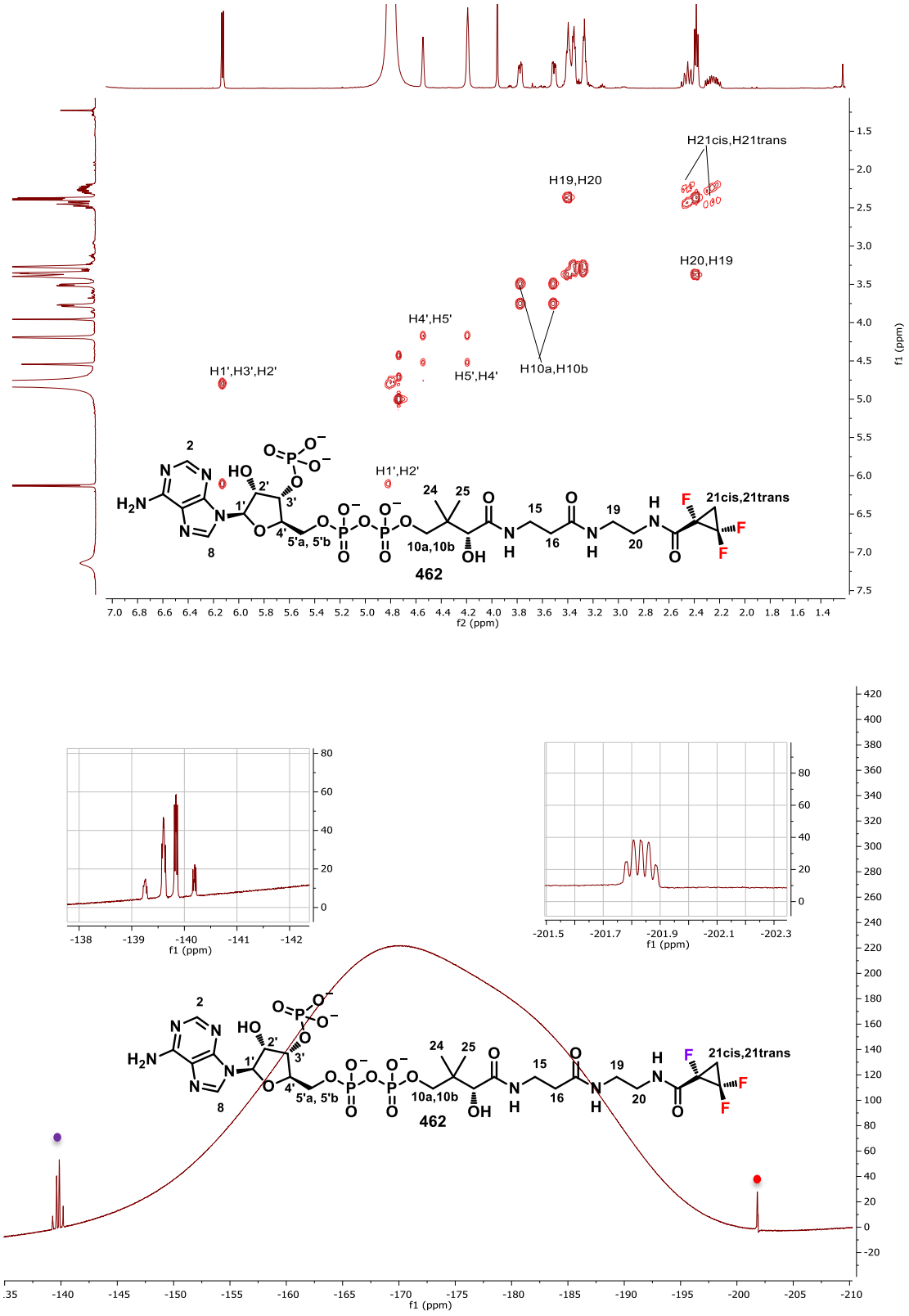

Figure 4.9. A) 2D-COSY and B) ^{19}F NMR spectra of α,β,β-trifluorocyclopropyl-CoA **462**.

α,β,β-Trifluorocyclopropyl-CoA **462** was successfully synthesized in good yield and was investigated as an inhibitor of citrate synthase using the protocol described in Chapter 2.

4.12. Citrate synthase inhibition with α,β,β-trifluorocyclopropyl-CoA 462

The inhibitory activity of **462** was assessed by calculating its IC_{50} with citrate synthase. The IC_{50} value (346.1 µM) was rather high with a Ki of 65.2 µM. This can be compared to the Km of acetyl-CoA (Km = 5.8 µM). Although there is some affinity with the enzyme, the steric effect of the cyclopropane is most probably impeding good binding (Figure 4.10).

$$\mathbf{IC_{50}} = 346.1\ (\pm\ 56.4)\ \mu M$$

$$\mathbf{K_i^{app}} = 65.2\ (\pm\ 11.0)\ \mu M$$

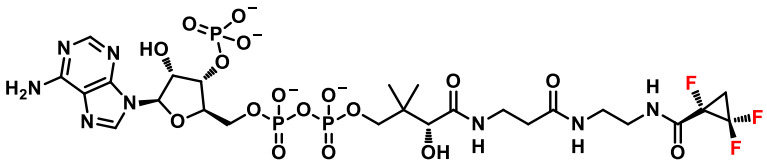

462

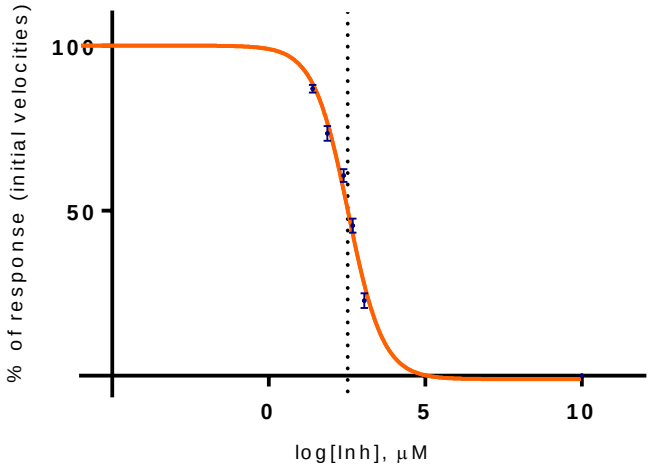

Figure 4.10. The IC_{50} and K_i computed values for *α,β,β*-trifluorocyclopropyl-CoA **462**.

4.13. Conclusions

Chapter 4 focused on the design of a difluoro ethyl thioether-CoA and a trifluoro cyclopropyl-CoA analogues of acetyl-CoA. Both acetyl-CoA analogues were accessed from their pantothenyl precursors via the three step biotransformation. [22,5]

Difluoro ethyl thioether diol **415** was prepared by the synthesis reported previously in Scheme 4.5. Precursor **415** was found to be unstable in the buffer conditions used for the biotransformation (pH 7-8) leading to fluorine elimination (Scheme 4.16).

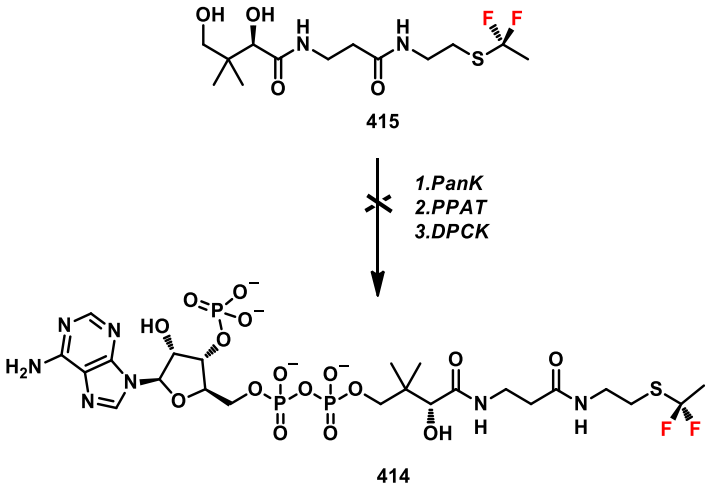

Scheme 4.16. Attempted synthesis of difluoro ethyl thioether-CoA **414**

As shown in Figure 4.4, paragraph 4.6, two experiments were set up to understand if the loss of fluorine was related to the buffer conditions used or whether something was happening in the enzymatic environment. From the test results, it is believed that the difluoroethyl moiety is unstable under the buffer conditions (pH 7-8) used for the enzymatic assay.

α,β,β-Trifluorocyclopropyl-CoA **462** was prepared by the three step biontrasformation from cyclopropane *α,β,β*-trifluorocyclopropyl pantetheinyl derivative **479** following the procedure described in Scheme 4.14. *α,β,β*-trifluorocyclopropyl-CoA **462** was found to be a poor inhibitor of porcine citrate synthase (Ki = 65.2 µM). It can be assumed that the *α,β,β*-trifluorocyclopropyl moiety does not fit properly in the enzyme cleft due to its bulkiness , hence affecting its binding affinity for the enzyme.

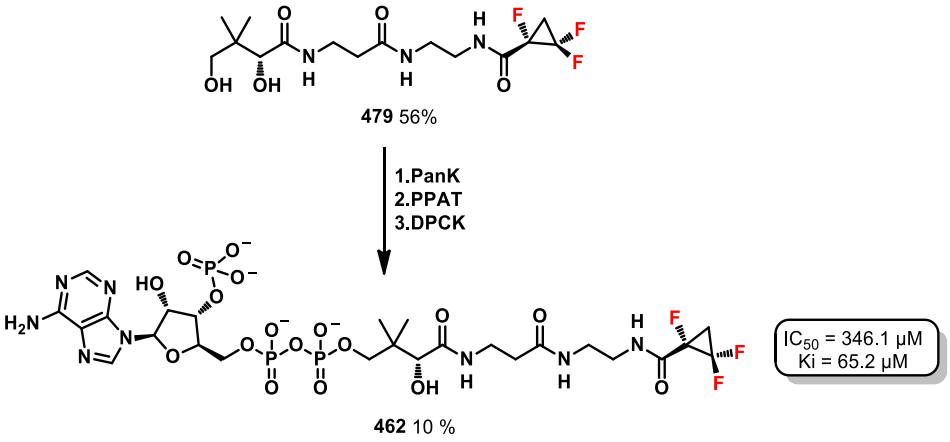

Scheme 4.17. The synthesis of *α,β,β*-trifluorocyclopropyl-CoA **462** and its investigation as inhibitor of porcine citrate synthase

Future work should be focused on the investigation of **462** as covalent inhibitor of citrate synthase and other acyl-CoA utilising enzymes such as malate synthase. Compound **462** will be incubated with the selected protein. Its molecular weight will be monitored by mass spectroscopy to detect any kind of variation.

4.14. References

1 N. A. Meanwell, *J. Med. Chem.*, **2018**, *61*, 5822–5880.

2 X. M. Ye, A. W. Konradi, J. Smith, D. L. Aubele, A. W. Garofalo, J. Marugg, M. L. Neitzel, C. M. Semko, H. L. Sham, M. Sun, A. P. Truong, J. Wu, H. Zhang, E. Goldbach, J. Sauer, E. F. Brigham, M. Bova, G. S. Basi, *Bioorg. Med. Chem. Lett.*, **2010**, *20*, 3502–3506.

3 M. N. Mattson, M. L. Neitzel, D. A. Quincy, C. M. Semko, A. W. Garofalo, P. S. Keim, A. W. Konradi, M. A. Pleiss, H. L. Sham, E. F. Brigham, E. G. Goldbach, H. Zhang, J. Sauer, G. S. Basi, *Bioorg. Med. Chem. Lett.*, **2010**, *20*, 2148–2150.

4 H. Xiamuxi, Z. Wang, J. Li, Y. Wang, C. Wu, F. Yang, X. Jiang, Y. Liu, Q. Zhao, W. Chen, J. Zhang, Y. Xie, T. Hu, M. Xu, S. Guo, H. Akber, Y. He, J. Shen, *Bioorg. Med. Chem.*, **2017**, *25*, 4904–4916.

5 M. G. Rubanu, D. Bello, N. Bandaranayaka, J. P. Götze, M. Bühl, D. O'Hagan, *ChemBioChem*, **2019**, *20*, 1174–1182.

6 T. F. Herpinb, M. J. Tozer, *Tetrahedron*, **1996**, *52*, 8620–8672.

7 M. F. Parisi, G. Gattuso, A. Notti , *J.Org.Chem*, **1995**, *60*, 5174–5179.

8 P. Kirsch, *Modern Fluoroorganic Chemistry*, **2004**, 3rd ed.

9 V. P. Reddy, R. Alleti, M. K. Perambuduru, U. Welz-biermann, H. Buchholz, G. K. S. Prakash, *Chem. Commun.*, **2005**, 654–656.

10 D. Bello, D. O'Hagan, *Beilstein J. Org. Chem.*, **2015**, *11*, 1902–1909.

11 D. Bello, R. A. Cormanich, D. O'Hagan, *Aust. J. Chem.*, **2015**, *68*, 72–79.

12 J. Salaun, *Chem Rev*, **1989**, *89*, 1247–1270.

13 G. Lemonnier, C. Lion, J. Quirion, J. Pin, C. Goudet, P. Jubault, **2012**, *20*, 4716–4726.

14 J. A. Shimshoni, M. Bialer, B. Wlodarczyk, R. H. Finnell, B. Yagen, *J. Med. Chem.*, **2007**, *50*, 6419–6427.

15 C. J. Thomson, Q. Zhang, N. Al-maharik, M. Bu, D. B. Cordes, A. M. Z. Slawin, D. O. Hagan, *Chem. Commun.*, **2018**, *54*, 8415–8418.

16 H. Amii, K. Oshiro, Y. Morimoto, *Synthesis*, **2010**, *12*, 2080–2084.

17 Billen et al., *US Patent No.148649*, **2005**.

18 W. C. Widdison, J.E. Baldwin, *J. Am. Chem. Soc.*, **1992**, *114*, 2245.

19 P. K. Mishra, D. G. Drueckhammer, *Chem. Rev.*, **2000**, *100*, 3283–3309.

20 M.P. Storz, C.K. Mauer, C. Zimmer, N. Wagner, C. Brengel, J.C. De Long, S. Lucas, M. M''Sken, S. Ha''ussler, A. Steinbach, R. Hartmann, *J.Am.Chem.Soc.*, **2012**, *134*, 16143-16146.

21 I. Nazi, K. P. Koteva, G. D. Wright, *Anal. Biochem.*, **2004**, *324*, 100–105.

22 Y. Li, X. Liu, D. Ma, B. Liu, H. Jiang, *Adv. Synth. Catal.*, **2012**, *354*, 2683–2688.

5. *EXPERIMENTAL SECTION*

5.1. General information

All commercially available reagents were purchased from Acros, Alfa Aesar, Fisher Scientific, Fluorochem or Sigma-Aldrich and used without further purification.

Reactions were performed under an atmosphere of argon using standard vacuum line techniques, unless otherwise stated. All glassware was oven-dried and allowed to cool down under high vacuum. All reactions that involved the use of HF-containing reagents were conducted in teflon round bottom flasks previously oven-dried and allowed to cool under high vacuum. Dry solvents dichloromethane, tetrahydrofuran, methanol were obtained from the MBraun SPS-800 Solvent Purification System, by passing the solvent through two drying columns under an argon atmosphere. Temperature of 0 °C was obtained using an ice/water bath. Reactions requiring heating or reflux were carried out using a heating block with a contact thermometer.

Thin layer chromatography (TLC) was performed using Merck TLC silica gel 60 F_{254} glass-backed plates. Compounds were visualised by either UV light (254 nm) or by the use of potassium permanganate stain or molybdenum-based stain. Reverse-phase preparative HPLC column chromatography were performed using a Shimadtzu Prominence® HPLC system (either using UV-Vis or diode array detectors), a Waters 600E multisolvent HPLC system coupled to a Waters 2487 dual wavelength absorbance detector or a Waters 2795 HPLC system coupled to a Waters LCT-MS mass detector, and a semipreparative Phenomenex Synergi® 4µ Polar-RP 80Å 250 x 10.0 mm column, eluting with mixtures of acetonitrile and water with or without using trifluoroacetic acid as a modifier. Optical rotations were measured in a 10 cm length cuvette using the Na_{589nm} on a Perkin Elmer 341 Polarimeter.

NMR spectra were recorded on Bruker Avance II 400 spectrometers (^{1}H at 400 MHz, ^{13}C at 100 MHz, ^{19}F at 376 MHz), or Bruker Avance III 500 spectrometers (^{1}H at 500 MHz, ^{13}C at 126 MHz, ^{19}F at 470 MHz) or Bruker Avance III spectrometer (^{1}H at 700 MHz, ^{13}C at 175 MHz, ^{19}F at 658 MHz).

Chemical shifts (δ) are reported in parts per million (ppm) and are quoted relative to the residual peak of $CDCl_3$, $(CD_3)_2SO$, CD_3OD, D_2O. Coupling constants (*J*) are given in Hertz (Hz). ^{13}C NMR were recorded with ^{1}H decoupling, and ^{19}F NMR spectra were recorded either with or without ^{1}H decoupling. Signal splitting patterns are described as: s – singlet, br s – broad singlet, d – doublet, t – triplet, tt – triplet of triplets, m – multiplet.

Mass spectrometric data were acquired by electron impact ionisation (EI), electrospray ionisation (ESI), and nano- electrospray ionisation (NSI) or chemical ionisation (CI), using Waters Micromass LCT (ESI) or GCT (CI) spectrometers (University of St

Andrews), or a Thermofisher LTQ Orbitrap XL spectrometer (APCI) (National Mass Spectrometry Service Centre, Swansea). Values are reported as a ratio of mass to charge (*m/z*). Melting points were determined in Pyrex capillaries using a Griffin Melting Point Apparatus and are uncorrected.

Enzymatic activity assays were carried out using a Thermo Scientific Evolution 220 UV-Vis spectrophotometer.[1]

5.2. (O,O'-Diacetyl)-D-pantothenic acid (294)[1,2]

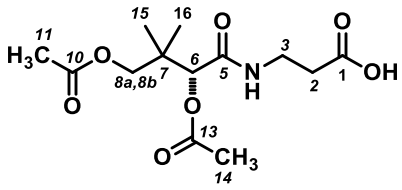

Compound **294** was synthesised according to the procedure reported by Tosin *et al*.[2] D-Pantothenic acid hemicalcium salt (5.0 g, 21.0 mmol, 14 equiv.) was suspended in acetic anhydride (100 mL), iodine (0.37 g, 1.5 mmol, 1 equiv.) was added and the resulting brown mixture was stirred for 16 hours at room temperature. The resulting gel was broken into pieces using a spatula and cooled down using an ice bath before adding a saturated solution of sodium hydrogen sulfite (50 mL) and water (100 mL). The mixture was strongly stirred for 1 hour and then concentrated under reduced pressure to remove the excess of acetic acid. Dichloromethane (100 mL) was added and the layers were separated. The aqueous layer was extracted with dichloromethane (50 mL), and the combined organic layers were dried onto magnesium sulfate, filtered and concentrated under reduced pressure to give a yellow oil. This material was dissolved in a 3:1 tetrahydrofuran/water mixture (100 mL) and stirred for 16 hours at room temperature. The mixture was then concentrated under reduced pressure. The crude was then dissolved in dichloromethane (100 mL), the layers were separated and the aqueous layer extracted with dichloromethane (50 mL). The combined organic layers were dried onto magnesium sulfate, filtered and concentrated under reduce pressure to afford a clear oil that crystallised into a colourless solid (obtained 4.10 g, 0.97 mmol, 65% yield). Diacetyl pantothenic acid was used either in both forms without affecting the reaction outcome.

Mp: 102-104 ºC; $[\alpha]^{20}_{D}$ = + 11.0 ° (c 0.01, $CHCl_3$)

^{1}H NMR (500 MHz, $CDCl_3$) δ 6.64 – 6.62 (t, J = 6.10 Hz, 1H, N*H*,), 4.96 (s, 1H,C*H*, H6), 4.03 (d, *J* = 10.9 Hz, 1H,CH_2, H8$_a$, H8$_b$), 3.82 (d, *J* = 10.9, 1H, CH_2, H8$_a$, H8$_b$), 3.62 - 3.56 (m, 1H, CH_2, H3), 3.52 - 3.46 (m, 1H, CH_2, H3), 2.60 (t, *J* = 5.44, 2H, CH_2, H2), 2.14 (s, 3H, CH_3, H11), 2.07 (s, 3H, CH_3, H14), 1.06 (s, 3H, CH_3, H16), 1.03 (s, 3H, CH_3, H15).

These data are in good agreement with the literature values.[1,2]

5.3. (O,O'-Diacetyl)-D-pantetheine (331)[1]

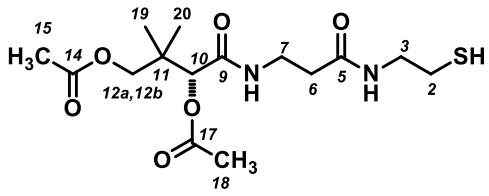

D-pantothenic acid diacetate **294** (2.52 g, 8.20 mmol, 1 equiv.) was dissolved in dry tetrahydrofuran (30 mL) under an atmosphere of argon and 1,1-carbonyl diimidazole (1.34 g, 8.20 mmol, 1 equiv.) was added portion wise to the reaction mixture which was then stirred for 2 hours at room temperature. After the production of gas had ceased, cysteamine hydrochloride (0.93 g, 8.20 mmol, 1 equiv.) was added and the resulting mixture was heated under reflux for 6 hours. The mixture was then cooled down to room temperature and concentrated under reduced pressure. The resulting crude was then dissolved in dichloromethane (60 mL). This mixture was then washed with saturated brine (50 mL), 2.0 N hydrochloric acid (50 mL), saturated sodium hydrogen carbonate aqueous solution (50 mL) and saturated brine (50 mL). The residue was dried onto magnesium sulfate, filtered and concentrated under reduced pressure to afford a colourless solid residue which was purified by silica gel flash chromatography eluting with a mixture of 5/95 methanol/dichloromethane, to give the desired compound as a colourless solid (obtained 1.97 g, 5.11 mmol, 66% yield).[1]

Mp: 58-60 ºC;

^{1}H NMR (500 MHz, $CDCl_3$) δ 6.96 - 6.93 (t, J = 6.3 Hz, 1H, N*H*), 6.56 - 6.54 (t, J= 6.5 Hz, 1H, N*H*), 4.84 (s, 1H, C*H*, H10), 3.98 (d, *J* = 11.5 Hz, 1H, CH_2, H12$_a$, H12$_b$), 3.79 (d, *J* = 11.5 Hz, 1H, CH_2, H12$_a$, H12$_b$), 3.53 - 3.30 (m, 4H, CH_2, H5, H3), 2.67-2.57 (m, 2H, CH_2, H2), 2.37 (t, *J* = 5.66 Hz, 2H, CH_2, H6), 2.10 (s, 3H, CH_3, H18), 2.02 (s, 3H, CH_3, H15), 1.40 (t, *J* = 8.37 Hz, 1H, S*H*), 1.01 (s, 3H, CH_3, H19), 0.98 (s, 3H, CH_3, H20);

^{13}C NMR (126 MHz, $CDCl_3$) δ 171.8 (*C*OCH_3, C17), 171.0 (*C*ONH, C9), 170.3 (*C*OCH_3, C14), 168.2 (*C*ONH, C5), 77.1 (*C*H, C10), 69.3 (*C*H_2, C12), 42.4 (*C*H_2, C3), 35.3 (*C*H_2, C6), 35.2 (*C*H_2, C7), 24.5 (*C*H_2, C2), 21.4 (*C*H_3, C18), 21.0 (*C*H_3, C15), 20.9 (*C*H_3, C20), 20.8 (*C*H_3, C19);

m/z (ESI$^+$): Found [M+Na]$^+$ 385.1394. $C_{15}H_{26}O_6N_2NaS$ requires M^+ 385.1404

5.4. Multistep synthesis of 259

5.4.1. Gold phthalimide complex (Au-1) L= John Phos (286)[3]

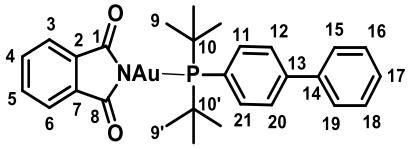

The catalyst was prepared according to the procedure reported by Han *et al*. [3]
Chloro (1,1'-biphenyl-2-yl)-di-tert-butyl phosphine gold (I) (0.30 g, 0.56 mmol, 1 equiv.) and potassium phthalimide (0.16 g, 0.85 mmol, 1.5 equiv.) were dissolved in acetone (6 mL) and the suspension was stirred for 3h at 45 °C. Upon completion, the mixture was filtered and the solid was washed with acetone (10 mL). Acetone was evaporated under pressure and the residue was further washed with water. The catalyst was obtained as a white solid (obtained 0.12 g, 0.19 mmol, 99 % yield).
^{1}H NMR (500 MHz, $CDCl_3$) δ 7.89 (td, 1H, J = 8.0 Hz, 1H, C*H*, H10), 7.67 (dd, *J* = 5.3, 3.0 Hz, 2H, CH_{aryl}, H3, H16), 7.57 (dd, *J* = 5.4, 3.0 Hz, 2H, CH_{aryl}, H4, H5), 7.54 – 7.46 (m, 2H, CH_2, H11, H21), 7.32 – 7.27 (m, 2H, CH_2, H12, H20), 7.19 – 7.12 (m, 2H, CH_2, H15, H19), 6.87 (t, J = 7.7 Hz, 2H, CH_2, H16, H18), 1.48 (s, 9H, CH_3, H9), 1.45 (s, 9H, CH_3, H9').
^{13}C NMR (126 MHz, $CDCl_3$) δ 177.9, 150.2 (d, J = 6 Hz, *C*=O), 142.4 (d, J = 6 Hz, $C_{quaternary}$), 136.7 (d, J = 3 Hz, *C*H, C3), 133.6 (d, J = 3 Hz, *C*H, C4), 132.9 (d, J = 6 Hz, *C*H, C5), 132.0, 130.4 (d, J = 2 Hz, CH_{Aryl}), 128.9, 128.4, 126.9, 126.6 (d = J = 6 Hz, CH_{Aryl}), 126.0 (d, J = 45 Hz, *C*H, C17), 121.4, 37.8 (d, J = 25 Hz, *C*H, C10), 30.9 (d, J = 6 Hz, CH_3, C9).
^{31}P NMR (162 MHz, Chloroform-*d*) δ 58.18.

These data are in good agreement with the literature values.[3]

5.4.2. N-(4-fluoropent-4-en-1-yl) phthalimide(282)[1,4]

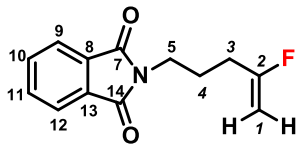

This compound was prepared following the synthetic procedure reported by Okoromoba *et al.*[1,4]

N-(4-pentynyl)-phtalimide (1.00 g, 4.68 mmol, 1 equiv.) was loaded in a Teflon round bottom flask under an atmosphere of argon. Dry chloroform (24 mL) was added followed by **286** (prepared accordingly to the method described by Han *et al.*[3] 0.01 M stock solution in chloroform, 9.36 mL, 0.094 mmol, 0.02 equiv.) and DMPU-HF (65% w/w 0.501 mL, 18.75 mmol. 4.00 equiv.) at room temperature. The reaction mixture was then stirred for 3 h at 55 °C. Upon completion, the reaction was quenched with a saturated sodium hydrogen carbonate solution (24 mL). The layers were separated and the aqueous phase was extracted with hexane (48 mL). The organic layers were combined and washed with brine (48 mL); dried onto anhydrous magnesium sulfate and filtered. The solvent was removed under reduced pressure and the residue was purified by flash column chromatography eluting with a mixture of 60/40 hexane: ethyl acetate to generate fluorovinyl phthalimide as a colorless oil (obtained 0.96 g, 4.10 mmol, 84% yield).

^{1}H NMR (400 MHz, $CDCl_3$) δ 7.93 – 7.79 (m, 2H, CH_2, H8, H12), 7.79 – 7.65 (dt, 2H, CH_2, H9, H11), 4.53 (dd, *J* = 17.5, 2.9 Hz, 1H, CH_2 , $H1_{cis}$), 4.29 (dd, *J* = 50.1, 2.9, 0.9 Hz, 1H, CH_2, $H1_{trans}$), 3.74 (t, *J* = 7.1 Hz, 2H, CH_2, H5), 2.36 – 2.17 (m, 2H, CH_2, H3), 1.98 – 1.80 (m, 2H, CH_2, H4).

^{19}F NMR (*with proton coupled*, 377 MHz, $CDCl_3$) δ -95.14 (m,1F, C*F*).

^{13}C NMR (126 MHz, $CDCl_3$) δ 168.3 (*C*O), 166.4 (*C*O), 134.0 (C_{Ar}, C9, C10), 132.0 (C_{Ar} C7, C12), 123.3 ($\underline{C}_{Ar}$), 90.1 (-C=*C*H_2, C1), 37.2 (*C*H_2, C5), 29.4 (*C*H_2, C3), 25.0 (*C*H_2, C4).

m/z (ESI$^+$): Found $[M+Na]^+$ 256.0740 [$C_{13}H_{12}O_2NFNa$] requires M^+ 256.0740.

These data are in agreement with the literature.[1,4]

5.4.3. 4-Fluoropent-4-en-1-amine (281)[1]

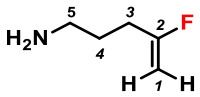

Fluorovinyl phtalimide (0.12 g, 0.52 mmol, 1 equiv.) was dissolved in ethanol (2mL), hydrazine monohydrate (124µL, 2.57 mmol, 5 equiv.) was added and the reaction was stirred for 4h. After completion, 5M Hydrochloric acid (HCl) (80 µL ,2.62 mmol, 5 equiv.) was added and the solvent was removed under vacuum. The crude was diluted with water and saturated sodium hydroxide aqueous solution (50 µL ,2.62 mmol, 5 equiv.) was added adjusting the pH to 13-14. The water layer was extracted with dichloromethane (5 mL), dried over anhydrous magnesium sulfate and the solvent was cautiously removed under pressure. The resulting concentrated dichloromethane solution was used in the next step without further purification due to high volatile amine.[1]

^{1}H NMR (500 MHz, $CDCl_3$) δ 4.54 (dd, *J* = 17.5 Hz, 2.7 Hz, 1H, CH_2, $H1_{cis}$), 4.26 (ddt, *J* = 50.2, 2.7 Hz, J = 0.9 Hz, 1H, CH_2, $H1_{trans}$), 2.77 (t, *J* = 7.0 Hz, 2H, CH_2, H5), 2.35 – 2.17 (m, 2H, CH_2, H3), 1.80 – 1.57 (m, 2H, CH_2, H4).

^{19}F NMR (*with proton coupled,* 471 MHz, $CDCl_3$) δ -94.74 (m, 1F, C*F*).

m/z (ESI^+): found $[M+Na]^+$ 126.1402, $[C_5H_{10}O_2FNNa]^+$ requires M^+ 126.1410.[1]

5.4.4. (O,O'-Diacetyl)-S-N-(4-fluoropent-4-en-1-yl)-D-pantothenamide (280)[1]

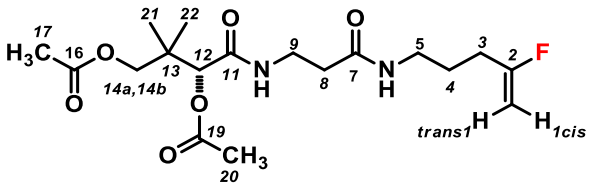

Fluorovinyl pentenamine **281** (0.21 g, 2.05 mmol, 1 equiv.) was dissolved in dichloromethane (8 mL), followed by O,O'-diacetyl-D-panthotenic acid (0.75 g, 2.46 mmol, 1.2 equiv.), 1-hydroxybenzotriazole hydrate (0.36 g, 2.46 mmol, 1.2 equiv.) and triethylamine (0.87 mL, 6.15 mmol, 3 equiv.). The solution was cooled down to 0 °C and N-(3-dimethylaminopropyl)-N'-ethylcarbodiimide hydrochloride (0.59 g, 3.08 mmol, 1.5 equiv.) was added. The reaction was stirred for 30 min at 0°C and at room temperature for 18 h. The mixture was diluted with dichloromethane (10 mL) and washed with 1 M hydrochloric acid (20 mL) and saturated sodium hydrogen carbonate aqueous solution (20 mL). After drying over anhydrous magnesium sulfate, the product was purified by flash column chromatography eluting with a mixture of 95/5 dichloromethane: methanol as a colourless oil (obtained 0.24 g, 0.61 mmol, 30% yield).[1]

$[\alpha]^{20}_{D}$ = + 12.4 ° (c 0.01, $CHCl_3$)

^{1}H NMR (500 MHz, $CDCl_3$) δ 6.92 (br t, J = 6.3, 1H, N*H*), 6.05 (br t, J = 6.2, 1H, N*H*), 4.89 (s, 1H, C*H*, H12), 4.51 (dd, *J* = 17.5, 2.8 Hz, 1H, CH_2, $H1_{cis}$), 4.31 – 4.18 (dd, J = 50.0 Hz, 3.0 Hz, 1H, CH_2, $H1_{trans}$), 4.00 (d, *J* = 11.0 Hz, 1H, CH_2, $H14_a$, $H14_b$), 3.82 (d, *J* = 11.0 Hz, 1H, CH_2, $H14_a$, $H14_b$), 3.60 – 3.40 (m, 2H, CH_2, H9), 3.20-3.31 (m, 2H, CH_2, H5), 2.36 (t, *J* = 5.8 Hz, 2H, CH_2, H8), 2.25 – 2.17 (m, 2H, CH_2, H3), 2.13 (s, 3H, CH_3, H17), 2.05 (s, 3H, CH_3, H20), 1.70 (p, *J* = 7.2 Hz, 2H, CH_2, H4), 1.04 (s, 3H, CH_3, H22), 1.00 (s, 3H, CH_3, H21).

^{19}F NMR (*with fluorine coupled,* 471 MHz, $CDCl_3$) δ -95.35 (m, 1F, C*F*).

^{13}C NMR (126 MHz, $CDCl_3$) δ 171.8 (*C*OCH_3, C19), 171.2 (*C*ONH, C11), 170.1 (*C*OCH_3, C16), 168.4 (*C*ONH, C7), 166.9 (*C*F=CH, C2), 164.8 (CH=*C*F, C2), 90.5, 90.3 (CF=*C*H, C1), 77.3 (*C*H, C12), 69.5 (*C*H_2, C14), 38.9 (*C*H_2, C9), 35.4 (*C*H_2, C8), 35.3 (*C*H_2, C5), 29.6, 29.4 (*C*H_2, C3), 26.2 (*C*H_2, C4), 21.5 (CO*C*H_3, C20), 21.0 (CO*C*H_3, C17), 21.0 (*C*H_3, C22), 20.9 (*C*H_3, C21).

m/z (ESI$^+$): found $[M+Na]^+$ 411.1897 [$C_{18}H_{29}O_6N_2FNa$]: requires M^+ 411.1902.[1]

5.4.5. (O,O'-Dihydroxy)-S-N-(4-fluoropent-4-en-1-yl)-D-pantothenamide (259)[1]

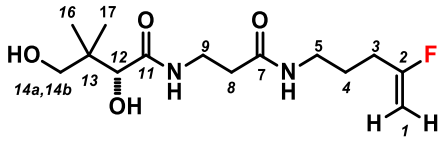

.

Derivative **280** (0.042 g, 0.11 mmol, 1 equiv.) was dissolved in methanol (8 mL) and cooled down to 0°C. Sodium methoxide (5.4 M solution in methanol, 60 µL, 0.32 mmol, 3 equiv.) was added and the reaction was stirred for 2h. The solvent was evaporated, water (5mL) was added and the crude was freeze dried. The crude product was purified by semipreparative HPLC (t_r = 20.0 min, gradient elution method: acetonitrile / water containing 0.05 % trifluoroacetic acid, from 0% to 25% of acetonitrile in 10 min, then from 25% to 60% for 10 min, 60% to 100% in 6 min to wash the column then down to 0% to equilibrate the column) to afford the product as a colourless deliquescent solid (obtained,15.1 mg, 0.050 mmol, 45 %).[1]

^{1}H NMR (400 MHz, $CDCl_3$) δ 7.51 (br t, J = 6.5 Hz, 1H, N*H*), 6.52 (br t, J = 6.4 Hz, 1H; N*H*), 4.55 (dd, *J* = 17.5 , 2.8 Hz, 1H, CH_2, $H1_{cis}$), 4.27 (ddt, *J* = 50.3, 2.9, 0.8 Hz, 1H, CH_2, $H1_{trans}$), 4.02 (s, 1H, C*H*, H12), 3.62 – 3.43 (m, 4H, CH_2, $H14_a$, $H14_b$, 8), 3.34 - 3.24 (m, 2H, CH_2, H8), 2.46 (t, *J* = 6.1 Hz, 2H, CH_2, H5), 2.32 – 2.13 (m, 2H, CH_2, H3), 1.73 (p, *J* = 7.3 Hz, 2H, CH_2, H4), 0.99 (s, 3H, CH_3, H17), 0.93 (s, 3H, CH_3, H16).

^{19}F NMR (*with proton coupled*, 471 MHz, $CDCl_3$) δ -95.21 (m, *J* = 17.9 Hz, C*F*).

^{13}C NMR (126 MHz, $CDCl_3$) δ 174.0 (*C*ONH, C11) , 171.7 (*C*ONH, C7) , 166.8 (*C*F=CH, C2) , 164.7 (*C*H=CF, C1), 90.5, 90.3 (CF=C<u>H</u>, C1), 77.4 (CH, C12), 70.8 (CH_2, C14), 39.4 , 38.9 (C<u>H</u>$_2$, C8), 35.9, 35.4 (C<u>H</u>$_2$, C9), 29.5, 29.3 (C<u>H</u>$_2$, C3), 26.1 (C<u>H</u>$_2$, 4), 21.4 (C<u>H</u>$_3$, C17), 20.6 (C<u>H</u>$_3$, C16).

m/z (ESI$^+$): found $[M+Na]^+$ 327.1686 [$C_{14}H_{25}O_4N_2FNa$]: requires M^+ 327.1691.[1]

5.5. Multistep synthesis of 260

5.5.1. 5-penten-1-en-phthalimide (298)[1,4]

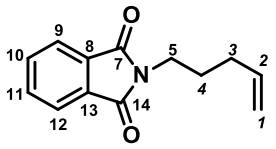

This compound was prepared according to the procedure described by Qi et al.[4]
5-bromopent-1-ene (2,00 g,13.42 mmol, 1 equiv.) was dissolved in dimethylfurane (16 mL) then potassium phtalimide (2.48 g, 13.42 mmol, 1 equiv.) was added and the reaction was heated at 60°C for 20h. The solvent was removed under vacuum and the crude was diluted with water (16 mL). The water layer was extracted with diethyl ether (48 mL) and the solvent was removed under pressure to yield the product as a yellow oil without further purification (obtained 2.74 g,12.78 mmol, 65% yield).[1,4]
^{1}H NMR (400 MHz, $CDCl_3$) δ 7.91 – 7.77 (m, 2H, C*H*, H8, H12), 7.75 – 7.65 (m, 2H, C*H*, H9, H11), 5.81 (ddt, *J* = 16.9, 10.2, 6.6 Hz, 1H, C*H*, H2), 5.12 – 4.91 (m, 2H, CH_2, H1), 3.77 – 3.65 (m, 2H, CH_2, H5), 2.12- 2.06 (m, 2H , CH_2, H4), 1.78 (m, 2H, CH_2, H3).
m/z (ESI$^+$): found $[M+Na]^+$ 238.2400 [$C_{13}H_{13}O_2NNa$] requires M^+238.2401.
These data are in agreement with the literature.[1,4]

5.5.2. Pentenyl-amine (299)[1,5]

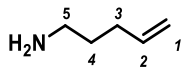

This substrate was synthetized following the procedure described by Du *et al.*[5]
5-penten-1-en-phthalimide **298** (1.04 g, 4.83 mmol, 1 equiv.) was dissolved in ethanol (21 mL) and hydrazine monohydrate (1.18 mL, 24.16 mmol, 5 equiv.) was added to the mixture. The reaction was stirred for 5 h. After completion, 5M Hydrochloric acid (HCl) (18 µL, 24.15 mmol, 5 equiv.) was added and the solvent was removed under pressure. The crude was re-dissolved with water (20 mL), 5M sodium hydroxide aqueous solution (NaOH) (450 µL, 24.16 mmol, 5 equiv.) was added adjusting the pH to 14 and the aqueous phase was extracted with dichloromethane (20 mL). The solvent was carefully removed under pressure and the resulted dichloromethane solution was used in the next synthetic step thus avoiding the loss of high volatile amine.[1,5]
^{1}H NMR (500 MHz, $CDCl_3$) δ 5.80 (ddt, *J* = 16.9, 10.2, 6.7 Hz, 1H, C*H*, H2), 5.09 – 4.84 (m, 2H, CH_2, H1), 2.69 (t, *J* = 7.1 Hz, 2H, CH_2, H5), 2.20 – 2.00 (m, 2H, CH_2, H3), 1.62 – 1.45 (m, 2H, CH_2, H4).
m/z (ESI$^+$): found $[M+H]^+$ 86.0965, $[C_5H_{12}N]^+$ requires M^+ 86.0964.
These data are in good agreement with the literature values.[1,5]

5.5.3. (O,O'-Diacetyl)-S-N-(pent-4-en-1-yl)-D-pantothenamide (300)[1]

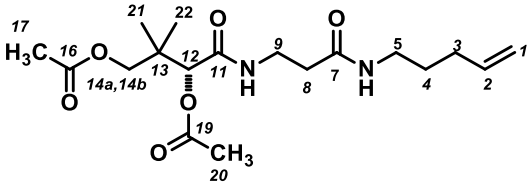

Pentenylamine **299** (0.50 g, 5.90 mmol,1eq) was dissolved in dichloromethane (8 mL), followed by O,O'-diacetyl-D-panthotenic acid **294** (2.13 g, 7.10 mmol, 1.2 equiv.), 1-hydroxybenzotriazole hydrate (1.00 g, 7.60 mmol, 1.3 equiv.) and triethylamine (2.5 mL, 17.60 mmol, 3 equiv.). The solution was cooled down to 0 °C and N-(3-dimethylaminopropyl)-N'-ethylcarbodiimide hydrochloride (1.70 g, 8.80 mmol, 1.3 equiv.) was added. The reaction was stirred for 30 min at 0°C and at room temperature for 18 h. The mixture was diluted with dichloromethane (10 mL) and washed with 1 M hydrochloric acid aqueous solution (20 mL) and saturated sodium hydrogen carbonate solution (20 mL). After drying over anhydrous magnesium sulfate, the product was

purified by flash column chromatography eluting with 95/5 dichloromethane: methanol to give the compound as a yellow oil (obtained , 0.87 g, 2.30 mmol, 40% yield).[1]

^{1}H NMR (500 MHz, $CDCl_3$) δ 6.92 (br t, J = 6.5 Hz, 1H, N*H*), 5.84 – 5.71 (br t, J = 6.4 Hz, 1H, N*H*, 1H, C*H*=CH_2, H2), 5.06 - 4.98 (m, 2H, CH_2=CH, H1), 4.93 (s, 1H, C*H*, H12), 4.02 (d, *J* = 11.0 Hz, 1H, C*H*, $H14_a$, $H14_b$), 3.83 (d, *J* = 11.0 Hz, 1H, C*H*, $H14_a$, $H14_b$), 3.61 – 3.43 (m, 2H, CH_2, H9), 3.29 – 3.17 (m, 2H, CH_2, H5), 2.36 (t, *J* = 5.8 Hz, 2H, CH_2, H8), 2.14 (s, 3H, CH_3, H20), 2.11 – 2.03 (m, 2H, CH_2, H3), 2.06 - 2.05 (s, 3H, CH_3, H17), 1.64 – 1.52 (m, 2H, CH_2, H4), 1.05 (s, 3H, CH_3, H22), 1.01 (s, 3H, CH_3, H21).

^{13}C NMR (126 MHz, $CDCl_3$) δ 171.8 (*C*OCH_3, C19), 171.3 (*C*ONH, C11) , 170.2 (*C*OCH_3, C16), 168.4 (*C*ONH, C7), 137.9 (*C*H=CH_2, C2), 115.7 (*C*H_2=CH, C1), 77.6 (*C*H, C12), 69.7 (*C*H_2, $C14_a$, $C14_b$), 39.5 (*C*H_2, C5), 37.5 (*C*H_2, C9), 35.5 (*C*H_2, C8), 31.4 (*C*H_2, C3), 29.0 (*C*H_2, C4), 21.7 (*C*H_3, C20), 21.3 (*C*H_3, C17), 21.2 (*C*H_3, C22), 21.1 (CH_3, C21).

m/z (ESI^+): found $[M+Na]^+$ found 393.1988 [$C_{18}H_{30}O_6N_2Na$]: requires M^+ 393.1996.[1]

5.5.4. (O,O- Dihydroxy)-S-N-(pent-4-en-1-yl)-D-pantothenamide (260)[1]

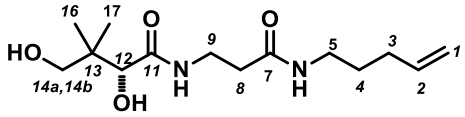

Compound **286** (0.17 g, 0.45 mmol, 1 equiv.) was diluted in methanol (10 mL) and cooled down to 0°C. Sodium methoxide (5.4 M solution in methanol) (249 µL, 1.34 mmol, 3 equiv.) was added and the reaction was stirred for 1h. The solvent was evaporated, water was added and the crude was freeze dried. The crude was purified by flash column chromatography eluting with 90:10 dichloromethane: methanol to give the compound as a colourless oil (0.038 g, 0.13 mmol, 38% yield).[1]

^{1}H NMR (500 MHz, $CDCl_3$) δ 7.26 (br t, J = 6.4 Hz, 1H, N*H*), 6.32 (br t, J = 6.5 Hz, 1H, N*H*), 5.74 (m, 1H, C*H*=CH_2, H2), 4.79 – 4.59 (m, 2H, CH_2=CH, H1), 3.67 (s, 1H, C*H*, H12), 3.38 – 3.03 (m, 4H, CH_2, H9), 2.89 (q, *J* = 6.7 Hz, 4H, CH_2, $H14_a$, $H14_b$, H5), 2.11 (t, *J* = 6.2 Hz, 2H, CH_2, H8), 1.75 (q, *J* = 7.4 Hz, 2H, CH_2, H4), 1.27 (h, *J* = 7.3, 6.8 Hz, 2H, CH_2, H3), 0.65 (s, 3H, CH_3, H17), 0.59 (s, 3H, CH_3, H16).

^{13}C NMR (126 MHz, $CDCl_3$) δ 174.4 (*C*ONH, C11), 171.9 (*C*ONH, C7), 137.9 (CH_2=*C*H, C2), 115.7 (*C*H_2=CH, C1), 77.5 (*C*H_2, C12), 71.1 (*C*H_2, C14) 39.5 (*C*H_2, C8), 36.1, 35.6 (*C*H_2, C5), 31.4 (*C*H_2, C3), 28.8 (*C*H_2, C4), 21.6 (*C*H_3, C17), 20.8 (*C*H_3, C16).

m/z (ESI^+): found $[M+Na]^+$ found 309.1783, [$C_{14}H_{26}O_4N_2Na$] requires M^+ 309.1783.[1]

5.6. Multistep synthesis of 312

5.6.1. (O,O'-Diacetyl)-S-methylthio(dethia)-D-pantetheine (310)[1]

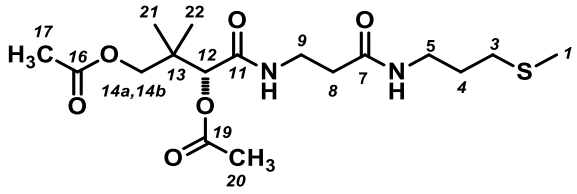

3-methylthio propylamine (0.50 g, 4.80 mmol, 1 equiv.) was dissolved in dichloromethane (18 mL), followed by O,O'-diacetyl-D-panthotenic acid **294** (1.72 g, 5.70 mmol, 1.2 equiv.), 1-hydroxybenzotriazole hydrate (0.83 g, 6.20 mmol, 1.3 equiv.) and triethylamine (2 mL, 14.00 mmol, 3 equiv.). The solution was cooled down to 0°C and N-(3-dimethylaminopropyl)-N'-ethylcarbodiimide hydrochloride (1.36 g, 7.10 mmol, 1.5 equiv.) was added. The reaction was stirred at 0 °C for 30 min then warmed up to room temperature and let it stirred for 18 h. The mixture was diluted with dichloromethane (18 mL) and washed with 1 M Hydrochloric acid (36 mL) and saturated sodium hydrogen carbonate aqueous solution (36 mL). The crude was dried over anhydrous magnesium sulfate and concentrated to generate the product as a white solid (obtained 1.41 g, 3.60 mmol, 76% yield).[1]

m. p. 64 - 67 °C. $[\alpha]^{20}_{D}$ = + 15.7 ° (0.01, $CHCl_3$)

^{1}H NMR (500 MHz, $CDCl_3$) δ 6.91 (br t, J = 6.5 Hz, 1H, N*H*), 5.98 (br t, J = 6.3 Hz, 1H, N*H*), 4.91 (s, 1H, C*H*, H12), 4.01 (d, *J* = 11.0 Hz, 1H, CH_2 , H14$_a$, H14$_b$), 3.82 (d, *J* = 11.0 Hz, 1H, CH_2, H14$_a$, H14$_b$), 3.60 – 3.43 (m, 1H, CH_2, H9), 3.38 - 3.28 (m; 2H, CH_2 , H4), 2.52 (t, *J* = 7.1, 4.6 Hz, 2H, CH_2, H2), 2.37 (t, *J* = 5.8 Hz, 2H, CH_2, H8), 2.14 (s, 3H, CH_3, H20), 2.06 (s, 3H, CH_3, H1), 2.09 (s, 3H, SCH_3, H17), 1.85 – 1.74 (m, 2H, CH_2, H3), 1.05 (s, 3H, CH_3, H22), 1.01 (s, 3H, CH_3, H21).

^{13}C NMR (126 MHz, $CDCl_3$) δ 171.6 (*C*OCH_3, C19), 171.5 (*C*ONH_2, C11), 171.0 (*C*OCH_3, C16), 170.0 (*C*ONH, C7), 77.0 (*C*H, C12), 69.4 (*C*H$_2$, C14$_a$, C14$_b$), 52.2 (*C*H$_2$, C2), 38.6 (*C*H$_2$, C9), 35.1 (*C*H$_2$, C8) , 31.6 (*C*H$_2$, C5), 28.5 (*C*H$_2$, C4) , 21.4 (CO*C*H$_3$, C20) , 21.0 (CO*C*H$_3$, C17), 21.2 (*C*H$_3$, C22), 20.4 (*C*H$_3$, C21) , 15.4 (S-*C*H$_3$, C1) .

m/z (ESI$^+$): Found [M+Na]$^+$ 413.1712 [$C_{17}H_{30}O_6N_2NaS$] requires M^+413.1717.[1]

5.6.2. (O,O'-Diacetyl)-S-methyl-D-pantetheine sulfoxide (311)[1]

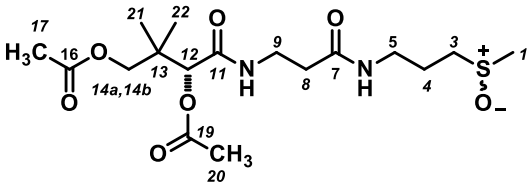

Derivative **310** (1.40 g, 3.60 mmol, 1 equiv.) was dissolved in dichloromethane (25 mL), followed by the addition of meta-chloroperoxybenzoic acid (0.63 g, 3.60 mmol, 1 equiv.). The reaction was stirred for 3h at room temperature. The organic layer was washed with saturated sodium bicarbonate solution (75 mL) and dried onto magnesium sulfate and concentrated. The crude was purified by flash column chromatography eluting with a mixture of 90/10 (dichloromethane: methanol) to afford a yellow oil (obtained 0.32 g, 0.80 mmol, 25% yield).[1]

^{1}H NMR (500 MHz, $CDCl_3$) δ 7.17 (br t, J = 6.4 Hz, 1H, N*H*), 6.94 (br t, J = 6.5 Hz, 1H, N*H*), 4.83 (s, 1H, C*H*, H12), 4.83* (s, 1H, C*H*, H12), 3.99* (dd, J= 11Hz , 1H, CH_2 , H14$_a$, H14$_b$), 3.81 (d, *J* = 10.9 Hz, 1H, CH_2, H14$_a$, H14$_b$), 3.52 – 3.43 (m, 2H, CH_2, H9), 3.43 - 3.35 (m, 1H, CH_2, H5), 3.35 - 3.25 (m, 1H, CH_2, H7), 2.81 – 2.66 (m, 2H, CH_2, H8), 2.56 (d, 3H, CH_3, H1), 2.36 (m, 2H, CH_2, H4), 2.10 (s, 3H, CH_3, H20), 2.03 (s, 3H, CH_3, H17), 2.03 - 1.89 (m, 2H, CH_2, H3), 1.02 (s, 3H, CH_3, H22), 0.99 (s, 3H, CH_3, H21).

^{13}C NMR (126 MHz, $CDCl_3$) δ 172.2, 172.1* (*C*OCH_3, C19), 171.0 (*C*ONH, C11), 170.3, 170.2* (*C*OCH_3, C16), 168.3, 168.2* (*C*ONH, C7), 77.2 (*C*H, C12) , 69.4 (*C*H_2, C14$_a$, C14$_b$), 51.9* (*C*H_2, C3), 37.3, 38.5* (*C*H_3, C1), 38.2, 37.2 (*C*H_2, C8), 35.5 , 35.5* (*C*H_2, C9), 35.2, 35.2* (*C*H_2, C5), 23.0 (*C*H_2, C4), 21.4, 21.0, 20.9* (CO*C*H_3, C20, C17), 20.8, 20.7* (*C*H_3, C21, C22).

m/z (ESI$^+$) Found [M+Na]$^+$: 429.1665, [$C_{17}H_{30}O_7N_2NaS$] requires M^+ 429.1666.[1]

*Double signals arising from two different isomers.[1]

5.6.3. (O,O'-Dihydroxy)-S-methyl-D-pantetheine sulfoxide (312)[1]

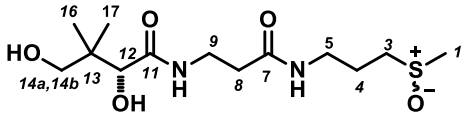

Compound **311** (0.17 g, 0.47 mmol, 1 equiv.) was dissolved in ethanol (13 mL) and cooled down to 0°C using an ice bath. Sodium ethoxide (0.053 mL, 1.40 mmol, 3 equiv.) was added and the reaction was stirred for 1h. The solvent was evaporated, water was added (1mL) and the crude was freeze dried. The crude was purified by flash column chromatography eluting with a mixture of 90/10 dichloromethane: methanol to afford the product as colourless deliquescent solid (obtained 0.080 g, 0.25 mmol, 53 % yield).[1]

^{1}H NMR (400 MHz, D_2O) δ 3.86 (s, 1H, C*H*, H12), 3.48, 3.16 (m, 6H, CH_2, H14$_a$, H14$_b$, H8, H9), 2.88– 2.69 (m, 2H, CH_2, H4), 2.59 (s, 3H, SOCH_3, H1), 2.39 (t, *J* = 6.5 Hz, 2H, CH_2, H5), 1.90 – 1.76 (m, 2H, CH_2, H3), 0.80 (s, 3H, CH_3, H17), 0.77 (s, 3H, CH_3, H16).

^{13}C NMR (126 MHz, D_2O) δ 175.0 (*C*ONH, C11), 174.0 (*C*ONH, C7), 75.6 (*C*H, C12), 68.3 (*C*H_2, C14$_a$, C14$_b$, C5) , 45.0 (*C*H_2, C3), 38.5 (*C*H_2, C8) , 38.0 , 36.5 (SO*C*H_3, C1), 35.4 , 35.2* (*C*H_2, C9), 22.0 (*C*H_2, C4) , 20.4, 19.0 (CO*C*H_3, C16, C17).

m/z (ESI$^+$): Found [M+Na]$^+$ 345.1451 [$C_{13}H_{26}O_5N_2NaS$] requires M^+ 345.1454.[1]

* Double signals arising from the two different isomers[1]

5.7. Multistep synthesis of (Z)-334 and (E)-335

5.7.1. (O,O'-Diacetyl)-S-(methoxycarbonylvinyl)-D-pantetheine((E)332/(Z)333)[1]

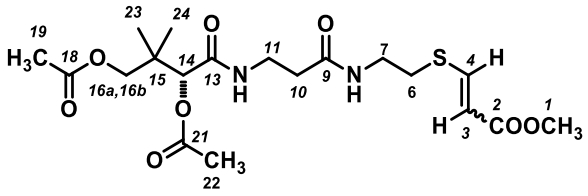

(Z)-**332** and *(E)*-**333** were prepared accordingly to the method reported by Carney *et al.*[6] In a round bottom flask, (O,O-diacetyl)-pantetheine **331** (0.19 g, 0.68 mmol, 1equiv.) and methyl propiolate (65 µL, 0.91 mmol, 1.1 equiv.) were diluted in tetrahydrofuran (4 mL) at room temperature and the reaction was cooled down to 5 °C. Then 1,8-Diazabicyclo [5.4.0] undec-7-ene (10 µL, 0.067 mmol, 0.010 equiv.) was added over a period over 3 minutes and the reaction was let stirred for 2h at room temperature. After completion, the solvent was removed under pressure and the residue was re-dissolved with dichloromethane and quenched with hydrochloric acid 1 M aqueous solution (5 mL). The organic layer was washed with brine (15 mL). After removing the solvent under reduced pressure, the crude was purified by column chromatography eluting with 95/5 dichloromethane: methanol to give the isomeric mixture of diacetyl-thioalkene *(E)*-**333**/*(Z)*-**332** (40:60, isomeric ratio calculated by ^{1}H NMR) (obtained 0.016 g, 0.51 mmol, 75% yield).[1]

^{1}H NMR (400 MHz, $CDCl_3$) δ 7.61 (d, *J* = 15.2 Hz, 1H, C*H*, $H4_{vinyl}$, *E*), 7.06 (d, *J* = 10.1 Hz, 1H, C*H*, $H4_{vinyl}$, *Z*), 6.91 (t, J = 6.4 Hz, 1H, N*H*), 6.55 - 6.45 (t, J = 6.3 Hz, 2H, N*H*), 5.92 – 5.87 (d, J = 10.0 Hz, 1H, C*H*, $H3_{vinyl}$, *Z*) , 5.88 – 5.84 (d, J = 15.1 Hz, 1H, C*H*, $H3_{vinyl,}$ *E*), 4.85, 4.86 (s, 1H, C*H*, H14, *E -Z*)* 4.00 (dd, *J* = 11.0, 2.7 Hz, 1H, CH_2, $H16_a$, $H16_b$), 3.82 (dd, *J* = 10.9, 2.0 Hz, 1H, CH_2, $H16_a$, $H16_b$), 3.70, 3.69 (s, 3H, CH_3, H1, *E-Z*)*, 3.58 – 3.35 (m, 4H, CH_2, H11, H7), 3.00 – 2.85 (m, 2H, CH_2, H6), 2.46 – 2.30 (m, 2H, CH_2, H10), 2.12 (s, 3H, CH_3, H22), 2.04 (s, 3H, CH_3, H19), 1.05 - 1.04 (s, 3H, CH_3, H24), 1.01 - 0.99 (s, 3H, CH_3, H123).

^{13}C NMR (126 MHz, $CDCl_3$) δ 171.8, 170.8, 170.0, 169.9, 168.1, 168.1 (*C*OCH_3, *C*ONH, C21, C14, C18, C9)*, 166.8, 165.5 (*C*OCH_3, C2, *E-Z*), 149.3 (*C*H_{vinyl}, C4, *Z*), 145.8 (*C*H_{vinyl}, C4, *E*), 113.9, 113.4 (*C*H_{vinyl}, C3, *E-Z*)*, 76.9 (*C*H, C14), 69.1 (*C*H_2, C16), 51.4, 51.1 (*C*H_3, C1)*, 39.3, 38.1, 36.8, 35.2, 35.1, 34.9, 34.9, 34.8 , 31.1 (*C*H_2, C11, C7, C10, C6)*, 21.1 (CO*C*H_3, C18), 20.7 (CO*C*H_3, C23), 20.6 (*C*H_3, C21), 20.5 (*C*H_3, C22);

m/z (ESI$^+$): Found $[M+Na]^+$ 469.160, $[C_{19}H_{30}O_8N_2NaS]$ requires M^+ 469.1615.

*double signals arising from E-Z isomers.[1]

5.7.2. (O,O'-Dihydroxy)-S-(Methoxycarbonylvinyl)-D-pantetheine((E)-335/(Z)-334)[1]

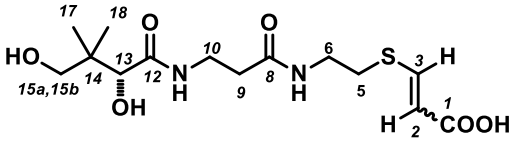

(Z)-**332** and *(E)*-**333** mixture (0.10 g, 0.22 mmol, 1 equiv.) was diluted in tetrahydrofuran (2.5 mL) then water (2.5 mL) and lithium hydroxide (0.034 g, 1.12 mmol, 5 equiv.) were added and the reaction was let stirred for 2h. After completion, tetrahydrofuran was removed under pressure and the crude was freeze dried to remove the remained water. The mixture of *(E)/(Z)* alkenes (60:40) were separated by semipreparative HPLC (gradient elution method acetonitrile / water containing 0.05 % of trifluoroacetic acid, Phenomenex Synergi® 4µ Polar-RP 80Å 250 x 10.0 mm, 0 to 20% acetonitrile in 10 min, then 20% acetonitrile for 10 min, then from 20% to 60% acetonitrile in 3 min to wash the column, then from 60% to 0% acetonitrile in 3 minutes, and 0% acetonitrile for 10 min to re-equilibrate the column) giving the (*E*)-**335** (retention time = 20.1 min) (obtained 0.020 g, 0.060 mmol, 25% yield) and the *(Z)*-**334** (retention time = 19.8 min) (obtained 0.023 g, 0.066 mmol, 30% yield) as a colourless oil. [1]

5.7.3. (E)-335

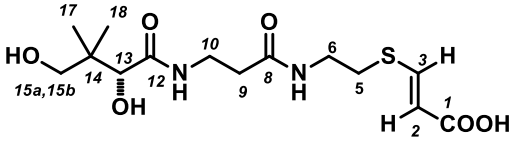

^{1}H NMR (500 MHz, D_2O) δ 7.54 (d, *J* = 15.2 Hz, 1H, C*H*, $H3_{vinyl}$), 5.85 (d, *J* = 15.2 Hz, 1H, C*H*, $H2_{vinyl}$), 3.94 (s, 1H, C*H*, H13), 3.55 – 3.42 (m, 5H, CH_2, H10, H6, $H15_a$, $H15_b$), 3.35 (d, *J* = 11.2 Hz, 1H, CH_2, $H15_a$, $H15_b$), 2.99 (t, *J* = 6.4 Hz, 2H, CH_2, H9), 2.46 (t, *J* = 6.5 Hz, 2H, CH_2, H5), 0.88 (s, 3H, CH_3, H18), 0.84 (s, 3H, CH_3, H17).
^{13}C NMR (176 MHz, D_2O) δ 175.0 (*C*ONH, C12), 174.0 (*C*ONH, C8), 163.1 (*C*OOH, C1), 117.1 (C_{alk}, C2), 115.4 (*C*H_{alk}, C3), 75.8 (*C*H, C13), 68.3 (*C*H_2, C15), 38.5 (*C*H_2, C6), 38.1 (*C*H_2, C10), 35.3, 35.2 (*C*H_2, C5), 30.8 (*C*H_2, C9), 20.4 (*C*H_3, C18), 19.0 (*C*H_3, C17). (m/z) ESI$^+$, Found $[M+Na]^+$ 371.1243, $C_{14}H_{24}O_6N_2NaS$ requires M^+ 371.1247.[1]

5.7.4. (Z)-334

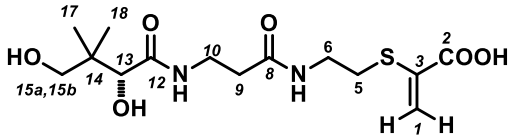

^{1}H NMR (500 MHz, D_2O) δ 7.15 (dd, *J* = 10.1, 4.1 Hz, 1H, C*H*, $H3_{vinyl}$), 5.82 (d, *J* = 10.1Hz, 1H, C*H*, $H1_{vinyl}$), 3.86 (s, 1H, C*H*, H13), 3.49 – 3.30 (m, 5H, CH_2, H10, H6, $H15_a$, $H15_b$), 3.26 (d, *J* = 11.3 Hz, 1H, CH_2, $H15_a$, $H15_b$), 2.84 (t, *J* = 6.5 Hz, 2H, CH_2, H9), 2.38 (t, *J* = 6.4 Hz, 2H, CH_2, H5), 0.79 (s, 3H, CH_3, H18), 0.75 (s, 3H, CH_3, H17).

^{13}C NMR (176 MHz, D_2O) δ 175.0 (*C*ONH, C12), 174.0 (*C*ONH, C8), 162.8 (*C*OOH, C2), 117.1 (S-CH=*C*H-COOH, C1), 115.6 (S-*C*H=CH-COOH, C3), 75.7 (*C*H, C13), 68.3 (*C*H_2, C15), 39.2 (*C*H_2, C6), 35.3 (*C*H_2, C10), 35.2 (*C*H_2, C9), 34.2 (*C*H_2, C5), 20.4 (*C*H_3, C18), 18.9 (*C*H_3, C17).

(m/z) ESI^+: Found $[M+Na]^+$ 371.1243 $C_{14}H_{24}O_6N_2NaS$ requires M^+ 371.1247.[1]

5.8. Multistep synthesis of 363

5.8.1. 2- iodosyl benzoic acid (484)[7]

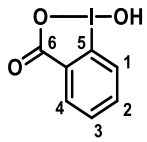

The compound was prepared according to the procedure described by Brand *et al.*[7]
2-Iodo benzoic acid (10 g, 40.32 mmol, 1 equiv.) was dissolved in glacial acetic acid (30 % v/v 80 mL) followed by the addition of sodium periodate (8.6 g, 40.32 mmol, 1 equiv.) was added to the mixture. The reaction was refluxed at 92 °C for 4 h. Upon completion, the reaction was quenched with cold water (210 mL) and allowed to cool down to room temperature. After 1 h, the product was filtered off and washed with cold water (100 mL) and cold acetone (100 mL). The desired photosensitive compound was dried affording a colourless solid. (obtained 9.50 g, 35.88 mmol, 89% yield).
^{1}H NMR (500 MHz, DMSO) δ 8.20 (s, 1H, O*H*), 8.16 (dd, *J* = 7.6, 1.5 Hz, 1H, CH_{Aryl}, H4), 8.11 (td, *J* = 8.6, 7.2, 1.5 Hz, 1H, CH_{Aryl}, H3), 7.99 (dd, *J* = 8.4, 0.8 Hz, 1H, CH_{Aryl}, H1), 7.85 (td, *J* = 7.3, 1.0 Hz, 1H, CH_{Aryl}, H2).
The data are in agreement with the reported literature values.[7]

5.8.2. Silyl Ethyl Benziodoxolone (366)[7]

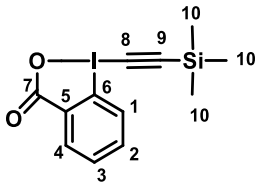

The title compound was prepared according to the procedure described by Brand *et al.*[7]
Trimethylsilyl triflate (3 mL, 16.66 mmol, 1.1 equiv.) was added to a suspension of compound **484** (4.00 g, 15.15 mmol, 1 equiv.) in dichloromethane (50 mL) at room temperature. The resulting yellow mixture was stirred for 1 h, followed by the dropwise addition of bis-(trimethylsylil)-acetylene (3.8 mL, 16.66 mmol, 1.1 equiv.). The resulting suspension was stirred for 6 hours at room temperature. A colourless solid was formed to wich sodium carbonate aqueous solution (30 mL) was added and the reaction was stirred until complete solubilisation of the solid. The two layers were separated and the organic was extracted with saturated sodium hydrogen carbonate solution and dried over magnesium sulfate, filtered and concentrated under reduced pressure. The resulting solid was re-crystallized with acetonitrile (50 mL) affording the compound as white crystals (obtained 3.49 g, 10.6 mmol, 70 % yield)

^{1}H NMR (500 MHz, $CDCl_3$) δ 8.52 – 8.32 (m, 1H, CH_{aryl}, H4), 8.30 – 8.10 (m, 1H, CH_{aryl}, H1), 7.78 (dtd, *J* = 8.5, 7.0, 1.6 Hz, 2H, C$H_{aryl,,}$ H2, H3), 0.32 (d, *J* = 6.6 Hz, 9H, CH_3, H10).

^{13}C NMR (126 MHz, DMSO) δ 166.1 (*C*=O, C7), 134.9, 132.1, 131.4, 131.2, 127.1, (*C*H, C1, C2, C3, C4), 115.7, 114.3 (CH_{alk}, C8, C9), 66.3, -0.5 (*C*H_3, C10).

The data are in agreement with the reported literature values.[7]

5.8.3. (O,O'-Diacetyl)-S-ethynyl-D-pantetheine (363)[1,7,8]

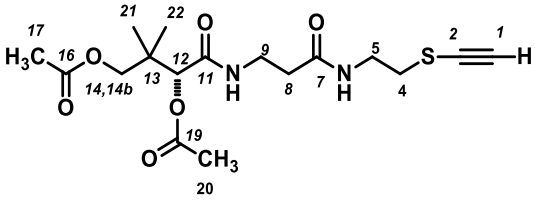

Diacetyl pantetheine **331** (14.70 g, 40.7 mmol, 1equiv.) was dissolved in tetrahydrofuran (300 mL) and tetramethylguanidine (5.6 mL, 44.7 mmol, 1.1 equiv.) was added. The resulting mixture was vigorously stirred at room temperature and a solution of EBX-TMS **366** (15.40 g, 44.7 mmol, 1.1 equiv. prepared according to the procedure reported by Waser *et al.*[7,8]), in tetrahydrofuran (50 mL), was slowly added. The resulting mixture was stirred for 2 hours at room temperature, then tetrabutylammonium fluoride trihydrate (14.10 g, 44.7 mmol, 1.1 equiv.) was added portionwise, and the resulting mixture was stirred for a further 4 hours. The mixture was then concentrated under reduced pressure, the resulting residue was taken up in dichloromethane (100 mL) and saturated aqueous sodium hydrogen carbonate (100 mL), the layers were separated and the aqueous layer was extracted with dichloromethane (2 x 100 mL). The combined organics were washed with brine (100 mL), dried onto magnesium sulfate, filtered and concentrated under reduced pressure. The residue was then purified by silica gel flash column chromatography eluting with a 5/95 mixture of methanol/dichloromethane gave the title compound as a colourless solid (obtained 10.10 g, 26. 05 mmol, 64% yield).[1,9,10]

Mp: 105-106 ºC. $[\alpha]^{20}_{D}$ = + 16.5 ° (c 0.01, $CHCl_3$)

^{1}H NMR (500 MHz, $CDCl_3$) δ 6.86 - 6.82 (br t, J = 6.3 Hz, 1H, N*H*), 6.27 - 6.23 (br t, J = 6.4 Hz, 1H, NH), 4.89 (s, 1H, C*H*, H12), 4.01 (d, *J* = 10.7 Hz, 1H, C*H*, H14$_a$, H14$_b$), 3.82 (d, *J* = 10.7 Hz, 1H, CH, H14$_a$, H14$_b$), 3.68 - 3.47 (m, 4H, CH_2, H9, H5), 2.87 - 2.84 (m, 2H, CH_2, H3), 2.78 (s, 1H, C*H*, H1), 2.40 (t, *J* = 5.91 Hz, 2H, CH_2, H5), 2.14 (s, 3H, CH_3, H20), 2.06 (s, 3H, CH_3, H17), 1.05 (s, 3H, CH_3, H22), 1.01 (s, 3H, CH_3, H21);

^{13}C NMR (126 MHz, $CDCl_3$) δ 171.9 (*C*OCH_3, C19), 171.1 (*C*ONH, C11), 170.1 (*C*OCH_3, C16), 168.2 (*C*ONH, C7), 82.8 (*C*H$_{alk}$, C2), 77.2 (*C*H, C12), 73.3 (*C*H$_{alk}$, C1), 69.4 (*C*H$_2$,

C14), 38.5 (*C*H_2, C8), 37.2 (*C*H_2, C9), 35.3, 35.2 (*C*H_2, C5), 34.4 (*C*H_2, C4), 21.5 (*C*H_3, C20), 21.1 (*C*H_3, C17), 20.9 (*C*H_3, C22), 20.9 (*C*H_3, C21);

m/z (NSI$^+$): Found $[M+H]^+$ 387.1584, $C_{17}H_{27}O_6N_2S$ requires M^+ 387.1584.[1,9,10]

5.9. Multistep synthesis of 362

5.9.1. (O,O-diacetyl)-S-methylthioster-D-pantetheine (365)[9]

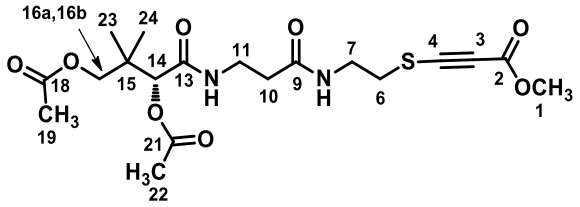

The compound was synthesised according to the procedure reported by Tsuji *et al*.[9]
A oven dried flask containing palladium chloride (II) (0.00050 g, 0.0026 mmol, 0.02 equiv.), coper chloride (II) (0.044 g, 0.33 mmol, 2.5 equiv.), sodium acetate (0.032 g, 0.40 mmol, 3.0 equiv.) in dry methanol (0.58 mL) was fitted with a septum. The flask was then purged with a vacuum line to flash out the air and a rubber balloon with carbon monoxide (1 atm) was attached. When higher pressures of carbon monoxide (50 bars) were used, the reaction was set up using an autoclave. Then, a solution of thioalkyne **363** (0.051 g, 0.13 mmol, 1 equiv.) in methanol (0.58 mL), was added to the mixture via cannula. The green solution turned to brown after 2.5 h and was stirred for 18h. Upon completion, the mixture was quenched with saturated aqueous ammonium chloride / ammonia (9:1). The aqueous phase was extracted with dichloromethane (10 mL). The combined organic layers were washed with brine (10 mL), dried over anhydrous magnesium sulfate, and concentrated under pressure. The residue was purified by silica gel column chromatography eluting with 95:5 dichloromethane: methanol to afford a yellow liquid (obtained 0.007 g, 0.017 mmol, 13 % yield).

^{1}H NMR (500 MHz, $CDCl_3$) δ 6.82 (br t, J = 6.4 Hz, 1H, N*H*), 6.32 (br t, J = 6.5 Hz, 1H, N*H*), 4.88 (s, 1H, C*H*, H14), 4.01 (d, J = 11.0 Hz, 1H, CH_2, H16$_a$, H16$_b$), 3.83 (d, J = 11.0 Hz, 1H, CH_2, H16$_a$, H16$_b$), 3.76 (s, 3H, CH_3, H1), 3.69 – 3.47 (m, 4H, CH_2, H11, H7), 2.96 (td, J = 6.2, 2.0 Hz, 2H, CH_2, H7), 2.42 (t, J = 5.8 Hz, 2H, CH_2, H10), 2.14 (s, 3H, CH_3, H22), 2.06 (s, 3H, CH_3, H19), 1.03 (s, CH_3, H24), 1.01 (s, CH_3, H23).
^{13}C NMR (126 MHz, $CDCl_3$) δ 172.1 (*C*OCH_3, C21), 171.1 (*C*ONH, C13), 170.1 (*C*OCH_3, C14), 168.3 (*C*ONH, C9), 153.3 (*C*O_2CH_3, C2), 87.6 (C_{alkyne}, C3), 83.2 (C_{alkyne}, C4), 77.0 (*C*H, C14), 69.4 (*C*H_2, C16), 52.7 (*C*H_3, C1), 38.9 (*C*H_2, C11), 35.2 (*C*H_2, C10), 35.1 (*C*H_2, C6), 34.8 (*C*H_2, C7), 21.5 (*C*H_3, C22), 21.0 (*C*H_3, C19), 20.9 (*C*H_3, C24), 20.8 (*C*H_3, C23).
HRMS (ES$^+$) m/z: found [M+Na$^+$] 467.1456, [$C_{19}H_{28}O_8N_2NaS$] *requires* M^+ 467.1459.

5.9.2. Bis-acetylene (372)

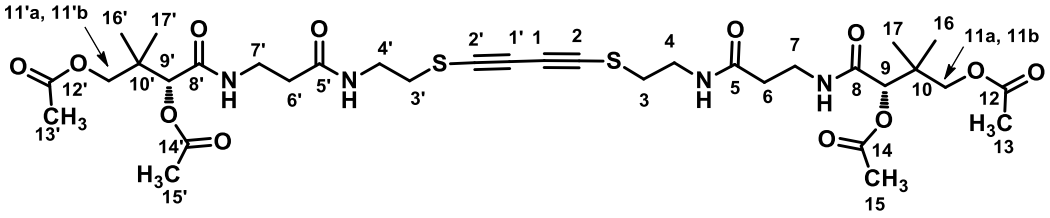

Bis acetylene was obtained as side product of the oxidative carbonylation of thioacetylene **363**. [9]

^{1}H NMR (500 MHz, $CDCl_3$) δ 6.98 (br t, J = 6.5 Hz, 1H, N*H*),6.59 (br t, J = 6.3 Hz, 1H, N*H*), 4.92 (s, 1H, C*H*, H9, H9'), 4.03 (d, *J* = 11.0 Hz, 1H, CH_2, H11$_a$, H11$_b$, H11'$_a$, H11'$_b$), 3.83 (d, *J* = 11.0 Hz, 1H, CH_2, H11$_a$, H11$_b$, H11'$_a$, H11'$_b$), 3.66 – 3.48 (m, 4H, CH_2, H7, H7', H4, H4'), 2.88 (td, 2H, CH_2, H6, H6'), 2.44 (t, *J* = 5.8 Hz, 2H, CH_2, H3, H3'), 2.16 (s, 3H, CH_3, H15, H15'), 2.08 (s, 3H, CH_3, H13, H13'), 1.07 (s, CH_3, H17, H17'), 1.05 (s, CH_3, H16, H16').

^{13}C NMR (126MHz, $CDCl_3$) δ172.1 (*C*ONH, C8, C8'),171.0 (*C*OCH_3, C14, C14'), 170.0 (*C*ONH, C5, C5'), 168.1 (*C*OCH_3, C12, C12'), 87.8 (C_{alk}, C1, C1'), 82.6 (C_{alk}, C2, C2'), 77.5 (*C*H, C9, C9'), 69.3 (*C*H_2, C11, C11'), 38.8 (*C*H_2, C7, C7'), 37.1 (*C*H_2, C4, C4'), 35.2 (*C*H_2, C3, C3'), 35.0 (*C*H_2, C6, C6'), 21.3 (*C*H_3, C15, C15'), 20.9 (*C*H_3, C13, C13'), 20.8 (*C*H_3, C17, C17'), 20.7 (*C*H_2, C16, C16').

m/z (NSI$^+$): Found $[M+Na]^+$793.2759, $[C_{34}H_{50}O_{12}N_4S_2Na]^+$ *requires* M^+ 793.2764.

5.9.3. N,N-diisopropyl-2,3-dimethyl-thio-imidazole (394)[10]

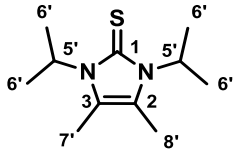

The title compound was synthesised according to the procedure reported by Talavera *et al.*[10]

Acetoin (10.13 g, 132.80 mmol, 1.2 equiv.) was added to a stirred solution of diisopropylthiourea (18.40 g, 115.00 mmol, 1 equiv.) in hexanol (110 mL) and the reaction was heated to 158°C for 12 h. Upon completion, the solution was cooled down to room temperature and the solid was filtered and washed with cold ethanol to afford the compound as a white solid (obtained 11.70 g, 80.50 mmol, 70 % yield).

^{1}H NMR (400 MHz, $CDCl_3$) δ 5.17-6.22 (br s, 1H, C*H*, H5'), 2.16 (s, 6H, CH_3, H7', H8'), 1.42 (d, J = 7.3 Hz, 12H, CH_3, H6').

The data are in agreement with the reported literature values.[10]

5.9.4. S-dibromo-N,N-diisopropyl-2,3-dimethyl-imidazole (395)[10]

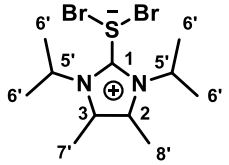

The title compound was synthesised according to the procedure reported by Talavera et al.[10]

Thiourea derivative **394** (11.70 g, 31.18 mmol, 1 equiv.) was dissolved in dry dichloromethane (50 mL) followed by the addition of bromine (2.82 mL, 31.18 mmol, 1 equiv.) at 0°C. The reaction was warmed up to room temperature and stirred for 3 hours. After the removal of all volatiles under reduced pressure, the product was generated as an orange solid (obtained 20.60 g, 0.071 mmol, 95 % yield).

^{1}H NMR (400 MHz, $CDCl_3$) δ 5.67 (2H, hept, J = 7.1 Hz, 1H, C*H*, H5'), 2.37 (s, 6H, CH_3, H7', H8'), 1.68 (d, J = 7.1 Hz, 12H, CH_3, H6').

The data are in agreement with the reported literature values.[10]

5.9.5. Ethyl thioester imidazolium derivative (382)[10]

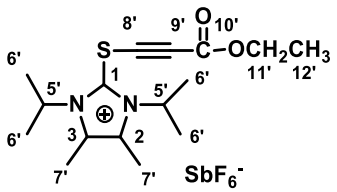

Silver ethyl propiolate (1.41 g, 6.87 mmol, 1.01 equiv.) was added to a solution of compound **395** (2.56 g, 6.87 mmol, 1.01 equiv.) in dry dichloromethane (20 mL) at room temperature. Silver hexafluoro antimonate (2.32 g, 6.75 mmol, 1 equiv.) was added after 5 minutes and the reaction was stirred at room temperature for 45 minutes. Silver salts were then filtered off and the solvent was removed under vacuum. The solid was washed twice with diethyl ether (20 mL) to afford the compound as a brown solid (obtained 3.48 g, 6.35 mmol, 93% yield).[10]

^{1}H NMR (400 MHz, $CDCl_3$) δ 5.17 (hept, J= 7.0 Hz, 1H, C*H*, H5'), 4.21 (q, J= 7.1 Hz, 2H, CH_2, H11'), 2.38 (s, 3H, CH_3, H7'), 1.62 (d, J = 7.0 Hz, 12H, CH_3, H6'), 1.24 (t, J = 7.1 Hz, 3H, CH_3, H12').

^{19}F NMR (400 MHz, $CDCl_3$) δ= -124.00 (sext, $J_{F\text{-}121\ Sb}$ = 1931 Hz).

^{13}C NMR (126 MHz, $CDCl_3$) δ 151.9 (*C*OCH_2CH_3, C10') , 132.2 (*C*H, C1), 88.2 (*C*H, C9'), 72.3 (*C*H, C8'), 63.3 (*C*H, C11'), 54.8 (*C*H, C5'), 21.5 (*C*H_3, C6'), 14.3 (*C*H_3, C12'), 10.9 (*C*H_3, C7').

The data are in agreement with the reported literature values.[10]

5.9.6. (O,O-Diacetyl)-S-ethyl-thioester-D-pantetheine (398)[10]

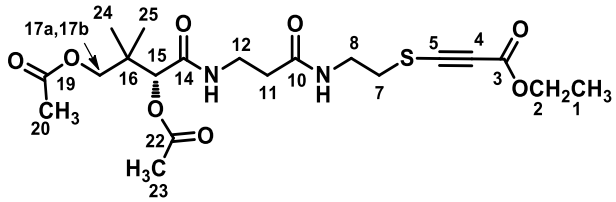

Compound **398** was prepared according to the procedure described by Alcarazo *et al.*[10] Diacetylated pantetheine **331** (0.092 g, 0.25 mmol, 1 equiv.) was dissolved in dry dichloromethane (0.9 mL). N,N-Diisopropylethylamine (44 µL, 0.30 mmol, 1.2 equiv.) followed by a dropwise addition of imidazolium sulfurane **382** (prepared according to Alcarazo *et al.*[10]) (0.17 g, 0.30 mmol, 1.2 equiv.) in dry dichloromethane (0.9 mL) at room temperature. The reaction was stirred for 1 h. The mixture was quenched with 1M of ammonium chloride aqueous solution (1.8 mL) and the aqueous layer was extracted with dichloromethane (2 mL). The combined organic layers were dried over magnesium sulfate and all the volatile components were removed under vacuum. The crude was purified sequentially by column chromatography eluting with 95:5 dichloromethane: methanol and HPLC (isocratic conditions acetonitrile: water 50:50) affording a white deliquescent liquid (obtained 11 mg, 0.025 mmol, 10 % yield).

^{1}H NMR (500 MHz, $CDCl_3$) δ 6.85 (br t, J = 6.4 Hz, 1H, N*H*), 6.35 (br t, J = 6.4 Hz, 1H, N*H*), 4.88 (s, 1H, C*H*, H15), 4.22 (q, J = 7.1 Hz, 2H, CH_2, H2) 4.01 (d, J = 11.0 Hz, 1H, CH_2, H17$_{a,}$ H17$_b$), 3.82 (d, J = 11.0 Hz, 1H, CH_2, H17$_{a,}$ H17$_b$), 3.70 – 3.46 (m, 4H, CH_2, H12, H8), 2.96 (td, J = 6.2, 2.1 Hz, 2H, CH_2, H7), 2.43 (t, 2H, CH_2, H11), 2.14 (s, 3H, CH_3, H23), 2.06 (s, 3H, CH_3, H20), 1.29 (t, J = 7.1 Hz, 3H, CH_3, H1), 1.07 (s, 3H, CH_3, H25), 1.03 (s, 3H, CH_3, H24).

^{13}C NMR (126 MHz, *CDCl$_3$*) δ 172.0 (*C*ONH, C14), 171.0 (*C*OCH$_3$, C22) , 170.9 (*C*ONH, C10), 168.4 (*C*OCH$_3$, C19), 152.8 (*C*OOCH$_2$CH$_3$, C3), 87.7 (C_{alk}, C4), 82.6 (C_{alk}, C5), 77.5 (*C*H, C15), 69.3 (*C*H$_2$, C17) , 62.0 (*C*H$_2$, C2), 38.8 (*C*H$_2$, C12), 35.2 (*C*H$_2$, C8) , 35.0 (*C*H$_2$, C7) , 34.6 (*C*H$_2$, C11) , 21.3 (*C*H$_3$, C23), 20.9 (*C*H$_3$, C20) , 20.8 (*C*H$_3$, C25), 20.7 (*C*H$_3$, C24) , 14.1 (*C*H$_3$, C1).

HRMS (ES$^+$) m/z: Found [M+Na$^+$] 481.1607, [$C_{20}H_{30}O_8N_2NaS$] *requires* M^+ 481.1615.

5.9.7. (O,O-Diacetyl)-S-fluorovinylthio-acrylate-D-pantetheine (362)

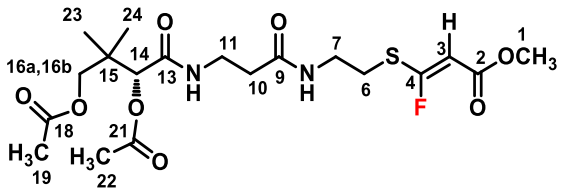

Compound **362** was prepared according to the procedure reported by Li *et al*.[11]
Diacetyl methyl thioester **365** (0.016 g, 0.035 mmol, 1 equiv.) was dissolved in a mixture of 20:1 acetonitrile: water (437µL) followed by silver fluoride (0.091 g, 0.072 mmol, 2 equiv.) and the reaction was stirred for 5 h at 80 °C in a stopped flask. The reaction was cooled down to room temperature. The solvent was removed carefully under pressure and the residue was re-diluted with ethyl acetate (3 mL). The solution was filtrated to remove silver salts and the solvent was removed under pressure to afford fluorovinyl thioacrylate as yellow oil without further purification (obtained 0.05 g, 0,010 mmol, 31 % yield).

^{1}H NMR (500 MHz, *CDCl$_3$*) δ 6.76 (br t, J = 6.3 Hz, N*H*), 6.09 (br t, J = 6.5 Hz, N*H*), 5.54 (d, $^{2}J_{HFtrans}$ = 31.0 Hz, 1H, C*H*, H3), 4.89 (s, 1H, C*H*, H14), 4.02 (d, J = 11.0 Hz, 1H, CH_2, H16$_a$, H16$_b$), 3.84 (d, J = 11.0 Hz, 1H, CH_2, H16$_a$, H16$_b$), 3.72 (s, 3H, CH_3, H1), 3.60 – 3.43 (m, 4H, CH_2, H11, H7), 3.01 (t, 2H, J = 6.2, 2.0 Hz, 2H, CH_2, H10), 2.41 (t, *J* = 5.7 Hz, 2H, CH_2, H6), 2.15 (s, 3H, CH_3, H22), 2.07 (s, 3H, CH_3, H19), 1.08 (s, CH_3, H24), 1.04 (s, CH_3, H23).

^{19}F NMR (*with proton decoupled*, 470 MHz, *CDCl$_3$*) δ -70.51 (s, C*F*=CH).

HRMS (ES$^+$) m/z: found [M+Na$^+$] 487.1507 [$C_{19}H_{29}O_8N_2FNaS$] requires M^+ 487.1521.

5.10. Multistep synthesis of 415

5.10.1. (O,O-Diacetyl)-S-difluoro ethyl thioether-D-pantetheine (433)[12]

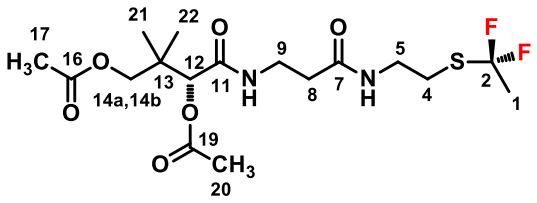

Derivative **433** was synthesized following the procedure described by Bello *et al.*[12]

In a polytetrafluoroethylene round bottom flask, *O,O'*-Diacetyl-*S*-ethynyl-D-pantetheine **363** (0.12 g,0.31 mmol, 1 equiv.) was diluted in dry dichloromethane (5 mL) and Olah's reagent (pyridine 30 %, hydrogen fluoride ~70 % 236 µL, 0.91 mmol, 3 equiv.) was added and the reaction was stirred for 15h . After completion, the reaction was quenched with a saturated sodium carbonate solution (20 mL) and extracted with dichloromethane (30 mL). The crude was purified by semipreparative HPLC (t_r = 17.00 min, isocratic conditions of 90:10 acetonitrile: water for 30 min) to yield an oil (obtained 0.022 g, 0.052 mmol, 17 % yield).

^{1}H NMR (500 MHz, $CDCl_3$) δ 6.85 (br t, J = 6.3 Hz, 1H, N*H*), 6.07 (br t, J = 6.4 Hz, 1H, N*H*), 4.91 (s, 1H, C*H*, H12), 4.02 (d, *J* = 11.0 Hz, 1H, CH_2, H14$_a$, H14$_b$), 3.83 (d, *J* = 11.0 Hz, 1H, , CH_2, H14$_a$, H14$_b$), 3.61 – 3.41 (m, 4H, CH_2, H9, H5), 2.97 (t, *J* = 6.5 Hz, 2H, CH_2, H4), 2.39 (t, *J* = 5.7 Hz, 2H, CH_2, H8), 2.14 (s, 3H, CH_3, H20), 2.06 (s, 3H, CH_3, H17), 1.92 (t, *J* = 16.8 Hz, 3H, CH_3, H1), 1.05 (s, 3H, CH_3, H22), 1.01 (s, 3H, CH_3, H21).

^{19}F NMR (*with proton coupled,* 471 MHz, $CDCl_3$) δ -66.23 (m, *J* = 16.7 Hz, CF_2).

^{13}C NMR (126 MHz, $CDCl_3$) δ 171.8 (*C*OCH_3, C19), 171.1 (*C*ONH, C11), 170.1 (*C*OCH_3, C16), 168.2 (*C*ONH, C7), 77.3 (*C*H, C12), 69.4 (*C*H_2, C14), 39.5 (*C*H_2, C8), 35.2, 35.1 (*C*H_2, C4, C9), 28.3 (CH_2, C5), 26.5 (*C*H_3F_2, J_{CF}= 25.8 Hz, C1), 21.5 (*C*H_3, C20), 21.0 (*C*H_3, C17), 20.9 (*C*H_3, C22), 20.9 (*C*H_3, C21).

m/z (ESI$^+$): Found $[M+Na]^+$ 449.1521, $C_{17}H_{28}O_6N_2F_2NaS$ requires M^+ 449.1528

5.10.2. (O,O-Dihydroxy)-S-difluoro ethyl thioether-D-pantetheine (415)

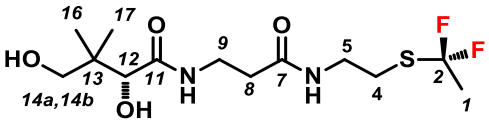

In a round bottom flask, derivative **433** (0.036 g, 0.085 mmol, 1 equiv.) was dissolved in methanol (24 mL). Sodium methoxide (5.4 M in methanol, 40 µL, 0.26 mmol, 3 equiv.) was added and the reaction was stirred for 2h. After completion, the solvent was removed under vacuum and freeze dried. The crude was purified by semipreparative HPLC (t_r =17.50 min, gradient elution method: acetonitrile / water containing 0.05 % trifluoroacetic acid, from 0% to 25% of acetonitrile in 10 min, then from 25% to 60% for 10 min, 60% to 100% in 6 min to wash the column then down to 0% to equilibrate the column) to give a colourless oil. (obtained 0.015 g, 0.058 mmol, 69% yield)

^{1}H NMR (400 MHz, D_2O) δ 7.39 (br t, J = 6.4 Hz, 1H, N*H*), 6.32 (br t, J = 6.3 Hz, 1H, N*H*), 4.00 (s, 1H, C*H*, H12), 3.67 – 3.35 (m, 6H, CH_2, H14$_a$, H14$_b$, H9, H5), 2.98 (t, *J* = 6.5 Hz, 2H, CH_2, H4), 2.52 – 2.36 (m, 2H, CH_2, H8), 1.93 (t, *J* = 16.8 Hz, 3H, CH_3, H1), 1.01 (s, 3H, CH_3, H17), 0.92 (s, 3H, CH_3, H16).

^{19}F NMR (*with proton decoupled,* 471 MHz, D_2O) δ -75.67 (CF_2).

^{13}C NMR (126 MHz, D_2O) δ 173.9 (*C*ONH, C11), 172.1 (*C*ONH, C7), 77.5 (*C*H, C12), 71.3 (*C*H_2, C14), 39.9 (*C*H_2, C8), 36.0, 35.6 (*C*H_2, C4, C9), 28.5 (*C*H_2, C5), 26.4 (*C*H_3, J_{CF} = 25.7 Hz, C1), 21.9 (*C*H_3, C17), 20.8 (*C*H_3, C16).

m/z (ESI$^+$): Found [M+Na] $^+$ 365.1311, $C_{13}H_{24}O_4N_2F_2NaS$ requires M^+, 365.1317

5.11. Multistep synthesis of 479

5.11.1. Pantothenic acid acetonide (480)[13]

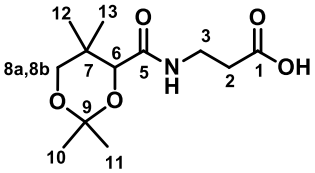

The desired compound was prepared according to the procedure reported by Storz *et al.* [13]

D-pantothenic acid hemicalcium salt (10 g, 0.04 mmol, 1 equiv.) was dissolved in acetone (15 mL) followed by the addition of anhydrous oxalic acid (18 g, 0.2 mmol, 5 equiv.). Then a solution of 2,2-dimethoxy propane (4.20 g, 0.04 mmol, 1 equiv.) in acetone (15 mL) was added and the reaction was refluxed for 16 h. Upon completion, the calcium oxalate was filtered off and the solvent was removed under pressure. The residue was dissolved in ethyl acetate (30 mL), washed with water (30 mL) and dried over magnesium sulfate. The solvent was removed under reduced pressure and the residue was triturated in hexane to give the desired compound as a white solid (obtained 7.80 g, 0.03 mmol, 75% yield).

m.p.87-89 °C

^{1}H NMR (400 MHz, $CDCl_3$) δ 7.03 (br t, J = 6.4 Hz, 1H, N*H*), 4.10 (s, 1H, C*H*, H5), 3.73 – 3.66 (d, J = 11.7 Hz, 1H, CH_2, H8$_a$, H8$_b$), 3.65 – 3.55 (m, 1H, CH_2, H3), 3.54 – 3.43 (m, 1H, CH_2, H3), 3.28 (d, *J* = 11.7 Hz, 1H, CH_2, H8$_a$, H8$_b$), 2.62 (t, *J* = 6.2 Hz, 2H, CH_2, H2), 1.46 (s, 3H, CH_3, H11), 1.43 (s, 3H, CH_3, H10), 1.03 (s, 3H, CH_3, H13), 0.97 (s, 3H, CH_3, H12).

These data are in agreement with the published procedure.[13]

5.11.2. α,β,β-trifluorocyclopropyl-carboxyamido-ethyl-carbamate (476)[14]

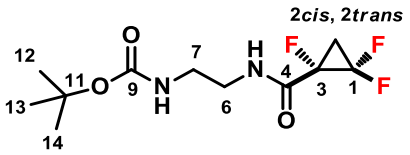

The product was prepared according to the procedure reported by Thomson *et al.*[14] Carbamic acid (0.70 g,3.56 mmol, 5 equiv.) was dissolved in dimethylformamide (6 mL), followed by α,β,β-trifluorocyclopropane-1-carboxylic acid **457** (supplied by Dr Q. Zhang from the university of St Andrews)[1] (0.10 g, 0.71 mmol, 1 equiv.), 1-hydroxybenzotriazole hydrate (0.19 g, 1.40 mmol, 2 equiv.) and triethylamine (501 µL, 3.60 mmol, 5 equiv.). The solution was cooled down to 0 °C. N-(3-dimethylaminopropyl)-N'-ethylcarbodiimide hydrochloride (0.27 g, 1.40 mmol, 2 equiv.) was added. The reaction was stirred for 30 min on ice and at room temperature for 18 h. The solvent was removed under reduced pressure and the crude was re-dissolved in dichloromethane (20 mL). The organic layer was washed with 1 M hydrochloric acid solution (20 mL) and saturated sodium hydrogen carbonate solution, (20 mL). After drying over anhydrous magnesium sulfate, the product was purified by flash column chromatography eluting with a mixture of 95/5 dichloromethane: methanol affording the product as a colourless oil (obtained 0.68 g, 2.40 mmol, 68% yield).

^{1}H NMR (500 MHz, $CDCl_3$) δ 7.29 (br t, J = 6.5 Hz, 1H, N*H*), 5.15 – 4.87 (br t, J = 6.4 Hz, 1H, NH), 3.46 (m, 2H, CH_2, H6), 3.33 (m, 2H, CH_2, H7), 2.62 – 2.47 (m, 1H, C*H*, $H2_{cis}$, $H2_{trans}$), 2.10 – 1.91 (m, 1H, C*H*, $H2_{cis}$, $H2_{trans}$), 1.43 (s, 9H, CH_3, H12, H13, H14).

^{13}C NMR (126 MHz, $CDCl_3$) δ 163.7 (d, J^2_{CF}= 18.5 Hz, *C*ONH, C4), 157.4 (*C*ONH, C9), 108.5 (tdd, $^1J_{CF}$= 296.3 Hz, $^2J_{CF}$=11.0 Hz, $^2J_{CF}$ = 4.6 Hz, *C*F_2, C2), 77.8 (*C*F hidden by $CDCl_3$ signal), 41.7 (*C*H_2, C6), 40.1(*C*H_2, C7), 28.7 (*C*H_3, C12, C13, C14), 22.2 (q, J^2_{CF} = 12.1 Hz, J^2 = 10.6 Hz , *C*H_2, C2).

^{19}F NMR (*with proton decoupled,* 471 MHz, $CDCl_3$) δ -139.30 (m, CF_2), -202.20 (m, C*F*).

m/z (ESI$^+$): Found [M+Na] $^+$ 305.1078, $C_{11}H_{17}O_3N_2F_3Na$ requires M^+, 305.1083

5.11.3. α,β,β-trifluorocyclopropyl-carboxyamido-ethyl amine (477)

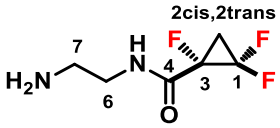

α, β, β-trifluorocyclopropyl-carboxyamido-ethyl carbamate **476** (0.060 g, 0.21 mmol, 1equiv.) was dissolved in dichloromethane (7 mL) and trifluoro acetic acid (421 µL, 26.59 mmol, 25 equiv.) was added to the mixture and the reaction was stirred for 3h. The solvent was removed under reduced pressure. The residue was diluted with water and the pH of the solution was adjusted to pH = 8 with a saturated aqueous solution of sodium hydrogen carbonate. The compound was loaded onto a C18 cartridge, washing first with water (10 mL) to remove the trifluoro acetic acid excess then with acetonitrile (10 mL) to flush down the compound. The solvent was carefully removed under pressure and the acetonitrile solution of amine was used in the next step to avoid the loss of the high volatile amine.

^{1}H NMR (400 MHz, MeOD) δ 3.65 – 3.45 (m, 2H, C*H*$_2$, H6), 3.07 (td, *J* = 5.8, 1.9 Hz, 2H, C*H*$_2$, H7), 2.48 (m, 1H, C*H*, H2$_{cis}$, H2$_{trans}$), 2.20 (m, 1H, C*H*, H2$_{cis}$, H2$_{trans}$).

^{19}F NMR (*with fluorine decoupled*, 377 MHz, MeOD) δ -77.14 (*trifluoroacetic acid*), -140.99 (ddd, $^{2}J_{FF}$ = 164.5 Hz, 122.2 Hz, ^{3}J$_{FF}$ = 10.6 Hz,1.8 Hz, C*F*$_2$), -203.96 (ddd, $^{3}J_{FF}$ = 47.6, 12.1, 1.8 Hz, C*F*).

m/z (ESI^{+}): Found [M+H] $^{+}$183.0737, [$C_6H_{10}ON_2F_3$] requires M^{+} 183.0740

5.11.4. (O,O-acetonide)-S-α,β,β-trifluorocyclopropyl-D-pantetheine (481)[14]

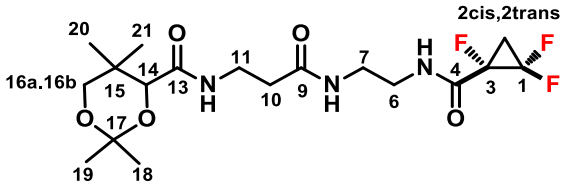

α, β, β-trifluorocyclopropyl-carboxyamido-ethyl amine **477** (0.019 g, 0.10 mmol, 1 equiv.) was dissolved in dimethylformamide (3 mL) followed by derivative **480** (0.032 g, 0.12 mmol, 1.2 equiv.), 1-hydroxybenzotriazole hydrate (0.018 g, 0.20 mmol, 2 equiv.) and triethylamine (43 µL, 0.31 mmol, 3 equiv.). The solution was cooled down to 0 °C and N-(3-dimethylaminopropyl)-N'-ethylcarbodiimide hydrochloride (0.030 g, 0.15 mmol, 1.5 equiv.) was added. The reaction was stirred for 30 min on ice bath and at room temperature for 18 h. The solvent was removed under reduced pressure and the crude was re-dissolved in dichloromethane (20 mL). The organic layer was washed with 1 M hydrochloric acid solution (5 mL) and saturated sodium hydrogen carbonate solution (5 mL). After drying over anhydrous magnesium sulfate, the product was purified by flash column chromatography eluting with a mixture of 95/5 dichloromethane: methanol affording the product as a colourless oil (obtained 0.020 g, 0.047 mmol, 46% yield).

^{1}H NMR (500 MHz, $CDCl_3$) δ 7.49 (br t, J = 6.3 Hz, 1H, N*H*), 7.04 (br t, J = 6.4 Hz, 1H, N*H*), 6.82 (br t, J = 6.5 Hz, 1H, N*H*), 4.07 (s, 1H, C*H*, H14), 3.67 (d, *J* = 11.7 Hz, 1H, CH_2, H16$_a$, H16$_b$), 3.60 – 3.36 (m, 6H, CH_2, H11, H10, H8), 3.27 (dd, *J* = 11.7, 1.9 Hz, 1H, CH_2, H16$_a$, H16$_b$), 2.55 (m, 1H, C*H*, H2$_{cis}$, H2$_{trans}$), 2.50- 2.43 (m, 2H, CH_2, H6), 2.02 (m, 1H, C*H*, H2), 1.45 (d, *J* = 1.5 Hz, 3H, CH_3, H18), 1.41 (s, 3H, CH_3, H19), 1.01 (s, 3H, CH_3, H21), 0.95 (s, 3H, CH_3, H20).

^{19}F NMR (*with proton decoupled*, 470 MHz, $CDCl_3$) δ -75.17 (*trifluoroacetic acid*) -139.22 (ddd, $^{2}J_{FF}$ = 165.1 Hz, $^{3}J_{FF}$ = 12.3 Hz, CF_2), -202.10 (dd, $^{3}J_{FFcis}$ = 47.3 Hz, 12.0 Hz, C*F*).

^{13}C NMR (126 MHz, $CDCl_3$) δ 172.4 (*C*ONH, C1), 170.6 (*C*ONH, C20), 163.3 (d, $^{2}J_{CF}$= 20.2 Hz, *C*ONH, C4),106.7 (td, $^{1}J_{CF}$ = 295.5 Hz, $^{2}J_{CF}$ = 8.3 Hz, *C*1) 77.3 (*C*H, C14), (*C*F signal hidden by chloroform signal), 71.4 (*C*H$_2$, C16), 40.6 (*C*H$_2$, C11), 39.5 (*C*H$_2$, C10), 36.4 (*C*H$_2$, C6), 34.9 (*C*H$_2$, C7), 29.5 (*C*H$_3$, C19), 22.1 (*C*H$_3$, C18), 21.87 (q, $^{2}J_{CF}$ = 10.4 Hz, *C*H$_2$, C2), 18.8 (*C*H$_3$, C21), 18.6 (*C*H$_3$, C20).

m/z (ESI$^+$): Found [M+Na]$^+$446.1864 [$C_{18}H_{28}O_5N_3F_3Na$]$^+$requires M^+ 446.1873

5.11.5. (O,O-acetonide)-S-α,β,β-trifluorocyclopropyl-D-pantetheine (478)

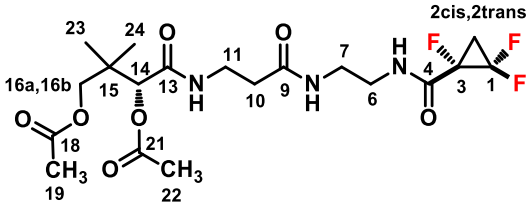

Compound **478** was prepared according to the same procedure described for **481** using compound **294** as protected pantothenic acid. The crude was purified by flash chromatography with a mixture of 90/10 dichloromethane: methanol to afford the desired compound as a colourless oil (obtained 0.007 g, 0.016 mmol, 16 % yield).

^{1}H NMR (500 MHz, $CDCl_3$) δ 7.50 (br t, J = 6.5 Hz, 1H, N*H*), 6.86 (br t, J = 6.4 Hz, 1H, N*H*), 6.63 – 6.44 (br t, 6.4 Hz, 1H, N*H*), 4.85 – 4.72 (s, 1H, C*H*, H14), 4.02 (dt, *J* = 11.1, 3.3 Hz, 1H, CH_2, H16$_a$, H16$_b$), 3.84 (dd, *J* = 11.0, 5.6 Hz, 1H, CH_2, H16$_a$, H16$_b$), 3.73 – 3.23 (m, 4H, CH_2, H11, H7), 2.53 (m, 1H, CH, H2$_{cis,}$ H2$_{trans}$), 2.47 – 2.31 (m, 1H, C*H*, H2$_{cis,}$ H2$_{trans}$), 2.14 (s, 3H, CH_3, H22), 2.10-1.97 (m, 2H, CH_2, H10), 2.06 (s, 3H, CH_3, H19), 1.34 - 1.20 (m, 2H, CH_2, H6), 1.05 (s, 3H, CH_3, H24), 1.03 (s, 3H, CH_3, H23).
^{19}F NMR (*with proton coupled,* 470 MHz, $CDCl_3$) δ -139.20 (m, CF_2), -201.98 (m, C*F*).
m/z (ESI$^+$): Found [M+Na]$^+$ 490.1768, [$C_{19}H_{29}O_7N_3F_3Na$]$^+$requires M^+ 490.1800

5.11.6. (O,O-Dihydroxy)-S-α,β,β-trifluorocyclopropyl-D-pantetheine (479)

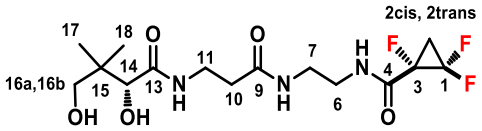

Derivative **481** (0.043 g, 0.10 mmol, 1 equiv.) was dissolved in a mixture of tetrahydrofuran: water (2:1, 4 mL) followed by the addition of para-toluene sulfonic acid (0.031 g, 0.16 mmol, 1.6 equiv.) and the reaction was stirred for 2h. Upon completion, the solvent was removed under pressure and the residue was freeze dried to remove the last traces of water. The crude was purified by semipreparative HPLC (r_t = 20 min gradient elution method: acetonitrile / water containing 0.05 % trifluoroacetic acid, from 0% to 25% of acetonitrile in 10 min, then from 25% to 60% for 10 min, 60% to 100% in 6 min to wash the column then down to 0% to equilibrate the column) to give the desired compound as colourless deliquescent solid (obtained 0.021 g, 0.056 mmol, 56% yield).

^{1}H NMR (500 MHz, D_2O) δ 3.99 (s, 1H, C*H*, H14), 3.59 – 3.28 (m, 8H, $H16_a$, $H16_b$, H11, H10, H7), 2.60 – 2.51 (m, 1H, C*H*, $H2_{cis}$, $H2_{trans}$), 2.49 (t, *J* = 6.6 Hz, 2H, CH_2, H6), 2.34 (m, 1H, C*H*, $H2_{cis}$, $H2_{trans}$), 0.92 (s, 3H, CH_3, H18), 0.89 (s, 3H, CH_3, H17).

^{13}C NMR (126 MHz, D_2O) δ 175.1 (*C*ONH, C13), 174.3 (*C*ONH, C9), 163.0 (q, $^{2}J_{CF}$ = 35.6 Hz, *C*ONH, C4), 116.37 (q, $^{1}J_{CF}$ = 291.8 Hz, *C*F_2, C2), 75.8 (*C*H_2, C14), (*C*F signal hidden by $CDCl_3$ signal), 68.4 (*C*H_2, C16), 38.9, 38.6, 38.5 (*C*H_2, C7), 35.4, 35.3 (*C*H_2, C5, C11), 21.7 (*q*, $^{2}J_{CF}$ = 10.5 Hz, *C*H_2, C3), 20.4 (*C*H_3, C18), 19.1 (*C*H_3, C17).

^{19}F NMR (*with proton decoupled,* 471 MHz, D_2O) δ -75.17 (*trifluoro acetic acid*), -139.63 (ddd, $^{2}J_{FF}$ = 164.6 Hz, CF_2), -201.86 (dd, $^{3}J_{FFcis}$ = 47.2 Hz, 12.0 Hz, C*F*).

m/z (ESI$^+$): Found $[M+Na]^+$406.1557 $[C_{15}H_{24}O_5N_3F_3Na]^+$ requires M^+ 406.1560.

5.12. Cloning and expression of PanK, PPAT, DPCK enzymes

The cloning and overexpression of PanK, PPAT and DPCK enzymes was carried out by Dr. Nouchali Bandaranayaka from the University of St. Andrews according to published procedures.[2,15] The plasmids were gifted by Dr. Manuela Tosin from the University of Warwick. [15]

PanK, PPAT, and DPCK were PCR amplified from E.Coli K12 genomic DNA using the following primer pairs.

PanK enzyme

Primers used for pET-29b plasmid

PanK p1 ACATGCATATGAGTATAAAAGAGCAAACGT NdeI

PanK p2 CTCCCCTCGAGATTATTTGCGTAGTCTGAC XhoI

PPAT enzyme

Primers used for pET-29b plasmid

PPAT1 forward GTCTCTAGAGCTAGCATGCAAAAACGGGCGATTTAT NheI

PPAT2 reverse CGCGGATCCAAGCTTCTACGCTAACTTCGCC BamHI

DPCK enzyme

Primers used for pETHISTEV plasmid

DPCKFP – 5'GGAACTGGATCCATGAGGTATATAGTTGCCTTAACGGGA BamHI

DPCKRP - CCGATTCTCGAGTTACGGTTTTTCCTGTGAGACAAACTG XhoI

5.13. General procedure for the enzymatic synthesis of acetyl-CoA analogues[1]

The enzymatic synthesis and characterization of the products have been performed following the protocol used for Fluoro vinylthioether-CoA ***212****.*[1]

The diol derivative (**259**, **260**, **312**, *(Z)*-**334**,*(E)*-**335**, **479**, 20 mg) was dissolved in 200 µL of a 1M aqueous buffer solution of Tris-HCl at pH 7.8 (50 mM) followed by adenosine 5'-trisphosphate disodium salt hydrate (40 mg, 20 mM), an aqueous solution of magnesium chloride (2 mM, 4µL). The resulting mixture was diluted with Milli-Q® water (1 mL). The pH was adjusted to 7.5 using a 30% aqueous solution of sodium hydroxide, and the stock solutions of PanK (5 mg/mL, 1 mL) and PPAT (5 mg/mL, 1 mL) were added, followed by Milli-Q® water to adjust the final volume to 4 mL. The resulting mixture was incubated for 20 hours at 37 ºC, then it was treated with chloroform (4 mL) to precipitate the enzymes. The mixture was shaken thoroughly and centrifugated at 4000 rpm for 10 minutes. The aqueous supernatant was pipetted out, and fresh Milli-Q® water (2 mL) was added, the protein pellet re-suspended and the mixture centrifugated at 4000 rpm for a further 10 minutes. The aqueous supernatant was removed and the combined aqueous layers were frozen in liquid nitrogen and freeze-dried. The crude material was purified by semipreparative HPLC using a linear gradient of acetonitrile and water containing 0.05 % trifluoroacetic acid and a Phenomenex Synergi® 4µ Polar-RP 80Å 250 x 10.0 mm. The eluted fractions were pooled, combined and the pH was corrected to slightly above 7.0 using a concentrated aqueous solution of ammonium hydroxide. The resulting mixture was gently concentrated under reduced pressure or a stream of argon gas to remove the acetonitrile, then it was frozen in liquid nitrogen and freeze dried, to afford the desired dephospho-coenzyme A intermediate as an ammonium salt.

The final phosphorylation at the 3' position on the ribose ring was achieved by dissolving the material obtained in the biotransformation described above (purified by HPLC) in Tris-HCl at pH 7.8 (200 µL, 50 mM). Adenosine 5'-trisphosphate disodium salt hydrate (40 mg, 20 mM) and an aqueous solution of $MgCl_2$ (2 mM, 4µL) were added, and the resulting mixture was diluted with Milli-Q® water (1 mL) and the pH was adjusted to 7.5 using a 30% aqueous solution of sodium hydroxide. Stock solutions of DPCK (5 mg/mL, 1mL) was added, followed by Milli-Q® water to bring up the final reaction volume to 4 mL. The resulting mixture was incubated for 20 hours at 37 ºC, then it was treated with chloroform (4 mL) to precipitate the protein. The mixture was shaken and centrifugated at 4000 rpm for 10 minutes. The aqueous supernatant was pipetted out, and fresh Milli-Q® water (2 mL) was added, the protein pellet re-suspended and the mixture centrifugated at 4000 rpm for a further 10 minutes. The aqueous supernatant was

removed and the combined aqueous layers were frozen in liquid nitrogen and freeze-dried. The resulting material was purified by semipreparative HPLC (Phenomenex Synergi® 4µ Polar-RP 80Å 250 x 10.0 mm). The eluted fractions were pooled, combined and the pH was adjusted to slightly above 7.0 using a concentrated aqueous solution of ammonium hydroxide. The resulting mixture was gently concentrated under reduced pressure and freeze dried to afford the final coenzyme-A analogue as an ammonium salt.[1]

5.13.1. S-Fluorovinyl-dethia-coenzyme A (261)[1]

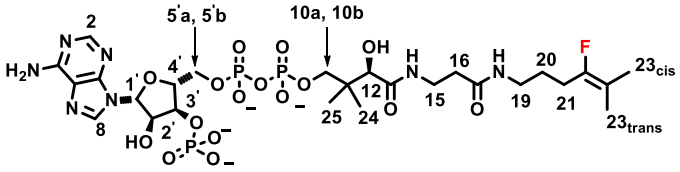

Compound **261** was synthesised accordingly to the general procedure described above. Fluoro dethia vinyl diol **259** (0.020 g, 0.025 mmol) was converted to Coenzyme A analogue **261** which was obtained as a colourless, highly hydroscopic solid in an overall yield of 25% (0.005 g as an ammonium trifluoroacetate salt) after purification by semipreparative HPLC chromatography using a Phenomenex Synergi® 4µ Polar-RP 80Å 250 x 10.0 mm column and a linear gradient of water and acetonitrile containing 0.05% trifluoroacetic acid (0 to 15% acetonitrile in 10 min, then 15% acetonitrile for 10 min, then from 15% to 80% acetonitrile in 3 min to wash the column, then from 80% to 0% acetonitrile in 3 minutes, and 0% acetonitrile for 10 min to re-equilibrate the column). Retention time: 15.0 min (detector: 215 nm).[1]

^{1}H NMR (700 MHz, D_2O) δ 8.54 (s, 1H, C*H*, H2), 8.25 (s, 1H,C*H*, H6), 6.15 (d, *J* = 6.7 Hz, 1H, C*H*, H1'), 4.84 - 4.73 (2H, m, C*H*, H2' and H3', signals partially hidden by water peak), 4.57 (s, 1H, CH, H4'), 4.51 (ddd, $J_{FH(cis)}$ = 18.5, 3.0 Hz, 1H, C*H*, $H23_{cis}$), 4.35 – 4.24 (dd, $J_{FH(trans)}$ = 50.0 , 3.0 Hz, 1H, C*H*, $H23_{trans}$), 4.22 (s, 2H, CH_2, H5'a, H5'b), 3.99 (s, 1H, C*H*, H12), 3.81 (dd, *J* = 10.1, 3.6 Hz, 1H, C*H*, $H10_a$, $H10_b$), 3.53 (dd, *J* = 10.1, 3.4 Hz, 1H, C*H*, $H10_a$, $H10_b$), 3.47 – 3.38 (m, 2H, CH_2, H15), 3.13 (t, *J* = 6.9 Hz, 2H, CH_2, H19), 2.41 (t, *J* = 6.6 Hz, 2H, CH_2, H16), 2.20 – 2.13 (m, 2H, CH_2, H21), 1.62 (p, *J* = 7.2 Hz, 2H, CH_2, H20), 0.86 (s, 3H, CH_3, H24), 0.73 (s, 3H, CH_3, H25).

^{19}F NMR (*with proton decoupled,* 659 MHz, D_2O) δ -76.01 (trifluoro acetic acid), -95.93 (m, CH_2=CHF).

m/z (ESI$^-$): Found $[M-H]^-$ 792.1585, $C_{24}H_{38}O_{16}N_7FP_3$ requires M^- 792.1577.

^{1}H NMR peak values were assigned by using 2D experiments (DQF-COSY) reported in Chapter 2 and by comparison with the structure of compound **212**.[1]

5.13.2. S-Vinyl-dethia-coenzyme-A[1](262)

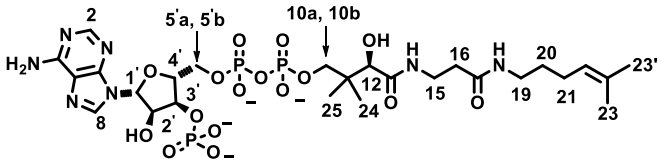

Compound **262** was prepared accordingly to the general procedure described above. Starting from diol **260** (0.020 g, 0.026 mmol), the coenzyme A mimetic **262** was obtained as a colourless, highly hydroscopic solid in an overall yield of 25% (0.005 g as an ammonium trifluoroacetate salt) after purification by semipreparative HPLC chromatography using a Phenomenex Synergi® 4µ Polar-RP 80Å 250 x 10.0 mm column and a linear gradient of water and acetonitrile with 0.05% trifluoroacetic acid (0 to 15% acetonitrile in 10 min, then 15% acetonitrile for 10 min, then from 15% to 80% acetonitrile in 3 min to wash the column, then from 80% to 0% acetonitrile in 3 minutes, and 0% acetonitrile for 10 min to re-equilibrate the column). Retention time: 15.1 min (detector: 215 nm).[1]

^{1}H NMR (500 MHz, D_2O) δ 8.50 (s, 1H, C*H*, H2), 8.21 (s, 1H, C*H*, H6), 6.12 (d, *J* = 6.9 Hz, 1H, C*H*, H1'), 5.76 (ddt, *J* = 17.0, 10.3, 6.6 Hz, 1H, C*H*, H22), 5.01 – 4.88 (m, 2H, CH_2, H23, H23'), 4.84 - 4.73 (m, 2H, C*H*, H2' and H3', signals partially hidden by water peak), 4.53 (br, 1H, C*H*, H4'), 4.18 (s, 2H, CH_2, H5'$_a$, H5'$_b$), 3.95 (s, 1H, C*H*, H12), 3.77 (dd, *J* = 9.8, 4.8 Hz, 1H, C*H*, H10$_a$, H10$_b$), 3.49 (dd, *J* = 9.8, 4.8 Hz, 1H, CH, H10$_a$, H10$_b$), 3.40 (td, *J* = 6.5, 3.0 Hz, 2H, CH_2, H15), 3.05 (t, *J* = 7.0 Hz, 2H, CH_2, H19), 2.38 (t, *J* = 6.6 Hz, 2H, CH_2, H16), 1.96 (q, *J* = 7.1 Hz, 2H, CH_2, H20), 1.47 (p, *J* = 7.2 Hz, 2H, CH_2, H21), 0.83 (s, 3H, CH_3, H24), 0.69 (s, 3H, CH_3, H25).

m/z (ESI$^-$): Found $[M-H]^-$ 774.1679, $C_{24}H_{39}O_{16}N_7P_3$ requires M^- 774.1672.

^{1}H NMR peak values were assigned by using 2D experiments (DQF-COSY) reported in Chapter 2 and by comparison with the structure of compound **261**.[1]

5.13.3. S-Sulfoxide-Coenzyme-A (305)[1]

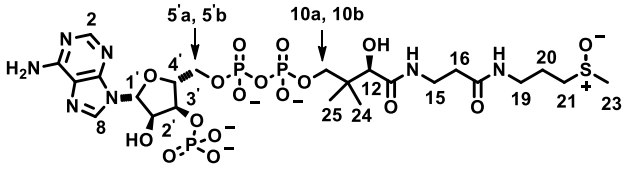

Compound **305** was synthesised following the general procedure described above. Diol **312** (0.020 g, 0.062 mmol) was converted to coenzyme A mimic **305** which was obtained as a colourless, highly hydroscopic solid in an overall yield of 30% (6 mg as an ammonium trifluoroacetate salt) after purification by semipreparative HPLC chromatography using a Phenomenex Synergi® 4µ Polar-RP 80Å 250 x 10.0 mm column and a linear gradient of water and acetonitrile containing 0.05% trifluoroacetic acid (0 to 15% acetonitrile in 10 min, then 15% acetonitrile for 10 min, then from 15% to 80% acetonitrile in 3 min to wash the column, then from 80% to 0% acetonitrile in 3 minutes, and 0% acetonitrile for 10 min to re-equilibrate the column). Retention time: 13.6 min (detector: 254 nm).[1]

^{1}H NMR (500 MHz, D_2O) δ 8.52 (s, 1H, C*H*, H2), 8.24 (s, 1H, C*H*, H6), 6.14 (d, *J* = 6.7, 1H, C*H*, H1'), 4.78 - 4.73 (m, 1H, C*H*, H2' and H3', signals partially hidden by water peak), 4.54 (br s, 1H, C*H*, H4'), 4.21 (br s, CH, 2H, H5'$_a$, H5'$_b$), 3.97 (s, 1H, C*H*, H12), 3.78 (dd, *J* = 9.9, 4.4 Hz, 1H, CH_2, *H*10$_a$, H10$_b$), 3.52 (dd, *J* = 8,6 Hz, 1H, CH_2, H10$_a$, H10$_b$), 3.43 (t, *J* = 6.6 Hz, 2H, CH_2, H15), 3.25 (t, *J* = 6.9 Hz, 2H, CH_2, H19), 2.89 - 2.76 (m, 2H, CH_2, H21), 2.65 (s, 3H, CH_3, H23), 2.42 (t, *J* = 6.6 Hz, 2H, CH_2, H20), 1.92 - 1.83 (m, 2H, CH_2, H16), 0.84 (s, 3H, CH_3, H24), 0.72 (s, 3H, CH_3, H25);

m/z (ESI$^-$): Found [M-H]$^-$ 810.1341, $C_{23}H_{39}O_{17}N_7P_3S$ requires M^- 810.1341.

^{1}H NMR peak values were assigned by using 2D experiments (DQF-COSY) reported in Chapter 2 and by comparison with the structure of compound **261** .[1]

5.13.4. Purification and separation of Co-enzyme-A analogues (Z)-319 and (E)-320[1]

Compound *(E)*-**320** and compound *(Z)*-**319** were synthesised accordingly to the general procedure described above. As described in Chapter 2, isomers diol (*E*)-**335** and *(Z)*-**334** (20.0 mg, 0.055 mmol) were progressed as a mixture to generate intermediates *(E)*-**337** and *(Z)*-**336** which were separated at this stage. Intermediates (E)-**337** and (Z)-**336** were finally converted to coenzyme-A analogues *(E)*-**320** and *(Z)*-**319**.[1]

5.13.5. S-(Z-propenoic-3-yl)-coenzyme A (Z)-319[1]

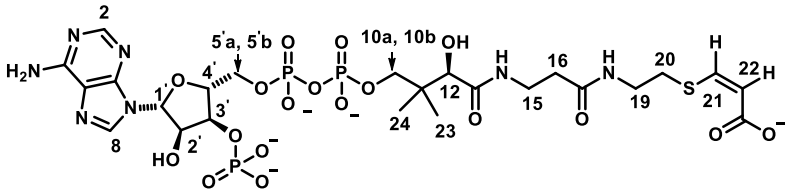

Compound (*Z*)-**319** was synthesised as a colourless, highly hydroscopic solid in an overall yield of 13% (0.006 g as an ammonium trifluoroacetate salt) after purification by semipreparative HPLC chromatography using a Phenomenex Synergi® 4µ Polar-RP 80Å 250 x 10.0 mm column and a linear gradient of water and acetonitrile containing 0.05% trifluoroacetic acid (0 to 15% acetonitrile in 10 min, then 15% acetonitrile for 10 min, then from 15% to 80% acetonitrile in 3 min to wash the column, then from 80% to 0% acetonitrile in 3 minutes, and 0% acetonitrile for 10 min to re-equilibrate the column). Retention time: 14.4 min (detector: 215 nm).

^{1}H NMR (500 MHz, D_2O) δ 8.55 (s, 1H, C*H*, H2), 8.28 (s, 1H, C*H*, H6), 6.93 (d, J_Z = 10.1 Hz, CH, 1H, C*H*, H21), 6.18 (d, J = 6.4 Hz, 1H, C*H*, H1'), 5.85 (d, J_Z = 10.0 Hz, 1H, C*H*, H22), 4.84 - 4.73 (m, 2H, CH_2, H2' and H3', signals partially hidden by water peak), 4.60 (br s, 1H , C*H*, H4'), 4.25 (s, 2H, CH_2, H5'$_a$, H5'$_b$), 4.01 (s, 1H, C*H*, H12), 3.83 (dd, J = 6.7 Hz , 1H , *CH$_2$,* H10$_a$, H10$_b$), 3.60 (dd, J = 6.6 Hz, 1H, CH_2, H10$_a$, H10$_b$), 3.47 (t, J = 6.7 Hz, 2H, CH_2, H15), 3.40 (t, J = 6.7 Hz, 2H, CH_2, H16), 2.85 (t, J = 6.8 Hz, 2H, CH_2, H19), 2.45 (t, J= 6.8 Hz, 2H, CH_2, H20), 0.89 (s, 3H, CH_3, H23), 0.76 (s, 3H, CH_3, H24).

m/z (ESI$^-$): Found [M-H]$^-$ 836.1145, $C_{24}H_{37}O_{18}N_7P_3S$ requires M$^-$ 836.1134 .

^{1}H NMR peak values were assigned by using 2D experiments (DQF-COSY) reported in Chapter 2 and by comparison with the structure of compound **261**.[1]

5.13.6. S-(E-propenoic-3-yl)-coenzyme A (E)-320[1]

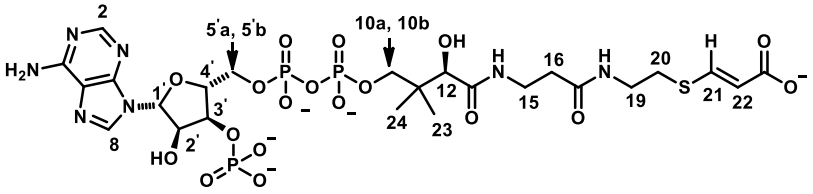

Coenzyme A mimic (*E*)-**320** was obtained as a colourless, highly hydroscopic solid in an overall yield of 15% (0.007 g as an ammonium trifluoroacetate salt) after purification by semipreparative HPLC chromatography using a Phenomenex Synergi® 4µ Polar-RP 80Å 250 x 10.0 mm column and a linear gradient of water and acetonitrile containing 0.05% trifluoroacetic acid (0 to 15% acetonitrile in 10 min, then 15% acetonitrile for 10 min, then from 15% to 80% acetonitrile in 3 min to wash the column, then from 80% to 0% acetonitrile in 3 minutes, and 0% acetonitrile for 10 min to re-equilibrate the column). Retention time: 13.9 min (detector: 215 nm).[1]

^{1}H NMR (500 MHz, D_2O) δ 8.54 (s, 1H, C*H*, H2), 8.26 (s, 1H, C*H*, H6), 7.47 (d, J_E = 15.3 Hz, 1H, C*H*, H21), 6.16 (d, *J* = 6.4 Hz, 1H, C*H*, H1'), 5.79 (d, J_E = 15.2 Hz, 1H, C*H*, H22), 4.84 - 4.73 (2H, m, H2' and H3', signals partially hidden by water peak), 4.57 (br, 1H, C*H*, H4'), 4.22 (s, 2H, CH_2, H5'$_a$, H5'$_b$), 3.98 (s, 1H, C*H*, H12), 3.79 (dd, *J* = 6.7 Hz, 1H, CH_2, H10$_a$, H10$_b$), 3.57 – 3.48 (dd, 1H, CH_2, H10$_a$, H10$_b$), 3.43 (t, *J* = 6.5 Hz, 2H, CH_2, H15), 3.39 (t, *J* = 6.5 Hz, 2H, CH_2, H16), 2.92 (t, *J* = 6.5 Hz, 2H, CH_2, H19), 2.42 (t, *J* = 6.5 Hz, 2H, CH_2, H20), 0.87 (s, 3H, CH_3, H24), 0.74 (s, 3H, CH_3, H23).

m/z (ESI$^-$): Found [M-H]$^-$ 836.1146, $C_{24}H_{37}O_{18}N_7P_3S$ requires M^- 836.1134.

^{1}H NMR peak values were assigned by using 2D experiments (DQF-COSY) reported in Chapter 2 and by comparison with the structure of compound **261**.[1]

5.13.7. S-α,α,β-trifluorocyclopropyl-Coenzyme-A (462)

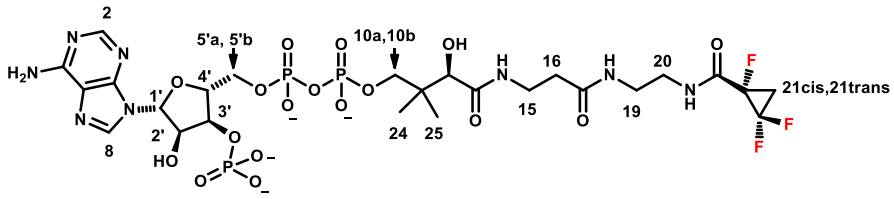

Compound **462** was prepared accordingly to the general procedure described above. Starting from a sample of diol **479** (0.020 g, 0.023 mmol), the coenzyme A analogue **462** was obtained as a colourless, highly hydroscopic solid in an overall yield of 10% (0.003 g as an ammonium trifluoroacetate salt) after purification by semipreparative HPLC chromatography using a Phenomenex Synergi® 4µ Polar-RP 80Å 250 x 10.0 mm column and a linear gradient of water and acetonitrile containing 0.05% trifluoroacetic acid (0 to 15% acetonitrile in 10 min, then 15% acetonitrile for 10 min, then from 15% to 80% acetonitrile in 3 min to wash the column, then from 80% to 0% acetonitrile in 3 minutes, and 0% acetonitrile for 10 min to re-equilibrate the column). Retention time: 16.2 min (detector: 215 nm).

^{1}H NMR (500 MHz, D_2O) δ 8.51 (s, 1H, C*H*, H2), 8.22 (s, 1H, C*H*, H8), 6.13 (d, *J* = 6.6 Hz, 1H, C*H*, H1'), 4.93 - 4.67 (m, 2H, C*H*, H2' and H3', signals partially hidden by water peak), 4.54 (s, 1H, C*H*, H4'), 4.19 (s, 2H, CH_2, H5'$_a$, H5'$_b$), 3.96 (s, 1H, C*H*, H12), 3.78 (dd, *J* = 9.8, 4.1 Hz, 1H, C*H*, H10$_a$, H10$_b$), 3.51 (dd, *J* = 9.8, 4.0 Hz, 1H, C*H*, H10$_a$, H10$_b$), 3.43 – 3.32 (m, 4H, CH_2, H15, H19), 3.27 (dq, *J* = 6.1, 3.6, 3.0 Hz, 2H, CH_2, H16), 2.52 – 2.41 (m, 1H, C*H*, H21$_{cis}$, H21$_{trans}$), 2.38 (t, *J* = 6.7 Hz, 2H, CH_2, H20), 2.34 – 2.14 (m, 1H, C*H*, H21$_{cis}$, H21$_{trans}$), 0.83 (s, 3H, CH_3, H25), 0.71 (s, 3H, CH_3, H24).

^{19}F NMR (*with proton decoupled,* 471 MHz, D_2O) δ -75.76 (*trifluoroacetic acid*), -139.82 (m, CF_2, $^{2}J_{FF}$ = 164.7 Hz), -201.83 (m, C*F*).

m/z (ESI$^+$): Found [M+Na]$^+$ 895.1157, $C_{25}H_{40}F_3N_8NaO_{17}P_3$ requires [M^++ Na] 895.1170.

5.14. Enzymatic inhibition assays[1]

5.14.1. Materials and methods[1]

Porcine heart Citrate Synthase was purchased from Sigma-Aldrich (C3260-KU, 1000 units) as an ammonium sulfate suspension. It was diluted with water (5 mL), affording a concentration of 13.47 μM (0.58 mg/mL, determined by using the A280 method on a Nanodrop® UV-Vis spectrophotometer). This mixture was then further diluted with TRIS buffer (200 mM, pH = 8.0) to afford stock solutions at the required concentrations as described for each assay.

Oxaloacetate (OAA) and dithionitrobenzoic acid (DTNB) were purchased from Sigma-Aldrich and the stock solutions and buffers prepared using MilliQ® water obtained from a MilliQ® apparatus. These were either used immediately or frozen in liquid nitrogen and stored at - 80 ºC.

Acetyl CoA trilithium salt was purchased from Sigma-Aldrich and diluted with phosphate buffer (5 mM, pH 6); the concentration of the resulting stock solution was then checked on a Thermo Spectrophotometer (path length 1 cm) at 260 nm (ε_{260} = 15400 cm^{-1} M^{-1}) and diluted accordingly using the phosphate buffer to the desired concentrations. Due to the intrinsic instability of acetyl CoA in solution, the mixture were either used immediately or frozen in liquid nitrogen and stored at - 80 ºC.

5.14.2. Determination of IC_{50} and K_i^{app} for the inhibition of citrate synthase

The procedure used to assess IC_{50} and K_i^{app} of compounds **261**, **262**, **305**, *(Z)*-***319***, *(E)*-***320***, **462** is fully described in Chapter 2.

IC_{50} values were estimated according to the protocol described in Chapter 2, using the software GraphPad® and applying the *log (inhibitor) vs. response - variable slope* model (Y = bottom + (Top - bottom) / {1+ 10^ [(Log IC_{50} - X)*HillSlope]}). The reported errors propagation values on IC_{50} and K_i^{app} measurements were derived from a standard error propagation calculator.

5.14.3. Fluorovinyl-dethia-coenzyme-A (261) IC_{50} and Ki^{app} [1]

The following results were obtained for compound **261** applying the general procedure described above. Stock solutions of compound **261** in MilliQ® water were prepared and their concentration accurately measured spectrophotometrically by using standard curves obtained from coenzyme A. The measurements were then carried out gradually increasing the concentration of compound **261** (20 µM, 63 µM, 282 µM, 489 µM, 1 mM) in duplicates.

Computed values for compound **261**:

$$\mathbf{IC_{50}} = 238.8\ (\pm\ 47.9)\ \mu M$$

$$\mathbf{K_i^{app}} = 44.8\ (\pm\ 9.2)\ \mu M$$

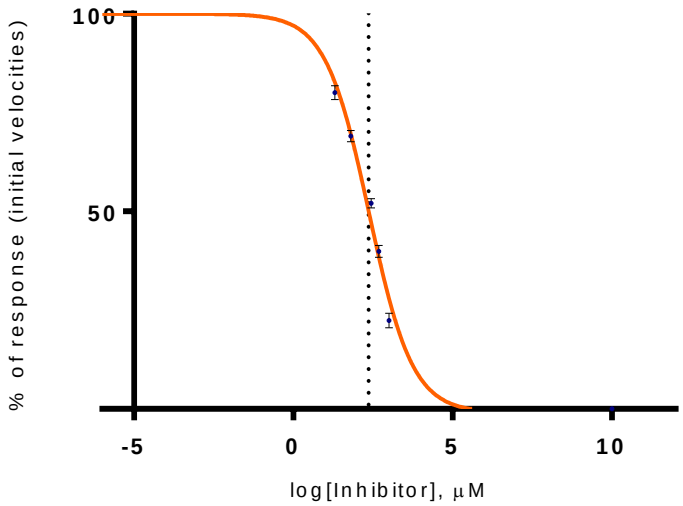

5.14.4. Vinyl-dethia-coenzyme-A (262) IC_{50} and Ki^{app} [1]

The following data were acquired for compound **262** as described in the general procedure reported above. Stock solutions of compound **262** in MilliQ® water were prepared and their concentration accurately determined spectrophotometrically by using standard curves obtained from coenzyme A. The measurements were then carried out gradually increasing the concentration of compound **262** (163 µM, 245 µM, 490 µM, 1.2 mM) in duplicates.

Computed values for compound **262**:

$$\mathbf{IC_{50}} = 281.9\ (\pm\ 32.4)\ \mu M$$

$$\mathbf{K_i^{app}} = 53.1\ (\pm\ 6.5)\ \mu M$$

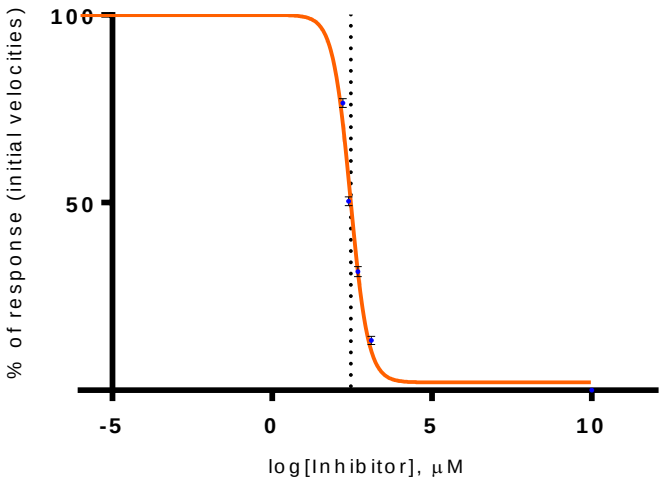

5.14.5. Sulfoxide Coenzyme A (305) IC_{50} and Ki^{app} [1]

The following data were obtained for compound **305** as described in the general procedure reported above and they are related to the diastereoisomeric mixture. Stock solutions of compound **305** in MilliQ® water were prepared and their concentration accurately determined spectrophotometrically by using standard curves obtained from coenzyme A. The measurements were then carried out gradually increasing the concentration of compound **305** (25 µM, 50 µM, 75 µM, 300 µM, 500 µM, 1.0 mM) in duplicate repeats.

Computed values for compound **305**:

$$\mathbf{IC_{50}} = 59.2\ \mu M\ (\pm 4.4)\ \mu M$$

$$\mathbf{K_i^{app}} = 11.1\ \mu M\ (\pm 0.9)\ \mu M$$

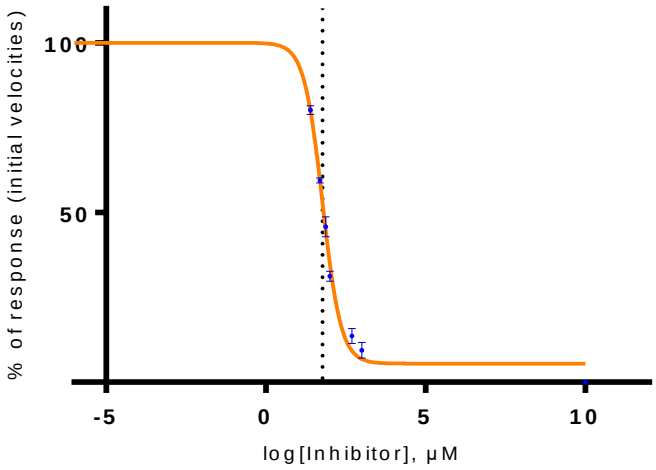

5.14.6. α, α, β-trilfuoro cyclopropyl-coenzyme-A (462) IC_{50} and Ki^{app} [1]

The following data were calculated for compound **462** according to the general procedure reported above. Stock solutions of compound **462** in MilliQ® water were prepared and their concentration accurately determined spectrophotometrically by using standard curves obtained from coenzyme A. The measurements were then carried out gradually increasing the concentration of compound **462** (26µM, 75 µM,250 µM,500 µM,1.1 mM) in duplicate repeats.

Computed values for compound **462**:

$$\mathbf{IC_{50}} = 346.1\ (\pm\ 56.4)\ \mu M$$

$$\mathbf{K_i^{app}} = 65.2\ (\pm\ 11.0)\ \mu M$$

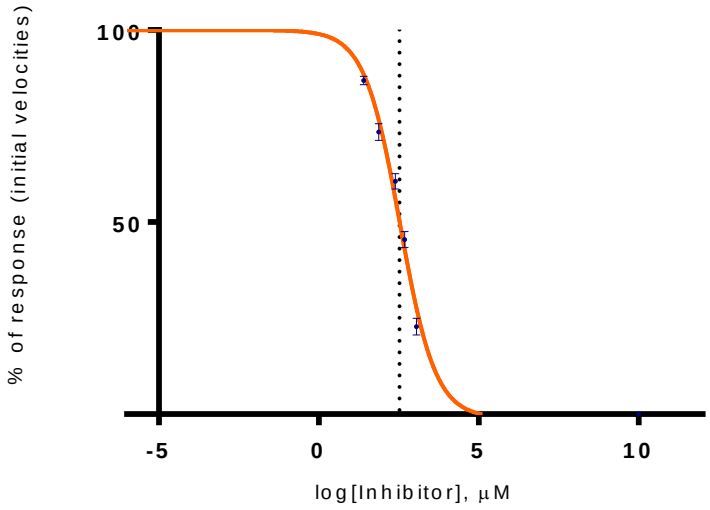

5.15. References

1 M. G. Rubanu, D. Bello, N. Bandaranayaka, J. P. Götze, M. Bühl, D. O'Hagan, *ChemBioChem*, **2019**, *20*, 1174-1182.

2 M. Tosin, D. Spiteller, J. B. Spencer, *ChemBioChem*, **2009**, *10*, 1714–1723.

3 J. Han, N. Shimizu, Z. Lu, H. Amii, G. B. Hammond, B. Xu, *Org. Lett.*, **2014**, *16*, 3500–3503.

4 O. E. Okoromoba, J. Han, G. B. Hammond, B. Xu, *J. Am. Chem. Soc.*, **2014**, *136*, 14381–14384.

5 W. Du, Q. Gu, Y. Li, Z. Lin, D. Yang, *Org. Lett.*, **2017**, *19*, 316–319.

6 Carney et al., *US Patent No.4*, **1989**, 5488-5494.

7 J. P. Brand, D. Fernández-González, S. Nicolai, J. Waser, *Chem. Commun.*, **2011**, *47*, 102–115.

8 R. Frei, J. Waser, *J. Am. Chem. Soc.*, **2013**, *135*, 9620–9623.

9 J. Tsuji, M. Takahashi, T. Takahashi, *Tetrahedron Lett.*, **1980**, *21*, 849–850.

10 G. Talavera, J. Peña, M. Alcarazo, *J. Am. Chem. Soc.*, **2015**, *137*, 8704–8707.

11 Y. Li, X. Liu, D. Ma, B. Liu, H. Jiang, *Adv. Synth. Catal.*, **2012**, *354*, 2683–2688.

12 D. Bello, R. A. Cormanich, D. O'Hagan, *Aust. J. Chem.*, **2015**, *68*, 72–79.

13 M. P. Storz, C. K. Maurer, C. Zimmer, N. Wagner, C. Brengel, J. C. De Jong, S. Lucas, M. Mu, S. Ha, A. Steinbach, R. W. Hartmann, *J. Am. Chem. Soc.*, **2012**, *134*, 16143–16146.

14 C. J. Thomson, Q. Zhang, N. Al-maharik, M. Bu, D. B. Cordes, A. M. Z. Slawin, D. O'Hagan, *Chem. Commun.*, **2018**, *54*, 8415–8418.

15 I. Nazi, K. P. Koteva, G. D. Wright, *Anal. Biochem.*, **2004**, *324*, 100–105.

6. *Appendix*

Acetyl coenzyme A analogues as rationally designed inhibitors of citrate synthase. / Bello, Davide; Rubanu, Maria Grazia; Bandaranayaka, Nouchali; Götze, Jan. P.; Bühl, Michael; O'Hagan, David.

ChemBioChem, Vol. 20, No. 9, 02.05.2019, p. 1174-1182.

https://doi.org/10.1002/cbic.201800700